

**EUROPEAN COMMISSION  
DG RTD**

SEVENTH FRAMEWORK PROGRAMME  
THEME 7  
TRANSPORT - SST  
SST.2007.4.1.2: Human physical and behavioral components  
GA No. 218740

**COVER**

**Coordination of Vehicle and Road Safety Initiatives,  
With a focus on Biomechanical coordination**

<b>Deliverable No.</b>	COVER D25	
<b>Deliverable Title</b>	Report on child safety research	
<b>Dissemination level</b>	Public	
<b>Edited By</b>	C Visvikis (TRL) and P Lemmen (Humanetics)	28/03/13
<b>Checked by</b>	J Carroll (TRL)	28/03/13
<b>Approved by</b>	Paul Lemmen (Humanetics)	29/03/13
<b>Issue date</b>	29/03/13	

## Executive summary

The problems arising from the growth in road traffic are looming ever larger in our daily lives and are impairing the quality of life of everyone. The citizens of Europe may legitimately demand clean, safe, intelligent, high-performance cars. Meeting this demand at competitive prices represents an enormous technological challenge for the European side of the automotive industry, and is also an essential prerequisite for maintaining, or even bolstering, its competitiveness in the future. At the same time traffic-related accidents are still a major threat to life in the European Union (EU), especially when the low average age of the victims is taken into account. In 2005 alone, around 41,600 people were killed and more than 1.7 million injured in European road accidents. Although the number of road fatalities declined to 34,817 in 2009, further efforts will have to be made to make European roads safer. This may be particularly challenging when taking the growing transportation needs of the elderly into account and the recent expansion of the EU with countries that historically have lacked effective safety standards.

Previous research in the field of vehicle passive safety has contributed to significant improvements in vehicle and road safety. However, the focus has been on protective measures optimised for “average occupants” (usually adults), whereas in the real world, substantial differences appear under a range of factors such as gender, age and size. Brought forward by stakeholders, this topic was recognised by the European Commission and put high on the research agenda. As a consequence, four projects were accepted in this field, which deal with two topics of particular importance:

- Child safety, addressing improved numerical and experimental test tools for younger children as well as adolescents;
- Thoracic injuries, addressing a body part which is placed at a high risk during collisions, as found in previous EU research projects, whilst being subject to large biomechanical variations over age, gender and size, due to geometry and material changes in bones and soft tissues.

The projects dealing with child safety are EPOCh (Enabling Protection of Older Children, GA No. 218744) and CASPER (Child Advanced Safety Project for European Roads, GA No. 218564). The projects dealing with thoracic injuries are THOMO (Development of a finite element model of the human thorax and upper extremities, GA No. 218643) and THORAX (Thoracic injury assessment for improved vehicle safety, GA No. 218516).

The aim of COVER, a Coordination and Support Action, is to develop a harmonised and consistent direction of research between these projects and to accelerate the implementation of research findings of four complementary research projects in the field of crash biomechanics. To maximise the benefits gained from the individual projects, synergies between the projects are exploited by coordinating the exchange of results, joining dissemination actions towards relevant stakeholders, and exchanging best practices and policies with respect to relevant aspects like test methods and deployment strategies. For the objective of dissemination (both towards relevant high-level stakeholders and the general public), a coordinated approach will be an important factor in providing a clear message and obtaining the necessary visibility.

A key part of these dissemination activities is to generate reports that integrating the results of projects involved in COVER. This includes reports on:

- Thoracic injuries, with content largely based on input from THOMO and THORAX;
- Child safety, with input from CASPER and EPOCh.

This report presents research findings related to child safety as obtained from the CASPER and EPOCH projects. . It provides a single source for the latest knowledge, tools and methods developed in these projects. Information on the following topics is included:

- Child restraint use and misuse observed during field observations undertaken in France, Germany and Italy;
- Injuries to children in collisions and the implications for legislation and dummy design;
- Child dummy developments, focussing on the Q-Series dummies and their instrumentation;
- The development of Injury criteria and performance limits for the Q-Series dummies;
- Child dummy and human body models.

---

## Contents

1	Introduction .....	7
1.1	The COVER project .....	7
1.2	Report structure .....	7
2	Field observations of child restraint use and misuse .....	8
2.1	Introduction .....	8
2.2	Basic data .....	8
2.3	Information on CRS .....	11
2.4	Information on misuse .....	13
2.5	Analysis of reasons leading to misuse .....	16
2.6	Sociological aspects about misuse .....	18
2.7	Consequences resulting from misuse based on accident reconstruction / misuse tests	21
2.8	Analysis of possibilities to reduce the misuse risk or to reduce the severity of consequences resulting from misuse .....	23
2.8.1	Solutions of CRS with integral harness .....	24
2.8.2	Solutions for boosters .....	26
2.9	Summary and conclusion .....	27
2.10	References .....	28
3	Injuries to children in road traffic collisions .....	30
3.1	Report on accident analysis – Deliverable 3.2.3 of the EC FP7 project CASPER	30
3.1.1	Introduction .....	30
3.1.2	Methodology .....	31
3.1.3	Overall overview of database .....	35
3.1.4	Frontal impacts .....	37
3.1.5	Lateral impacts .....	54
3.1.6	Safety technologies .....	74
3.1.7	Comparison of injury recording systems .....	77
3.1.8	Discussion and conclusions .....	83
3.1.9	References .....	89
3.2	EPOCH Task 1.1 - Literature review, accident analysis and injury mechanisms....	89
3.2.1	Introduction .....	89
3.2.2	Background .....	90
3.2.3	Overview of collision studies .....	104
3.2.4	Mechanisms of injury in older children .....	108
3.2.5	Discussion .....	109
3.2.6	Conclusions .....	111
3.2.7	Recommendations .....	111
3.2.8	Acknowledgements .....	112
3.2.9	References .....	112

---

4	Child dummy developments .....	115
4.1	Auxiliary equipment for Q3 and Q6 to improve belt interaction response .....	115
4.1.1	Introduction: general use of child dummies in the frame of research.....	115
4.1.2	Possible shortcomings in Q3 dummy affecting the dummy response.....	118
4.1.3	Assessment of the lumbar region stiffness in flexion .....	124
4.1.4	Proposals to improve the dummy response by removing the gap at the groin 129	
4.1.5	Presentation of the prototypes .....	135
4.1.6	Preliminary evaluation of the prototypes .....	137
4.1.7	Conclusions and perspectives .....	142
4.1.8	References .....	142
4.2	Abdominal pressure twin sensors for the Q dummies: from Q3 to Q10 .....	144
4.2.1	Introduction.....	144
4.2.2	Discussion and conclusions .....	154
4.3	Q10 biofidelity – dummy validation in certification-type loading .....	157
4.3.1	Introduction.....	157
4.3.2	Method.....	157
4.3.3	Anthropometry .....	158
4.3.4	Biofidelity .....	160
4.3.5	Sensitivity .....	165
4.3.6	Repeatability .....	172
4.3.7	Durability.....	174
4.3.8	Certification procedures .....	175
4.3.9	Summary and conclusions .....	178
4.3.10	References .....	179
5	Injury criteria and performance limits.....	180
5.1	Estimating Q-dummy injury criteria using the CASPER project results and scaling adult reference values .....	180
5.1.1	Introduction.....	180
5.1.2	Methods.....	181
5.1.3	Results.....	186
5.1.4	Discussion .....	194
5.1.5	Conclusion.....	195
5.1.6	Acknowledgement .....	195
5.1.7	References .....	195
5.1.8	Appendices.....	196
5.2	Development of injury risk curves for the Q10 dummy .....	199
5.2.1	Introduction.....	199
5.2.2	Scaling approach .....	200
5.2.3	Head acceleration.....	201

---

5.2.4	Head excursion.....	204
5.2.5	Neck .....	204
5.2.6	Thorax .....	207
5.2.7	Thorax acceleration .....	213
5.2.8	Summary and discussion.....	213
5.2.9	Conclusions .....	214
5.2.10	References .....	215
6	Numerical simulation.....	218
6.1	Numerical simulation in the area of child safety using Q dummy models .....	218
6.1.1	Q dummy model status .....	219
6.1.2	New hardware dummy development – the Q10 .....	220
6.1.3	Improving Q6 model and validation tests .....	220
6.1.4	First experience with FE Q-dummies .....	221
6.1.5	Human body modelling .....	228
6.1.6	Acknowledgements.....	229
6.1.7	References .....	229
6.2	Development of a 3-year-old child head-neck finite element model and derivation of a novel head injury criteria.....	230
6.2.1	Introduction.....	230
6.2.2	Methods.....	234
6.2.3	Results.....	239
6.2.4	Discussion .....	241
6.2.5	Conclusions .....	242
6.2.6	Acknowledgements.....	242
6.2.7	References .....	242
6.3	Six-years-old child head-neck finite element modelling application to the Interaction with airbag in frontal and lateral Impact .....	244
6.3.1	Introduction.....	244
6.3.2	Materials and methods.....	245
6.3.3	Results.....	256
6.3.4	Discussions .....	262
6.3.5	Conclusions .....	262
6.3.6	Acknowledgement .....	262
6.3.7	References .....	263
7	Summary .....	265

## 1 Introduction

### 1.1 The COVER project

COVER is a Coordination and Support Action under the 7th Framework Programme (FP7) of the European Commission. It includes four research projects dealing with human physical aspects. Figure 1-1 depicts the participating initiatives in a diagram with respect to age and output of the project.

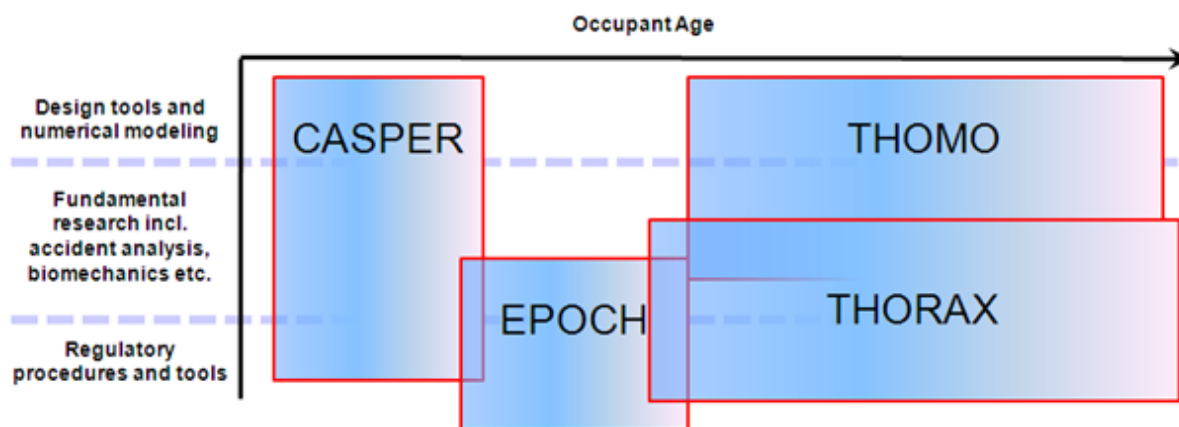


**Figure 1-1: Overview of the FP7 projects participating in COVER**

Under the implementation of COVER, these projects will:

- 1) Install a structure of joined research activities that optimise outcomes and implementation of results of each of the individual initiatives;
- 2) Exchange information and best practices (internal dissemination);
- 3) Develop and execute a joint agenda for external dissemination.

### 1.2 Report structure

This report collates the principal research findings related to child safety from CASPER (Child Advanced Safety Project for European Roads) and the EPOCH (Enabling Protection for Older Children) project. It provides a single source for the latest knowledge, tools and methods developed in these projects. The report is structured as follows:

- Chapter 2 presents the findings of field observations of child restraint use and misuse undertaken in France, Germany and Italy;
- Chapter 3 examines the injuries to children in collisions and the implications for legislation and dummy design;
- Chapter 4 describes the latest child dummy developments, focussing on the Q-Series dummies and their instrumentation;
- Chapter 5 presents the latest developments on injury criteria and performance limits for the Q-Series dummies;
- Chapter 6 comprises research on the development of child dummy and human body models.

The main technical content of the report was derived from previously published material. This included published project deliverables and papers presented at international conferences such as IRCOBI (International Research Council on Biomechanics of Injury), Protection of Children in Cars and ICRASH (the International Crashworthiness Conference).

## 2 Field observations of child restraint use and misuse

The use of a child restraint system is mandatory when travelling in cars in all Member States of the European Union, in line with Directive 91/671/EEC, as amended by 2003/20/EC. The Directive requires that children less than 150 cm in height are restrained by a child restraint, approved to United Nations (UN) Regulation 44.03 (or later). Certain exemptions are provided for special categories of vehicles, such as taxis, and Member States are permitted to mandate the use of child restraints for children up to 135 cm in height, rather than 150 cm, if they wish.

Such legislation, combined with education and information campaigns, has undoubtedly increased the use of child restraint systems. However, observation studies regularly find that child restraints are fitted incorrectly or they are inappropriate for the child's size. The way a child restraint system is used is likely to affect its performance in a collision. Some mistakes may be more serious than others, nevertheless, the benefits of high levels of child restraint use may not be being realised fully.

This chapter describes an observation study undertaken within the CASPER project. It comprises a paper presented at the International Crashworthiness Conference in 2012 and reproduced here in its entirety. The full reference of the paper is:

Müller, G., Johannsen, H., Eisenach, A., Lesire, P., Chevalier, M-C., Beillas, P., Fiorentino, A. and Schnottale, B. (2012). Misuse of child restraint systems – an important problem for child safety. *Proceedings of the International Crashworthiness Conference 2012*. London: Taylor & Francis Group.

### 2.1 Introduction

Besides the dynamic performance of Child Restraint Systems (CRS) in sled tests, the actual use of the system has an important effect on child safety. Past experience from field studies and accident investigations show that a majority of children are not correctly restrained when travelling in cars [1- 4]. This includes cases of unrestrained children, children using the car belt without CRS, CRS that are not correctly installed in the car, children that are not correctly restrained in the CRS and the use of an inappropriate CRS.

Within the CASPER project field studies were conducted in order to analyse the restraining situation of children in different European regions. In addition to the technical data of the CRS installation and restraining situation of the child, a sociological approach helped to better understand the circumstances that lead to incorrect restraining of children. Furthermore the risk resulting from misuse was analysed based on comparative sled tests and last but not least published solutions to reduce the risk were reviewed.

The interviews for the field study took place in Naples, Berlin and Lyon and surrounding areas. They were divided into two parts. The first one was the observation and assessment of the securing situation of the child in the car; the second part was a short interview with the car driver. As basis for the analysis of the study 104 cases from both areas Berlin and Lyon as well as 108 cases from Naples were analysed. That means the data base consists of 316 cases.

### 2.2 Basic data

A look to the age distribution (Figure 2-1) of the children in this study shows that there are few observations in the group from 10 to 12 years and limited numbers in the group up to one year of age, which is normally the group of rearward facing CRS. In this



lower age group, some differences may be observed: 20% of children are younger than 1 year in the Berlin data while about 4% in Lyon and 8% in Naples samples. Statistical tests performed with the CHI-2 test confirm these observations:  $p < 0.05$  when comparing Berlin and Lyon or Berlin and Naples samples while the age distributions are not statistically different between Naples and Lyon data ( $p = 0.22$ ). The data collection strategy (mostly near a city park with recreational facilities in Lyon, in a variety of locations in Berlin and in connection with the company Christmas party in Naples) may have affected this distribution.

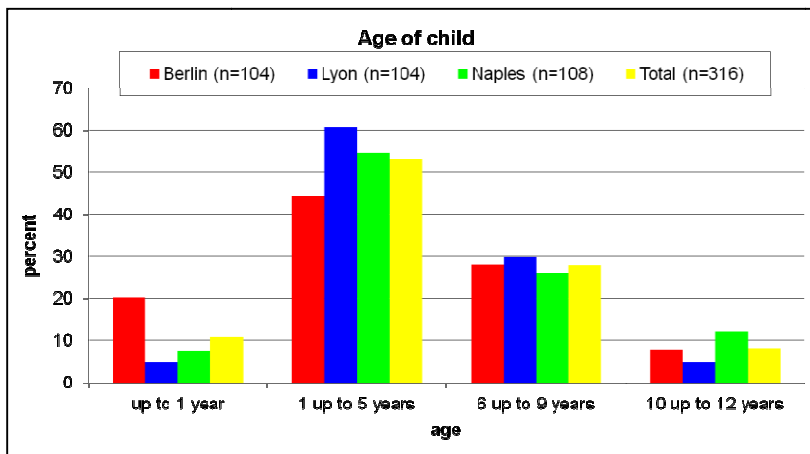
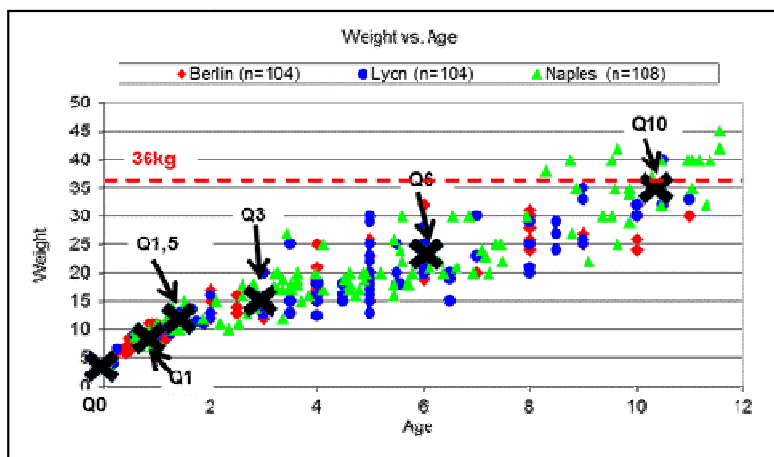
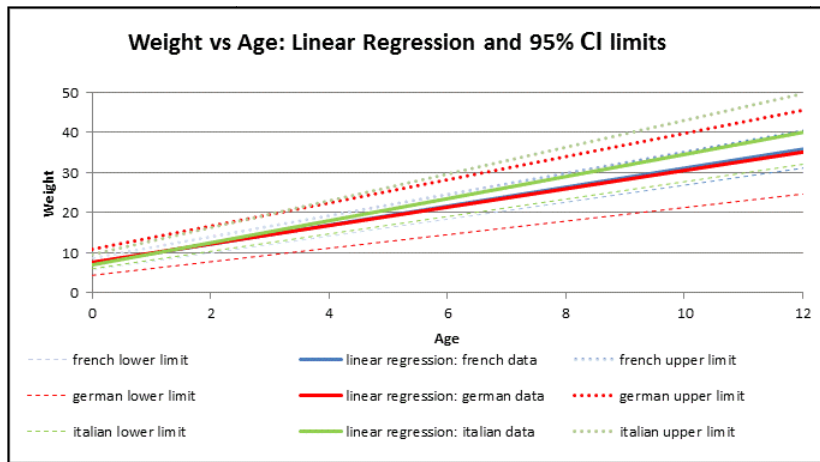


Figure 2-1: Distribution of age

The comparison of age and weight of the children from Berlin, Lyon and Naples is shown in Figure 2-2a. Linear regressions were performed with calculation of confidence interval at 95% (Figure 2-2b): no significant differences between Berlin, Lyon and Naples data were found in the limit of this interval. For all groups the scatter of weight increased with increasing age. The relationship between weight and age was well in line with the dummy characteristics (Figure 2-2a).



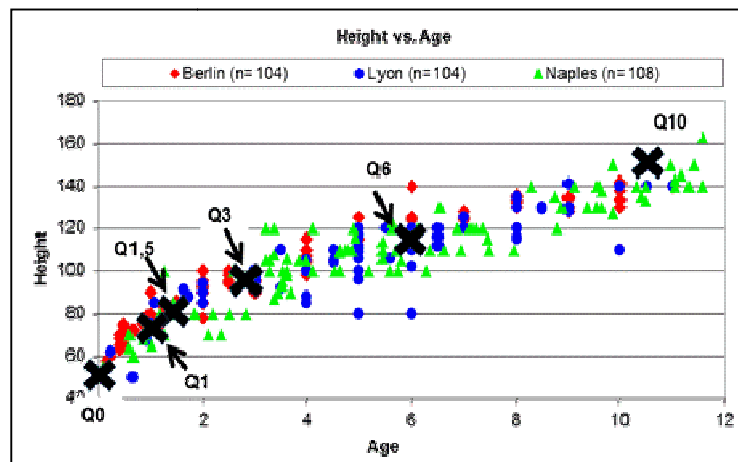
a)



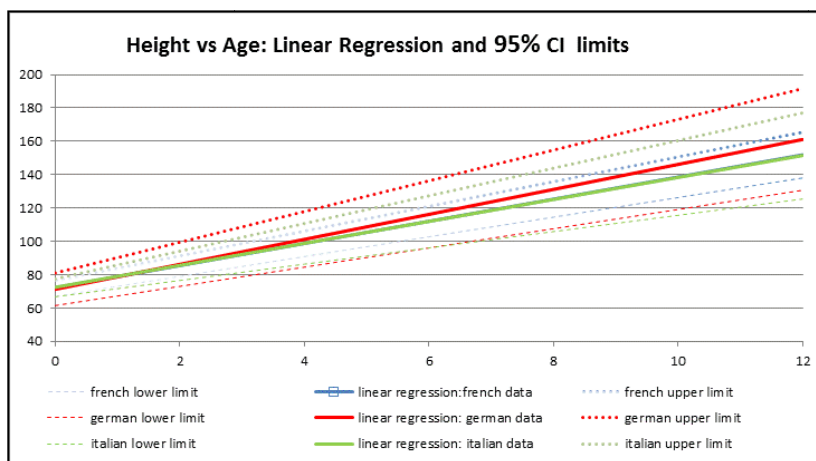
b)

**Figure 2-2: a) Comparison of weight and age for the children of the misuse study and the Q-dummies (top) b) Linear regression and 95% confidence intervals (bottom)**

A similar picture emerges when comparing body size and age of children (Figure 2-3a). The distributions are statistically similar for all three survey locations within a confidence interval at 95% (Figure 2-3b) and again, the Q-dummies fit well within the cloud. Only the Q10 dummy, which represents a 10.5 years old child, is at the upper limit of the stature of the children. However, only limited data was collected for this age group.



a)



b)

**Figure 2-3: a) Comparison of height and Age for the children of the misuse study and the Q -dummies (top) b) Linear regression and 95% confidence intervals (bottom)**

### 2.3 Information on CRS

The distribution of the CRS which was in use shows differences between Berlin, Naples and Lyon data (Figure 2-4 and Figure 2-5). Most striking here is certainly the high rate of non-use cases in Naples: Sixty percent of all children were not secured, only secured with the vehicle's seatbelt or were travelling on an adult's lap. In contrast, the non-use cases were 16% in Lyon and 3% in Berlin, respectively. However it has to be noted that there were different selection criteria of cases at the three locations. While in Berlin cases were only collected when the child was sitting in a CRS, in Naples all children in vehicles were considered. In Lyon an intermediate approach was used: all children below 12 years old in a car were considered for the study, if at least one of the children was secured in a CRS. These different selection criteria have to be taken into account when comparing the results of the individual regions. Also, based on the feedback from the investigation teams, regional differences are very likely. A non-use rate of 60%, as it was recorded in Naples would not be the case in Berlin, not even taking into account all the children who were seen in cars. According to research of the BAST, the usage rate of CRS in Germany is at 84%, another 14% of children are secured only by the safety belt [1].

The high rate of infant carriers (UN Regulation 44 Group 0+ seats) in Berlin compared to other survey sites is partly explained by the different age distribution. In addition, it must be noted that ISOFIX seats are still seldom used. On all three survey locations less than five percent of the children were secured in an ISOFIX seat.

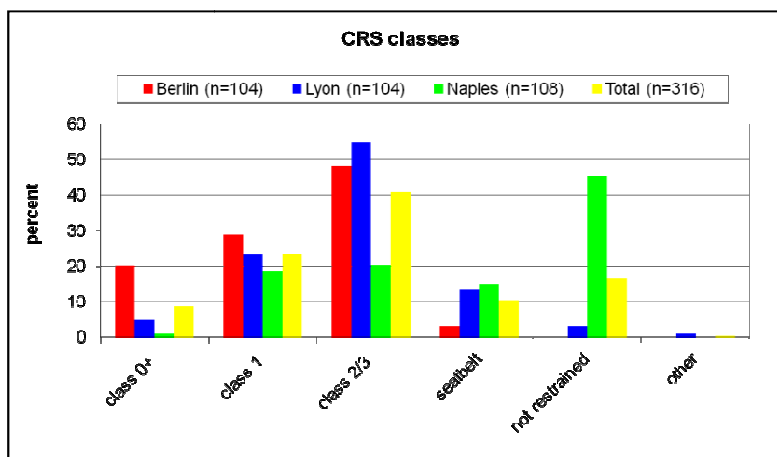


Figure 2-4: Distribution of CRS classes

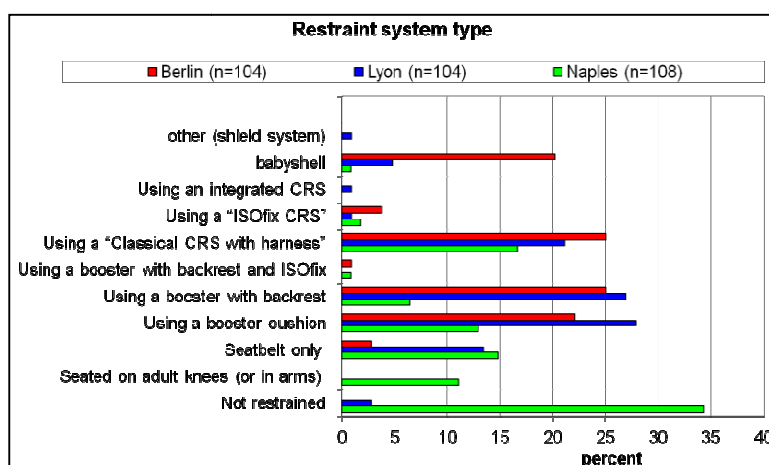


Figure 2-5: Restraint system type

Plotting the CRS classes as a function of the age of the children suggests an overall age-appropriate selection of CRS classes (Figure 2-6). Infant carriers (class 0+) are used mainly for all children up to one year; some are still in the age group 1 to 5 years in use. While CRS in Class 1, suitable for children aged 9 to 18 kg, are mainly used by the 1 to 5 year old, some are in use for younger children. In most cases, these seats are not suitable for children in this age group and their use constitutes a misuse. CRS of class 2/3 (15 to 36 kg) are suitable for children from about 4 to 5 years. According to the distribution shown in Figure 2-6, their use is age-appropriate. Unsecured children, or children restrained only by the safety belt were observed in all age groups.

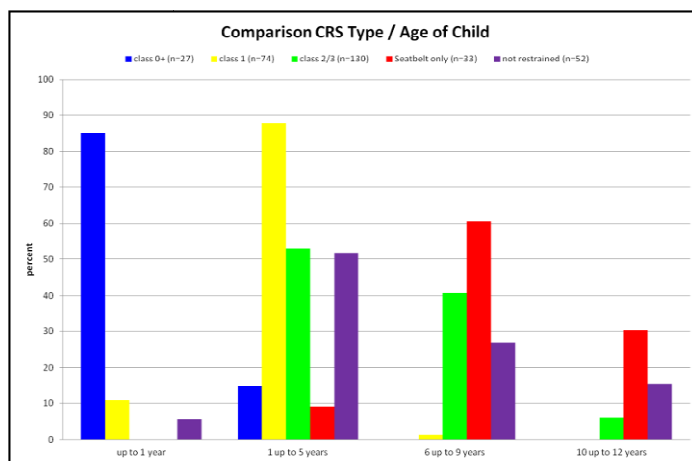


Figure 2-6: Comparison of CRS type and age of the child

## 2.4 Information on misuse

For the evaluation of the securing situation, it should be first defined how to deal with cases where the children were secured in a CRS or were secured only by the safety belt in the car. Since the term "misuse" refers to the misuse of CRS, and is used in this sense in the current study, the term "misuse" can only be applied to cases where a CRS was in use in some way. Accordingly, only those cases are considered for the following analyses. This classification is consistent with older field studies [1-4]. Only the following diagram (Figure 2-7) takes into account all cases, to present an overall picture of the current securing situation in the comparison of the three study regions.

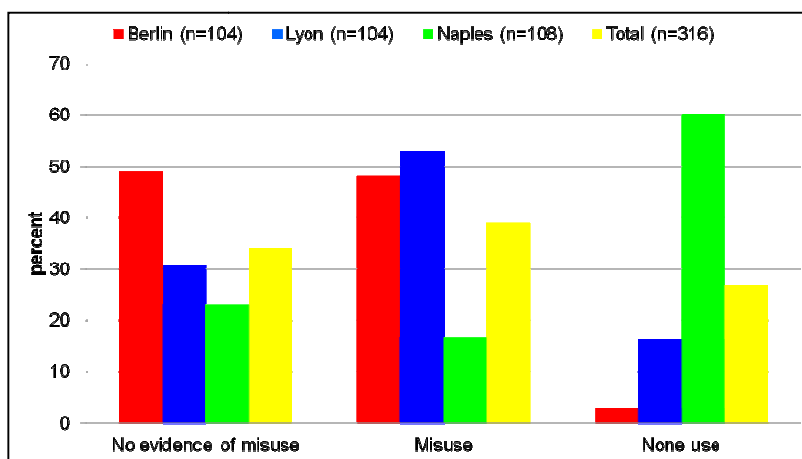


Figure 2-7: Securing quality

In general the results of this study confirm the results of former evaluations [1-4]: only one third of the children are properly secured in the vehicle, two thirds are wrongly or not secured. However, in the older studies, cases were selected only, if a CRS was in use, which was the same selection criterion in Berlin.

Depending on the region, differences could be observed. While in Berlin the rate of correct use was about 49%, it was only 31% in Lyon and 23% in Naples in part due to the non-use of CRS. If removing the non-use cases out of the three locations, the correct use rate becomes 50% (n=101) in Berlin, 37% (n=87) in Lyon and 58% (n=43) in Naples, and the average becomes 47% (n=231).

Grouping data from all sites leads to a misuse rate (taking into account only cases where a CRS was used) of 53% (Figure 2-8). It is important to note that this rate does

not reflect the protection of children in cars as children without CRS, which are especially at risk, are not considered. Taking only into account the data from Berlin gives similar results (50% misuse). Regional differences may be more marked on the rate of non-use (as already seen above between Lyon and Naples).

Overall, these results could suggest a reduction of the CRS rate of misuse with time. While this could be an encouraging trend, it needs to be taken with caution as methodology; sampled population and investigator training may differ between studies and locations. This is illustrated by the difference of age distribution between locations. Future studies and analyses should be performed to determine if it is a positive trend or a methodological artefact.

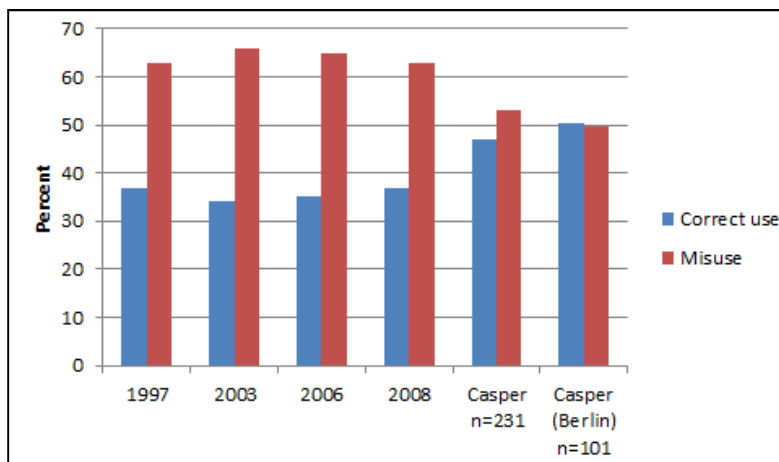


**Figure 2-8: Comparison of misuse rate with older field studies [1 - 4] [Only the cases for which a CRS was used were included for the three locations]**

A look at the distribution of misuse suggests that more misuse occur when securing the child in the CRS (securing misuse) than misuse in relation with the installation of the CRS in the car (installation misuse). However both misuse types were often observed (Figure 2-9).

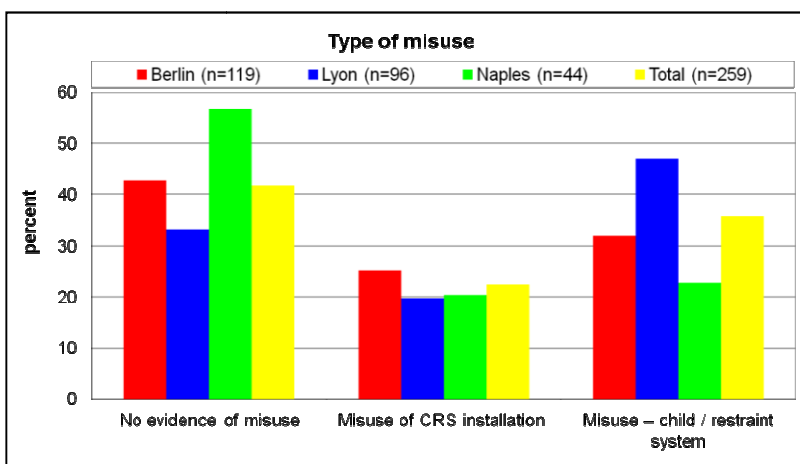


**Figure 2-9: Type of misuse**

A closer look at the securing misuse shows what problems arise most often. The most common is the slack in the belt system of the CRS, which can be detected in more than 25% of all misuse cases. Furthermore, twisted belts in the CRS or in the vehicle were found in 13% of the cases, however, it has usually no direct impact on the safety of the occupants, but it can cause belt slack because the belt cannot be tightened properly.

The non-use of the lower lap belt guides in class 2/3 seats is another common problem. This could result in some accident cases in the direct loading of the abdominal region by the belt, which might obtain abdominal injuries. Belt under the arm (7%) could also result in inappropriate loading of the thoracic and abdominal regions and injuries.

Quite often (6%) the children are too small (very seldom too large) for the used CRS, which means that its belt geometry cannot be properly adjusted for the child. In the worst case, the child is clearly too small for a Class 1 seat, and thus could be more exposed to the risk of neck injuries that it will suffer because of his large head weight in comparison to the neck muscles, which also occur in relatively small car decelerations.

Most often observed securing misuse:

- Slack in harness (baby shell, class 1) 26%
- Lower belt guide not used (class 2/3) 18%
- Car belt twisted (class 2/3) 13%
- Wrong shoulder belt position (class 1; 2/3) 11%
- CRS belt under arm of child (class 2/3) 7%
- Child too small for CRS (class 1; 2/3) 6%

Looking at the types of misuse related to the installation of the CRS in the car (Figure 2-10), the most common problems are the car belt path, the lack of shoulder belt guide use in a class 2/3 seat with a backrest, the insufficiently tightened car belt and the bulk seat fixation. These misuses are critical and may lead to serious injuries if an accident occurred. The most common misuses have in common that they could be prevented by the use of ISOFIX.

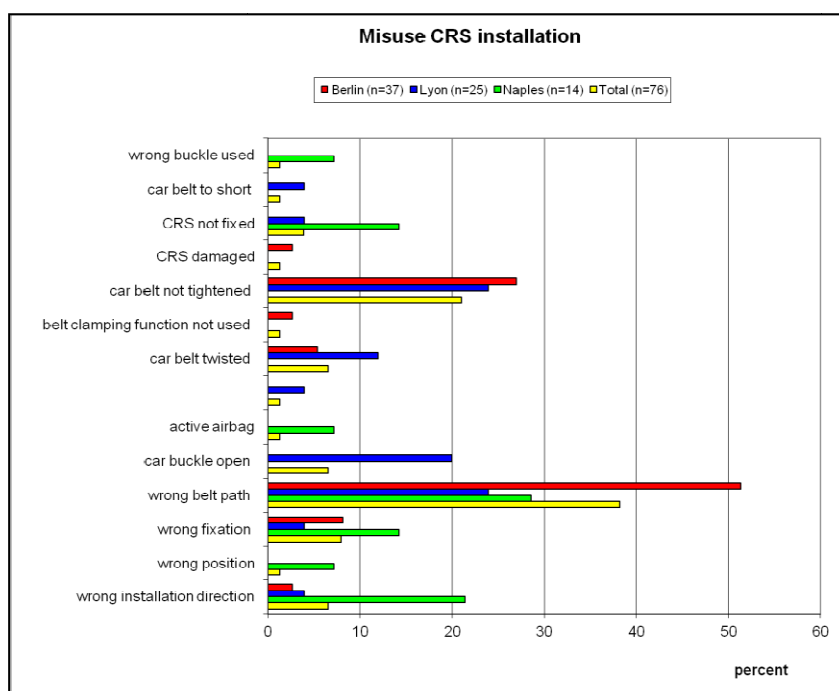


**Figure 2-10 Misuse in connection with the installation of CRS in the car**

The assessment of the installation misuse shows that most of the cases were rated by the interviewers as severe misuse. There are some differences between the three study regions, but these were probably due to the small sample size and the general difficulty in assessing the severity of errors.

## 2.5 Analysis of reasons leading to misuse

Apart from the details directly related to the technical aspects of the restraint conditions, information about the transport situation was collected. The aim was to better understand the situation and try to find which specific circumstances could lead to misuse. The following analysis includes cases where the child was not secured in a CRS and includes data from all three regions.

First, the travel time was compared with the misuse frequency (Figure 2-11). The correct use of a child safety seat seems to increase with travel time, however the tendency is not very pronounced. This trend cannot be seen for misuse or non-use cases.

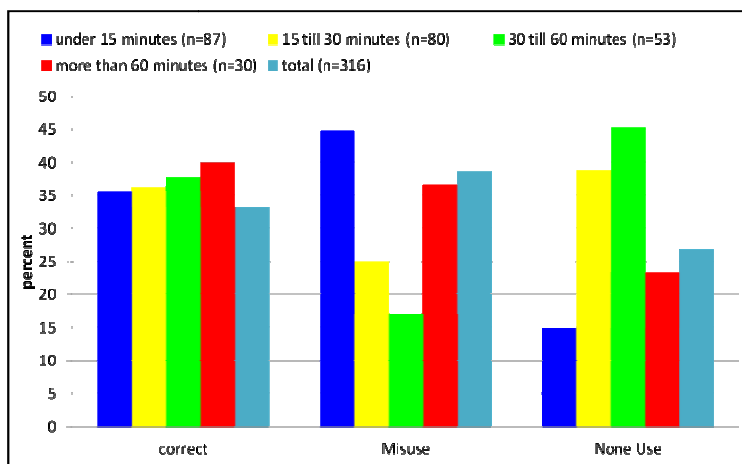


Figure 2-11: Misuse depending on travel time

Another interesting point is a possible link between the securing quality and the travel purpose. In the questions, the travel purpose could be: ride to school / nursery, shopping, vacation, leisure activity and other rides. This analysis suggests that there is a relationship between securing quality and travel purpose (Figure 2-12). Driving to school, kindergarten or shop, which may be associated with a certain time pressure, was more likely to lead to poor restraint of the child, children in leisure or recreational trips tend to be better secured. Because of the special situation in Naples, where all interviews took place in conjunction with a company Christmas party, there is a large group of “other” in the statistics of the travel purpose.

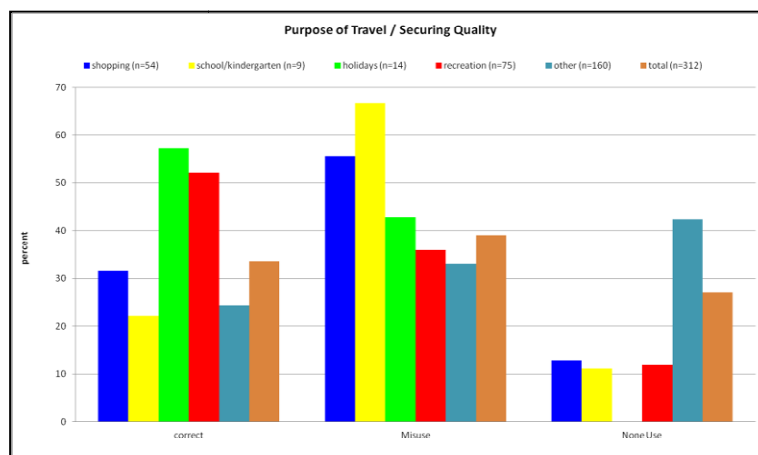


Figure 2-12: Comparison of purpose of travel and securing quality



During the interview, all drivers were asked whether they believe that their child was secured in the vehicle correctly. A majority of respondents replied “yes”, and only a small proportion was unsure or stated that this was not the case (Figure 2-13). However the comparison of these data with the actual installation quality shows that misuses were present in almost 60% of the situations that were perceived as correct by the drivers. In cases where the drivers were not sure or not expecting that everything was done correctly, the misuse rate was even higher (Figure 2-14).

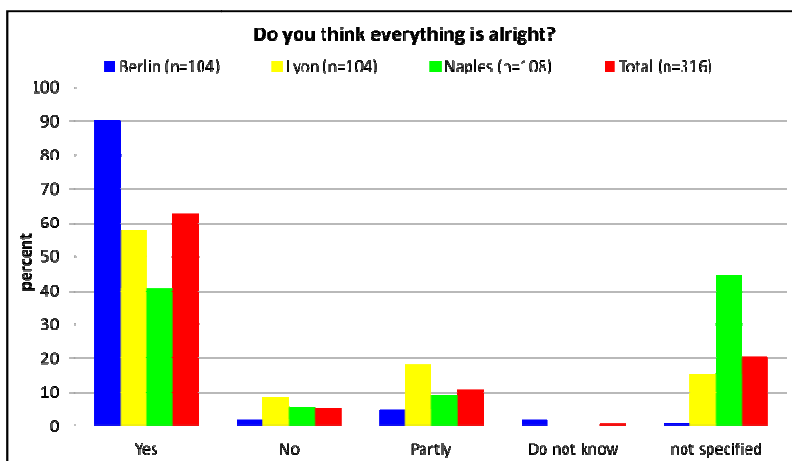


Figure 2-13: Self-assessment of the situation

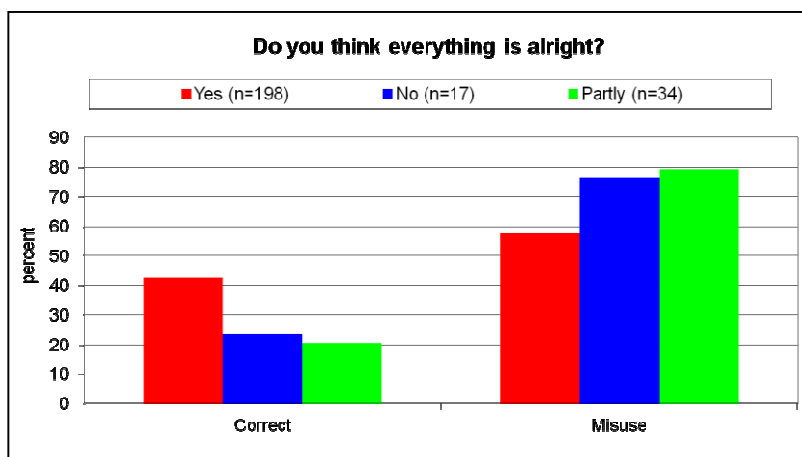


Figure 2-14: Comparison of self-assessment and misuse rate

According to this result, a majority of drivers believes that the restrained child is properly secured and is not aware of the misuse. The misuse is not a known situation that the driver accepts while knowing better, but seems the result of a lack of knowledge about the correct use of CRS. It is also unknown if some parents could have been aware but refused to admit it in front of the investigators.

The study has shown that external factors, such as the trip purpose, have influence on the securing quality. The ride to kindergarten or to school, which is a daily situation where parents may have less time, resulted in a higher rate of misuse. Trips with greater travel time or a relaxed environment, such as vacation trips, was associated with a better securing quality.

Finally, the results of the study and the interviews with the drivers have shown that parents want to secure their child correctly. However, lack of information or a misunderstanding of the user manual lead to a high misuse rate. Obviously there is still a great need for the simplification of the usability of CRS. At the same time it should be

the aim of the manufacturer of CRS to ensure that also frequently observed misuse does not automatically lead to a significant loss of the protective potential of child CRS.

## 2.6 Sociological aspects about misuse

The misuse survey included several questions that could help understanding some of the sociological aspects associated with CRS misuse, such as parental attitudes, habits and behaviours and driver perception relating to child transportation in cars.

Globally the sample is composed by 317 observations, equally distributed between the three countries (104 Germany, 104 France, 109 Italy) but for time constraints the collection of this information was not always possible. The “unknown” or missed answers are excluded by each variable percentage. The driver was always the person answering the question even when there were other adult occupants in the vehicle.

- **Gender (n=314):** The whole survey was mainly composed by males (61%), highlighting the fact that men are more likely those who drive the car with their family. Women were only the 39% of the cases.
- **Age (n=261):** Most of the men were between 36 and 45 years of age (57%), and the majority of the women were between 31 and 40 years (55%).
- **Family situation (n=221):** The great majority of drivers reported they lived as couple (91%), with one child (43%). Consequently the average number of children per family in the sample is 1.40, which is not representative of the three countries where the survey was given.
- **Educational level (n=175):** The majority of the driver sample had a high level of education (95%). This is comprehensive of high school (47%) graduate 1%, university 47%.
- **Driving experience (n=240):** 90% of the sample had a considerable amount of experience on the road. They had been driving for more than 10 years, and the 49% of them had been involved in a road accident as driver.
- **Location of residence (n=230):** 50% of the drivers reported that they lived in a large town, about one third of participant reported that they lived in a small town (34%), 16% of participants reported that they lived in the countryside.
- **Age of the car (n=289):** 27% of drivers had a car of the last two years (2010-2009), 55% had a car between 3 and 10 years old, 18% of the participants had a car older than 10 years.
- **CRS purchasing (n=162):** 82% of the driver bought the CRS in a specialist shop (nursery shop) or in a supermarket and they did not ask for advices at selling point (56%).

As explained at the beginning of this paper, the misuse survey is composed by of 316 cases and misuses were detected in 59% of the cases: misuse of CRS installation (17%) and misuse of fixing the child in the child restraint system (39%). Considering the whole survey (n= 317 observations), misuses were detected in 53% of the cases (n=167 observations), even if in 32 observations both kind of misuses (CRS installation and securing child in CRS) were detected at the same time. For this reason, considering the possibility to have the same observation with one or two misuses, the misuse sample was composed by 199 cases 61 misuses of CRS installation (31%) and 138 misuses of securing the child in CRS (69%).

When a misuse was detected, the main responsible for the misuse was the driver (Figure 2-15 and Figure 2-16). In details:

- Considering only the misuses in CRS installation (61 cases), the driver was mainly responsible for 66% of the cases (Figure 2-15);
- Considering only the misuse in securing child in CRS (138 cases) the driver was responsible for 57% of the cases (Figure 2-16). For this kind of misuse the percentage of children that secure themselves (25%) was relevant and 78% of the driver thought that the child protection was alright.

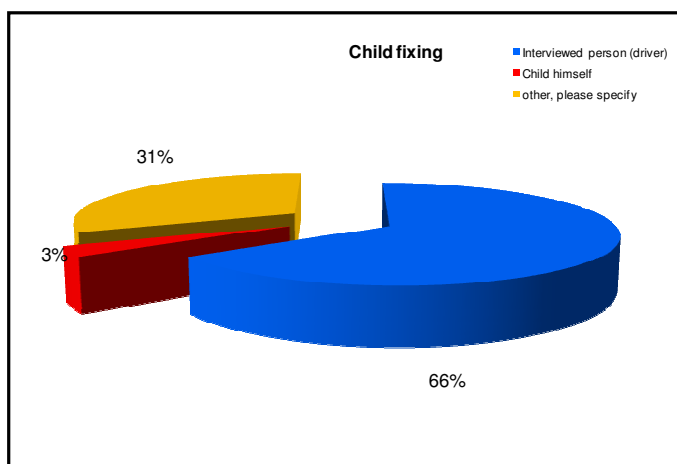


**Figure 2-15: Misuse and CRS installation (n=61)**

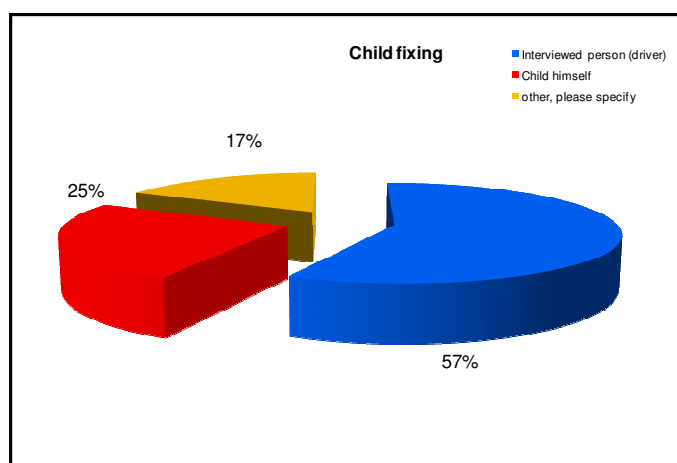


**Figure 2-16: Misuse and child securing (n=138)**

With reference to the gender of driver and to the kind of misuse, as shown in Figure 2-17 below, a misuse was caused more often by driver males (54%) than by driver females (46%). The misuse gender distribution is quite similar to whole sample, but analysing the misuse types it is very interesting to point out that:

- Driver males generally made misuse when securing the child in the CRS (64%, vs. 36% for females);
- Instead, the driver females made misuse when fixing CRS to the car (53%, vs. 47% of the males).

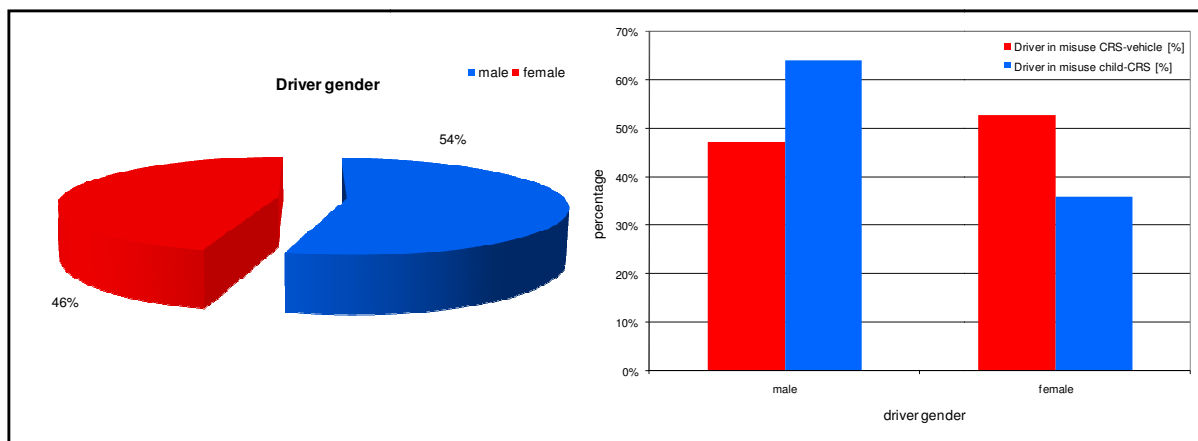


**Figure 2-17: Driver’s gender and misuse type (n=199)**

Another interesting analysis is related to the relationship between the driver’s age and the misuse status (Figure 2-18):

- Younger drivers (until 35 years) were most likely to make a misuse (45%, against the 29% of no misuse cases). The younger drivers’ misuses are mainly related to fixing the CRS to the car (57%).
- The distribution between misuse cases and no misuse cases was similar in the age group 36-40. For this age group, when a misuse was detected, it was mainly linked to securing the child into the CRS (36%).
- “No misuses” were more relevant in the age group over 40 years old (40% of correct use against 27% of misuse cases). For this group when a misuse was detected, it was mainly related to securing the child into the CRS (37%). The older parents (over 40 years), had mainly 1 child (76%), with an average age of 6 years. When a misuse was detected it was mainly related to securing the child into the CRS (37%); they didn’t have difficulty in CRS installation because they used mainly seat belt (41%), or booster (with backrest and only cushion – 27%).

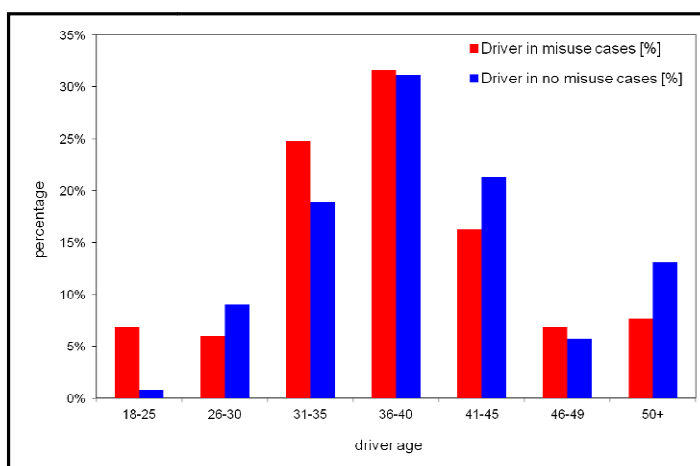


**Figure 2-18: Driver’s age and misuse (n=349)**

Finally when a misuse is detected, as shown in Figure 2-19 below, the main responsible person for the misuse is the driver. He is responsible of 72% of misuse in CRS installation and of 60% in fixing the child in the CRS.

About misuse in fixing the child in CRS, 29% of children fix themselves, and generally the driver does not check the correct use of the restraint by the child before the trip.

This percentage goes up until 37% if the analysis is linked only to misuse in fixing the child into the CRS.

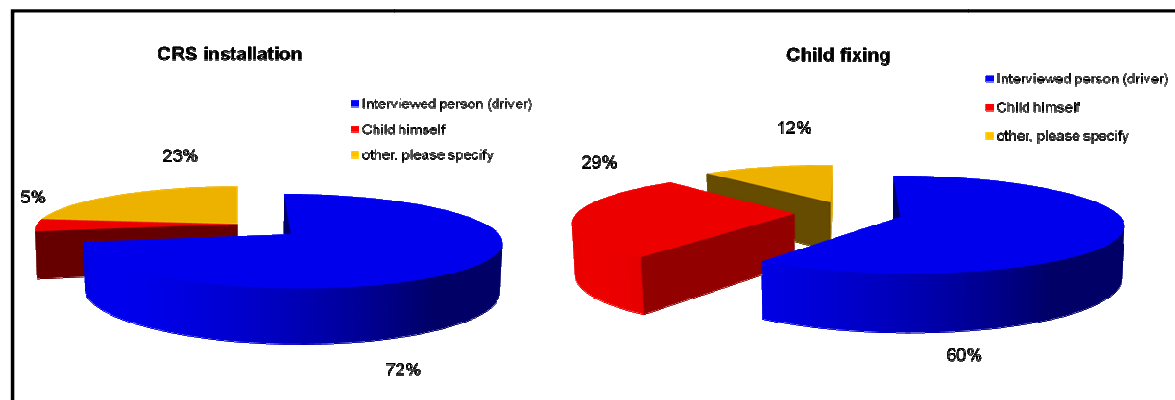


Figure 2-19: Misuse, CRS installation and child fixing

## 2.7 Consequences resulting from misuse based on accident reconstruction / misuse tests

During the EC CHILD project, field studies on the situation of use and misuse of CRS were conducted and considering that this point was a major issue in the child safety area, the decision to create an ad-hoc group on the item of misuse was taken. The aim was to increase the partnership already existing in the CHILD consortium to other participants such as CRS and car safety devices manufacturers. This group based on the exchange of voluntary work, has been looking at available field data, through their own way of collection but also to the material available in the accident in-depth investigation cases of the CHILD project. After this, a dynamic testing program has been set up to define the effect of misuse on the protection of children. Results were reported in a document made publicly available at the end of the project [6]. This public report is regularly updated and can be found on the CASPER website. Results have also been published at the end of the CHILD project [7].

The test set up is depending on the possibilities of the test facilities but with a common methodology: misuse tests are compared with a reference test performed according to UN Regulation 44, so the test severity cannot be considered as the cause of any failure. In the end, 77 tests in bodies in white tests and 16 regulation bench tests were conducted in the first period leading to the study of the situation of 160 child dummies. In addition to this previous works, more than 60 configurations have been tested in the frame of the CASPER project, with the performance of 25 tests in car environment and 13 on regulation bench.

Of course all misuses do not represent the same danger in terms of protection decrease. The evaluation of this point is somewhere delicate and subject to interpretation of the evaluator. Recently some works have been conducted on this point that confirms this statement [8]. In the following paragraph, the evaluation is done for frontal impact (the most frequent configuration) and it is based on two main parameters: the dummy readings, and the visual observation of the dummy kinematics on the high speed videos. It seems that both are necessary because in case of reproduction of an event (e.g. head impact), child dummies are often the best tool to use (indications on duration of event, level of severity), but they are not sufficient indicators in case of “non-event”, which does not correspond necessarily to the absence of injury risk. For example, if there is an excessive dummy head excursion during a test but that no impact occurs, the risk of head injury by impact on a rigid vehicle component is higher in that case than in the reference test, even if

measurements from the child dummy show similar results. In configurations with non-event, videos are then, the most appropriate tool to be used to compare differences between the reference tests and misuse configurations.

It is important to note that one of the limits of the analysis is the fact that results are only valid for the tested CRS in the environment of the test. For example, a misuse reproduced on a high quality CRS could lead to no evidence of decrease of protection, but the same misuse occurring on a lower quality system could lead to a total breakage of the system. Knowing this and taking into account the fact that tests were mostly performed with CRS that could be ranged from “reasonably good performance” to “excellent ones”, the first global statement is still that in none of the misuse situations show better protection than the reference tests. For nearly all types of CRS, the head is more at risk in case of misuse because of the larger displacement of the head (risk of head impact). CRS for which the seatbelt is used to restrain children show a higher risk of injuries in the abdominal area.

For further analysis, it is necessary to put the different misuses reproduced into categories (illustrated on Figure 2-20). The first one is the wrong fixation of the CRS to the car using the seatbelt or ISOFIX connectors (e.g. wrong seatbelt route, only one ISOFIX connector engaged, wrong support leg adjustment, etc. ...). In some cases, the integrity of the CRS is not ensured anymore and base and shell are separated. This leads to a high risk of ejection of the children, or at least to a severe impact with the car interior. The risk is similar if the CRS integrity is kept but that the CRS is not restrained anymore. Most of the other situations are giving more liberty of freedom to the CRS which correspond to a higher risk of sustaining an impact with the vehicle interior or that could lead to a structural rupture in case of more severe event.



**Figure 2-20: Misuse of CRS fixation (left), misuse of restraining child in CRS (centre), misuse of seatbelt restraining the child (right)**

The second category of misuse is the wrong adjustment of the parts restraining the child in its CRS. This kind of misuse is often observed in field studies and different configurations have been tested. The first strong result is that for an important part of misuses of this category, the dummies do not respond in the expected way. Effectively, through the in-depth accident studies of frontal impacts, it is assumed that in case of excessive slack in a harness, the child is moving forward, the shoulders slip-off from the harness and the upper part of the torso being not restrained anymore, the child's head is continuing its movement forward with a high risk of impacting the front seatback in front of the child or the B pillar of the vehicle.

Tests performed in this program and accident reconstructions have shown that independently of the amount of slack introduced into the harness, the child dummy had a too rigid torso and shoulders that make it stay restrained by the harness. It has then been difficult to give a more scientific point of view than the one of the experts in accidentology in these configurations. When the harness is located under the arms or when it has been transformed into a three point (in a wrong re-assembling process

after washing the cover for example) the buckle of the harness tends to penetrate the abdominal area, and becomes a source of injuries. This can sometimes be combined with the penetration of the lower straps of the harness in the abdomen of the dummy. Of course in case of excessive slack in one of the adjustable part of the CRS, the risk of ejection from the restraint system is high and would lead to no protection at all.

The third category is the wrong route of the seatbelt to restraint the child which leads to very impressive kinematics in a lot of cases. Most of the time, the abdominal area is overloaded by the pelvic or thoracic parts of the seatbelt, and sometime by both of them. In case of restraint applied only to the lower part of the trunk, the risk of hard impact of the head against a rigid part of the car is very high. Some seatbelt routes observed in field studies with children on boosters nearly lead into the ejection of the child from the body in white.

Inappropriate use (Figure 2-21) and postural tests performed were not necessarily considered as misuse situations but leads to similar results: children with a too small stature are at risk considering ejection (but still difficult to show with a dummy), CRS in which children heavier than the range for which it is approved can sustained structural damages as the loadings will be higher than the ones it is approved for. Risk of projection becomes then high.



**Figure 2-21: Inappropriate use Q0 (left) and Q6 (right) in a G1 harness CRS**

Tests with dummies using the seatbelt of the vehicle (with or without booster systems) positioned in postures close to the one observable in the real life were conducted and compared to results of test in standard positions. It was difficult to discriminate wrong postures tests from the ones of the regulation tests using only the standard dummy readings except in case of head impact. The abdominal pressure sensor developed in the CHILD and CASPER projects and that is used in the Q dummies was the only predictive indicator of a major injury risk. Videos were also helpful to check the most appropriate dummy kinematics. It is important also to note that the posture used by children often lead to misuse of the seatbelt because of comfort issue (seatbelt under the arm, additional excessive slack, etc.).

## **2.8 Analysis of possibilities to reduce the misuse risk or to reduce the severity of consequences resulting from misuse**

Before going into a detailed analysis of technical solution, it is important to notice that some CRS products on the market are proposing isolated solutions, such as visual and/or audio indicators of correct adjustments of the different parts of the CRS. These types of solutions are helpful for parents that have little knowledge in the safety area and that are in need for help [9]. Their generalisation could lead to a global reduction of

the misuse situation of CRS on the roads. But as most of these indicators are not mandatory, it is up to each CRS manufacturers to equip their systems with such solutions to make them easier to use. The CASPER project has been reviewing some existing solutions and concludes that it was difficult to find solutions that were acceptable for all parts involved in the „child safety chain“, from the engineering and commercial services of the CRS manufacturer to the children and parents including legislators and scientific researchers in child safety. Nevertheless, these relatively simple indicators of correct use were often considered as a good balance for all parts and have been rated for most of them with positive score. Most of the proposed solutions by CRS manufacturers have been presented in the International Conference “Protection of Children in Cars” that is one of the most important yearly conferences on the field of child safety in vehicles. The following section is based on the review of the proceedings from this conference. Possible technical solutions for different CRS and misuse types were presented from 2003 to 2010 and were analysed with regard to technical solutions for misuse.

In a first step the solutions can be separated between solutions for CRS with integral harness and solutions for boosters.

### **2.8.1 Solutions of CRS with integral harness**

For harness systems, the most important or most frequently seen misuse types are “incorrect seatbelt route” and “harness not sufficiently tightened”. In addition rearward facing CRS are found installed forward facing. Group 1 CRS are often used too early (for children from 6 month) and left also too early for the use of booster seats.

The discussed solutions are partly already available on the market, regulatory solutions in different countries or concept studies.

To address the problem of the not sufficiently tightened harness, two concepts were shown in [10 - 12]. The first system gives a visual indication of the harness tension. A mechanical working flap is attached to the harness strap, implemented in the shoulder padding. As long as the harness is not properly tensioned, the flap is in a raised position. In this position a corresponding negative pictogram is visible. When the harness tension is adjusted properly, the flap comes down flat to the shoulder padding and a positive pictogram is visible. The second described solution is an audible indicator. When the correct harness tension is reached during the tensioning procedure, this is indicated by audible clicks.

The revised Australian and New Zealand CRS standard includes a seating height related marking [13]. Stickers on the CRS indicate the height of the shoulders of a child that fits in the restraint. The markings show the lowest shoulder height, below which the CRS should not be used and the highest shoulder height, above which the CRS has to be changed. In parallel, dimension controls have been included in the Australian and New Zealand standard to ensure that the categories of CRS are linked to each other (maximum size of one CRS fits to the minimum size of the next CRS).

A concept Group I CRS addressing numerous misuse cases by technical solutions was presented in [14] (Figure 2-22). To control the seat belt route and the tension, the vehicle belt has to be routed using one of the upper belt guide clamps. Spring-load levers with an integrated push button on both sides of the guide allow detecting the correct belt tension and belt path. The installation direction (forward/ rearward) as well as the upright position of the CRS is controlled by push buttons on the back of the CRS. This ensures the fitment to the backrest of the vehicle seat.



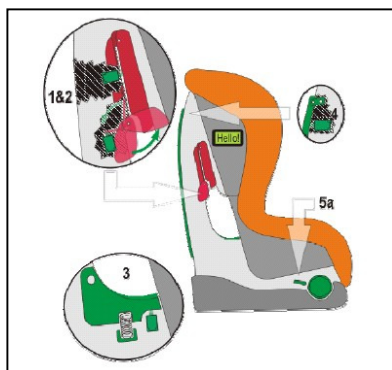


**Figure 2-22: Concept Group I CRS [14]**

The incorrect harness tightening is addressed by a new harness tensioning device. The integrated harness is tensioned by large turning handles on both sides of the CRS. For the consumer the tensioning is easier due to the reduction of the needed force and the better positioning. The correct harness tension will be indicated by a haptic feedback, as soon as an integrated slipping clutch detects sufficient belt force (Figure 2-23).

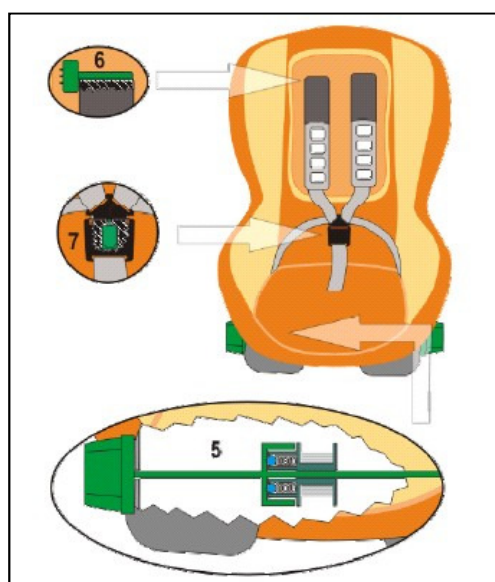


**Figure 2-23: Harness tensioning and buckle control [14]**

Two accelerometers, on the backrest of the CRS and on the upper part of the shoulder harness, analyse the angle between the shoulder harness and the CRS seat back. Here the correct position of the shoulder harness is controlled (Figure 2-24). A miniature switch inside the buckle of the integrated harness connected to a sound interface gives a warning, if the child unbuckles during a trip. To make it possible for consumers to check whether a CRS was exposed to an accident, a very thin conductor with a small weight was attached to the back of the CRS. The conductor will break after a certain level of acceleration is reached and give a visible indication on the possible exposure to an accident. Information on mistakes during the installation process is given to the user via a LC-display. An interface like this display can give a direct feedback to the consumer about a misuse and can offer information on the solution.

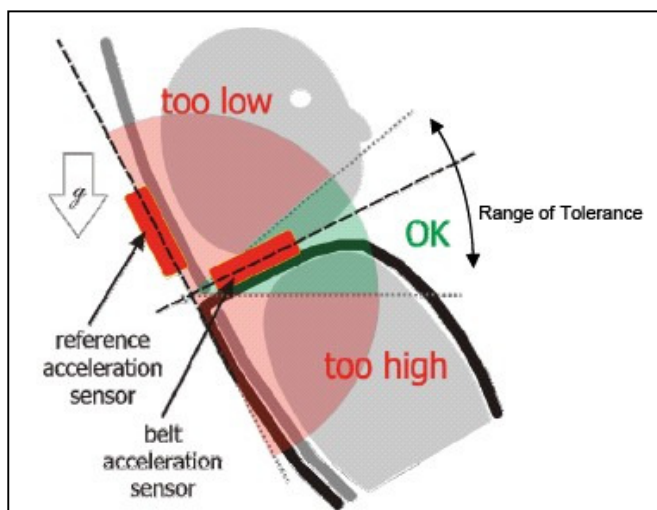


**Figure 2-24: Harness position control [14]**

Specific to ISOFIX child restraint systems, [15] describes the design of a global indicator for ISOFIX and Top Tether fixation. The Top Tether includes an elastic indicator adjusted to the correct tension of the tether. The elastic indicator is connected to the central positioner of both ISOFIX connectors of the CRS. All three anchorages, both ISOFIX connectors and the Top Tether have to be correctly attached to the vehicle to receive a positive visual indication of correct installation (Figure 2-25).

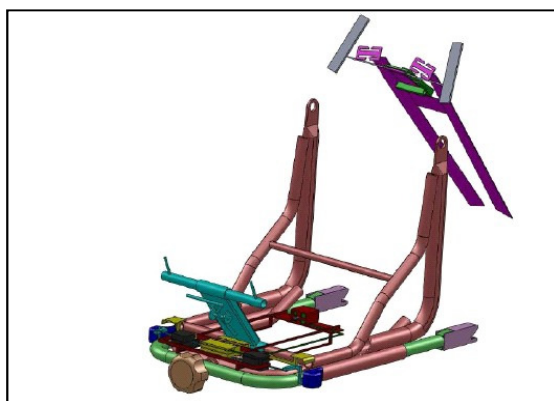


**Figure 2-25: Global indicator for ISOFIX and top tether control [15]**

### 2.8.2 Solutions for boosters

For booster with and without backrest, the most common misuse cases are the seat belt under the arm during the driving phase, incorrect seatbelt routing, and misuse based on geometrical incompatibility between the booster and the vehicle. The non-use of CRS increases especially for older children.

One solution described in [16 - 19] are integrated CRS. In [16, 19] it is seen, that booster seats integrated in the vehicle are more accepted by the children (less childish). This could increase the use of boosters for older children from an age of 8 years on. Additionally the handling of integrated boosters was seen easy and fast. So the correct usage of the booster could be increased. [18] shows the possibility of 2-stage booster cushions with a high position for smaller children up to a height of 1.20 m and a lower position for the taller children. The 2-stages approach allows a better thigh support for a more upright seating position. The increased height and the booster being designed together with the vehicle allow the children to participate in the safety benefits of the car related safety systems.

In [17] the concept of a self-adjusting integrated child restraint system is demonstrated. The child (or adult) is detected by a webcam. After several image processing steps, the actual height of the occupant is distinguished. A motor driven mechanical system modifies the seating height to a correct position according to the height measurement. Based on an anthropometric database the seat is adjusted to the best position for the use of the 3-point belt system for this occupant. The system adjusts the height and the side protection (Figure 2-26).

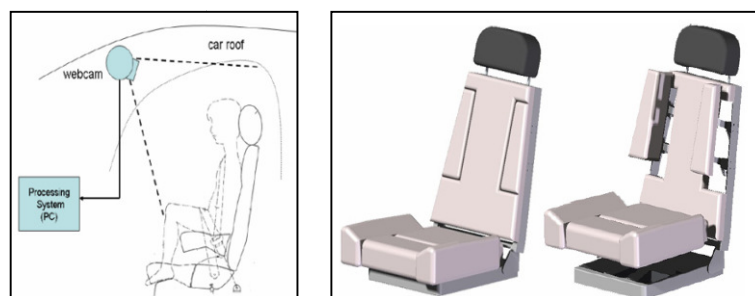


**Figure 2-26: Self-adjusting integrated child restraint system [17]**

Harness systems and lap belt positioning devices in addition to the booster seat can be used on the Australian market. [20] shows different possibilities according to the Australian/ New Zealand Standard 1754:2004. The harness system restrains the upper part of the body and stays in position even if the child moves during the travel. An additional lab belt positioning device, attached to the booster shall keep the lap belt of the vehicle and also a harness system correctly positioned.

[21] analysed the vehicle rear seats to get an impression whether it could be possible to modify this seat in a way, that could allow children (aged 6 years and above) to use the 3-point seatbelt only. The use of pre-tensioner and seat ramps and the modification of the belt anchorage points could lead to rear seat that could be used by taller children without CRS. A problem that was not addressed was the incompatibility between the thigh length of children and the length of the seat cushion. The cushion was too long for the children's legs.

The CRS presence and orientation detection was demonstrated by [22]. Presence and orientation of a CRS equipped with resonators can be detected on a vehicle seat with adequate sensors. The gathered information can be used for the passenger airbag deactivation for rearward facing CRS on the passenger seat. Additionally the information can be used to address individualized strategies for safety systems for different CRS types.

## 2.9 Summary and conclusion

Recent field studies that were conducted in Berlin, Lyon and Naples showed that approximately two thirds of the children travelling in cars are not correctly restrained. However, important regional differences exist. Slack in the harness, slack in the car's belt and wrong belt path were reported most often. Most of the interviewed parents believe that they do restrain their children correctly so it is concluded that misuse is mainly a result of lack of knowledge.

Within the analysed sample males and young drivers are overrepresented to install CRS incorrectly. Sled tests show higher risks for the head in misuse conditions mainly caused by larger head displacement. In cases with booster seats abdominal loading normally increases in misuse conditions. One problem that was observed in accident studies was impossible to be reproduced in dummy tests. While in a number of

accident it was concluded that the harness slipped off the shoulders during the accident it remained under all possible circumstances (slack in harness, harness position far outside but on the shoulders) at the dummy shoulders. Different dummy postures were only possible to be “detected” by the abdominal loading. Other parameters did not correlate with the subjective rating of the respective situation.

Several solutions for avoiding misuse situations are proposed or on the market already, e.g., audible, visible or tactile information regarding the correct harness tension. These systems were not yet seen in the misuse field observation therefore it is hardly possible to judge their effectiveness in real-world live conditions. The same is true for ISOFIX CRS, which were observed in less than 5% of the cases.

## 2.10 References

- [1] Siegner, W.: “Sicherung durch Gurte, Helme und andere Schutzsysteme 2009”; Kontinuierliche Erhebungen zum Schutzverhalten von Verkehrsteilnehmern 2009 Bericht zu Forschungsprojekt 82.354/2008, Bundesanstalt für Straßenwesen.
- [2] Langwieder, K.; Stadler, P.; Hummel, Th.; Fastenmeier, W.; Finkbeiner, F.: „Verbesserung des Schutzes von Kindern in Pkw“, Bericht der BAST, Heft M37, Bergisch Gladbach, 1997.
- [3] Langwieder, K.; Hummel, Th.; Finkbeiner, F.; Roselt, Th.: „Kinder im Auto“, Studie zur Verwendung von KSS und Verbesserungspotentiale durch ISOFIX, 0304, GDV Bericht, 2003.
- [4] Fastenmeier, W.; Lehnig, U.: „Fehlerhafte Nutzung von Kinderschutzsystemen in Pkw“, Bericht der BAST, Heft M178, Bergisch Gladbach, 2006.
- [5] Hummel, Th.; Finkbeiner F.; Kühn, M.: “Misuse of Child Restraint Systems – A 2008 Observation Study in Germany”, 6th International Conference Protection of Children in Cars, 4-5 December 2008, München, Germany.
- [6] CHILD Deliverable 1.2.2 for the EU Project “CHILD”, <http://www.casper-project.eu/previous-studies/child/>
- [7] Lesire, P.; Cuny, S.; Alonzo, F.; Cataldi, M.: “Misuse of Child Restraint Systems in Crash Situations - Danger and Possible Consequences” Annual Proceedings of the Association for the Advancement of Automotive Medicine, 2007.
- [8] Misuse severity assessment – Mueller & al. - March 2012; final workshop for EU Project “CASPER”, <http://www.casper-project.eu/news/workshop-march-13-15-2012/>
- [9] Deliverable D3.1.1. for the EU Project “CASPER”, <http://www.casper-project.eu/>
- [10] F. Bendjellal, M. Bennett, S. Carine: “Reducing Misuse of Child Restraint Systems – An Attempt to Treat Loose Harness Problem”; Protection of Children in Cars, 4th International Conference; Munich 2006.
- [11] F. Bendjellal, S. Carine, E. Böhringer: “Child Restraint Systems: History, Present and Future Safety Challenges”; Protection of Children in Cars, 5th International Conference; Munich 2007.

- 
- [12] F. Bendjellal: “Misuse: Recent Evaluations in Ireland and France – The need for a continuous and consistent parents’ education and development of technical solutions”; Protection of Children in Cars, 6th International Conference; Munich 2008.
- [13] M. Lumley: “Revised Australian and New Zealand CRS Standard”; Protection of Children in Cars, 7th International Conference; Munich 2009.
- [14] G. Müller, J.-P. Borgmann, H. Johannsen: “Technical options for reduction of misuse group 1 CRS”; Protection of Children in Cars, 7th International Conference; Munich 2009.
- [15] D. Gallegos, F. Liesa, A. Longton, G. Tejera: “Analysing Misuse Trends in Child Restraint Systems. The Idea of Including a Global Indicator for ISOFIX and Toptether Correct Fixation.”; Protection of Children in Cars, 8th International Conference, Munich 2010.
- [16] K. Bohman, O. Boström, M. Eriksson, A.-L. Osvalder: “Frontal Impact Protection of Children on Booster Cushions – an Attitude, Handling and Safety Approach”; Protection of Children in Cars, 4th International Conference, Munich 2006
- [17] P. Boyraz, M. Acar, J. Bennett: “Self- adjusting, Integrated Child Restraint System”; Protection of Children in Cars, 5th International Conference; Munich 2007.
- [18] L. Jakobsson, H. Wiberg, I. Isaksson-Hellman, J. Gustafsson: “Rear Seat Safety for Children Aged 4 and Above – a New Integrated 2-stage Booster Cushion”; Protection of Children in Cars, 5th International Conference; Munich 2007.
- [19] L. Jakobsson, I. Isaksson-Hellman, M. Lindman: “Positive trend of proper restraint usage – injury reduction for children aged 4-12”; Protection of Children in Cars, 7th International Conference; Munich, 2009.
- [20] M. Lumley: “Improving Occupant Safety of Booster Seats”; Protection of Children in Cars, 7th International Conference; Munich 2009.
- [21] H. Johannsen, M. Schipper, V. Schindler: “Is it possible to optimise the rear seat for children (6 YO and above) and adults?”; Protection of Children in Cars, 8th International Conference; Munich 2010.
- [22] F.-H. Brämig:” Child Seat Presence and Orientation Detection CPOD (ISOcare)”; Protection of Children in Cars, 6th International Conference; Munich 2006

### 3 Injuries to children in road traffic collisions

The number of children killed or seriously injured in road traffic collisions has fallen steadily in Europe over the last 10 years. UN Regulation 44 has made a significant contribution by ensuring that child restraints meet minimum standards of performance in front impact collisions. Nevertheless, continuing to monitor the performance of child restraints in real collisions is essential if this progress is to be maintained. Such analyses typically reveal the body regions that are injured in children, the types of injuries they receive and their mechanisms (along with details about the circumstances of the collisions). This information can be used to target improvements in child restraint performance; for example, by updating regulatory and consumer test procedures, including child dummies and their injury criteria, to ensure they reflect injuries that are observed in the field.

Representative databases such as the German In-Depth Accident Study (GIDAS) and the United Kingdom Cooperative Crash Injury Study (UK CCIS), for example, are often used for collision analysis studies; however, they typically feature relatively few cases of serious injury to children due, in part, to the sampling strategies that are used. CASPER has compiled a database, which includes cases from previous European Commission Framework Projects; CREST and CHILD. The database provides a valuable resource for child safety researchers who wish to undertake detailed analyses, although the findings cannot be applied when weighing the costs and benefits of a safety intervention and cannot be used to draw comparisons across different types of child restraints.

This chapter comprises a comprehensive analysis of the CASPER database, performed by the project partners, along with an analysis of injuries to older children undertaken within the EPOCh project. It features a published deliverable from each project, reproduced here in their entirety. The full references for each deliverable are:

Kirk, A. and Lesire, P. (2012). *Report on accident analysis – Deliverable 3.2.3 of the EC FP7 project CASPER.*

Visvikis, C., Pitcher, M., Girard, B., Longton, A. and Hynd, M. (2010). *Task Number 1-1 - Literature review, accident analysis and injury mechanisms.* Retrieved March 23, 2013, from: <http://www.epochfp7.org/Publications.aspx>

#### 3.1 Report on accident analysis – Deliverable 3.2.3 of the EC FP7 project CASPER

##### 3.1.1 Introduction

###### Overall background – WP3 and Task 3.2

It is important that the work of the CASPER project is both set in the context of the real world and is scientifically driven by real world data. This is generally the purpose of Work Package 3, but more specifically Task 3.2 concentrates on children in road accidents.

Task 3.2 makes studies at different levels for the protection of children transported in cars:

- The size of the issue,
- Determining the main injury and fatality reasons,
- The restraint conditions, and
- Crash configurations.

Injury mechanisms for restrained children are studied and reported.

### **Objectives of Sub tasks 3.2.2 and 3.2.4 - Road accident data collection and analysis**

The primary **objective of subtask 3.2.2** is to collect road accident cases involving restrained child car occupants, with a good detailed understanding of crash severity and configuration and quality of restraint use. These cases are selected in order to provide real-world data that are essential to improve or to develop crash test dummies and models and to obtain injury criteria (WP1 and WP2). Accident data are used to validate injury mechanisms (physical and numerical).

The review of car accident investigations leads to proposed test procedures that are closer to the real travelling conditions of children than the test conditions currently used for the approval of CRS (integrated in the WP4 solutions). Also misuse situations observed in the road accident cases further the understanding of the effect of misuse on injury outcome and provide real world situations to feed into the misuse testing activities of CASPER. This data are integrated by WP4 in the proposed solutions.

The primary **objectives of subtask 3.2.4** are to analyse and to report main results by crash configuration and restraint type for restrained in the accident database.

### **3.1.2 Methodology**

#### **Process**

##### **Review**

Rather than cases just being added to the database, CASPER has a process of review to ensure that cases are suitable to the scientific aims of the project and of sufficient quality. Importantly the combined experience of the group during case review adds to the quality of each case. Comments are made and discussions held regarding injury mechanisms, child restraint type, misuse situations and crash severity. If required, additional information has to be provided before deciding to include an accident in the database or to reject it.

##### **Crash conditions / severity**

In particular, during case review, consideration is made of vehicle structure engagement and involvement to understand the effect that crash circumstance (direction, intrusion, impact area) and severity has had on the injury outcome of the occupants. This is considered in parallel with occupant age, restraint conditions and restraint quality.

In particular the following are considered:

- Engagement of the crash energy management structures (frontal and side) and stiff structure involvement;
- Comparison of injuries across occupants of vehicle;
- EES and Delta V.

##### **Consideration of misuse - identification during investigation**

Misuse (use of CRS not according to user manual instructions) can be difficult to find in investigations – the priority is to remove the child from the vehicle for medical treatment as soon as possible. Certainly low severity misuse (for example, small level of seat belt or harness slack) is more difficult to assess after an accident than severe misuse as the evidence is less likely to present itself in terms of injury or physical damage to the CRS or vehicle. As CASPER is the third project to utilise a review process as

described above a good level of experience has been established in the group in identifying severe misuse injury patterns and real world circumstances that can lead to misuse.

Examination of the CRS or evidence from photographs can indicate many misuse situations including; belt routing is incorrect, CRS is incorrectly in a position with a frontal airbag, harness strap height is incorrect, slack is present (both CRS to car and belts restrained children) and unexpected belt routing marks (if CRS is not still attached in the car) or for booster systems that are not necessarily directly fixed to the car.

Projection and excursion that is not in keeping with crash conditions can indicate poor restraint of either the CRS or the child. If the child restraint is reported as being ejected or found loose in the vehicle (by those immediately at the scene) it could be possible that belt routing for the CRS attachment to the vehicle is incorrect. Marks or damage to the door could indicate only attachment on one side. Extreme projection of the head (for example reaching the B pillar) with low or moderate crash severity can show problems with CRS or child restraint.

Unusual injury patterns that do not relate to expected restraint routing can show problems. For example, if detailed injury records mention thoracic bruising under the arm but nothing to the shoulder it could be possible that the seat belt is under the arm rather than over the shoulder.

Information from parents/carers (when appropriate and possible) regarding common travelling conditions can provide insight into misuse situations. For example, some parents will admit that the child typically repositions the seat belt away from the neck by putting it under the arm. Also background into the overall family situation can be informative. For example, an older sibling may have recently moved up from a group 1 harness seat to a booster seat, making the group 1 seat available to a younger sibling. This can be a reason for the harness straps being too high for the younger sibling, if the parents have forgotten to make the adjustment for the younger, smaller, child.

Even so the levels of misuse that are recorded in the database are lower than the actual levels (found during misuse field surveys) and it likely that at best the database is considering severe misuse, rather than being able to highlight slight misuse.

CHILD & CASPER children: 14% misuse positively identified  
CASPER children: 20% misuse positively identified

### Consideration of Inappropriate use

Inappropriate use is considered to occur when the restraint system used by the child is not approved for their weight / height (or age if height and weight are unknown).

The CRS type being used or just the use of the adult seat belt can clearly be identified as being appropriate, or not, if data is available regarding weight, height and age. Appropriate use can be more difficult to record if only age is available. In particular, whether it is appropriate for a 3 year old to be in a booster seat, as some children would not yet be 15 kg at that age whilst others would be exceeding 18 kg. Likewise, for older children, for example of 10 years old, it is not possible to be sure if the child exceeds 36 kg or is above the height criteria for an adult seat belt only to be appropriate. Further information on how inappropriate use is considered is given in the table given in Definitions and procedure, below.



### Sampling criteria

The cases found in the CASPER dataset are not proportionally representative of the accident situation across Europe, or in individual countries.

The real world accident cases are collected to ensure that information on child kinematics, injury causation, injury criteria and CRS performance (including misuse where understood) is available to the project in order to further activities in injury criteria, dummy/model development and the understanding of misuse. To achieve this case selection, criteria are used that generally favour more severe cases, in terms of both injury severity and impact severity. To also provide a full range of data for injury criteria and an understanding across the injury severity spectrum, cases of high crash severity but low injury severity are also included.

- At least one child up to and including the age of 13 years old in a passenger car designed for up to 9 occupants (case vehicle). Car-to-vehicle or car-to-fixed-obstacle accidents are considered.
- The child should be correctly restrained in a child restraint system (CRS) or adult seat belt. Cases with misuse can be included if the conditions of the misuse are well defined and possible to reproduce in a sled test or reconstruction.
- Frontal, lateral or rear impact (not just rollover)
- Rollover only crashes not considered. If rollover has occurred in combination with a frontal, lateral or rear impact, then the injuries must be clearly attributed to the frontal, lateral or rear impact.
- The child or another restrained occupant in the case car has at least an AIS 2 injury (AIS 2 concussion not included). If not:
  - A frontal impact must have a Delta V of at least 40 km/h;
  - A lateral impact must have at least 200mm of intrusion with the child on the struck side;
  - Rear impacts reviewed on a case by case basis.

Other than the inclusion of 12 and 13 year olds and rear impacts, the same set of criteria was used in the previous EC projects (CREST and CHILD).

Due to this selection process, the cases are generally more severe in terms of both injury and crash severity than would be seen in the overall child car passenger crash population. As an example of crash severity, 82% of restrained children in frontal impacts are in an impact with an Energy Equivalent Speed (EES – see Definitions and procedure) over 40 km/h. For the overall child car passenger crash population in frontal crashes the crash severity would be lower. Similarly, in the general child crash population involved in lateral impact crashes, average passenger compartment intrusion would be much lower than the cases selected for the database.

The database does give an indication of which body regions are being injured in different CRS types or for different ages of children and gives insights into restraint conditions that lead to injury. It is important that any analysis carried out is set in the context of the selection criteria presented above.

### Limitations of the data

Although all teams follow up cases as thoroughly as possible it is not always possible to gather as much data as would be preferable. For example, for the restrained children with known injury severity the following is recorded:

Type of restraint:	99%
Age:	100%

Height or weight of child: 43% of cases

Without contact with the parents, or if in a fatality this information is not recorded in the medical notes, it can be difficult to get height and weight of children and therefore there is a reliance on age in many cases for selecting testing dummies for further CASPER activities and suggesting if CRS use is appropriate.

#### Definitions and procedure

**Adult seat belt:** When the restraint type is referred to as the adult seat belt the only restraint is the adult seat belt with no additional child restraint system

**CDC:** Collision Deformation Classification, an alphanumeric code to describe the nature and location of direct contact to a vehicle. Devised by SAE (Recommended Practice J224b).

**Child:** Occupant of car up to and including 13 years of age

**CRS:** Child restraint system (additional to the vehicle or integrated)

**Restrained:** Using a child restraint system or adult seat belt (includes inappropriate use or misuse)

**Appropriate use:** Restraint system used by child is approved for their weight / height (or age if height and weight are unknown). Table 3-1 gives the rules used to code children on the database as being appropriately or not appropriately restrained

**Table 3-1: Rules for the coding of appropriate use**

CRS type group	Approved weight (kg)	Height (cm)	Age (expert)
Rearward facing infant carrier group 0	<10	-	up to 12 m
Rearward facing infant carrier group 0+	<13	-	up to 18 m
Carrycot group 0	<10	-	up to 12 m
Forward facing group 1	9 to 18	-	from 9 m up to 47 m
Rearward facing group 1	9 to 18	-	from 9 m up to 47 m
Booster group 123	9 to 36	-	from 9 m up to 11 y
Booster group 23	15 to 36	<140 cm	from 3 y to 11 y
Booster group 3	22 to 36	<140 cm	from 5 y to 11 y
Group 2	15 to 25	<140 cm	from 3 y to 6 y
Adult seat belt	>36	>140 cm	from 12 y and more

**Misuse:** Use of CRS not according to user manual instructions

**Shell system:** CRS designed to be used with a harness or a shield to restrain its occupant, rearward facing or forward facing

**Struck side:** The side of the vehicle on which the main impact occurred during the crash

**Direct intrusion:** The occupant is in the area in which the car sustained deformations due to a contact with an external object/obstacle or another vehicle

**AIS:** All Injuries are coded according to the Abbreviated Injury Scale (AIS) (AAAM, 1998) and in CASPER are doubly coded to AIS 2005 (updated 2008)

**MAIS:** Maximum Abbreviated Injury Score, the highest injury score for the occupant to any body region. Can also be connected to a particular body region to give the highest injury score for that body region - for example, MAIS (thorax)

**EES:** Energy Equivalent Speed, the equivalent speed at which a particular vehicle would need to contact any fixed rigid object in order to dissipate the deformation energy corresponding to the observed residual crush. (ISO/DIS 12353-1:1996(E))

**Sample Size:** The sample sizes in the analyses presented may differ slightly from overview statistics. This is due to different filtering and different focuses in each

analysis. For instance, a case may be filtered out if a variable pertinent to that investigation is not available (e.g. side structure intrusion)

### 3.1.3 Overall overview of database

#### Introduction

The CASPER accident database includes cases from the previous EC child safety studies CREST and CHILD. The fundamental case selection criteria are the same for all three projects (see Section 0), the only changes for CASPER being the inclusion of 12 and 13 year olds and rear impacts (although the rear impact numbers are low).

Rather than an analysis of any particular area this chapter is a statement of the data that are available in the accident database regarding overall numbers, source of the data and overall injury levels. Further chapters will focus on frontal and lateral impacts.

#### Overall case and occupant numbers

Table 3-2 gives an overview of the case numbers and number of restrained child occupants from each project (children who are not restrained appear on the database when they are in the same vehicle as a child who does fit the sampling criteria but are not considered here). Restrained children are up to and including 13 years old.

**Table 3-2: Overall case numbers – All impacts**

EC Project	Cases	Vehicles	Overall Occupants	Restrained children	Vehicles with restrained children
CREST	405	746	1832	645	432
CHILD	264	465	1146	431	279
CASPER	137	251	611	225	152
<b>Total</b>	<b>806</b>	<b>1462</b>	<b>3589</b>	<b>1301</b>	<b>863</b>

Table 3-3 shows the number of restrained children distributed by impact type and the general restraint type used – child restraint system or adult seat belt only.

**Table 3-3: Restrained children by impact type, n=1301**

EC Project	All Impacts		Frontal		Lateral		Rear	
	Seatbelt only	CRS	Seatbelt only	CRS	Seatbelt only	CRS	Seatbelt only	CRS
CREST	220	425	165	306	55	119	0	0
CHILD	166	265	117	196	49	68	0	1
CASPER	74	151	61	109	10	40	3	2
<b>Total</b>	<b>460</b>	<b>841</b>	<b>343</b>	<b>611</b>	<b>114</b>	<b>227</b>	<b>3</b>	<b>3</b>

If the CHILD and CASPER cases are combined, 34% of the 656 restrained children in the resulting dataset are from cases collected in the CASPER project and 66% from the CHILD project.

Table 3-4 shows the same information but for restrained children where the MAIS is known to be 3 or above or injuries are fatal.

**Table 3-4: Restrained children by impact type – MAIS ≥ 3 or fatality, n=384**

EC Project	All Impacts		Frontal		Lateral		Rear	
	Seatbelt Only	CRS	Seatbelt Only	CRS	Seatbelt Only	CRS	Seatbelt Only	CRS
CREST	71	110	51	73	20	37	-	-
CHILD	34	78	16	51	18	26	0	1
CASPER	20	71	14	53	5	16	1	2
<b>Total</b>	<b>125</b>	<b>259</b>	<b>81</b>	<b>177</b>	<b>43</b>	<b>79</b>	<b>1</b>	<b>3</b>

If the CHILD and CASPER cases are combined, 45% of the 203 MAIS ≥ 3 or fatality injured restrained children in the resulting dataset are from cases collected in the CASPER project and 55% from the CHILD project.

**Type of impact (restrained children)**

Figure 3-1 gives an overview of the type of impact for the restrained children in each project. The impact used for analysis is the one that had the most influence on the injury outcome of the children in the vehicle. This is judged during case review of the accident, where the effect of multiple impacts or any rollover on injury outcome is also evaluated.

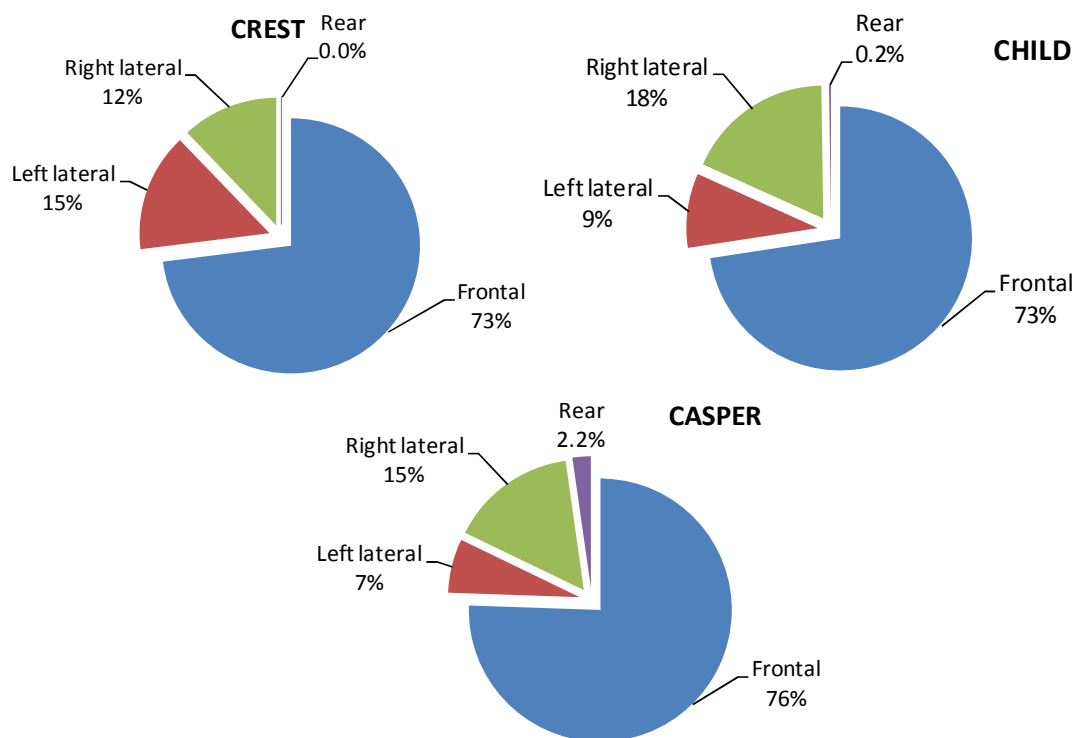


**Figure 3-1: Type of impact – CREST, CHILD and CASPER datasets**

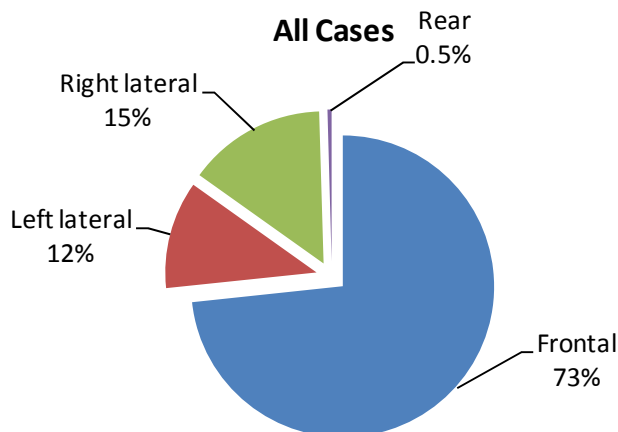


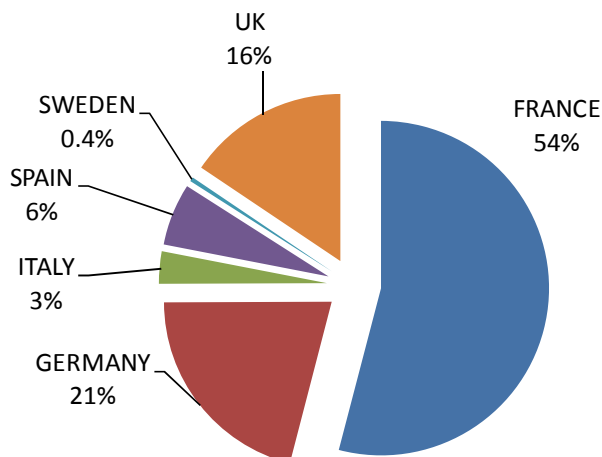
**Figure 3-2: Type of impact – All cases, n=1301 (restrained children)**

Overall, around one quarter of restrained children are in lateral impacts for each project dataset. In the CHILD and CASPER projects twice as many restrained children are in right side lateral impacts than left side lateral impacts.

### 3.1.4 Frontal impacts

#### Introduction

The accident database has available the cases of the combined CREST, CHILD and CASPER datasets to inform the development of injury criteria and the understanding of injury causation. Crashworthiness in frontal impacts has improved due to new testing programs. For the analysis of frontal impacts in this section the CHILD and CASPER data, which is more recent than CREST data, are utilised to investigate the most injured body regions. Whilst it is recognised that CHILD cases are not particularly recent – the project ran from 2002 to 2006, with cases that occurred before this being entered as well – it is considered by the authors that the majority of cars are of a ‘EuroNCAP’ generation with vehicle structures and core restraint systems that are recognisable in more modern cars. Likewise, the CRS designs in the CHILD dataset are generally of designs that are recognisable today. Although improvements have of course been made in CRS designs and materials there has not been a step change in design that makes the CRS present in the CHILD dataset look particularly out of date. Although it is recognised that individual products have of course introduced novel features. Of the combined CHILD and CASPER database, 483 restrained children are in frontal impacts, 73.6% of the total (656).



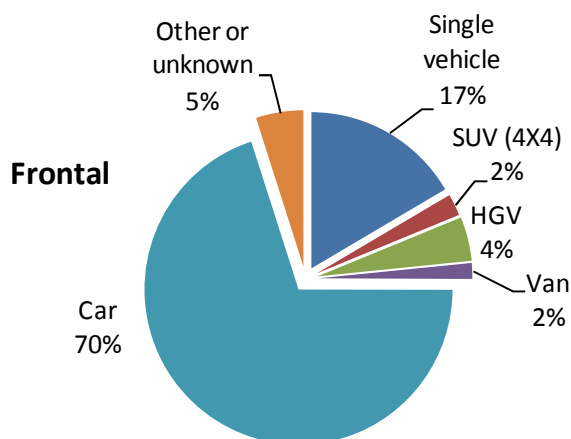
**Figure 3-3: Distribution of restrained children by country of origin – Frontal impacts, n=483**

Figure 3-3 shows the country of case origin for the 483 restrained children in frontal impacts.

### Crash and restraint parameters

#### Crash opponent

Figure 3-4 and Figure 3-5 show the distributions of crash opponent for restrained children in frontal impacts, the first for all restrained children and the second for MAIS ≥ 3 restrained children or those with fatal injuries, sometimes with injuries not known.



**Figure 3-4: Distribution of crash partner – Restrained children n=483**

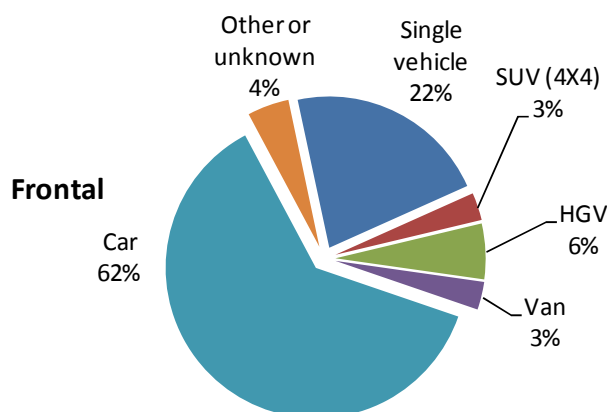


**Figure 3-5: Distribution of crash partner – Restrained children, MAIS ≥ 3 or fatality, n=134**

Whilst in both figures another car is the most often struck opponent when the sample is shifted to serious and fatal injury the proportion of cars reduces, with an increase in the second most frequent category of single vehicle impact (with obstacle). When the crash opponent is not another vehicle, 76% of the children are in a car that has an impact with a tree/pole (same for MAIS ≥ 3 or fatal).

The MAIS distributions for the main crash partner categories are given in Figure 3-6.

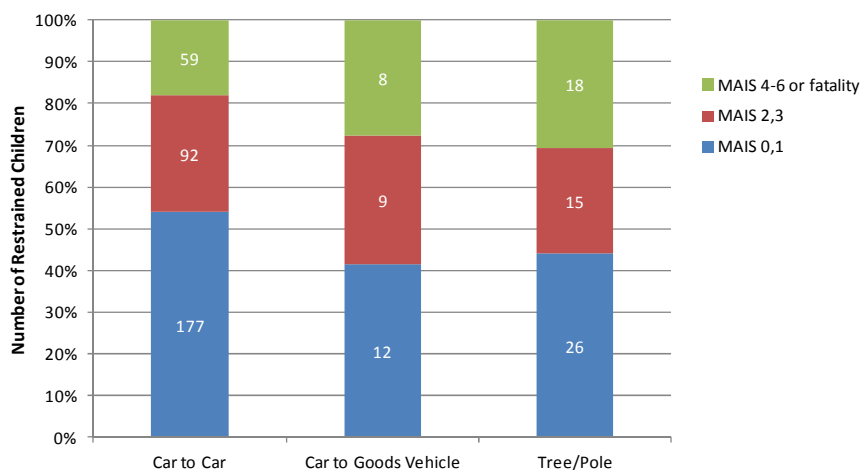


**Figure 3-6: Distribution of MAIS by crash opponent – Frontal impacts n=416**

There is a shift to a greater proportion of  $MAIS \geq 2$  restrained children for crashes involving goods vehicles and trees/poles.

**Seating position (restrained children)**

Seat position distribution can have an effect on injury outcome due to intrusion - especially for lateral impacts (struck or non-struck side) but also for frontal impacts - or restraint design - traditionally front seats have more advanced restraint systems (e.g. airbags, pretensioners and load limiters). The top figure (Figure 3-7) shows all restrained children, the bottom figure (Figure 3-8) shows  $MAIS \geq 3$  restrained children with injuries known or those with fatal injuries.

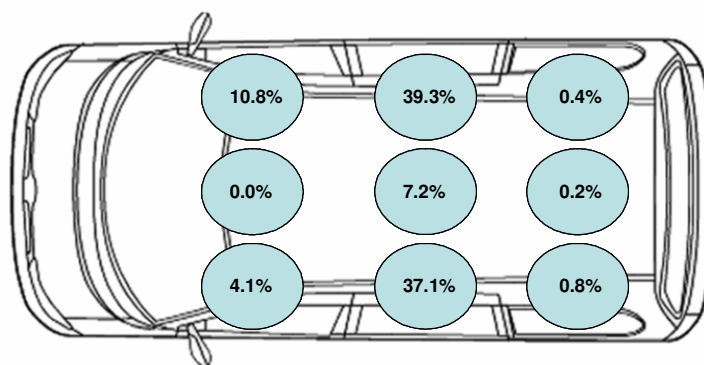


**Figure 3-7: Distribution of seating position – Frontal impacts, n=483**

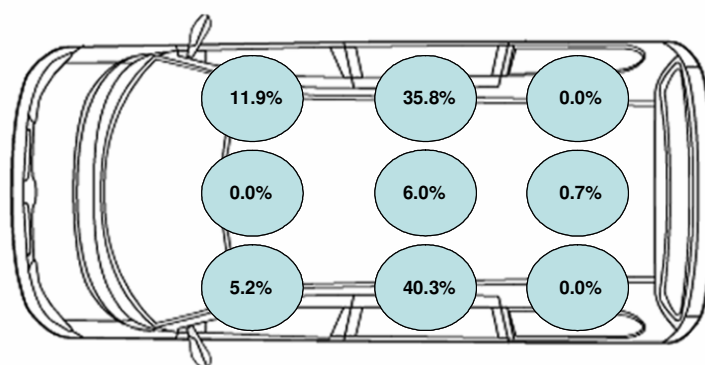
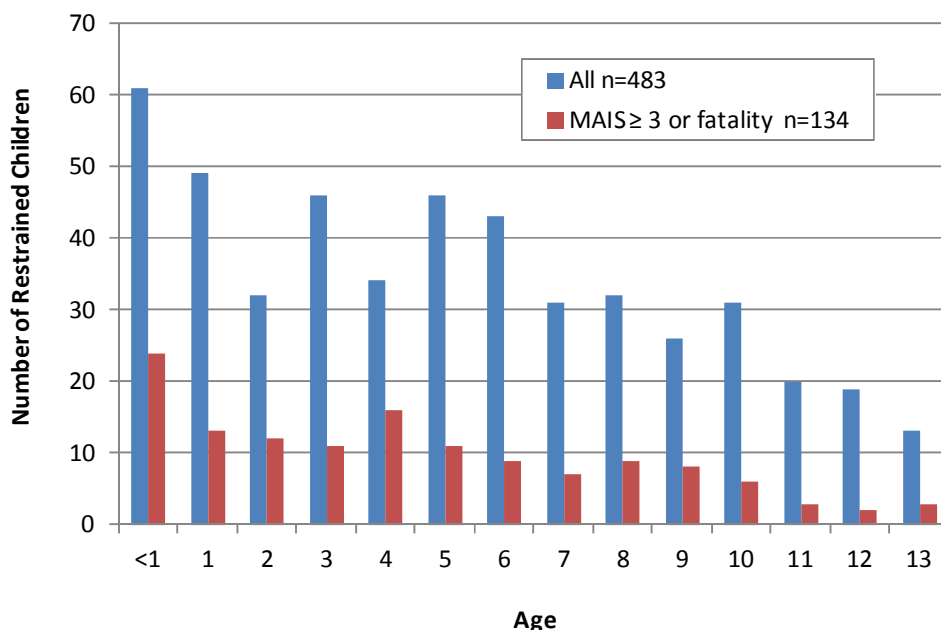


**Figure 3-8: Distribution of seating position – Frontal impacts, MAIS ≥ 3 or fatality, n=134**

For both injury samples the majority of restrained children are in the second row of seats. Of the severely or fatally injured group, 17% are seated in the front row of the car.

**Age**

The following figure (Figure 3-9) illustrates the distribution of age for the restrained children.



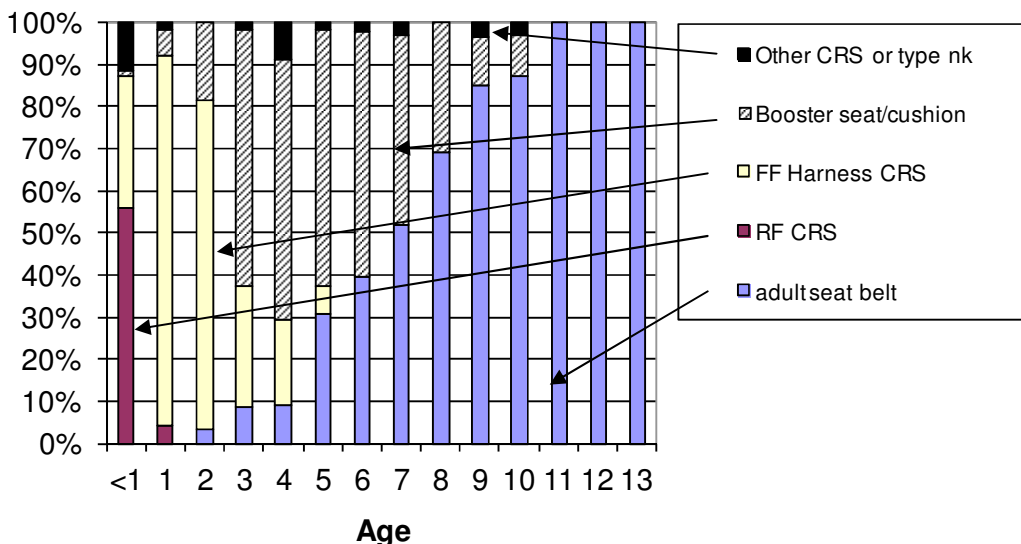
**Figure 3-9: Restrained children by age – Frontal impacts**

Figure 3-9 shows there is generally a good spread of ages across the frontal impact sample although there is a fall in number towards higher age. This may be a feature of the case sampling, resistance to injury as age increases, population or exposure (distance travelled). Also, 12 and 13 year old children were not in the inclusion criteria of the previous research projects, so some occupants of that age were present in vehicles, but cases with only children of that age were not presented/accepted.



### Restraint type by age

Figure 3-10 shows the type of restraint being used at the time of impact for all restrained children in the combined database in frontal impacts. This is only an indication of appropriate use as age is used. The ideal situation would be to have weight, height and age available for each child.



**Figure 3-10: Restraint condition by age – Frontal impacts, n=483**

The majority of the inappropriately restrained children are in adult seat belts rather than dedicated child restraint systems. At the age of 7 years old the majority of restrained children are using just the adult seat belt when at this age most should be restrained by booster systems. As the database is a sample biased towards higher severity injuries and impact severity it could be expected that the level of inappropriate use, if inappropriate use is expected to increase injury risk, may be higher than in the crash population as a whole. There is an overall picture of the use of rearward facing to forward facing to booster CRS and then just the adult seat belt towards greater age.

### Overall Injury Situation in frontal impacts

There are 450 restrained children in the dataset in frontal impacts with type of restraint and injuries known (or it is known that no injury has occurred). Of these children, 45% have a MAIS ≥ 2 and 25% have a MAIS ≥ 3.

There are a further 19 restrained children with fatal injuries but the actual injuries by AIS and body region are not known.

### Fatalities

Of the 483 restrained children in frontal impacts, there are 55 fatalities. The distribution of MAIS for restrained children with fatal injuries is given in Figure 3-11. MAIS (Maximum Abbreviated Injury Score) is used to indicate the highest injury severity that an occupant has received to any body region.

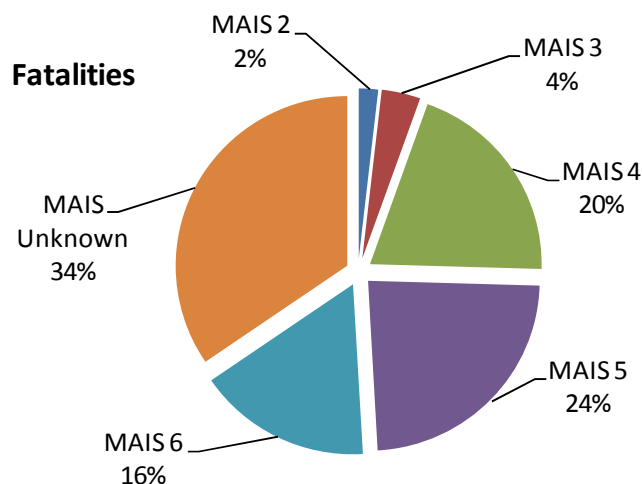


**Figure 3-11: MAIS for fatalities – Frontal impacts, n=55**

Unfortunately detailed injuries are not available for some of these fatalities (19 out of 55), with the MAIS recorded as unknown.

**MAIS Distribution – Overall and by restraint type**

The overall distribution of MAIS for restrained children in frontal impacts is given in Table 3-5.

**Table 3-5: MAIS distribution restrained children frontal impact, n=483**

MAIS	Restrained children	
	Frequency	Percentage
0	59	12.2%
1	187	38.7%
2	90	18.6%
3	38	7.9%
4	48	9.9%
5	19	3.9%
6	9	1.9%
Unknown MAIS (but known to be fatality)	19	3.9%
Unknown MAIS (not fatality)	14	2.9%
<b>Total</b>	<b>483</b>	<b>100%</b>

Of the children with known MAIS, 13% are not injured, 45% have a MAIS ≥ 2 and 25% have a MAIS ≥ 3.

The type of restraint that the child is using can be recorded in the database to a detailed level. For the analysis here the CRS types have been grouped into the common UN Regulation 44 group classifications; Rearward facing CRS (Group 0, 0+ or Group 1), Forward facing with harness (Group 1), Booster seats or cushions (Group 2, 3). There are 3 shield systems (two Group 1 and one Group 2) in the CHILD/CASPER dataset and they have been placed in the ‘other’ category. Other examples of CRS in the other group are carrycots, belt guides and CRS type unknown. Unknown was

recorded if, for example, the child was taken to hospital in the CRS but the type was not recorded.

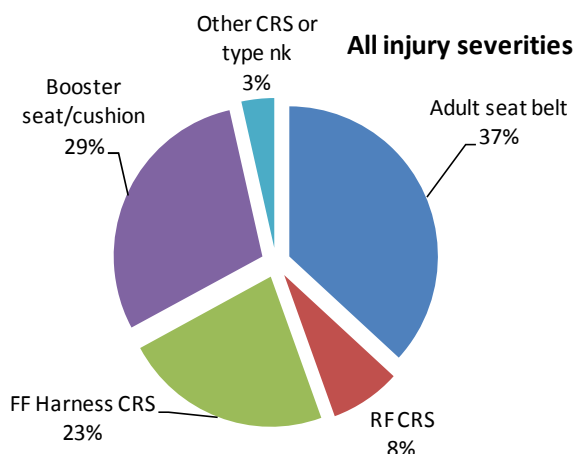


**Figure 3-12: Restraint type distribution – Frontal impacts – all injury severities, n=483**

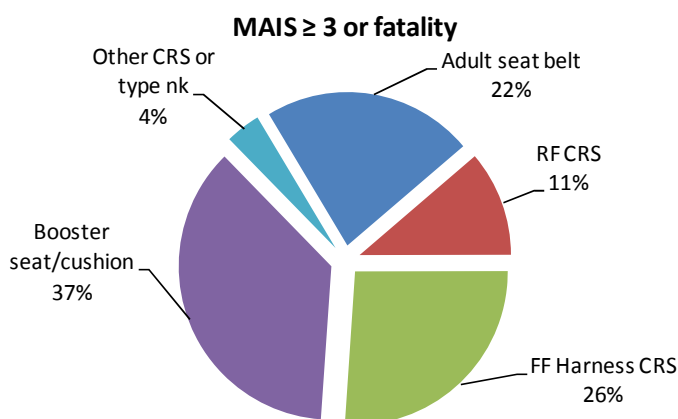


**Figure 3-13: Restraint type distribution – Frontal impacts MAIS ≥ 3 or fatality, n=134**

Comparing all injury severities to the serious and fatal injury sample, the proportion of restrained children using dedicated child restraint systems increases with a corresponding drop in the use of just adult seat belts.

Figure 3-14 is a statement of the situation found in the accident database for frontal impacts regarding restraint type use – those with known MAIS or known to have fatal injuries are selected. Comparisons cannot be made across the child restraint types as appropriateness must be taken into account and crash parameters (in simple terms ‘average’ crash severity) are not necessarily comparable.

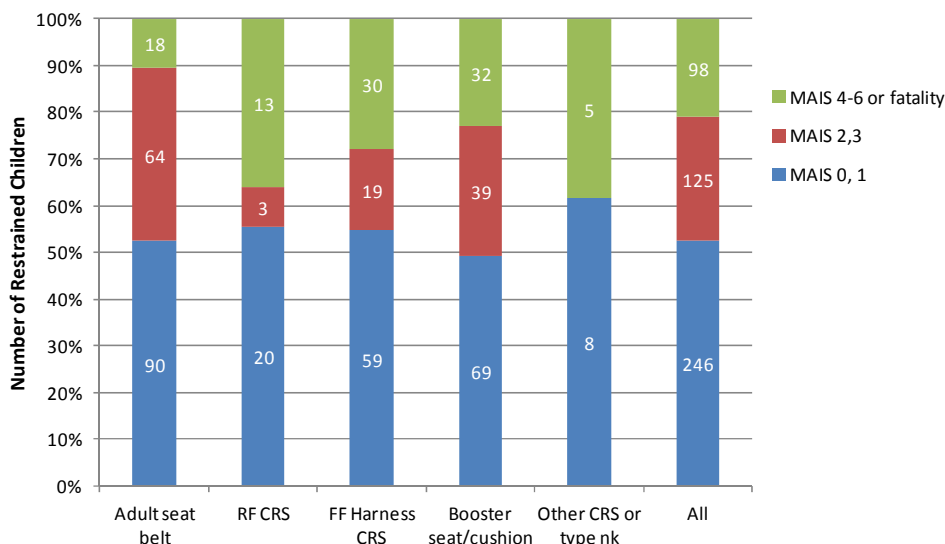


**Figure 3-14: Overall Injury by CRS Type – Frontal impacts n=469**

In the sample, the highest proportion of serious and fatal cases are for children restrained in booster systems and the lowest proportion (of the known CRS types) are restrained in rearward facing CRS. At the MAIS ≥ 2 level there is little difference though. The highest proportion of MAIS ≥ 4 and fatalities is for rearward facing children and the lowest for just adult seat belt restrained children.

**Quality of restraint use**

It is possible to record if misuse is present and the type of misuse. For analysis just two categories are used ‘Misuse identified’ and ‘No misuse identified’. Misuse is a complex issue and it is important to understand that sometimes it is not possible from the available evidence to identify misuse, especially if injury levels are low or not known or it has not been possible to examine the CRS. Therefore the definition of ‘No misuse identified’ should be read as ‘No misuse identified with the evidence available’.

**Table 3-6: Distribution of misuse identification by restraint type – Frontal impacts, n=469**

Restraint type	Misuse identified	No misuse identified
Adult seat belt	7.6%	92.4%
RF CRS	36.1%	63.9%
FF Harness CRS	29.6%	70.4%
Booster seat/cushion	12.1%	87.9%
Other CRS or type not known	15.4%	84.6%
<b>Total n=469</b>	<b>16.4%</b>	<b>83.6%</b>

The overall rate of misuse identified (16%) is lower than figures found in misuse field studies (surveys and checking days). It is likely that at best the database is considering severe misuse, rather than being able to highlight slight misuse.

Figure 3-15 shows banded injury severity by appropriate use and misuse. It is important to note that in the analysis below, appropriateness is often a judgement, as

often weight and/or height are not known. Misuse has been positively identified in the misuse cases and not identified or unknown in the 'no misuse identified' category.

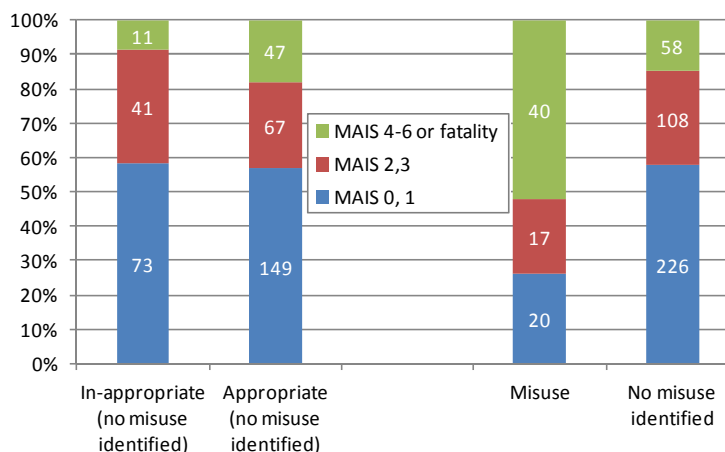


**Figure 3-15: Quality of restraint – Overall injury levels**

A relationship between misuse and injury level is apparent in Figure 3-15 with higher MAIS  $\geq 2$  injury levels for restrained children in the sample where it has been possible to identify misuse, compared to those restrained children with misuse not identified. There is no control for crash parameters (the cases with misuse may be of overall higher crash severity).

The same relationship is not apparent for appropriate use. This may be due to the definitions of inappropriate injury used, especially when weight and/or height are not known. In particular the recording of restrained child up to and including 11 years old being inappropriately restrained in just the adult seat belt (where otherwise no information is known regarding weight and/or height) is quite strict. Also there is no control for crash parameters - the cases with inappropriate use may simply be of overall higher crash severity.

#### Parameters for frontal impacts – Crash severity

It is important to not suggest that one CRS type is worse than another in terms of injury risk as this sample is not representative, crash parameters are not necessarily comparable across CRS and quality of restraint use and airbag deployment must be taken into account. Also overall practical considerations must be projected onto the data that take into account the changes in child anatomy, physiology, strength and therefore injury tolerances as they get older. And, although it would afford them the best protection, children over the age of 4 are not likely to be agreeable to travelling rearward facing or have the space to do so.

Confounding factors in using general measures of crash severity for child occupants, compared to adult occupants, are, in particular, quality of restraint use (appropriateness, misuse and pre-crash positioning) and airbag deployment (especially for rear facing restrained children). Also seen during case review is the influence of intrusion in sideswipes or narrow frontal impacts.

The direction of force (DOF) for an impact is available from the CDC code. For the frontal impacts the distribution of direction of force for restrained children is given in Table 3-7.

**Table 3-7: Distribution of direction of force – Frontal impacts**

Direction of force	MAIS known or fatality n=469	MAIS ≥ 3 or fatality n=134
10 o'clock	0.4%	1.5%
11 o'clock	19.8%	19.4%
12 o'clock	67.4%	73.1%
1 o'clock	12.4%	6.0%
2 o'clock	0.0%	0.0%

The largest proportion of children can be seen to be injured in 12 o'clock impacts, followed by 11 o'clock impacts. This doesn't change a large amount when selecting only MAIS ≥ 3 children or fatalities.

To quantify the crash severity in frontal impact, EES (Equivalent Energy Speed) has been used. EES is a translation of the energy absorbed by the car during the crash (based on structural deformation) into an impact speed against a rigid object to obtain equivalent deformations in a crash test. Different methods are used by different collection teams:

1. Estimation method based on comparing structural deformations of the case car to deformations sustained during crash tests;
2. Calculation of energy from crush measures;
3. PC Crash scene dynamics impact and rest points.

The distribution of crash severity (EES) (when available) is given in Figure 3-16 for restrained child with known MAIS injury level or it is known that injuries are fatal. If the impact is narrow or a sideswipe, intrusion is seen in certain cases to be a large problem leading to severe injury. Here there is no selection for intrusion, direction of force or appropriate use.

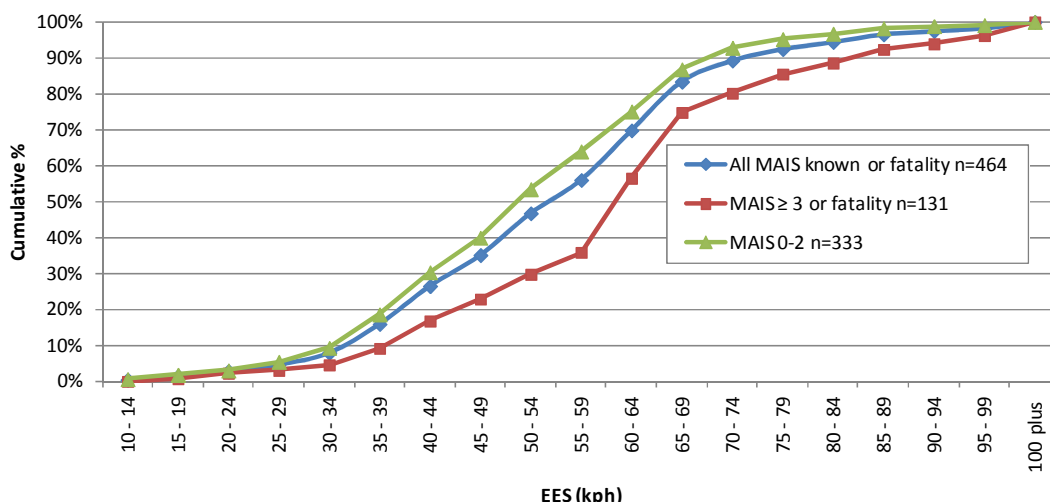


**Figure 3-16: Distribution of crash severity (EES) in frontal impacts**

As would be expected there is a general trend for a shift in the cumulative % graph towards higher EES for higher overall injury level. Of the MAIS ≥ 3 children or those with fatal injuries, approximately half are in a vehicle for which the EES is over 60 km/h

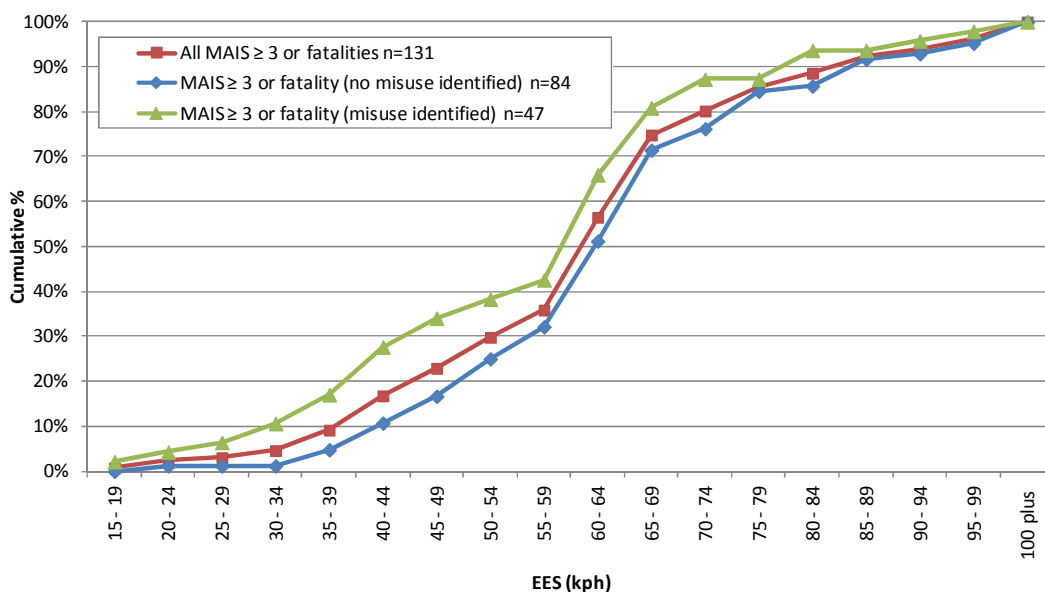
and approximately 25% over 70 km/h, exceeding the design criteria of cars and CRS (UN Regulation 44 frontal impact test conditions).

Figure 3-17 shows the distribution of crash severity (EES) (when available) for restrained child with known MAIS ≥ 3 injury level or fatalities. Selection for misuse is introduced compared to Figure 3-16. It is worth noting again that ‘No misuse identified’ should be understood to be ‘No misuse identified with the evidence available’.

Including severe injury and misuse in this analysis does introduce complexities, in particular the identification of misuse. For 19 of the fatalities injury details are not known (shown in Figure 3-11). Injury patterns are one of the main ways of identifying misuse so it is more likely that misuse will not be positively identified for such fatalities.

It is expected here that larger differences in EES are observed in the figure for lower severities than higher, if the hypothesis is that misuse is causing serious injury or fatalities at otherwise low crash severities. The effect of misuse is likely to be more masked at higher severity as the natural effects of higher severity - higher loads on the body and intrusion - play a larger role.

There are 3 cases where the child is identified as being ‘out of position’ pre-crash. This is not necessarily misuse but has an effect on injury outcome. These three cases have been included in the misuse identified category for the purposes of Figure 3-17. Further cases identify the child as ‘sleeping’ or ‘relaxed’ but this does not necessarily imply a poor restraint condition and in this analysis these cases have not been assigned as ‘misuse identified’, unless misuse has also been recorded separately in the case, for example slack being introduced into the seat belt.



**Figure 3-17: Distribution of crash severity (EES) in frontal impacts – MAIS ≥ 3 and fatalities**

Figure 3-17 indicates that at lower crash severities misuse is a factor when MAIS ≥ 3 and fatalities occur, with separation of the misuse and no misuse identified category lines on the figure.

A confounding factor is the actual type of frontal impact. Cases are apparent that are not side swipes (the direct contact overlap is more than 10 cm) but the frontal overlap is such that the particularly stiff frontal structures of the vehicle have not been engaged, for instance the longitudinal beam can be seen not to have been loaded. These cases

can lead to high levels of deformation along the side of the car, especially if the opposite vehicle is a goods vehicle but also in car to car impacts. Intrusion can reach child occupants causing serious injury and in some cases damage to restraint systems. In order to only include cases where children have been in a frontal impact with the likelihood of deformation of the car’s primary stiff frontal structure, Figure 3-18 excludes cars with an overlap of only 20% or less.

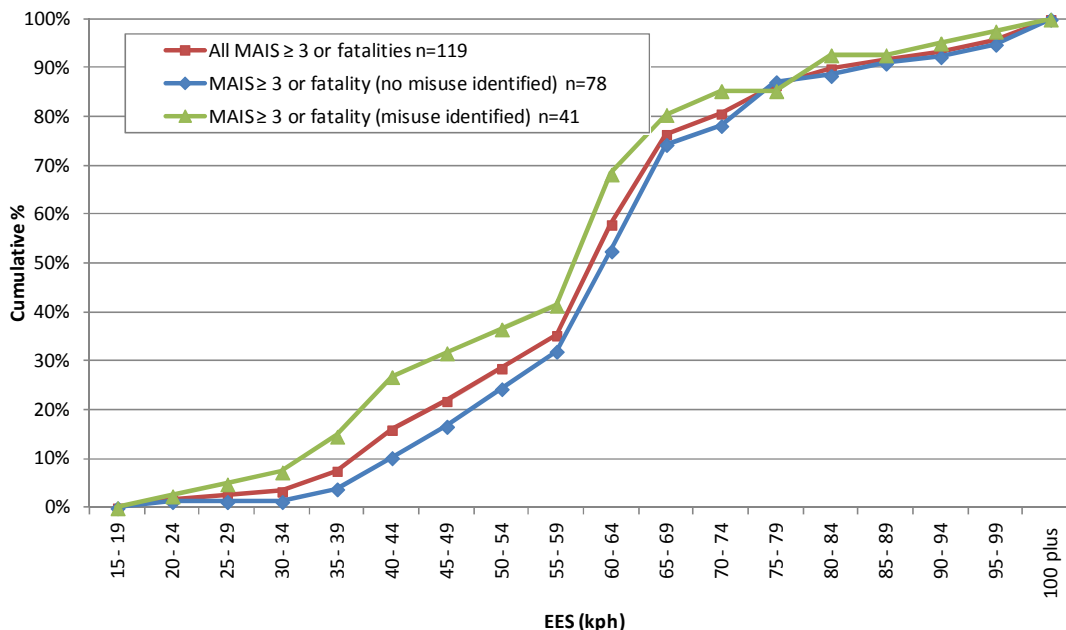


**Figure 3-18: Distribution of crash severity (EES) in frontal impacts – MAIS ≥ 3 and fatalities – Only cars with more than 20% frontal overlap**

Whilst controlling for frontal overlap the pattern for EES distribution in Figure 3-18 is similar to Figure 3-17.

**Maximum injury severity by restraint type**

As this section addresses injury by body region and restraint type, restrained children with injuries not known or restraint type not known are excluded.

Figure 3-19 gives the proportions of restrained children by restraint type that have an injury to each body region at the MAIS ≥ 2 level (body region). For example, of the 33 children in the dataset restrained rearward facing 36% have a head injury of AIS 2 or above. The MAIS ≥ 2 (head) rate is therefore 36%. Likewise Figure 3-20 addresses MAIS ≥ 3 injury rates. It is important to remember that this sample is not representative. An extreme example of this would be to note the high levels of head injury to rear facing restrained children. For each frontal impact that a child in a rearward facing child is involved in across Europe, there is not such a high chance (36%) of a head AIS ≥ 2 injury in every impact.

This analysis shows the general patterns of injury across the different restraint types. The neck, thorax and abdominal regions include the relevant region of the spine. ‘Head’ does not include the face. The MAIS ≥ 2 (external) rate is zero for all and not shown on the figures.



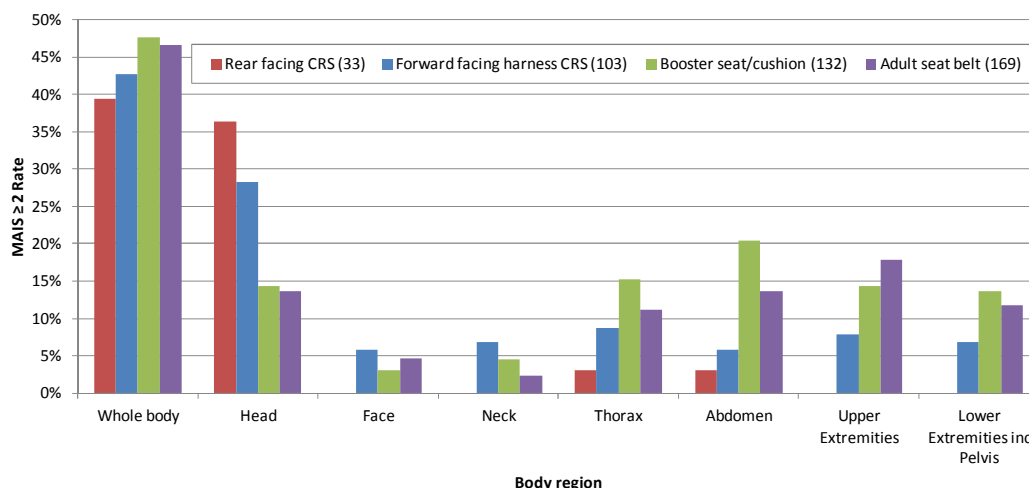


**Figure 3-19: Proportion of restrained children with an AIS ≥ 2 injury by body region and restraint type – Frontal impact, n=437**

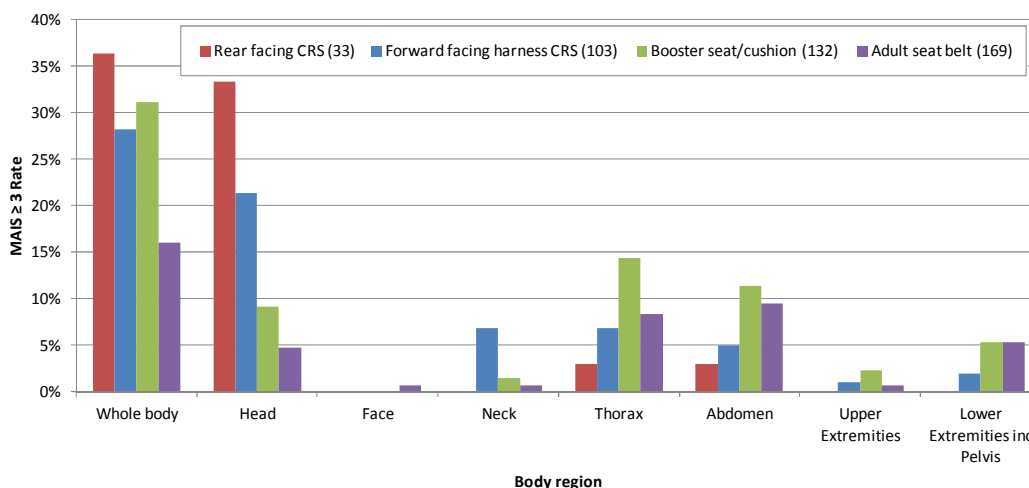


**Figure 3-20: Proportion of restrained children with an AIS ≥ 3 injury by body region and restraint type – Frontal impact, n=437**

**Rear facing CRS** Even though case numbers are small it is clear that the head is the most seriously injured body region, this is a good example of how this data can identify areas to consider in severe crashes, but is not representative of the whole injury population.

**Forward facing harness CRS** Again, as for rearward facing systems, it is clear that the head is the most seriously injured body region with 28% of the 103 children in this sample receiving an AIS ≥ 2 injury head injury. At the AIS ≥ 2 level, the other body regions start to feature equally but increasing the AIS to ≥ 3 shows the neck, abdomen and thorax are more prominent than the face and extremities.

**Booster seat/cushion** Serious injuries are more distributed across the body regions than for harness shell systems with both upper (14%) and lower extremity (14%) regions, the abdomen (21%) and the thorax (15%) featuring strongly at the AIS ≥ 2 level, along with the head (14%). At the AIS ≥ 3 level the thorax features as the most injured body region with 14% of the children in this sample having such an injury. The abdominal and head regions are also evident at 11% and 9% respectively.

**Adult seat belts** For children just restrained by the adult seat belt the extremities, upper extremities (18%) and lower extremities and pelvis (12%), feature strongly at the

AIS  $\geq 2$  level, along with the head (14%) and abdomen (14%), followed by the thorax (11%). At the AIS  $\geq 3$  level the abdomen has an AIS  $\geq 3$  injury for 10% of the 169 children, followed by the thorax (8%) and then the head and lower extremities are equally prevalent at 5%.

The following sections look at each restraint type individually at an injury level rather than the maximum injury level for each body region.

### Injury to body regions by restraint type

#### Rearward facing CRS

There are 33 children using rearward facing child restraint systems, of which 13 are not injured. Multidirectional ('convertible'), 2 way child restraints, are included when they are being used rearward facing. 94% are below 1 year old and 6% are 1 year old.

There are 20 injured children in rearward facing CRS, sustaining 47 injuries of all severities. Of these children, 13 have AIS  $\geq 2$  injury(ies) with 28 AIS  $\geq 2$  injuries in total.

Figure 3-21 shows how the 28 individual AIS  $\geq 2$  injuries for rearward restrained children are distributed across the body regions. For example, 93% of all the individual AIS  $\geq 2$  injuries for this sample are to the head.

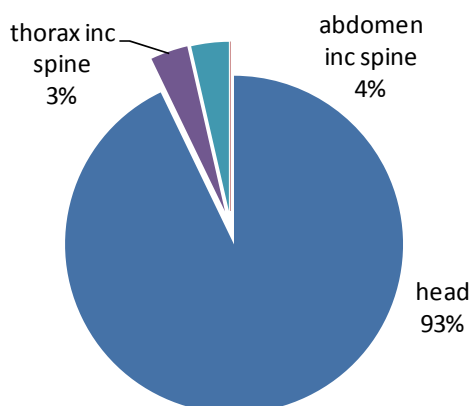


**Figure 3-21: AIS  $\geq 2$  Injury distribution for rearward facing CRS - Frontal impacts known injuries - 28 AIS  $\geq 2$  injuries in total**

As in Figure 3-19 and Figure 3-20 it is clear that the head is by far the most injured body region for the children in this sample, with 26 (93%) of the 28 AIS  $\geq 2$  injuries being to the head. Of these AIS  $\geq 2$  injuries 18 are brain injuries and 8 are fractures, with no crush or penetration injuries.

This is a small sample but of the 12 casualties with AIS  $\geq 2$  cranium injury, 11 are in the front passenger seat. In 3 cases contact with the dashboard is recorded and in another 7 there is a deployed frontal airbag. The casualty in the rear sustained brain haemorrhage due to excessive slack in the harness allowing contact with the carrying handle.

Fracture is present for 7 casualties along with brain injury, whilst 4 casualties have just brain injury and 1 casualty having just fracture. This skull fracture (which was AIS 2) was caused by a wooden toy mounted on the carrying handle of the CRS.

The only child without head injury sustained a thoracic crush injury with the centre console when the strap between the legs failed during the crash.

### Forward facing harness CRS

There are 103 children using forward facing child restraint systems with a harness, of which 21 are not injured. Convertible, two-way child restraints are included when they are being used forward facing with a harness. The simple distribution of age is given in Figure 3-22, showing that most are 1 year old.

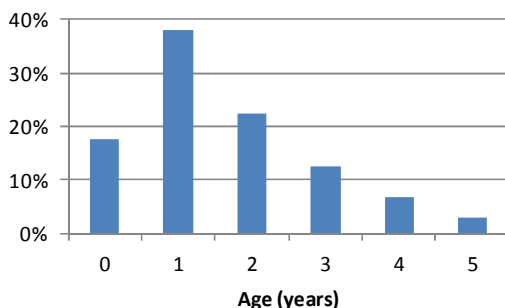


**Figure 3-22: Restrained child age distribution for Forward Facing CRS Harness – Frontal impacts known injuries**

There are 82 injured children using forward facing child restraint systems with a harness, with a total of 228 injuries of all severities. Of these children 44 have AIS ≥ 2 injury(ies) with 116 AIS ≥ 2 injuries in total.

Figure 3-23 shows how the 116 individual AIS ≥ 2 injuries for forward facing restrained children are distributed across the body regions. For example, 51% of all the individual AIS ≥ 2 injuries for this sample are to the head.

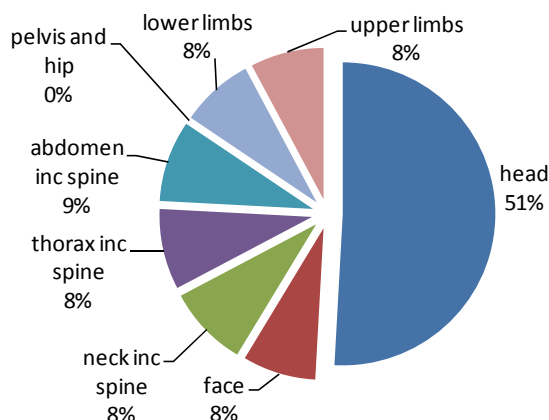


**Figure 3-23: AIS ≥ 2 Injury distribution for forward facing CRS – Frontal impacts known injuries - 116 AIS ≥ 2 injuries in total**

As in Figure 3-21 it is clear that the head is by the most injured body region for the children in this sample, with 51% of the 116 AIS ≥ 2 injuries being to the head. The distribution of AIS ≥ 2 injuries between remaining body regions is then very similar (except for the pelvis and hip where there are no AIS ≥ 2 injuries). Of the 44 MAIS ≥ 2 casualties, 3 are in the front passenger seat, the rest in the middle rear row.

Of the casualties with AIS ≥ 2 head injuries, when a contact is identified (75% of cases), it is to the seat back in front in 48% of cases and to the B pillar in 18%. Combining the own kinematics and deceleration fields gives 23%. 46 of the AIS ≥ 2 head injuries are to the brain, 12 are fractures and 1 is a crush or penetrating injury. 17 children have just a brain injury, 5 just a fracture and 6 both types of injury.

The injury causes to the extremities can be difficult to attribute but the seatback and the dashboard are given as possible causes.

### Booster systems

There are 132 children using booster child restraint systems either with or without backrests, of which 13 are not injured. The simple distribution of age is given in Figure 3-24, showing that the peak is at 3 years old - often the changeover point for children from harness to booster.

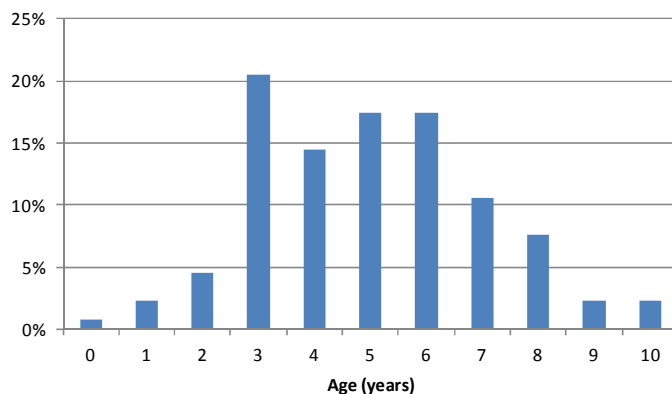


**Figure 3-24: Restrained child age distribution for booster systems – Frontal impacts known injuries**

There are 119 injured children using a booster system, with a total of 358 injuries of all severities. Of these children, 63 have AIS  $\geq 2$  injury(ies) with 184 AIS  $\geq 2$  injuries in total. Figure 3-25 shows how the 184 individual AIS  $\geq 2$  injuries for booster system restrained children are distributed across the body regions. For example, 20% of all the individual AIS  $\geq 2$  injuries for this sample are to the head.

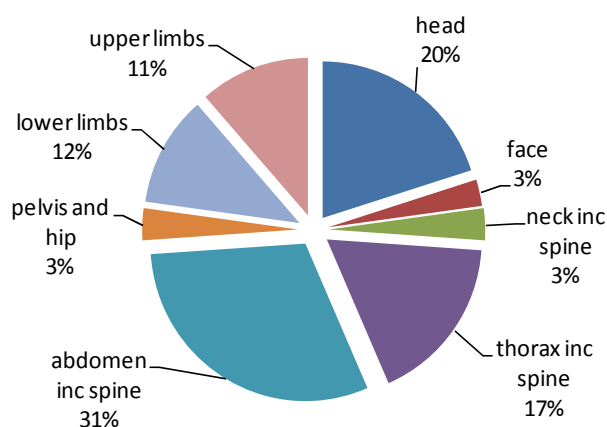


**Figure 3-25: AIS  $\geq 2$  Injury distribution for booster systems – Frontal impacts known injuries - 184 AIS  $\geq 2$  injuries in total**

Figure 3-25 shows that the abdomen region accounts for just under a third of all AIS  $\geq 2$  injuries for this sample of children. The head accounts for 20% of all AIS  $\geq 2$  injuries followed by the thoracic region at 17%. The extremities added together cover 23% of the 184 AIS  $\geq 2$  injuries. Of the 132 MAIS  $\geq 2$  casualties, 10 are in the front passenger seat, 121 in the middle rear row and 1 in the third row (rear).

Of the casualties with AIS  $\geq 2$  abdominal region injuries, when a contact is identified (96% of cases), it is to the seat belt in all cases. The same is found for thoracic AIS  $\geq 2$  injuries.

The injury causes to the extremities can be difficult to attribute and show a higher use of 'unknown' for probable injury cause than for other body regions.

**Only adult seat belt**

There are 169 children using just the adult seat belt, of which only 10 are not injured. The simple distribution of age is given in Figure 3-26, showing an expected rise starting at 5 years old.

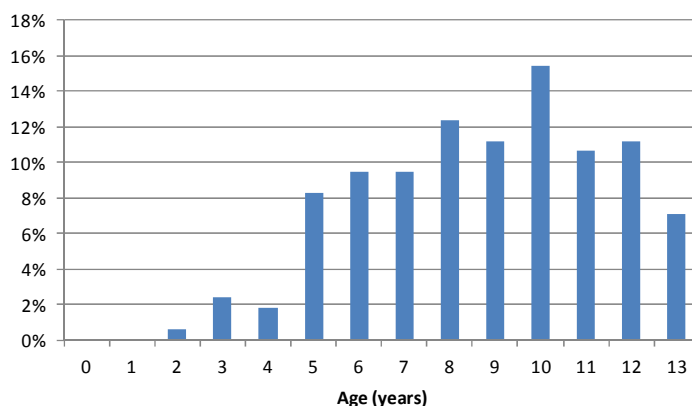


**Figure 3-26: Restrained child age distribution for adult seat belts – Frontal impacts known injuries**

There are 159 injured children using just the adult seat belt, with a total of 560 injuries of all severities. Of these children, 79 children have AIS ≥ 2 injury(ies) with 189 AIS ≥ 2 injuries in total. Figure 3-27 shows how the 189 individual AIS ≥ 2 injuries for only adult seat belt restrained children are distributed across the body regions. For example, 17% of all the individual AIS ≥ 2 injuries for this sample are to the head.

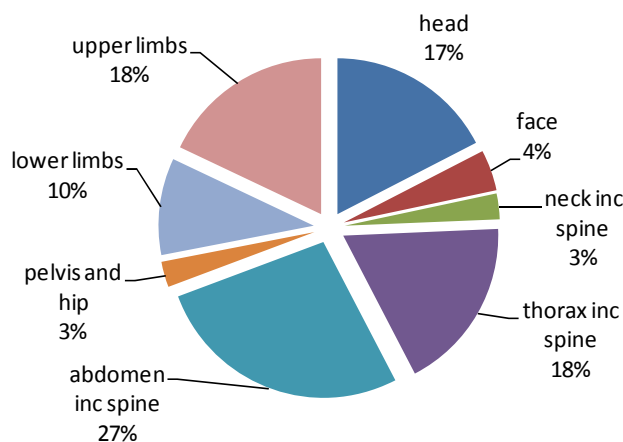


**Figure 3-27: AIS ≥ 2 Injury distribution for adult seat belts – Frontal impacts known injuries - 189 AIS ≥ 2 injuries in total**

Figure 3-27 shows that AIS ≥ 2 extremity injuries account for 28% of all the AIS ≥ 2 injuries for this sample of children and then the abdominal region features strongly at 27%, followed by the thorax and head with similar proportions (18% and 17%).

Children restrained with the adult seat belt only are more spread around in terms of seating position than those with dedicated CRS. Of the 169 MAIS ≥ 2 casualties, 33 are in the front passenger seat, 131 in the middle rear row and 5 in the third row (rear).

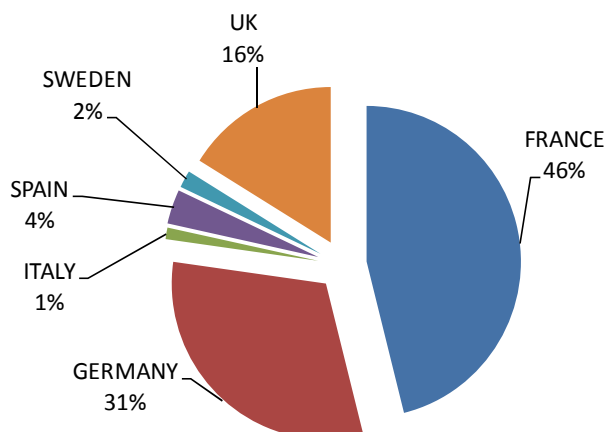
As with booster systems, abdominal injuries are mainly attributed to the seat belt, as are the thoracic injuries.

### 3.1.5 Lateral impacts

#### Introduction

The same dataset (CHILD and CASPER) is used for lateral impacts as in the frontal impact analysis. It is important to consider that the data is sampled against certain criteria and is not representative of the child crash population. However, as with frontal impacts, it can be used to give an indication of which body regions are being injured in different CRS types.

Of the combined CHILD and CASPER database, 167 restrained children are in lateral impacts, 25.5% of the total (656).



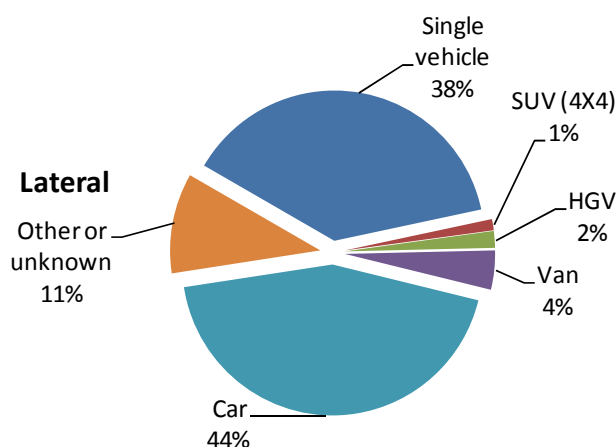
**Figure 3-28: Distribution of restrained children by country of origin – Lateral impacts, n=167**

Figure 3-28 shows the country of case origin for these 167 children.

#### Crash and Restraint Parameters

##### Crash opponent

Figure 3-29 and Figure 3-30 show the distribution of crash opponent for restrained children in lateral impacts.



**Figure 3-29: Distribution of crash partner – Restrained children, n=167**

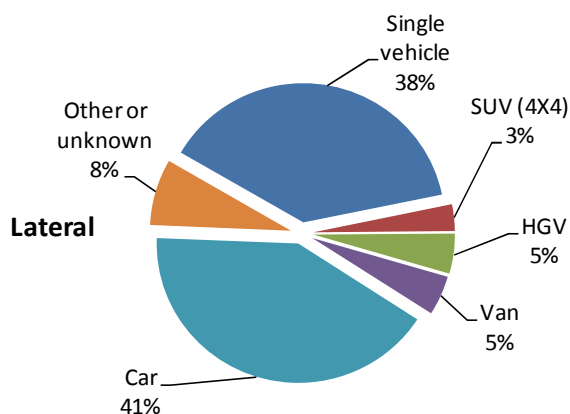


**Figure 3-30: Distribution of crash partner – Restrained children, MAIS ≥ 3 or fatality, n=65**

The division between car to car impacts and single vehicle impacts is similar, for both injury selections. When the crash opponent is not another vehicle, 83% of the children are in a car that has an impact with a tree/pole (80% for MAIS ≥ 3 or fatal).

The MAIS distributions for the main crash partner categories are given in Figure 3-31.

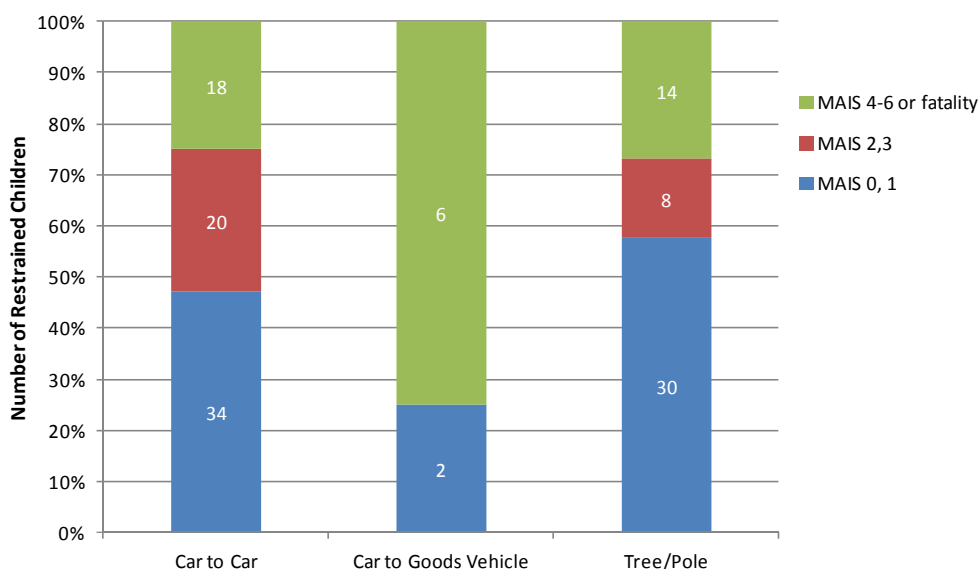


**Figure 3-31: Distribution of MAIS by crash opponent – Lateral impacts n=132**

In the lateral impact sample the rate of serious injury is highest for restrained children involved in crashes with goods vehicles, although overall they form a small proportion of the sample.

**Seating position (restrained children)**

Seat position distribution can have an effect on injury outcome due to intrusion - especially for lateral impacts (struck or non-struck side) but also for frontal impacts - or restraint design - traditionally front seats have more advanced restraint systems (e.g. airbags, pretensioners and load limiters). The top figure is all restrained children, the bottom figure MAIS ≥ 3 restrained children with injuries known or those with fatal injuries.

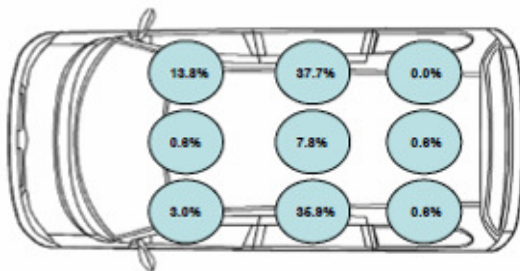


**Figure 3-32: Distribution of seating position – Lateral impacts, n=167**

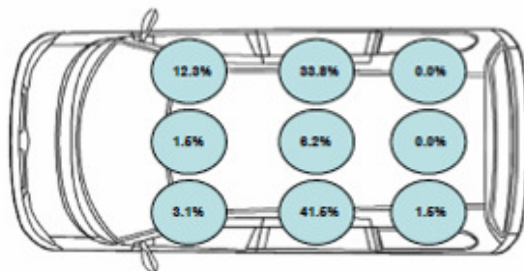


**Figure 3-33: Distribution of seating position – Lateral impacts, MAIS ≥ 3 or fatality, n=65**

For both injury samples the majority of restrained children are in the second row of seats. Of the severely or fatally injured group, 17% are seated in the front row of the car and when in the second row more are sat on the left side than the right.

**Age**

The following figure (Figure 3-34) illustrates the distribution of age for the restrained children.

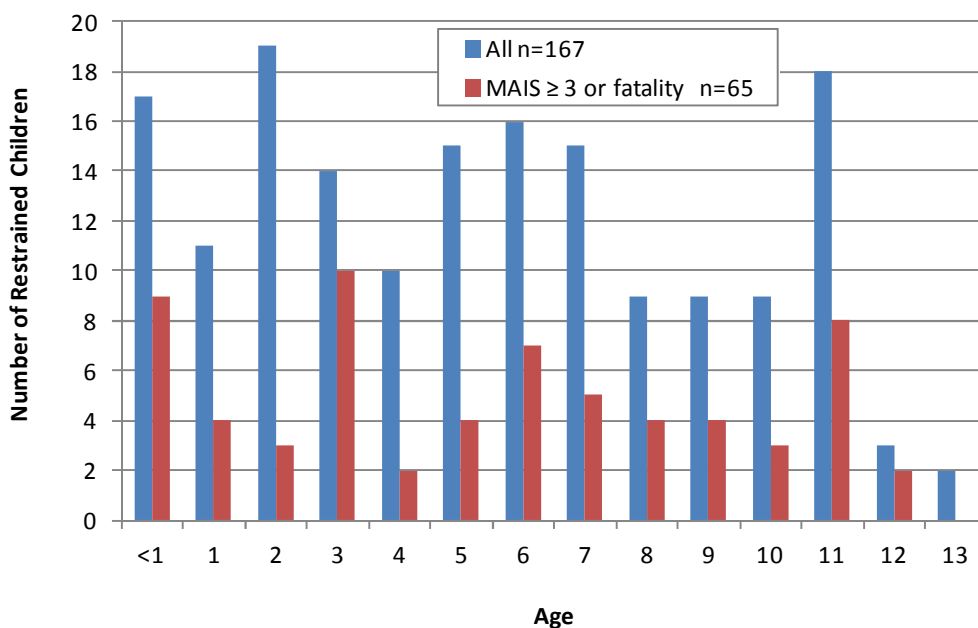


**Figure 3-34: Restrained children by age – Lateral impacts**

Figure 3-34 shows that the distribution of age across the lateral impact sample is not uniform but each part of the age spectrum reflecting the CRS grouping system is



represented. As with frontal impacts there is a fall in number for 12 and 13 year olds. This may be a feature of the case sampling combined with resistance to injury as age increases and the inclusion of older children mainly for CASPER cases.

### Restraint type by age

Figure 3-35 shows the type of restraint being used at the time of impact for all restrained children in the combined database in lateral impacts. This is only an indication of appropriate use as age is used. The ideal situation would be to have weight, height and age available for each child.

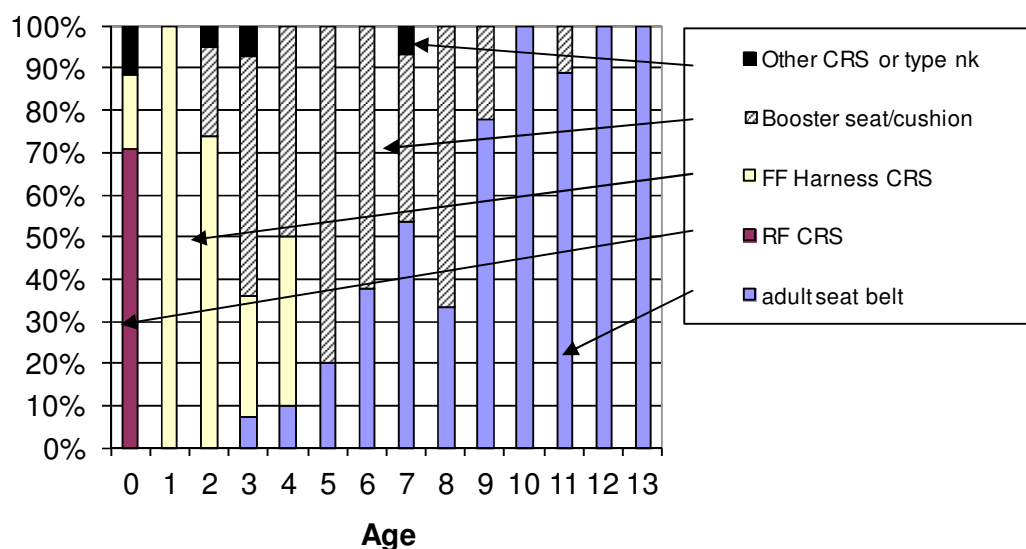


**Figure 3-35: Restraint condition by age – Lateral impacts, n=167**

The majority of the inappropriately restrained children are in adult seat belts rather than dedicated child restraint systems. At the age of 7 years old the majority of restrained children are using just the adult seat belt when at this age most should be restrained by booster systems – although there is then a reduction in just adult seat belt use for 8 years old. As the database is a sample biased towards higher severity injuries and impact severity it could be expected that the level of inappropriate use, if inappropriate use is expected to increase injury risk, may be higher than in the crash population as a whole. There is an overall picture of the use of rearward facing to forward facing to booster CRS and then just the adult seat belt towards greater age.

### Overall injury situation on lateral impacts

There are 148 restrained children in the dataset in lateral impacts with type of restraint and injuries known (or it is known that no injury has occurred). Of these children, 46% have a MAIS  $\geq 2$  and 34% have a MAIS  $\geq 3$ .

There are a further 15 restrained children with fatal injuries but the actual injuries by AIS and body region are not known.

### Fatalities

Of the 167 restrained children in lateral impacts, there are 34 fatalities. The distribution of MAIS for restrained children with fatal injuries is given in Figure 3-36. MAIS (Maximum Abbreviated Injury Score) is used to indicate the highest injury severity that an occupant has received to any body region.

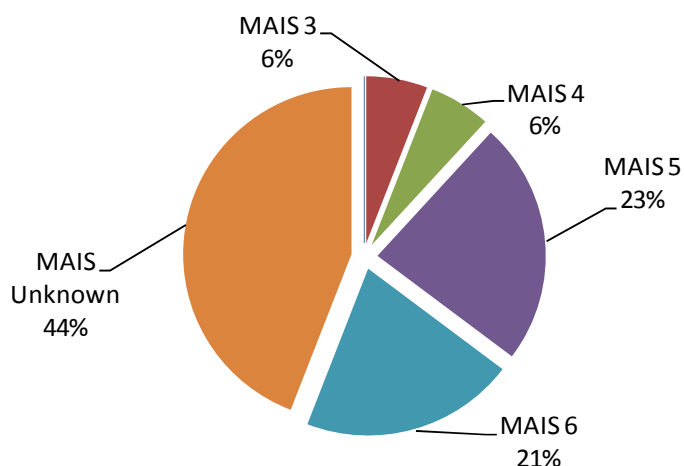


**Figure 3-36: MAIS for fatalities – Lateral impacts, n=34**

Unfortunately detailed injuries are not available for some of these fatalities (15 out of 34), with the MAIS recorded as unknown.

**MAIS distribution – Overall and by restraint type**

The overall distribution of MAIS for restrained children in lateral impacts is given in Table 3-8.

**Table 3-8: MAIS distribution restrained children - Lateral impact, n=167**

MAIS	Restrained children	
	Frequency	Percentage
0	25	15.0%
1	55	32.9%
2	18	10.8%
3	19	11.4%
4	12	7.2%
5	12	7.2%
6	7	4.2%
Unknown MAIS (but known to be fatality)	15	9.0%
Unknown MAIS (not fatality)	4	2.4%
<b>Total</b>	<b>167</b>	<b>100.0%</b>

Of the children with known MAIS (n=148), 17% are not injured, 46% have a MAIS ≥ 2 and 34% have a MAIS ≥ 3.

The type of restraint that the child is using can be recorded in the database to a detailed level. For the analysis here the CRS types have been grouped into the common UN Regulation 44 group classifications; Rearward facing CRS (Group 0, 0+ or Group 1), Forward facing with harness (Group 1), Booster seats or cushions (Group 2, 3). There are 3 shield systems (two Group 1 and one Group 2) in the CHILD/CASPER dataset and they have been placed in the ‘other’ category. Other examples of CRS in the other group are carrycots, belt guides and CRS type unknown. Unknown was

recorded if, for example, the child was taken to hospital in the CRS but the type was not recorded. The following figures include only restrained children with known injuries.

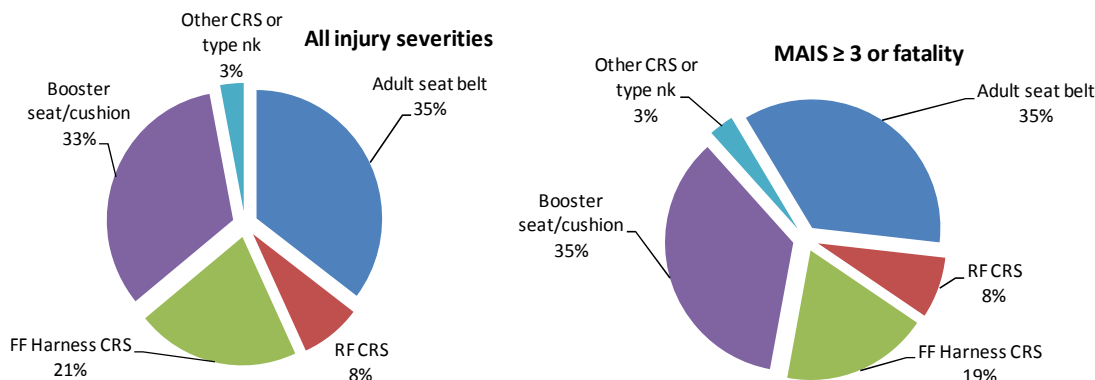


**Figure 3-37: Restraint type distribution – Lateral impacts**

Comparing all injury severities to the serious and fatal injury sample the restraint type distribution is very similar.

Figure 3-38 is a statement of the situation found in the accident database for lateral impacts. Comparisons cannot be made across the child restraint types as appropriateness of restraint type for each age must be taken into account and crash parameters (in simple terms ‘average’ crash severity) are not necessarily comparable. Figure 3-38 includes restrained children with known MAIS or known to have fatal injuries in lateral impact.

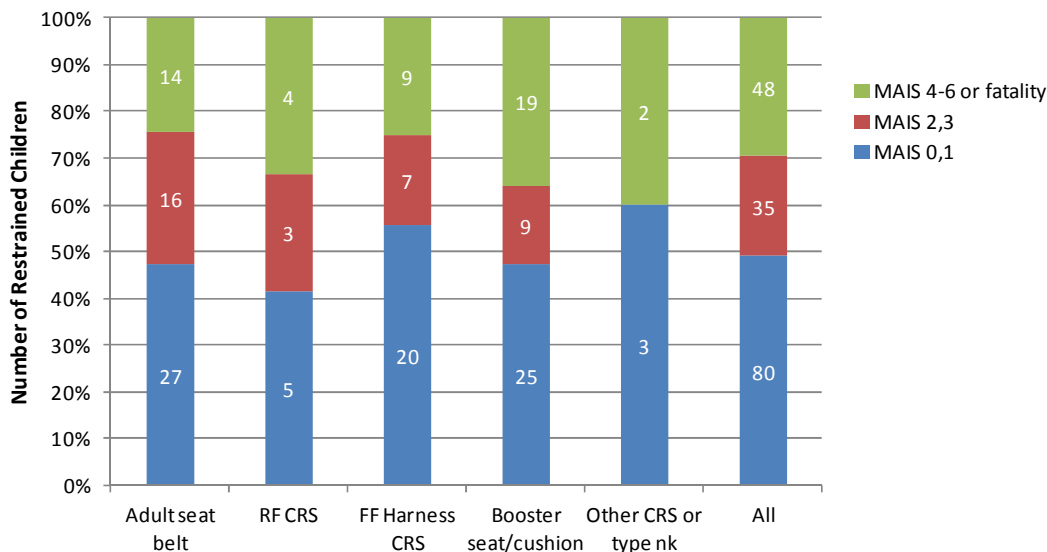


**Figure 3-38: Overall Injury by CRS type – Lateral impacts n=163**

In the sample, the highest proportion of serious and fatal cases are for children restrained in rear facing child restraints and the lowest proportion (of the known CRS types) are restrained in forward facing harness CRS. The highest proportion of MAIS ≥ 4 and fatalities (of the known CRS types) is for children using booster systems and the lowest equally for children using just the adult seat belt and forward facing harness systems.

**Quality of use**

It is possible to record if misuse is present and the type of misuse. For analysis just two categories are used ‘Misuse identified’ and ‘No misuse identified’. Misuse is a

complex issue and it is important to understand that sometimes it is not possible from the available evidence to identify misuse, especially if injury levels are low or not known or it has not been possible to examine the CRS. Therefore the definition of ‘No misuse identified’ should be read as ‘No misuse identified with the evidence available’.

**Table 3-9: Distribution of misuse identification by restraint type – Lateral impacts, n=163**

Restraint type	Misuse identified	No misuse identified
Adult seat belt	-	100.0%
RF CRS	8.3%	91.7%
FF Harness CRS	16.7%	83.3%
Booster seat/cushion	11.3%	88.7%
Other CRS or type nk	20.0%	80.0%
<b>Total</b>	<b>8.6%</b>	<b>91.4%</b>

Overall the rate of identified misuse in lateral impact (8.6%) is approximately half the rate in frontal impacts (16.4%). Injury mechanisms that identify misuse can be more obvious in frontal impacts than in lateral impact. For example, in a frontal impact head projection of a sizeable distance can indicate poor restraint condition, such as slack in the harness or seat belt, but in lateral impact on the struck side the distance before head contact is smaller so does not necessarily identify slack in harness or seat belt.

Figure 3-39 shows banded injury severity by appropriate use and misuse. It is important to note that in the analysis below, appropriateness is often a judgement, as often weight and/or height are not known. Misuse has been positively identified in the misuse cases and not identified or unknown in the ‘no misuse identified’ category.

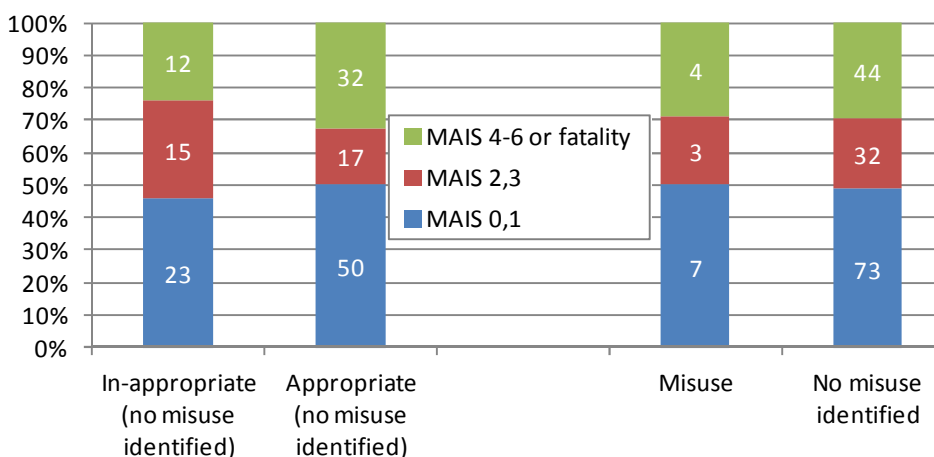


**Figure 3-39: Quality of restraint – Overall injury levels – Lateral impacts**

A relationship between misuse and higher injury levels is not apparent in Figure 3-39 for lateral impacts, as it was for frontal impacts in Figure 3-15. In fact as discussed above the number of cases where misuse has been identified is very low at only 11. There is no control for crash parameters (the cases with misuse may be of overall higher crash severity).

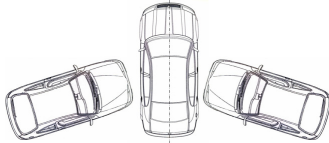
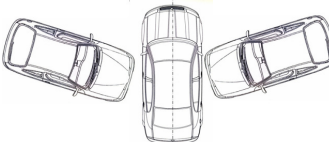
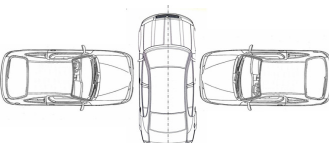
The proportion of children defined as appropriately restrained with no or minor injuries is higher than the in-appropriately restrained group, but the difference is small and does not hold for MAIS 4 to 6 and fatally injured children. This may be due to the

definitions of inappropriate injury used, especially when weight and/or height are not known. In particular the recording of restrained child up to and including 11 years old being inappropriately restrained in just the adult seat belt (where otherwise no information is known regarding weight and/or height) is quite strict. Also there is no control for crash parameters - the cases with inappropriate use may be of overall higher crash severity.

#### Parameters for lateral impacts

The direction of force (DOF) for an impact is available from the CDC code and is shown in relevant groups in Table 3-10.

**Table 3-10: Direction of force for lateral impacts**

DOF		Distribution - All injury severities	Proportion with MAIS $\geq$ 2 or fatality
Lateral from rear 07 08 04 05 o'clock		17 10.4%	41.2%
Lateral from front 01 02 10 11 o'clock		84 51.5%	50.0%
Pure lateral 09 03 o'clock		61 36.8%	54.1%
Other	-	2 1.2%	50.0%
All		100%	-

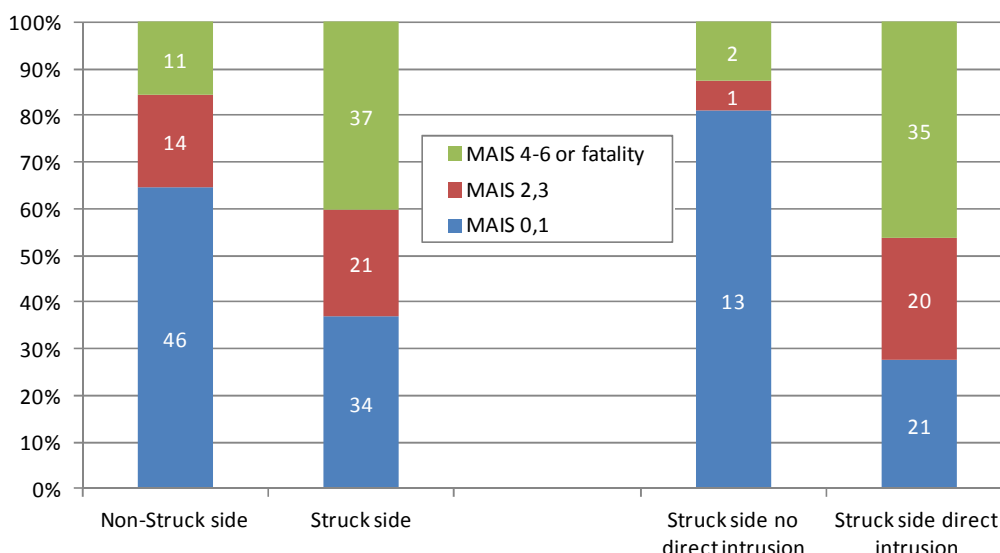
'Lateral from front' and 'pure lateral' together are the impacts experienced the by large proportion of restrained children in lateral impacts. The proportion of children with MAIS  $\geq$  2 or fatal injuries is highest for purely lateral impacts (54%), followed by lateral from front (50%) and then lateral from rear (41%).

#### Lateral impact by struck side

It is known whether the occupant is on the struck side or non-struck side of the car. Being in the centre is considered to be non-struck side.

#### Injury severity

There are 92 restrained children sitting on the struck side in a lateral impact and 71 are non-struck side. Figure 3-40 shows the distribution of MAIS by struck/non-struck side and by direct intrusion for struck side occupants.



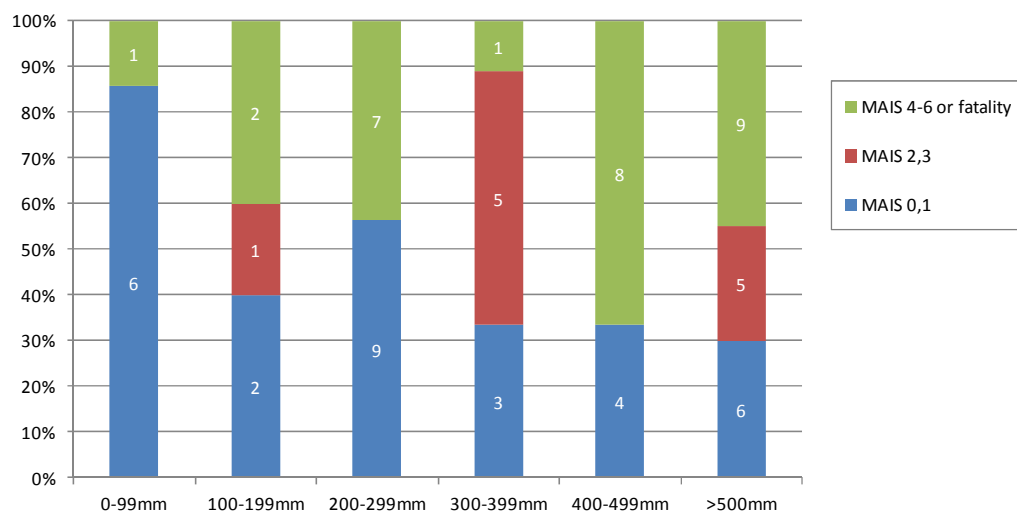
**Figure 3-40: MAIS – Non / struck side and direct intrusion – Lateral impacts restrained children, n=163**

Figure 3-40 shows that the distribution of MAIS for restrained children sitting on the struck side is different than for the non-struck side. There are more children on the struck side and they have a higher rate of  $MAIS \geq 2$  and a greater proportion of  $MAIS$  4-6 and fatal injury. This indicates that children seated on the struck side in lateral impacts have a more serious injury outcome in the sample than those on the non-struck side. But it also shows that serious and fatal injury is present for non-struck side passengers, often when high levels of intrusion effectively put them on to the struck side or poor restraint conditions project them across the car.

Figure 3-40 also shows that being on the struck side is not the sole parameter influencing the severity of injury outcome and it is visible that having direct intrusion (on the struck side) gives a higher proportion of serious injury than no direct intrusion. The sample of children on the struck side but not in the area of intrusion is small but it shows the best proportion of not injured or slightly injured children. Therefore to make significant progress for the protection of children in side impact, it is important that the side impact test procedure used for CRS approval simulates the intruding parts of the vehicle.

**Injury severity distribution by maximum intrusion – Struck side restrained children**

Figure 3-41 shows the maximum intrusion for struck side restrained children by overall injury severity (MAIS). The intrusion value is the highest value recorded for the general area that the child is seated. For children in the front seat that is the B pillar and forwards. For children in the rear, the B pillar and rearwards. Therefore it is possible to have intrusion (especially from a tree or pole) at the B pillar and not necessarily at the child's head position.



**Figure 3-41: Injury severity distribution by maximum intrusion – Struck side restrained children, n=69**

Examining the MAIS 0,1 children with >500mm of intrusion some are in shell CRS and the intrusion is on the B pillar but not necessarily high at the children's actual position, especially if the child is young and the impact is purely lateral. Conversely if the impact has a forward component the head excursion can put the head into the area of B pillar intrusion leading to high levels of injury.

The amount of maximum intrusion around the child's position has a link with the level of injury severity for children on the struck side in the area of the intrusion (direct intrusion), with an overall increase in maximum injury severity towards higher intrusion. Although it should be noted that the 100-199mm band has more serious injury than might be expected. This is mainly linked to case inclusion criteria that are in lateral impact more than 200mm of intrusion on the compartment of the vehicle or  $\text{MAIS} \geq 2$  for at least one occupant. Lateral impact cases present in the CASPER database with less than 200mm of intrusion must have at least one  $\text{MAIS} \geq 2$  occupant which can be the child. Another explanation can be that if the intrusion occurs on the engine block (stiff structure – often low deformation) the level of deceleration for occupants is high and the risk of projection is increased, very often such impacts are combined with a large rotation of the vehicle as the impact occurs away from its centre of gravity, leading to other possibilities of impact location in the vehicle. In addition, the sample in the category of less than 200 mm of intrusion is low.

At over 300 mm of maximum intrusion, 68% of the 41 restrained children on the struck side are  $\text{MAIS} \geq 2$  children, 44% are  $\text{MAIS} \geq 4$  or have fatal injuries.

### Maximum injury severity by restraint type – Struck side

As this section addresses injury by body region and restraint type, restrained children with injuries not known or restraint type not known are excluded.

Figure 3-42 gives the proportions of restrained children (lateral impact – struck side) by restraint type that have an injury to each body region at the  $\text{MAIS} \geq 2$  level (body region). For example, of the 29 children in the dataset restrained in a shell system, 35% have a head injury of AIS 2 or above. The  $\text{MAIS} \geq 2$  (head) rate is therefore 35%. Likewise Figure 3-43 addresses  $\text{MAIS} \geq 3$  injury rates. Shell systems are rear and forward facing harness systems (including multidirectional 'convertible', 2 way child restraints). It is important to remember that this sample is not representative and that the sample size when broken down into categories is not very large for each group. An extreme example of this unrepresentativeness would be to note the high levels of head

injury to shell system restrained children. For each lateral impact that a child in a rearward facing child is involved in across Europe in a struck side position, there is not such a high chance (35%) of a head AIS ≥ 2 injury in every impact.

This analysis shows the general patterns of injury across the different restraint types. The neck, thorax and abdominal regions include the relevant region of the spine. ‘Head’ does not include the face. The MAIS ≥ 2 (external) rate is zero for all and not shown on the figures.

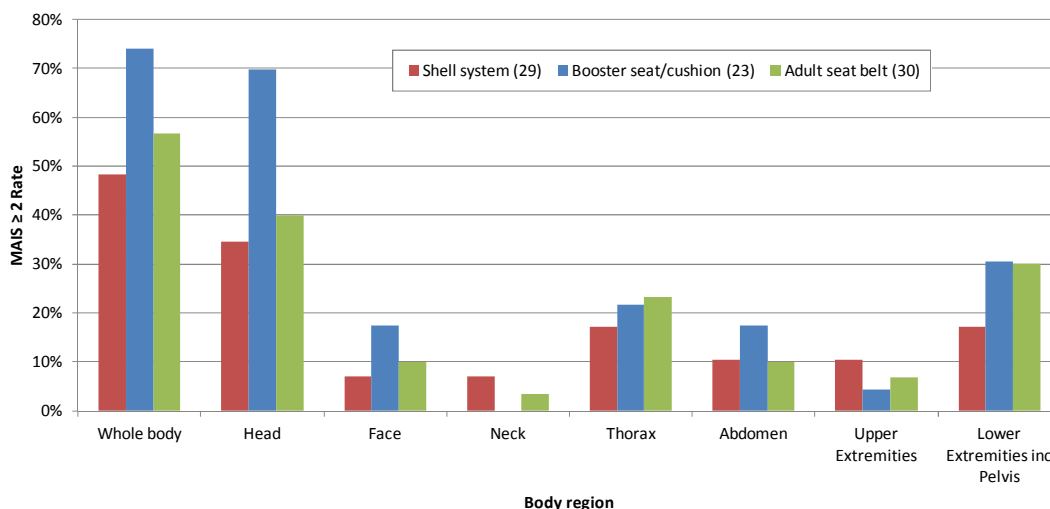


**Figure 3-42: Proportion of restrained children with an AIS ≥ 2 injury by body region and restraint type – Lateral impact, struck side, n=82**

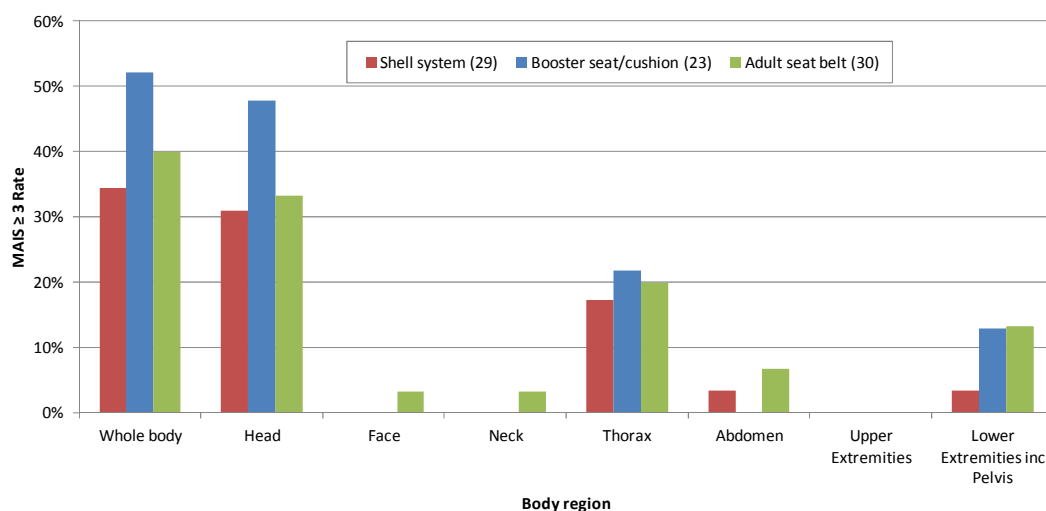


**Figure 3-43: Proportion of restrained children with an AIS ≥ 3 injury by body region and restraint type – Lateral impact, struck side, n=82**

**Shell System CRS** The head is the most seriously injured body region, followed equally by the thorax and lower extremities at the AIS ≥ 2 level and strongly by the thorax at the AIS ≥ 3 level.

**Booster seat/cushion** The rate of serious injury to the head is very high, in itself and compared to the shell system and adult seat belt restrained children. Abdominal injuries do feature at the AIS ≥ 2 level but at a lower rate than lower extremities and the thorax and equal to the face. At the AIS ≥ 3 level, injuries are only seen for the head, then thorax and lower extremities.



**Adult seat belts** The rate of serious injury to the head is slightly higher than for shell systems. At the AIS  $\geq 2$  level, lower extremity injuries have the second highest injury rate, followed by the thorax. This relationship between the lower extremities and the thorax is reversed at the AIS  $\geq 3$  level.

Globally, it can be said that shell systems seem to have lower rates of AIS  $\geq 3$  injuries than other systems and that the repartition of severe injuries across the body segments is similar for the different types of restraint systems: head, thorax and lower extremities.

The following sections look at each restraint type individually at an injury level rather than the maximum injury level for each body region.

### Injury to body regions by restraint type

#### Shell systems – Struck side

There are 29 children using shell systems with a harness, of which 4 are not injured. The simple distribution of age is given in Figure 3-44, showing a spread from new born to 4 years old.

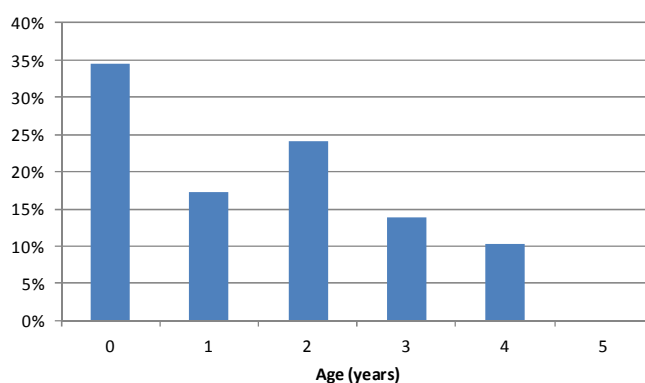


**Figure 3-44: Restrained child age distribution for shell systems – Lateral impacts, struck side, known injuries**

There are 25 injured children in shell systems with harness, sustaining 103 injuries of all severities. Of these children, 14 have AIS  $\geq 2$  injury(ies) with 46 AIS  $\geq 2$  injuries in total.

Figure 3-45 shows how the 46 individual AIS  $\geq 2$  injuries for shell system restrained children are distributed across the body regions. For example, 48% of all the AIS  $\geq 2$  individual injuries for this sample are to the head.

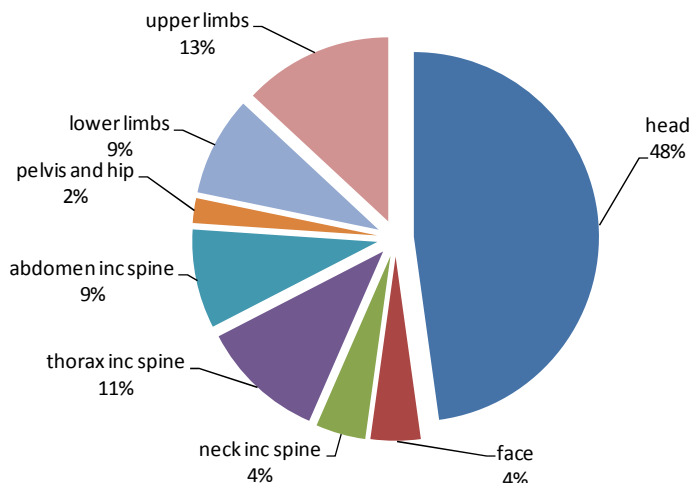


**Figure 3-45: AIS ≥ 2 Injury distribution – Non-struck side restrained children – Shell systems - 46 AIS ≥ 2 injuries in total**

As in Figure 3-42 and Figure 3-43 it is clear that the head is by far the most injured body region for the children in this sample, with 22 (48%) of the 46 AIS ≥ 2 injuries being to the head. Of these AIS ≥ 2 injuries 12 are brain injuries, 7 are fractures and 3 are crush or penetration injuries. Skull fracture is present for 3 casualties along with brain injury, whilst 6 casualties have just brain injury. Upper limbs represent the second body region with the most AIS ≥ 2 injuries, followed by the thorax and the lower limbs and abdomen equally. Of the 5 AIS ≥ 2 thoracic injuries, all involve lung contusion, there are no fractures.

All of the 10 casualties with AIS ≥ 2 head injury are sat in the rear of the car (5 on the left, 5 on the right). Regarding injury causation, known contacts are varied: window lateral (3), pillar B (1), object external to the vehicle (2), door panel (2), own kinematics (1).

**Booster systems – Struck side**

There are 23 children using booster systems, of which 2 are not injured. The simple distribution of age is given in Figure 3-46, showing a spread from 2 to 11 years old.

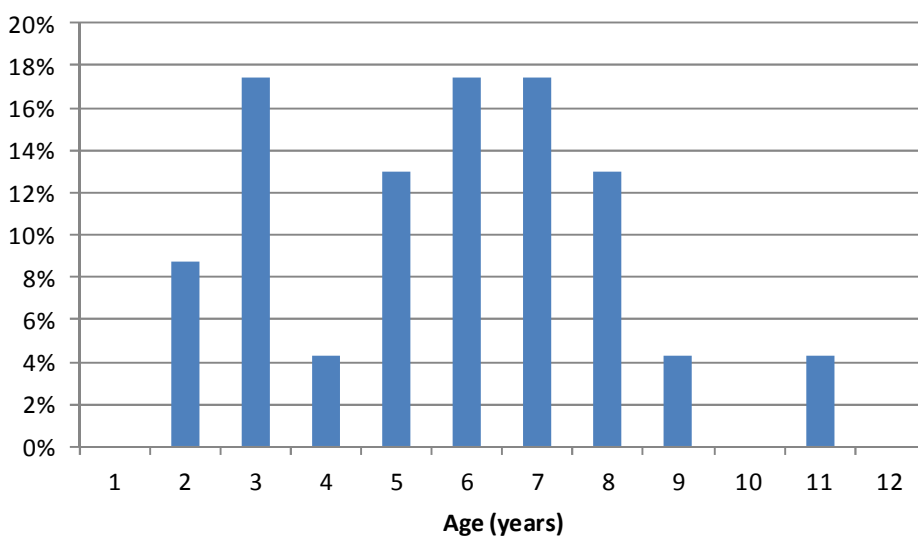


**Figure 3-46: Restrained child age distribution for booster systems – Lateral impacts, struck side, known injuries**

There are 21 injured children in booster systems, sustaining 130 injuries of all severities. Of these children, 17 have AIS  $\geq 2$  injury(ies) with 59 AIS  $\geq 2$  injuries in total.

Figure 3-47 shows how the 59 individual AIS  $\geq 2$  injuries for booster system restrained children are distributed across the body regions. For example, 54% of all the individual AIS  $\geq 2$  injuries for this sample are to the head.

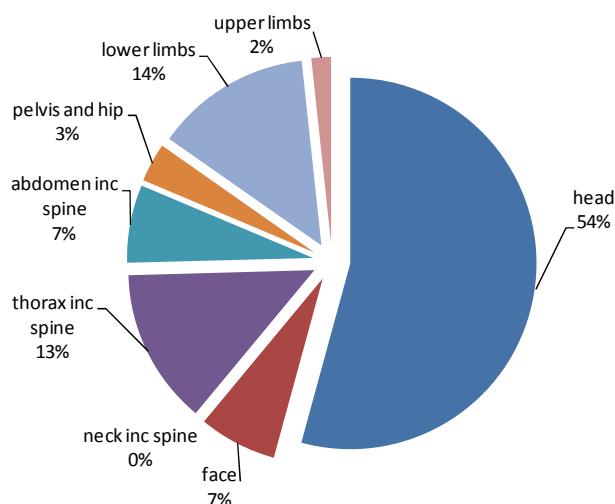


**Figure 3-47: AIS  $\geq 2$  Injury distribution for booster systems – Lateral impact restrained children - 59 AIS  $\geq 2$  injuries in total**

The head is by far the most injured body region for the children in this sample, with 32 (54%) of the 59 AIS  $\geq 2$  injuries being to the head. Of these AIS  $\geq 2$  injuries 23 are brain injuries, 8 are fractures and 1 is a crush or penetration injury. Skull fracture is present for 5 casualties along with brain injury, whilst 10 casualties have just brain injury. Compared with shell systems upper limb injuries decrease whilst lower limb increase.

Of the 16 casualties with AIS  $\geq 2$  head injury, 14 are sat in the rear of the car and 2 are front seat passengers. Regarding injury causation, known contacts are varied: window lateral (5), B pillar (1), C pillar (4), object external to the vehicle (1), door panel (2), own side (2).

The 5 casualties with AIS  $\geq 2$  thoracic injuries have those injuries attributed to the door panel in 3 cases and CRS in one case (1 unknown). Of the 8 AIS  $\geq 2$  thoracic injuries, 1 is a rib fracture and 1 is a crush injury. For the lower limbs the most frequent contact is with the door panel.

#### Only adult seat belt – Struck side

There are 30 children using only the adult seat belt, of which 3 are not injured. The simple distribution of age is given in Figure 3-48, showing a spread from 4 to 13 years old, although ages are concentrated in the 6 to 11 year old range, with a dip for 8 year olds.

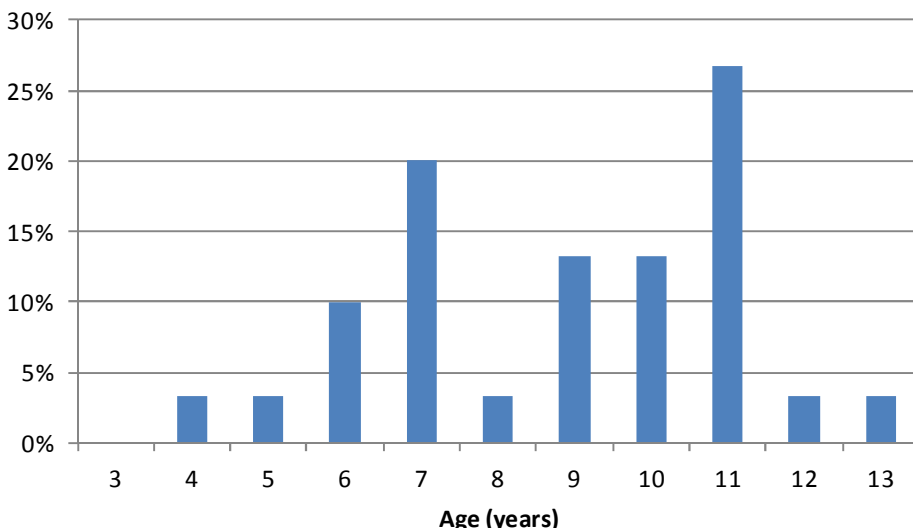


**Figure 3-48: Restrained child age distribution for just adult seat belts – Lateral impacts, struck side, known injuries**

There are 27 injured children using just adult seat belts, sustaining 149 injuries of all severities. Of these children, 17 have AIS ≥ 2 injury(ies) with 79 AIS ≥ 2 injuries in total.

Figure 3-49 shows how the 79 individual injuries for restrained children using just the adult seat belt are distributed across the body regions. For example, 49% of all the individual AIS ≥ 2 injuries for this sample are to the head.

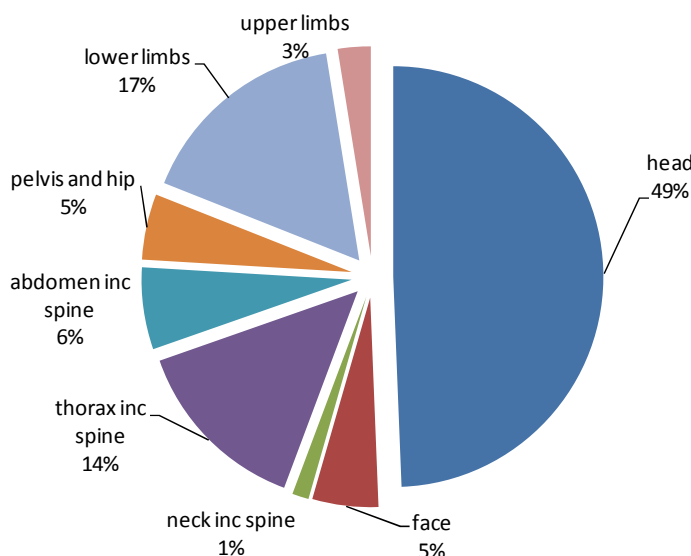


**Figure 3-49: AIS ≥ 2 Injury distribution for just adult seat belts – Lateral impact restrained children - 79 AIS ≥ 2 injuries in total**

Compared to frontal impacts, where for children just using the adult seat belt the injured body regions become more distributed than for the dedicated CRS, a similar pattern is seen in Figure 3-49 to booster systems for lateral struck side impacts, with half the AIS ≥ 2 being to the head and lower limb injuries being prominent. Compared with shell systems upper limb injuries decrease whilst lower limb increase (as with booster systems).

Of the 39 AIS  $\geq 2$  head injuries 32 are brain injuries and 7 are fractures. Skull fracture is present for 5 casualties along with brain injury, whilst 7 casualties have just brain injury.

Of the 12 casualties with AIS  $\geq 2$  head injury, 6 are sat in the rear of the car and 6 are front seat passengers. Regarding injury causation, known contacts are varied: window lateral (1), roof (1), object external to the vehicle (4), door panel (1). For the lower limbs the most frequent contact is with the door panel although contacts for limbs are also often unknown. The 7 casualties with AIS  $\geq 2$  thoracic injuries have those injuries attributed to the door panel in 4 cases and own side in 1 case (2 unknown). Of the 11 AIS  $\geq 2$  thoracic injuries, 3 are fractures.

### Maximum injury severity by restraint type – Non-struck side

As this section addresses injury by body region and restraint type, restrained children with injuries not known or restraint type not known are excluded.

Figure 3-50 gives the proportions of restrained children (lateral impact – non-struck side) by restraint type that have an injury to each body region at the MAIS  $\geq 2$  level (body region). For example, of the 14 children in the dataset restrained in a shell system, 14% have a head injury of AIS 2 or above. The MAIS  $\geq 2$  (head) rate is therefore 14%. Likewise Figure 3-51 addresses MAIS  $\geq 3$  injury rates. Shell systems are rear and forward facing harness systems (including multidirectional ‘convertible’, 2 way child restraints).

It is important to remember that this sample is not representative. An extreme example of this would be to note the high levels of head injury to shell system restrained children. For each lateral impact that a child in a rearward facing child is involved in across Europe in a non-struck side position, there is not such a high chance (14%) of a head AIS  $\geq 2$  injury in every impact.

This analysis shows the general patterns of injury across the different restraint types. The neck, thorax and abdominal regions include the relevant region of the spine. ‘Head’ does not include the face. The MAIS  $\geq 2$  (external) rate is zero for all and not shown on the figures.

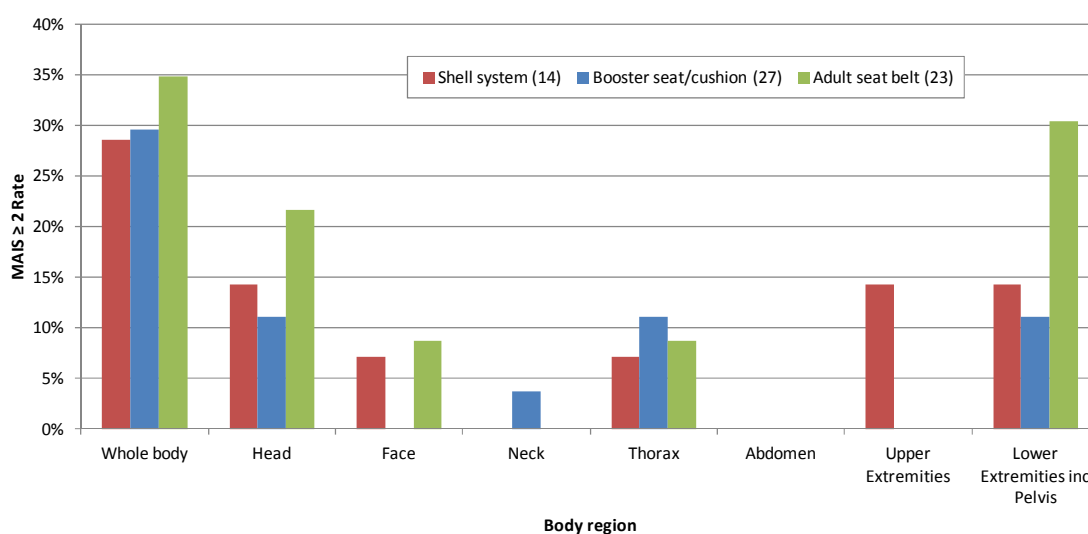


**Figure 3-50: Proportion of restrained children with an AIS  $\geq 2$  injury by body region and restraint type – Lateral impact, non-struck side, n=64**

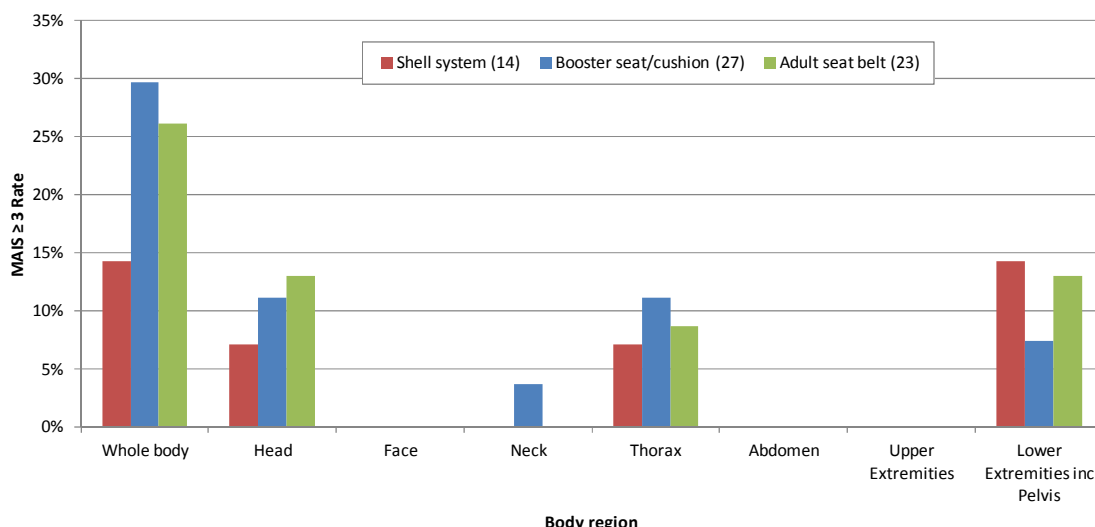


**Figure 3-51: Proportion of restrained children with an AIS ≥ 3 injury by body region and restraint type – Lateral impact, non-struck side, n=64**

**Shell System CRS** The number of children is low with only 14 in the sample. The rate of AIS ≥ 2 injury to both the lower and upper extremities is equivalent to that for the head. At the AIS ≥ 3 level, upper extremity injuries fall away leaving the highest rate for lower extremity injuries.

**Booster seat/cushion** The rate of AIS ≥ 2 injury to both the lower extremities and thorax is equivalent to that for the head. At the AIS ≥ 3 level, thoracic and the head give the highest rate of injury.

**Adult seat belts** In this sample, the rates of head and lower extremity injuries are high at both AIS ≥ 2 and AIS ≥ 3 levels, followed by thoracic injuries.

The following sections look at each restraint type individually at an injury level rather than the maximum injury level for each body region.

**Injury to body regions by restraint type**

**Shell systems – Non-struck side**

There are 14 children using shell systems with a harness, of which 4 are not injured. The simple distribution of age is given in Figure 3-44, showing mainly children under 1 year old to 2 years old.

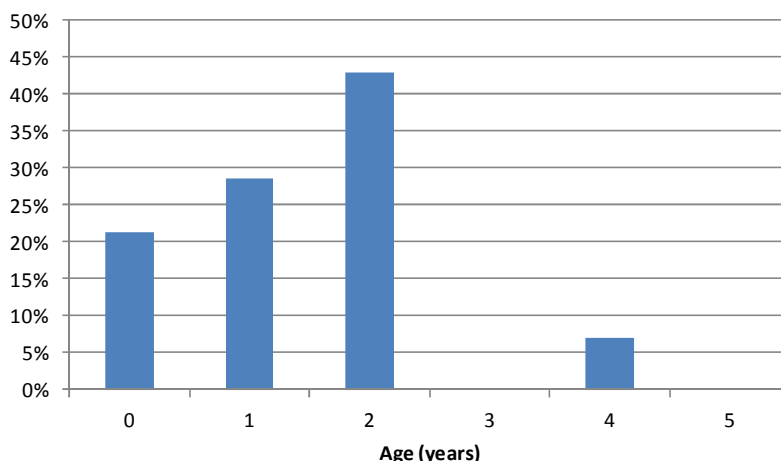


**Figure 3-52: Restrained child age distribution for shell systems – Lateral impacts, non-struck side, known injuries**

There are 10 injured children in shell systems with harness, sustaining 22 injuries of all severities. Of these children, 4 have AIS ≥ 2 injury(ies) with 9 AIS ≥ 2 injuries in total. Figure 3-53 shows how the 9 individual AIS ≥ 2 injuries for shell system restrained children are distributed across the body regions. For example, 22% of all the AIS ≥ 2 individual injuries for this sample are to the head.

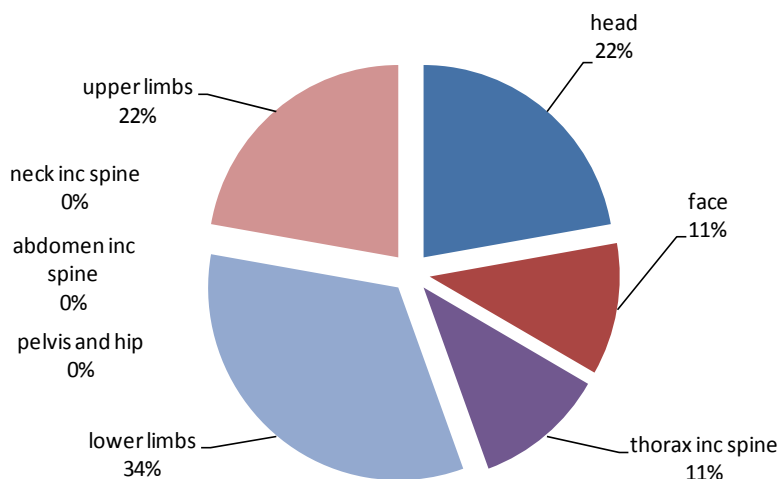


**Figure 3-53: AIS ≥ 2 Injury distribution – Non-struck side restrained children – Shell systems - 9 AIS ≥ 2 injuries in total**

The number of individual AIS ≥ 2 injuries is small and only applies to 4 children. In this sample the injuries are distributed five body regions, with extremities combined at the highest number.

**Booster systems – Non-struck side**

There are 27 children using booster systems, of which 6 are not injured. The simple distribution of age is given in Figure 3-54, showing a spread from 2 to 11 years old.

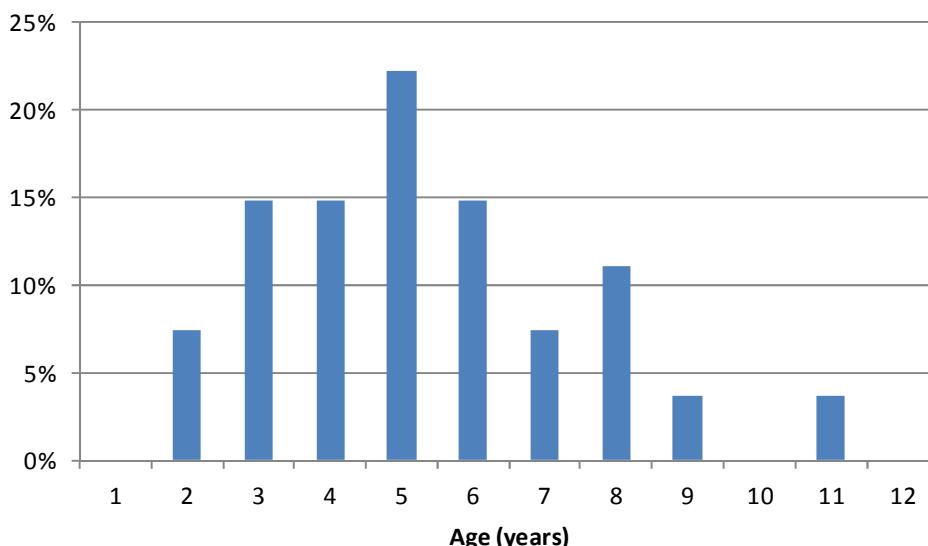


**Figure 3-54: Restrainted child age distribution for booster systems – Lateral impacts, non-struck side, known injuries**

There are 21 injured children in booster systems, sustaining 51 injuries of all severities. Of these children, 8 have AIS ≥ 2 injury(ies) with 13 AIS ≥ 2 injuries in total.

Figure 3-55 shows how the 13 individual AIS ≥ 2 injuries for booster system restrained children are distributed across the body regions. For example, 46% of all the individual AIS ≥ 2 injuries for this sample are to the head.

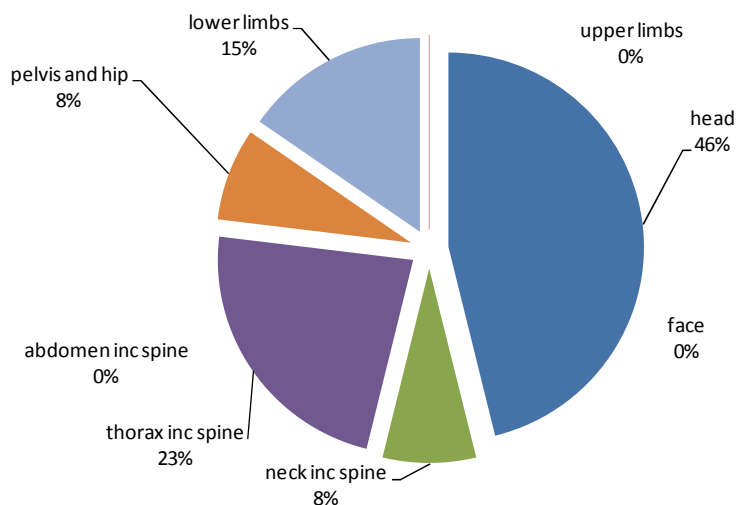


**Figure 3-55: AIS ≥ 2 Injury distribution – Non-struck side restrained children – Booster systems - 13 AIS ≥ 2 injuries in total**

The number of individual AIS ≥ 2 injuries is small and only applies to 8 children. In this sample the injuries are distributed across the body regions, with the head having the highest number.

**Only adult seat belt – Non-struck side**

There are 23 children using only the adult seat belt, of which 6 are not injured. The simple distribution of age is given in Figure 3-56, showing a spread from 3 to 13 years old, although ages there are peaks at 10 and 11 years olds.



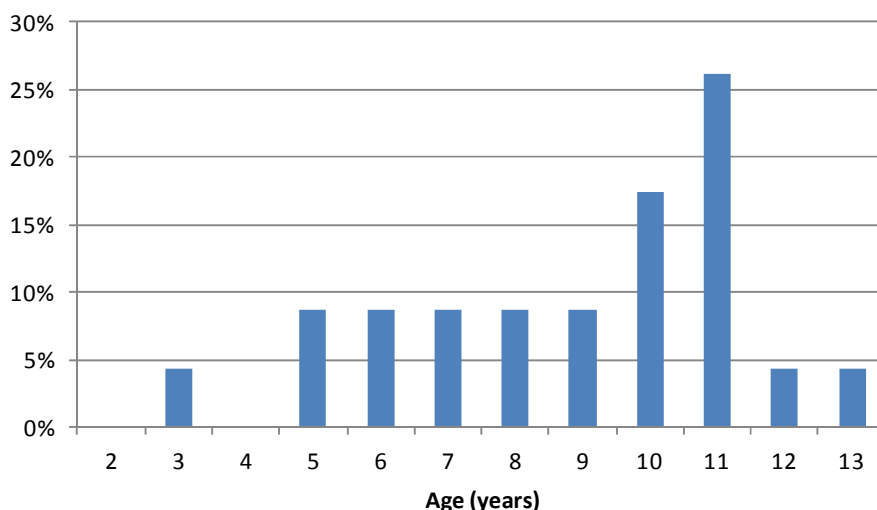


**Figure 3-56: Restrainted child age distribution for just adult seat belts – Lateral impacts, non-struck side, known injuries**

There are 17 injured children using just adult seat belts, sustaining 49 injuries of all severities. Of these children, 8 have AIS ≥ 2 injury(ies) with 22 AIS ≥ 2 injuries in total. Figure 3-57 shows how the 22 individual injuries for restrained children using just the adult seat belt are distributed across the body regions. For example, 45% of all the individual AIS ≥ 2 injuries for this sample are to the head.

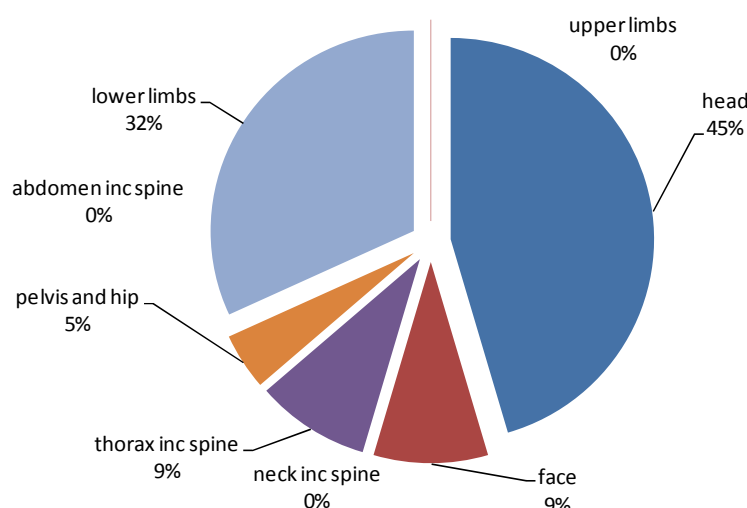


**Figure 3-57: AIS ≥ 2 Injury distribution for just adult seat belts – Lateral impact restrained children - 22 AIS ≥ 2 injuries in total**

The number of individual injuries is small and only applies to 8 children. In this sample the injuries to the head are the most numerous, followed by the lower limbs.

**Non-struck side - Injury causation**

Examining the whole non-struck side sample. The 10 children with AIS ≥ 2 head injuries have the following known contacts; B pillar (1), object internal to the vehicle (1), door panel (2) and seat backrest (1). The 10 children with lower extremity AIS ≥ 2 injuries have the following known contacts: luggage (1), other occupant (1), door panel (1) and seat backrest (4). Of the 6 AIS ≥ 2 thoracic injuries, 5 involve lung contusion and 1 is a spinal injury, cord contusion with dislocation due to own kinematics. Contacts for the lung contusions are various: Safety belt, CRS, other occupant (twice) and CRS.

Looking at the injury distribution through the different types of restraint systems in Figure 3-51, it is seen that the head that is better protected in shell systems than with other systems on the non-struck side. This is likely to be due to children in such systems being linked to the CRS with a harness and that the CRS movement is limited when the seatbelt route is correct. The scenario with boosters and only adult seat belt can be an escape from the restraint system of the upper part of the child. This can lead to a higher displacement and then more risk for sustaining a head impact again a rigid part of the car or be placed into the area where the intrusion is occurring.

### 3.1.6 Safety technologies

To maximise the data regarding safety technologies the CREST, CHILD and CASPER are used in this Section.

Whilst it would be beneficial to be able to indicate the effectiveness of safety technologies such as pretensioners, load limiters and airbags in reducing injury the numbers in the database when spread across crash situation (type and severity), presence of misuse, child age and restraint type make it difficult. Here a statement is made regarding the information in the accident database regarding safety technologies. It is more likely that experiences here can be put with reconstruction or misuse testing results to start to form a more complete picture of the effectiveness of safety technologies (car or CRS) for restrained children.

No evaluation of primary safety systems has been made or is possible with the road accident database. Also no causation analysis is undertaken. The main focus of the road accident database is to collect information on secondary (passive) safety aspects for restrained children.

Safety technologies are often introduced primarily to protect adult occupants and the benefit or problems for children travelling in these seating positions equipped with these safety functions is not one of the first considerations. This can lead to the following situations:

- Safety benefit also for children;
- No benefit for children, but also no danger;
- Dangerous situation due to the safety function.

### Seat belt technologies

#### Front and rear passenger compartments

As part of the introduction of airbags and associated crash structures (EuroNCAP era) restraint systems often also incorporate pretensioners and load limiters - but often only in the front seats. This is shown in Figure 3-58. Side airbags refer to door or (more often) seat mounted side airbags. Head airbags refer to side mounted airbags in the roof rail (tube or curtain).

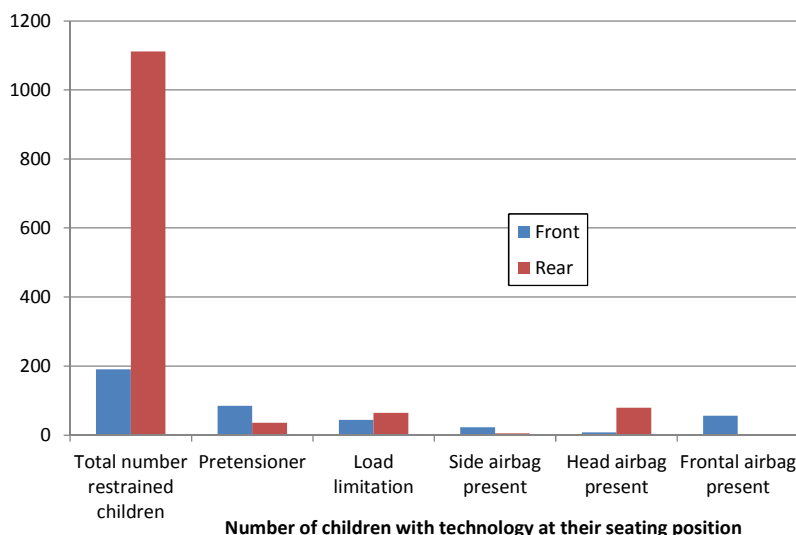


**Figure 3-58: Number of restrained children with certain technologies present at their seating position**

Although the majority of children are in the rear rows of seats (85%) this proportion is not reflected in the technologies present at children’s seating positions.

**Airbags**

**Disabled frontal airbags**

In the database it has been recorded that frontal airbags (all in the front seats) have been disabled for 6 child occupants, in all cases with rear facing CRS. There are 15 occasions recorded in the database of a frontal airbag and a rear facing CRS. In 8 cases the frontal airbag has deployed, in 1 case it did not deploy as the impact was lateral rather than frontal and it has been disabled in 6 cases.

There is one example of CPOD transponder technology (Child Seat Presence and Orientation Detection) in the accident database. It has proved effective in disabling the passenger frontal airbag in a 50 km/h (EES) frontal impact where a rear facing infant carrier was present. There were no injuries to the child.

**Deployed frontal airbags and rear facing CRS**

There are 8 cases with a deployed frontal airbag and a rear facing CRS, with all children in the front passenger position. In 7 of the cases the EES is below 45 km/h with no intrusion of the passenger compartment. In the other case (number 4 in Table 3-11) the EES was 72 km/h but with no intrusion to the front passenger area. The eldest being 8 months old, 3 of the children died and 5 survived. Figure 3-11 gives a summary of the highest head injury severities recorded for these 8 children.

**Table 3-11: Injury summary – rear facing children with deployed frontal airbag**

Child	Highest AIS severity	
	Brain injury	Skull fracture
1 - killed	6	2
2 - survived	4	-
3 - survived	4	2
4 - survived	4	-
5 - survived	4	3
6 - killed	4	3
7 - killed	5	4
8 - survived	3	2

Table 3-11 shows that each child had injury or injuries to the brain, 6 of them also reported as having skull fracture. Like the general rear facing sample injuries are characterised by a lack of injury to other body regions away from the head. All these injuries are attributed to contact with the deploying frontal airbag.

#### Deployed frontal airbags and forward facing children

There are 35 instances of a deployed frontal airbag and a known forward facing restrained child. Of these, 27 occurred in frontal impacts (where the predominate impact causing injury has been recorded as frontal) - 20 adult seat belts, 2 forward facing harness CRS and 5 Booster seat/cushion).

The highest severity injury that has been recorded to contact with a deployed frontal airbag is to 4 year old in a group 1 harness system. The AIS 4 pulmonary contusion (bilateral) is attributed to the deploying airbag but is it noted that also harness contact could have made a contribution to the injury. This was the only AIS  $\geq 3$  injury and the child survived. The EES of the head on impact with another car was 70 km/h and the delta v was 79 km/h (maximum deformation of 920 mm) with intrusion to the passenger compartment starting. This is a substantial impact and without the airbag deployment, head excursion to the dashboard may have occurred with associated head injury being possible. Further detail in the case shows that the CRS was badly damaged during the impact with failure of the structure. The airbag therefore may have paid a part in the protection of the child from worse injury.

**Figure 3-59: Views of seating position and general state of CRS after the accident**

## Side airbags

### *Seat or door mounted*

There are 8 instances of a deployed side airbag in a position with a restrained child (6 with adult seat belts and 2 in rear facing CRS). One child is in the rear. Of these, 3 occurred in frontal impacts and 5 in lateral impacts (the predominate impact causing injury being recorded). Of the 5 children involved in a lateral impact, only 1 has AIS 3 level injuries, which is a relatively low number in regard with the general severity of this database. Additional investigations could be conducted, examining each case with side airbag deployment and making comparison to another child of a similar age, restrained in the same type of CRS with similar intrusion but with no airbag fitted. This would be a way to estimate the safety benefit of the combination of 'car and side airbag'. This activity will be done in further analysis as it is very time consuming to find the correct case without any guarantee of sound results.

### *Head level (tube or curtain)*

There are more instances (23) of a deployed head level side airbag in a position with a restrained child than a seat or door mounted airbag as these systems often cover the front and rear passenger compartments. Of these, 13 occurred in frontal impacts and 10 in side impacts (the predominate impact causing injury being recorded). Eleven children are restrained with adult seat belts, 1 in rear facing CRS, 6 in forward facing harness CRS and 5 using a booster seat/cushion. There are no injuries attributed to head level side airbag deployment. The same work will be conducted as for seat or door mounted side airbags in order to check that the airbag deployment is not the origin of injuries of children and to investigate safety benefit.

## Child restraint systems

### Integrated CRS

There are 6 children restrained with integrated booster systems in the database, 2 are in the same vehicle. Two are in lateral impacts and 4 in frontal impacts. It is therefore difficult to conduct an analysis of such systems with such low numbers. No failure of integrated CRS has been reported and no misuse has been mentioned.

### ISOFIX

The number of child occupants using ISOFIX to restrain their child restraint in the accident database is low at 7, with 3 of these children in the same vehicle. All cases with children using ISOFIX are in the CASPER dataset (rather than the earlier datasets). Surprisingly, given that they are a relatively recent addition to the CRS market, 6 of the 7 children are restrained in ISOFIX booster seats, and one in a forward facing harness system.

### 3.1.7 Comparison of injury recording systems

#### Background

The previous CREST and CHILD projects used the AAAM AIS90 system for recording injuries. At the beginning of the CASPER project it was decided that all previous cases would be changed from AIS90 to AIS98, and AIS98 would become the primary injury recording system for CASPER. Additionally, when possible, all new CASPER cases would be coded to AIS2005 (updated 2008) for child occupants. This would be an exploration of the most recent AIS injury recording system whilst keeping the link with previous cases and the injury risk curve work already undertaken.

In the following two sections, overall comparisons are made regarding the injury recording systems. The first evaluates the change from AIS90 to AIS98 as the primary

recording system and the second an indication of the level of change, in comparison to AIS98, if using AIS2005 in the future as the primary injury system.

### Change from AIS90 to AIS98

#### Main considerations

It was thought that for children the major change from AIS90 to AIS98 would be for femur fractures. In AIS90, 5 AIS codes are available that can reduce the AIS severity score from 3 to 2 for occupants below 12 years old (femur not further specified, condylar, shaft, subtrochanteric and supracondylar). The below 12 years old codes are not available in AIS98 and therefore no severity score reduction takes place. Away from age specific codes other main changes are (from AIS90 to AIS98):

- AIS severity for heart contusions reduced from AIS 3 to AIS 1 (441099, 441002 and 441004);
- AIS severity for certain duodenum laceration codes reduced from AIS 3 to AIS 2 (541020 and 541022);
- Flail chest (unstable chest wall) not further specified is reduced from AIS 4 to AIS 3;
- Rib cage fracture NFS (not further specified) (450210) AIS 1 changes to multiple rib fractures not further specified AIS 2 (same code).

In each body region in AIS98, codes are available with AIS 9 severity scores that reflect that it is known that some injury has occurred in that region but the injury is not known. These codes are not available for all body regions in AIS90. Codes are also added in AIS98 for death without specific injury information. For example, 115999.9 – Died without further evaluation; no autopsy, which builds upon 115099.9 – closed head injury NFS (Use also for traumatic brain injury NFS).

#### Maximum abbreviated injury score (MAIS)

Injuries in only the CREST and CHILD datasets were recorded with AIS90. Therefore the comparison here of AIS90 and AIS98 selects only the CREST and CHILD datasets and children that are restrained with known MAIS. Children with MAIS unknown are excluded even if it is known that injuries were fatal.

Figure 3-60 and Figure 3-61 show the Maximum Abbreviated Injury Score for the same set of CREST and CHILD restrained children under the AIS90 and AIS98 injury recording systems.

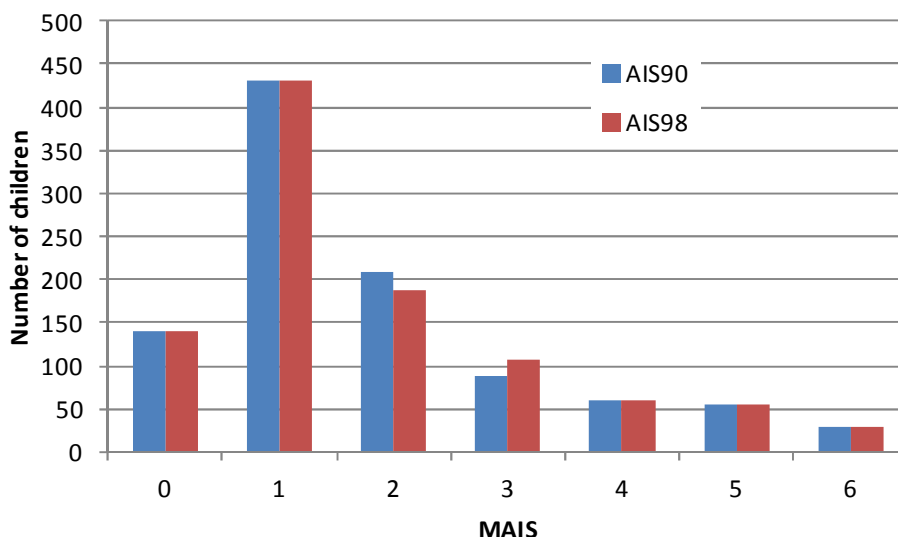


**Figure 3-60: MAIS severity by recording system (1008 restrained children)**

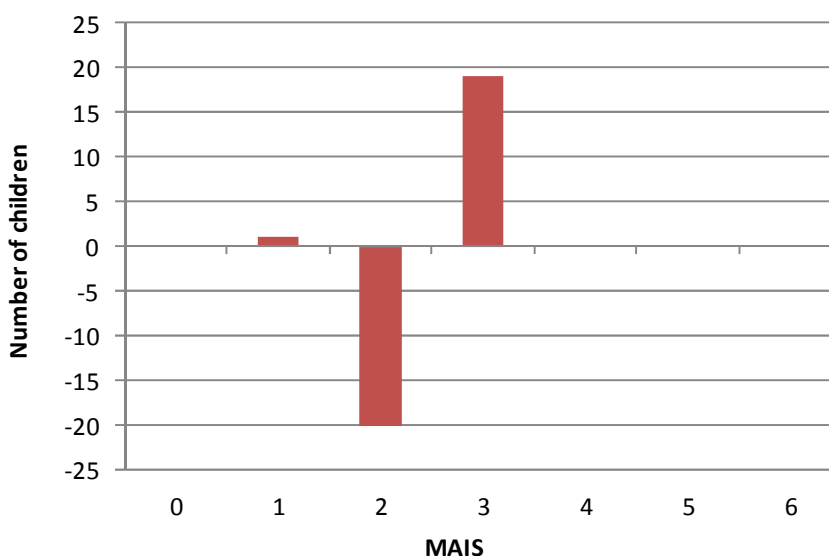


**Figure 3-61: MAIS severity differences AIS90 and AIS98 (1008 restrained children)**

In Figure 3-61 the columns indicate the situation in AIS98 compared to AIS90. For example, there are 19 more MAIS 3 children in the sample when using the AIS98 system than in AIS90. Differences can clearly be seen between the MAIS 2 and 3 levels and one child has a MAIS changed to 1. Although across this number of children (1008) only 20 are affected, which is a small proportion.

**MAIS by body region**

To find which body regions are causing the differences shown in Figure 3-60 and Figure 3-61, Figure 3-62 illustrates the MAIS ≥ 3 rate by body region – the proportion of children with AIS ≥ 3 injuries in each body region.

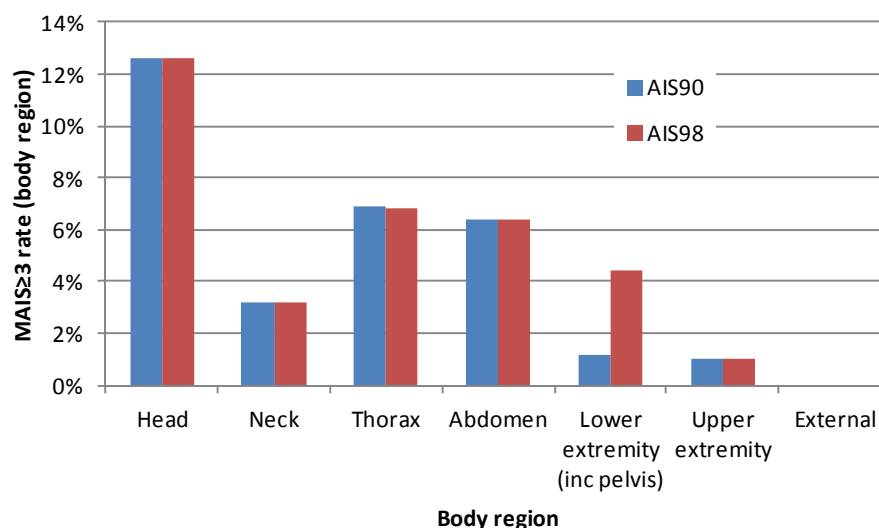


**Figure 3-62: MAIS  $\geq$  3 (body region) by recording system (1008 restrained children)**

Figure 3-62 shows that the majority of the difference between the recording systems is shown to be in the lower extremities, with an increase for AIS98. Inspection of the cases shows these injuries to be femur fractures. There is a decrease in AIS severity (from AIS90 to AIS98) for one restrained child in the thoracic region. This is a reduction in heart contusion from AIS 3 to AIS 1 (441002).

### Comparison of AIS98 and AIS2005

#### Main considerations

There are major differences between the AIS98 and AIS2005 (updated 2008) injury recording systems, changes that are much more pronounced than those between AIS90 and AIS98.

In AIS90 there are 1,331 individual injury codes, in AIS2005 this number increases to 2,104 (Barnes 2009). Overall, not concentrating on any particular body region, changes are introduced both in actual injury severity levels for individual injuries and reflecting the level of detail required from the medical information to be able to code an injury to a particular severity level.

The first major set of changes consider advances in medical care that lower the threat to life of particular injuries. The second set of changes is a consideration that more detailed injury information is often required in AIS2005 to assign a certain severity level than in AIS98. For example, cerebrum intraventricular hemorrhage (140678) is AIS 4 in AIS98. But in AIS2005 just this knowledge of the injury allows only AIS 2 to be recorded. If associated coma of over 6 hours is known then AIS 4 can be recorded. In this overview it is not possible to cover the many changes but, as an example, one injury that does appear often in the dataset is 'concussion', which is AIS 2 in AIS98 but in AIS2005 if no time of unconsciousness is available (NFS) then the injury is AIS 1.

#### Maximum abbreviated injury score (MAIS)

All child occupants in the CASPER dataset were recorded with both AIS98 and AIS2005 injuries. Many children in the CHILD dataset have also been coded with AIS2005 injuries.

There are 452 restrained child occupants recorded in the database with information for both AIS 98 and AIS2005 systems, with 87 uninjured (MAIS 0) and 51 having unknown



injuries (MAIS 9). The comparison here selects only the restrained children with known MAIS. Children with MAIS unknown are excluded even if it is known that injuries were fatal.

Figure 3-60 and Figure 3-61 show the Maximum Abbreviated Injury Score for the same set of CHILD and CASPER restrained children under the AIS98 and AIS2005 injury recording systems.

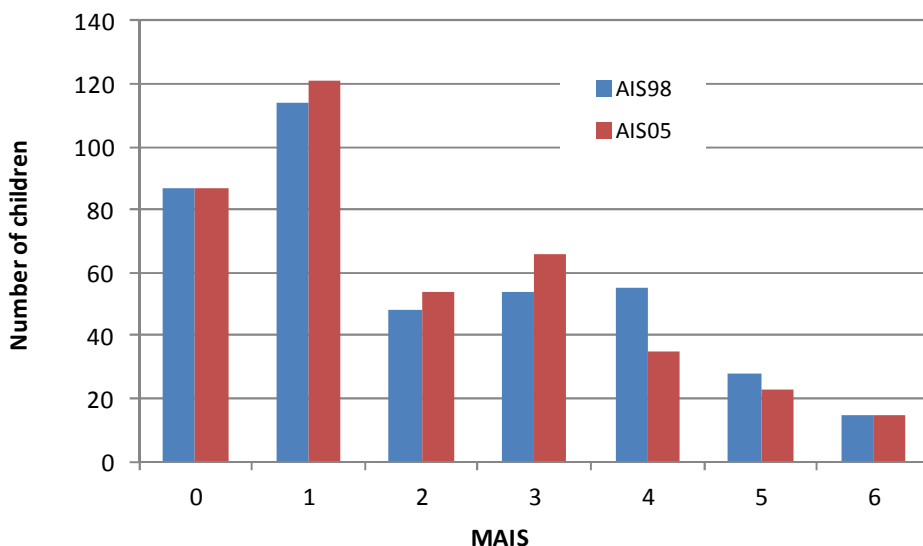


**Figure 3-63: MAIS severity by recording system (401 restrained children)**

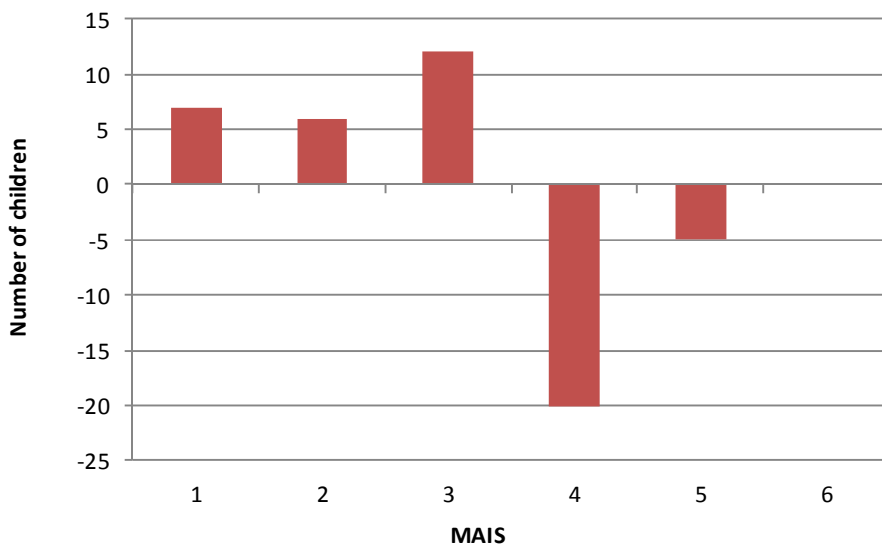


**Figure 3-64: MAIS severity differences AIS98 and AIS2005 (401 restrained children)**

In Figure 3-64 the columns indicate the situation in AIS2005 compared to AIS98. For example, there are less MAIS 4 children in the sample when using the AIS2005 system than in AIS98. A shift from MAIS 4 and MAIS 5 to lower MAIS values can be seen, involving 25 of the 316 children.

AIS severity by injury

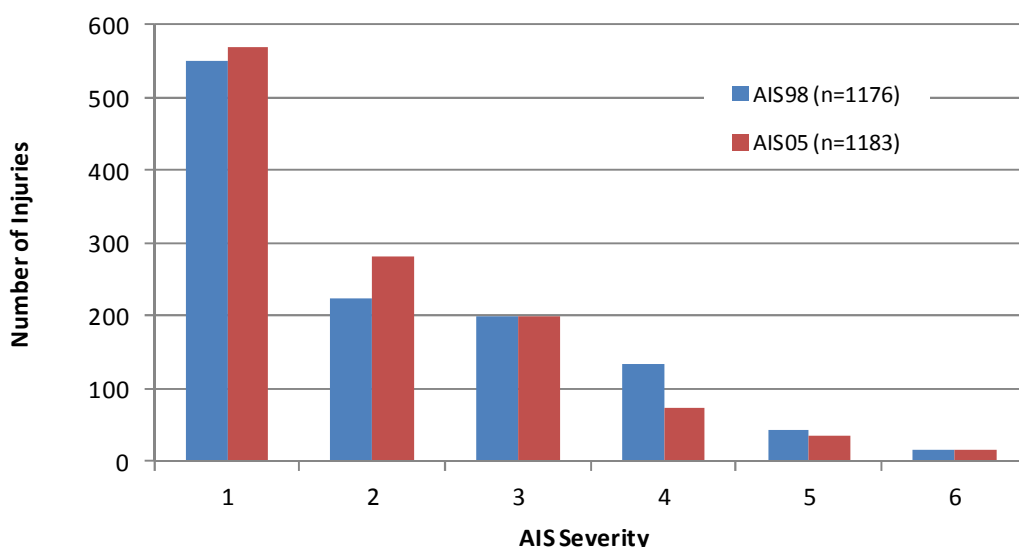


**Figure 3-65: AIS severity for all injuries by recording system (401 restrained children)**

Figure 3-66 shows the differences at each AIS severity point between the AIS98 and AIS2005 recording systems. As an example there are 61 less AIS 4 injuries recorded in the AIS2005 system than the AIS98 system for the same group of 401 restrained children (with some injury).

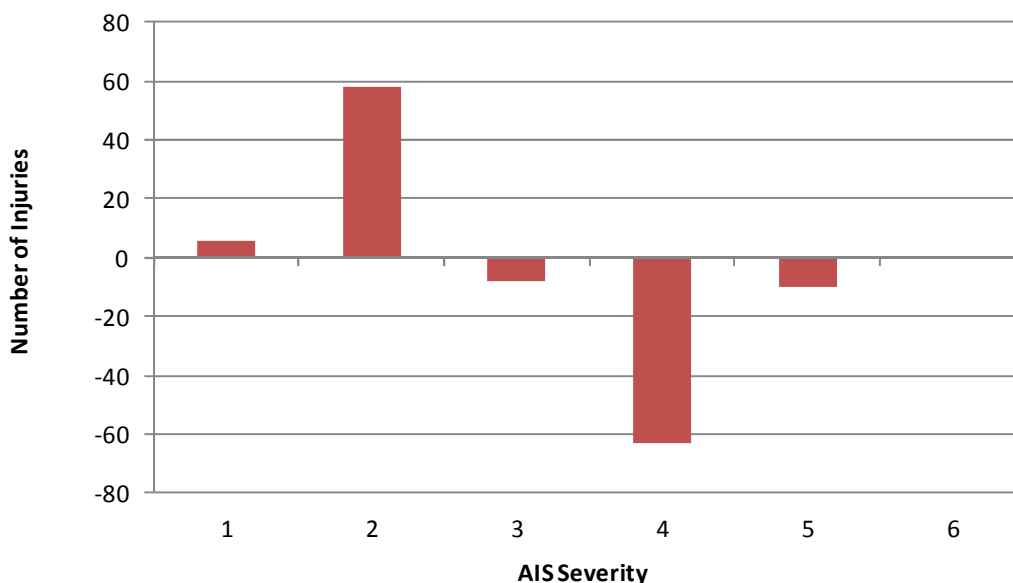


**Figure 3-66: AIS severity differences for all injuries between AIS98 and AIS2005 (401 restrained children)**

In Figure 3-66 the columns indicate the situation in AIS2005 compared to AIS98. For example, there are more AIS 2 injuries for this sample when using the AIS2005 system than in AIS98 and less AIS 4 injuries.

MAIS by body region

The largest difference in injury severity in Figure 3-66 is seen between AIS 2 and AIS 4. Therefore, to find which body regions are causing the differences, Figure 3-67

illustrates the MAIS  $\geq 3$  rate by body region – the proportion of children with AIS  $\geq 3$  injuries in each body region.

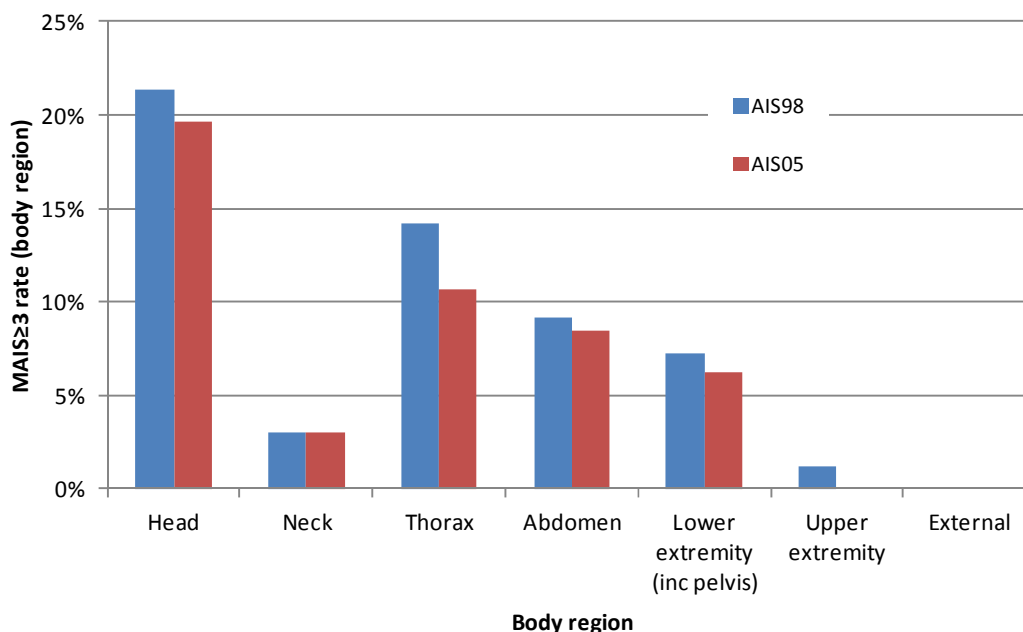


**Figure 3-67: MAIS  $\geq 3$  (body region) by recording system (401 restrained children)**

Figure 3-67 shows that the differences between the recording systems is shown to be in the spread across the body regions but in particular the largest percentage drop is for thoracic injuries. Looking at the actual thoracic injuries that have decreased in AIS severity from being AIS 3 in AIS98, the majority involve lung contusion, with unilateral ‘not further specified’ and ‘minor’ reducing to AIS 2 in AIS2005. Similarly, but in lower numbers, pneumothorax also features, especially ‘not further specified’ (442202) which reduces to AIS 2 in AIS2005.

Of the 8 head injuries reduced from AIS  $\geq 3$  in AIS98 to below AIS 3 in AIS2005; 4 are cerebrum intraventricular hemorrhage (AIS 4 to 2), 2 are cerebrum subarachnoid hemorrhage –one slight and one not associated with coma - (AIS 3 to 2) and 2 are cerebrum hematoma petechial hemorrhages - not further specified - (AIS 3 to 2).

### 3.1.8 Discussion and conclusions

#### Methodology

Whilst the in-depth investigation of collisions involving restrained children is complex, with the addition of dedicated restraint systems adding a layer of investigation compared to studying adults, it is believed that the process used of group discussion gives the best opportunity to ensure consistency and the best quality of information possible. By establishing the parameters to be collected at the start, with a common database, teams are able to focus on important considerations whilst carrying out the investigations and seek advice from the wider group when required. Crash severity and injury mechanisms in particular benefit from this approach of the combined groups’ experiences.

#### Sampling

As made clear during this report the cases found in the CASPER dataset are not proportionally representative of the accident situation across Europe, or in individual countries. Cases are collected to reflect the scientific aims of the project regarding new injury criteria and being sufficient in detail to accurately replicate the crashes in full

scale physical reconstructions or virtual simulations with a high degree of confidence. The case selection criteria and the severity of the impacts limits the conclusions that can be drawn from analysis of the database but as long as these limitations are kept in mind the accident is important for identifying the body regions that are being injured in different types of CRS.

### Quality of restraint use

The consideration of misuse remains a challenge and the knowledge continues to grow with the collection of further accident cases, experiences from field surveys and sled testing. In particular it can be difficult to appreciate low level misuse (for example, small amounts of slack), especially in low severity impacts, and to separate injury outcome from normal crash circumstance and injury outcome from misuse in high severity crashes.

The overall rate of misuse identified (16%) in frontal impacts is lower than figures found in misuse field studies (surveys and checking days). It is likely that at best the database is considering severe misuse, rather than being able to highlight slight misuse. In the sample most misuse is seen for rear facing infant carriers. This is due to the clear misuse of the CRS being in the place of a deployed frontal airbag, leading to serious injury. For forward facing CRS with harness, misuse situations are well defined and can be found from evidence during investigation, for example, poor seat belt routing (in situ or from marks on CRS), incorrect harness strap height. For booster systems and just the adult seat belt, the restraint situation between the CRS and car and between the seat belt and child is lost. So, although of course there are still possibilities to identify misuse from CRS marks and injuries, the possibilities are less. The lower rates identified for booster and seat belts may also correspond with fewer possibilities for misuse errors as the restraint systems become less complex.

Care has been taken in the group, and should be taken into consideration in similar future activities, that misuse can still be present but the evidence is not available. This can be both practically, for example the CRS is not present during investigation, or crash severity is too low for misuse to be apparent.

Inappropriate use is difficult to analyse fully when height or weight are often unknown during data collection, leading age to be relied upon as an estimation of appropriate use (when height and/or weight are not known). The approach taken in CASPER of a set of rules for the coding of appropriate use is recognised as being limited when height or weight are not known, but is thought to be the best approach possible with data collection across multiple teams (consistency is ensured) and when no further information is available.

## Frontal impacts

### Overall

There are 450 restrained children in the dataset in frontal impacts with type of restraint and injuries known (or it is known that no injury has occurred). Of these children, 45% have a MAIS  $\geq 2$  and 25% have a MAIS  $\geq 3$ . There are a further 19 restrained children with fatal injuries but the actual injuries by AIS and body region are not known.

There is a general trend for a shift in cumulative EES % graph towards higher EES for higher overall injury level, as expected. Of the MAIS  $\geq 3$  children or those with fatal injuries, approximately half are in a vehicle for which the EES is over 60 km/h and approximately 25% over 70 km/h, exceeding the design criteria of cars and CRS (UN Regulation 44 frontal impact test conditions).

Selecting MAIS  $\geq 3$  children or those with fatal injuries and filtering by whether misuse is identified, shows that the cases with misuse identified are shifted towards a lower EES distribution than cases with no misuse identified. The difference is less apparent at higher EES values as the effect of misuse is likely to be more masked at higher severity as the natural effects of higher severity - higher loads on the body and intrusion - play a larger role. Overall, there are higher MAIS  $\geq 2$  injury levels for restrained children in the sample where it has been possible to identify misuse, compared to those restrained children with misuse not identified.

The same relationship is not apparent for appropriate use. This may be due to the definitions of inappropriate injury used, especially when weight and/or height are not known. In particular the recording of restrained child up to and including 11 years old being inappropriately restrained in just the adult seat belt (where otherwise no information is known regarding weight and/or height) is quite strict.

### Restraint types

**Rearward facing CRS:** In the CHILD/CASPER dataset there are 33 children using rearward facing child restraint systems, of which 13 are not injured. Even though case numbers are small it is clear that the head is the most seriously injured body region with 36% having a head injury of AIS  $\geq 2$ . Of the 28 AIS  $\geq 2$  injuries for rearward restrained children, 26 are to the head. There are no AIS  $\geq 2$  injuries to the neck or extremities.

**Forward facing CRS:** In the CHILD/CASPER dataset there are 103 children using forward facing child restraint systems with a harness, of which 21 are not injured. It is clear that the head is the most seriously injured body region with 28% of the children sustaining an AIS  $\geq 2$  head injury and 51% of all the 116 AIS  $\geq 2$  injuries being to the head. At the AIS  $\geq 2$  level, half of the head injuries are attributed to the seat back in front and a quarter to the 'own kinematics' and 'deceleration fields' combined. At the AIS  $\geq 2$  level, the other body regions start to feature equally but increasing the AIS to  $\geq 3$  shows the neck, abdomen and thorax are more prominent than the face and extremities.

**Booster systems:** In the CHILD/CASPER dataset there are 132 children using booster systems either with or without backrests, of which only 13 are not injured. Serious injuries are more distributed across the body regions than for harness shell systems with both upper (14%) and lower extremity (14%) regions, the abdomen (21%) and the thorax (15%) featuring strongly at the AIS  $\geq 2$  level, along with the head (14%). At the AIS  $\geq 3$  level the thorax features as the most injured body region with 14% of the children in this sample having such an injury. The abdominal and head regions are also evident at 11% and 9% respectively. Of the 184 individual AIS  $\geq 2$  injuries just under one third are to the abdomen with seat belt contact given as the contact, when identified, in all cases, as with thoracic injuries.

**Adult seat belts only:** In the CHILD/CASPER dataset there are 169 children using just the adult seat belt, of which only 10 are not injured. At the AIS  $\geq 2$  level the extremities, both upper extremities (18%) and lower extremities and pelvis (12%), feature strongly, along with the head (14%) and abdomen (14%), followed by the thorax (11%). At the AIS  $\geq 3$  level the abdomen has an AIS  $\geq 3$  injury for 10% of the 169 children, followed by the thorax (8%) and then the head and lower extremities are equally prevalent at 5%. As with booster systems, abdominal injuries are mainly attributed to the seat belt, as are the thoracic injuries.

## Lateral impacts

### Overall

There are 148 restrained children in the dataset in lateral impacts with type of restraint and injuries known (or it is known that no injury has occurred). Of these children, 46% have a MAIS  $\geq 2$  and 34% have a MAIS  $\geq 3$ . This MAIS  $\geq 3$  is higher than the frontal impact sample. There are a further 15 restrained children with fatal injuries but the actual injuries by AIS and body region are not known.

The proportion of misuse situations identified is half that in the frontal impact sample and a relationship between misuse and a rate of higher injury is not apparent. It is possible that misuse is more difficult to identify in lateral impact or has less of an effect on injury outcome in a higher proportion of circumstances (for example, struck side 90 pure lateral impacts).

'Lateral from front' and 'pure lateral' together are the impacts experienced the by large proportion of restrained children in lateral impacts. As this is a sample with a shift toward serious injury selection this could indicate a higher risk of injury with a pure lateral impact or a frontal component, although exposure rates for different impacts are not known – there could simply be less lateral impacts with a rear component. The proportion of children with MAIS  $\geq 2$  or fatal injuries is highest for purely lateral impacts (54%), followed by lateral from front (50%) and then lateral from rear (41%).

There are 92 restrained children sitting on the struck side in a lateral impact and 71 are non-struck side. Struck side children have greater proportions of both MAIS 2-3 and MAIS 4-6 or fatality than non-struck side children. For these struck side children the rates of higher injury levels are much higher when there is direct intrusion to the area in which they are seated. Generally the level of maximum intrusion around the struck side child's position has a link with the level of injury severity, with an overall increase in maximum injury severity towards higher intrusion. At over 300 mm of maximum intrusion, 68% of the 41 restrained children on the struck side are MAIS  $\geq 2$ , 44% are MAIS  $\geq 4$  or have fatal injuries. This analysis would benefit from individual case review as the injury outcome can be very dependent upon the exact position of intrusion, the principal direction of force and type of CRS.

Illustrations of the difference in risk of getting an AIS  $\geq 2$  injury are shown in Figure 3-12. It is visible in terms of the rate of children injured at the AIS  $\geq 2$  level in the sample with a coherence for all restraint systems considered and it is also true looking at the number of injuries sustained by each severely injured child which is on average 1.74 times higher on the struck side than for injured children on the non-struck side. Combining frequency and number of injuries per injured child leads to a rate of AIS  $\geq 2$  injury per child 3.2 higher on the struck side. This table also underlines the efficiency of shell systems on the struck side with a rate of AIS  $\geq 2$  injuries per child 1.65 times lower than for these just using the adult seatbelt.

**Table 3-12: Difference of injury risk struck vs non struck side**

	Struck side				Non-struck side			
	shell	booster	seatbelt	total	shell	booster	seatbelt	total
Number children	29	23	30	82	14	21	23	58
AIS ≥ 2 children	14	17	17	48	4	8	8	20
% AIS ≥ 2 children	48%	74%	57%	59%	29%	38%	35%	34%
AIS ≥ 2 injuries	46	59	79	184	9	13	22	44
AIS ≥ 2 injuries per AIS ≥ 2 child	3.29	3.47	4.65	3.83	2.25	1.63	2.75	2.20
AIS ≥ 2 injuries per child	1.59	2.57	2.63	2.24	0.64	0.62	0.96	0.76

### Restraint types

**Shell System CRS:** On the struck side there are 29 children using shell systems with a harness, of which 4 are not injured. The head is the most seriously injured body region, followed equally by the thorax and lower extremities at the AIS ≥ 2 level and strongly by the thorax at the AIS ≥ 3 level. For the head injuries known contacts to rigid parts vary as expected, according to direction of impact and crash partner. On the non-struck side there are only 14 children using shell systems with a harness, of which 4 are not injured. The number of individual AIS ≥ 2 injuries is small (9 injuries only applying to 4 children) and they are distributed across five body regions.

**Booster seat/cushion:** On the struck side there are 23 children using booster systems, of which 2 are not injured. The rate of serious injury to the head is very high, in itself and compared to the shell system and adult seat belt restrained children. Abdominal injuries do feature at the AIS ≥ 2 level but at a lower rate than lower extremities and the thorax, and equal to the face. At the AIS ≥ 3 level, injuries are only seen for the head, then thorax and lower extremities. On the non-struck side there are only 8 children with AIS ≥ 2 injury(ies) with injuries distributed across the body regions but with the head having the highest number followed by the thorax.

**Adult seat belts** On the struck side there are 30 children using only the adult seat belt, of which 3 are not injured. The rate of serious injury to the head is slightly higher than for shell systems. At the AIS ≥ 2 level, lower extremity injuries have the second highest injury rate, followed by the thorax. This relationship between the lower extremities and the thorax is reversed at the AIS ≥ 3 level. On the non-struck side there are only 8 children with AIS ≥ 2 injury(ies). The rates of head and lower extremity injury are high at both AIS ≥ 2 and AIS ≥ 3 levels, followed by thoracic injuries.

### Safety technologies

It continues to be difficult to collect a significant number of data regarding new safety technologies across all ages, restraint conditions and crash types/severities. New technologies (except side head airbags) are concentrated on the front seats whilst the majority of crash data is for children seated in the rear. Whilst future investigation activities will collect data on new technologies in the rear (for example, during the time of CASPER thoracic side airbags in the rear have started to slowly appear) an approach of revisiting the cases already collected and combining individual case reviews with results from reconstruction or misuse testing results could start to form a more complete picture of the effectiveness of safety technologies (car or CRS) for restrained children. It would also be advantageous to record type of airbag in more

detail in the database, for example, mounting for passenger airbags or size and extent of side airbags.

There are still only 7 children using an ISOFIX system in the database, 3 of them in the same vehicle. There could be different explanations for this. The numbers of ISOFIX in the fleet could still be low. Parents/carers who spend the extra money on ISOFIX systems may be less likely to be involved in an accident and when they are involved the vehicle may be more expensive, newer or larger. When accidents occur ISOFIX systems may protect their occupants to such a degree that they do not appear in notifications, although the CASPER criteria also includes high severity low injury impacts so they should still be included. Within this task the possibility of these points being realised is not addressed but could be investigated in further studies by using sales data, marketing or CRS use surveys and CRS testing data.

Eight cases are available of deployed passenger airbags and rear facing infant carriers. Whilst 5 of the children are reported as having survived, the children are very young and the brain injuries are likely to be important at a critical time of development.

### **Injury recording**

The situation regarding injury recording is an interesting one for the on-going work in the area of child passenger biomechanics due to the balance between using the newest and most accurate recording systems and being able to link back to previous work (especially the CREST and CHILD projects).

#### **AIS90 to AIS98**

The noticeable change in using AIS98 instead of AIS90 as the core injury recording system is the increase in MAIS value (to 3) for 20 children due to the below 12 year old femur fracture codes not being available in AIS98. Whilst this is not a large change as a proportion of the entire sample (1008), as it focuses on one body region it should be taken into account in any injury criteria work that may compare previous results to CASPER results in this body region.

#### **AIS98 to AIS2005**

Regarding differences between the AIS98 and AIS2005 it is no surprise that revisions in the AIS system show an overall reduction in the injury severity score of certain regions as advances are made in medical care. But it is also clear that AIS2005 is a more demanding system in terms of the medical information and evidence required (for example, volume of loss, depth, length, time) and this can lead to injuries coded in AIS98 being given lower severity scores due to the extent of the injury being not as well documented. Sometimes, 2 or 3 AIS2005 codes that cover just one code in AIS98 are building to the same injury severity as the AIS98 code but more information on the extent is required to be able to code the highest injury severity. For example, cerebrum intraventricular hemorrhage (140678) is AIS 4 in AIS98. But in AIS2005 just this knowledge of the injury allows only AIS 2 to be recorded. If associated coma of over 6 hours is known then AIS 4 can be recorded. Another example is that 'concussion' is AIS 2 in AIS98 but in AIS2005 if no time of unconsciousness is available then the injury is AIS 1 (NFS).

The proportion of restrained children  $\text{MAIS} \geq 3$  in AIS98 is 37.9% and AIS2005 34.7%, similarly for  $\text{MAIS} \geq 4$  the proportion drops from 24.4% in AIS98 to 18.2% in AIS2005. Currently it is not clear what proportion of the decrease is due to a genuine reduction in the injury severity score (medical progress) and what proportion is due to the greater level of injury detail required in AIS2005 for certain injuries.



It is recommended that any future activities are coded with both AIS98 and AIS2005, to ensure consistency with previous biomechanics work and enable injuries in new road accident cases to be recorded as accurately as possible.

### **Further work**

For lateral impacts a review of individual cases to understand intrusion levels with reference to child age, restraint type and importantly specific direction of impact, but also intrusion levels for specific body regions.

A case by case analysis could also be conducted to enlarge the understanding of some extreme crash conditions to which child have been surviving and the same approach could be used to evaluate the potential benefit of airbags in frontal and side impacts. Individual case review to separate booster systems into just cushions and those with backrests, with further separation as to whether the backrest endeavours to provide lateral impact.

Combination of individual case reviews with results from reconstruction or misuse testing results to start to form a more complete picture of the effectiveness of safety technologies (car or CRS) for restrained children.

Deeper analysis regarding the reduction in injury severities from AIS98 to AIS2005 to understand the contribution of injuries with a genuine reduction in severity compared to a lack of medical information leading to reduction.

### **3.1.9 References**

Ernst Tomasch, Graz University of Technology, AT. 'Accident Reconstruction Guidelines, Part of Deliverable D4', EC PENDANT Project, October 2004.

Gennerelli, T.A., and Wodzin, E. (2005) editors, The Abbreviated Injury Scale, AAAM, Illinois 2005.

J Barnes, A Hassan, R Cuerden, R Cookson, J Kohlofer. 'Comparison of injury severity between AIS 2005 and AIS 1990 in a large injury database', AAAM 2009  
The Abbreviated Injury Scale 1990 revision, AAAM, Des Plaines Illinois 1990.  
The Abbreviated Injury Scale 1990 revision - Update 1998, AAAM, Des Plaines Illinois, 1998.

## **3.2 EPOCH Task 1.1 - Literature review, accident analysis and injury mechanisms**

### **3.2.1 Introduction**

The implementation of Directive 2003/20/EC, dated 8 April 2003 (which amends Directive 91/671/EEC) means that children aged 3 or more years old and up to 150 cm in height or 12 years old, must use a child restraint appropriate to their size when travelling in cars or goods vehicles fitted with seat belts. The effect of this legislation has led to children remaining in child restraints until they are older (up to 12 years old, depending on their height).

Research into the anatomy and development of older children has been conducted to help identify the injury mechanisms of older children. A review of current and existing research was also conducted with particular interest in how and where older children are being injured whilst travelling in vehicles. This included a review of the work from the previous research projects; CHILD and NPACS. Accident data that was reviewed

previously by the NPACS and CHILD projects along with recent data from the CCIS and CARE databases has been analysed to highlight accidents involving older children.

This has enabled the main priorities for the body areas that need to be protected by restraint systems designed for older children to be established, for both front and side impact. This has then allowed requirements for the measurement capabilities of the dummy to be identified.

### 3.2.2 Background

In order to understand better the scope of the project, this section summarises the anatomy and development of older children, current practices in restraint design, legislation on child restraint use and corresponding trends, and finally, collision data.

#### Anatomy and development of older children

Young children tend to have a continuous growth rate; however, on entering puberty, they experience growth spurts of 7 to 8 cm per year. These are due to an increase, of up to 8 fold, of the growth hormone in the body system. Children of 10 to 12 years of age are on average 140 to 150 cm in height. Girls usually reach their peak height at around 12 years of age whereas boys reach peak at around 14 years of age. Both sexes see weight increases in relation to their growth in height, however the largest increase is seen later on in puberty. Older children weigh between 30 and 40kg irrespective of sex, which can be extrapolated to being half of their future adult weight. At this stage of growth, most of the weight gain comes from the developing bones and musculature in the limbs and the spine (Tanner, 1989).

Growth starts initially from the limbs. The bones grow in length through ossification centres, at their endings. The bones become stronger and more plastic from their centre out, as the lengthening process occurs. These changes are accompanied by muscle strengthening which ensures protection and support for the growing bones. During puberty, growth is more noticeable as the feet and hands grow larger followed by the arms and legs (Tanner, 1989).

The torso lengthens, which allows thoracic breathing to occur. The lengthening is mainly due to vertebral growth. The vertebrae grow in height and become stronger and compact. The cushioning discs between the vertebrae also mature and extend to offer stronger protection. The joints between the vertebrae change angle, which modifies the child's posture and the rib cage descends. This is accompanied by a rise in lung volume, due to increased rib displacement referred to as the bucket handle movement. The ribs rise vertically as well as horizontally thus increasing the volume of the chest. This movement combined with the expanding number of breathing pockets called alveoli, allows for greater respiratory capacity (Brant *et al.*, 2008). Hip widening also occurs, which allows the abdominal contents to drop down and also helps to allow thoracic breathing. This is found especially in girls, due to the presence of oestrogen, a sex hormone that activates ossification centres at the hip joints. In younger children, the abdomen is prominent resulting in the "pot-belly" effect. This is because the torso and the hips are not wide enough to allow the contents to sit lower down in the abdomen. As the hips widen, the abdominal muscles also strengthen which reduces the "pot-belly" and pushes the contents gradually into place. Until this occurs, the major organs such as the liver, which is the abdomen's largest organ, the stomach, the spleen, which is crucial for blood production, and the gastrointestinal tract, are fully exposed (Nahum and Melvin (eds.), 2001; MacGregor, 2000).

Finally, the shoulders widen, which also helps in terms of thoracic breathing. This is emphasised for boys through sex hormones which also induces a distinct increase in muscle mass compared to that with girls (MacGregor, 2000; Tanner, 1989).

Another body area of interest for this project is the head and neck. Bone thickening and the closing of the space between the bones of the skull occur earlier in childhood. However, older children experience a change in their facial features, for example the forehead lengthens, the brow ridge becomes more prominent, the jaw extends forward and the facial muscles develop. As mentioned earlier, the vertebrae mature and the child's posture changes. The neck muscles also increase in size to provide stronger support for the head (Nahum and Melvin (eds.), 2001).

All these changes happen over a period of 5 to 6 years depending on the individual, and careful consideration needs to be given to the fact that children aged 10 to 12 years are only at the very beginning of these processes. Thus their body is not fully mature like an adults, nor immature as in young children.

### **Current practices in child restraint design for older children**

Currently, there are different types of child restraint systems (CRSs), which are made in different sizes to fit different mass groups of children, corresponding to United Nations Economic Commission for Europe (UN-ECE) Regulation 44. The main seats used for older children are booster systems with or without a backrest. Booster systems with backrests are referred to as booster seats and those without backrests are referred to as booster cushions. To conform to the Regulation, a child restraint must meet a series of design and construction requirements and pass a series of performance tests, the main ones of which are summarised briefly below.

Booster systems, with 'Universal' approval, are all non-integral restraints which use the adult seatbelt to restrain both the child to the CRS and the CRS to the vehicle. Booster cushions raise the child in order to guide the adult seat belt to fit on the lap just below the pelvis. Booster seats provide enhanced protection over a booster cushion by also routing the diagonal portion of the adult belt over the shoulder and providing some protection from side impacts through wing-like extensions around the torso and head.

The CRS must be secured to the car structure. The child or a carer must be able to remove the belt from the child and remove the child independently. For this group of restraint the child must also be able to remove the belt on their own.

Different performance tests are carried out on the booster systems and these include dynamic frontal impacts, overturning tests and energy absorption tests. The impact tests are accomplished with the use of child anthropometric devices (child dummies) appropriate for the restraint. The restraint should prevent the motion of the child continuing forward beyond a certain distance relative to a point on the test bench and mitigate loading above a set level. No parts on the restraint should break and the belt should not unlock or move from the belt guides.

Most seats are injection moulded with polystyrene inserts and are designed to absorb as much energy as possible in front impacts. The cover of the seat must also meet toxicity and flammability requirements.

An overturning test rotates the restraint with a child dummy and assesses how much the dummy's head moves past a set distance compared to the original position relative to the seat.

### **Legislation on child restraint use for older children**

The European Directive 2003/20/EC states that occupants of motor vehicles must wear seat belts and use appropriate child restraint systems. This Directive also states that children who are below 150cm in height and/or under 12 years of age must be seated in a child restraint. The Directive currently allows countries to restrain children with the minimum height of 135cm by the adult seatbelt; however, it is thought to be only temporary. Germany, Italy, Austria, Ireland, Luxembourg, Greece, Hungary, Poland, Portugal have already enforced the 150cm rule whereas other European countries opted for the 135cm requirement.

Child restraint systems must conform to UN Regulation 44. The Regulation classifies restraints by child mass, which for older children only goes up to 36kg. This corresponds to Group III (children of 22kg to 36kg), which is the largest group currently available in the Regulation. This classification reflects that Regulation 44 was developed to allow assessment of CRSs designed for children up to the age of about 10 years. This now needs updating to allow provision of restraint systems that are designed for children up to a height of 150cm.

The retention system of a child restraint may be of two classes; integral and non-integral. An integral restraint is where the retention of the child within the restraint system is independent of any means directly connected to the vehicle. A non-integral restraint is where the retention of the child within the restraint system is dependent upon any means directly connected to the vehicle.

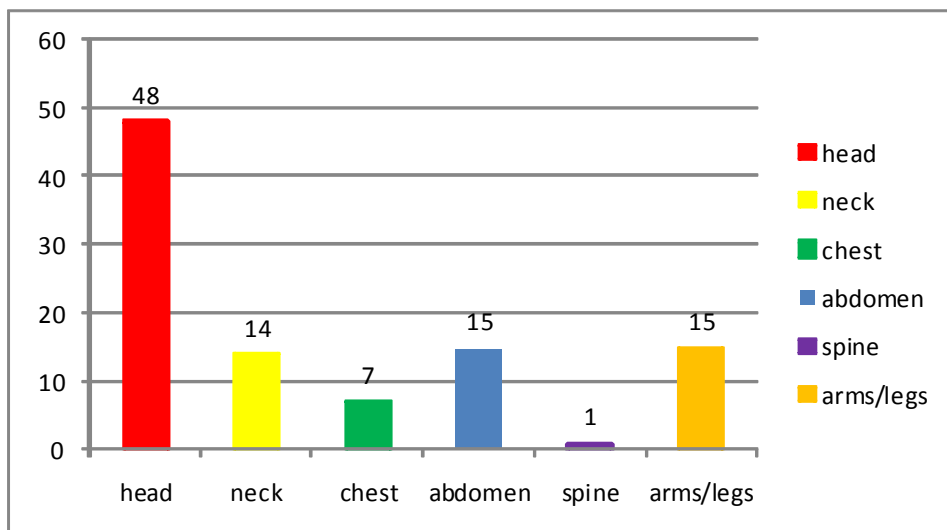
### **Trends in restraint use by older children**

Before the European Directive 2003/20/EC came into effect it was common for children above the age of four years to be restrained by only the adult belt and very unlikely for a child above six years old to be on a booster system. The current situation, as mentioned above, is that some countries require children to be in a CRS until they are 150cm in height or have reached twelve years old, whilst others require children to be in CRSs until they are 135cm in height or have reached twelve years old. This has led to the use of booster systems by older children and to the availability of 'high backed' booster systems in the market place.

From accident analysis data, it was shown that in Belgium, even though the restraint use is compulsory it is poorly respected, or the restraint system is not used correctly (Javouhey *et al.*, 2006). The majority of older use only the adult seat belt (99%) rather than booster cushions (1%) (Vesentini and Willems, 2007).

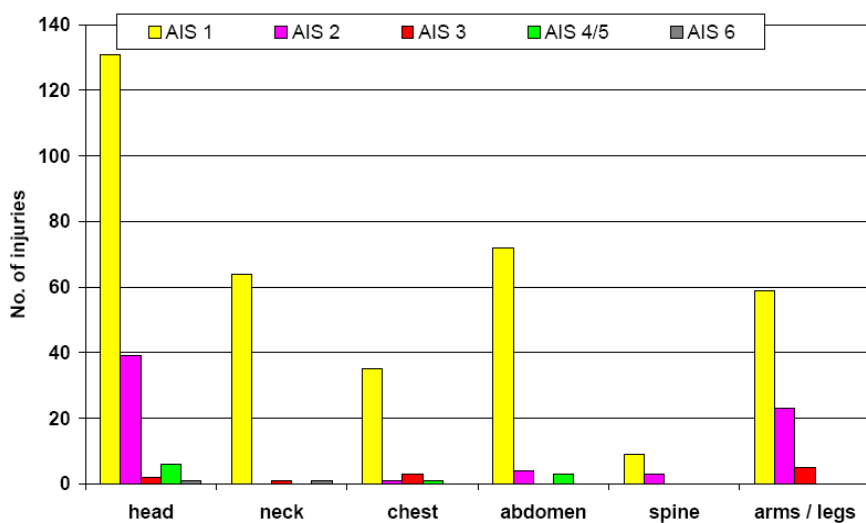
### **Involvement of children in collisions**

An accident study, looking at children of all ages, from the late 1990's (Johannsen, 2004) showed that 48% of the children using a CRS properly suffered head injuries and 15% suffered injuries to the abdominal area (Figure 3-68). In this sample, head injuries are the most prevalent. Abdominal injuries and injuries to the extremities rank as the second body region sustaining injuries. This does not, however show specifically the effects of children travelling in booster systems or identify how many older children the data relate to.



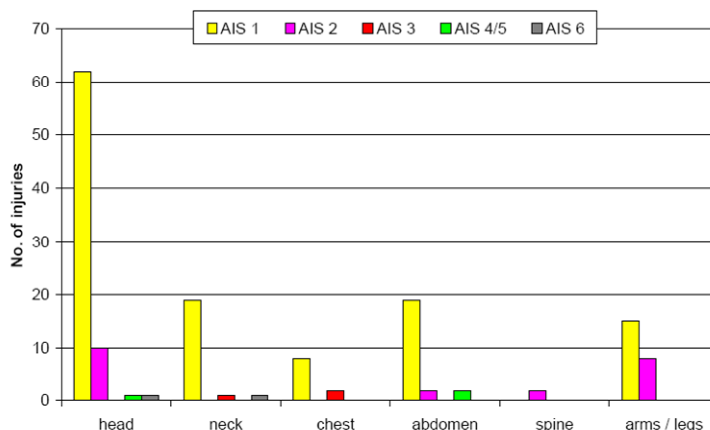
**Figure 3-68: Percentage distribution of injuries by body region for children using CRS properly (reproduced from Johanssen, 2004)**

Figure 3-69 shows the injury severity of the different body regions of 415 children of all ages and restraint use. The head region received the majority of injuries, followed by the abdomen, neck, limbs and chest. The most severe injuries were found in the head, followed by the limbs.



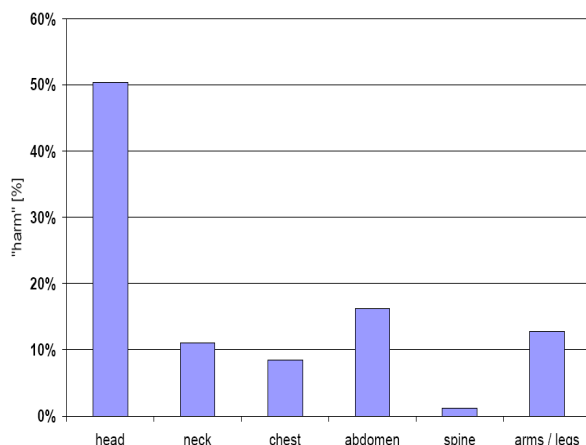
**Figure 3-69: Injuries of 415 children of all ages and restraint use (reproduced from Johanssen, 2004)**

Figure 3-70 shows the picture for 200 children of all ages and using a CRS and is broadly similar to that above.



**Figure 3-70: Injuries of 200 children using a CRS (reproduced from Johannsen, 2004)**

Johannsen refers to an assessment of “harm”, which is a weighted injury frequency, in Figure 3-71. This shows that the body region most likely to be injured is the head followed by the abdomen.



**Figure 3-71: Calculated harm for different body regions of 415 children (reproduced from Johannsen, 2004)**

This data is from a publication written in 1997 and as such it is unlikely any older children included in the sample were seated on child restraints. At the immature development stage of younger children the head and neck need a high level of protection. In older children, due to the anthropometric changes, the priority relies on the head, chest and abdomen.

**Front impact**

*Injury patterns for children in front impact*

For children using a Booster seat and adult seat belt (group II/III):



Wismans *et al.* (2008) looks at children using booster systems. The study was carried out before older children were using child restraint systems and those children using child restraints are likely to be aged between 3 and 6 years. The report concluded that the head is the most important body region, in terms of frequency of severe injuries.

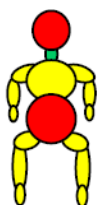
The relative importance of abdominal injuries increases with such restraint systems compared to child restraints with a harness. This is because the penetration of the lap section of the seat belt into the abdomen of the child can cause injuries to the liver, spleen, and kidneys. The protection of the abdominal area is therefore a high priority to ensure good protection of children using a CRS that uses the adult seat belt to restrain the occupant directly.

Chest injuries are not frequently reported for children seated on booster seats with a backrest. However, as the chest cavity protects vital organs, it remains an important body segment. In general chest injuries occur through chest compression, but often occur without rib fractures due to the chest compliance of children.

The pelvis rarely suffers serve injuries in frontal impact and therefore is not a priority body region.

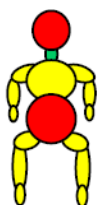
Limb fractures often occur, but were reported to be generally low in severity and therefore are not a major priority in terms of child protection.

Booster cushion and adult seat belt (group II/III):



Wismans *et al.* (2008) also reported that the main body regions, for this limited age range of children, injured on booster cushion type CRSs are the same as for booster seats. In comparison with booster seats, an increase of the number of chest injuries is found, due to the fact that children using these CRSs are generally older (less compliant chest) than the ones using booster seats. From the age of the sample and the typical restraint use at that time, the older children referred to using booster systems in the report are likely to be from 3 to 6 years old.

Adult seat belt:



Wismans *et al.* (2008) also found that in many of the accident cases where older children were injured they were only restrained by the adult seat belt, while if they had been using a CRS, their injuries would have been reduced.

The main body regions injured when only using the adult seat belt are similar to the ones using booster cushions. However the injuries are generally more severe especially in the abdominal area.

The European Enhanced Vehicle-safety Committee (EEVC) Working Group 18 Report: Child Safety - February 2006 (EEVC, 2006) compared the injuries suffered by children using a booster cushion and those who only used the adult seat belt. From the age of the sample and the typical restraint in use at that time, the older children referred to in the report, using booster systems are likely to be aged between 3 to 6 years old. An increase in abdominal injuries was observed in cases without the booster cushion. It was concluded that this was due to a difference in kinematics of the child due to the poor positioning of the lap section of the seat belt.

Table 3-13 shows a comparison of injuries sustained by children using a booster cushion compared to only using the adult seat belt. The table shows that there were a higher percentage of AIS 3+ neck injuries to children on boosters, whilst there were more AIS 3+ chest injuries sustained by children using only the adult seat belt. In both cases a high number of limb fractures were observed.

**Table 3-13: Comparison of injuries: booster cushion and seat belt only (reproduced from EEVC, 2006)**

	Booster cushion + Seat belt		Adult seat belt only	
	AIS1+	AIS 3+	AIS1+	AIS 3+
Number of children with medical information	108		148	
Number of Injuries for:				
Head	39	7	44	8
Neck	22	11	25	6
Chest	24	9	45	18
Abdomen	28	9	68	27
	AIS1+	Fracture	AIS1+	Fracture
Limbs	53	25	88	38

Both EEVC (2006) and Wismans *et al.* (2008) concluded that in a frontal impact, the main priority should be to protect the head of the occupant for all types of child restraints for older children.

The chest and abdominal injuries increase in frequency and severity for older children over the age of 3 years compared to the younger children who are in a harness restraint type system. Therefore based on the findings from these reports, the recommended body regions to be protected, for children who have outgrown harness systems, are the head, neck, chest, abdomen, lumbar spine and pelvis.

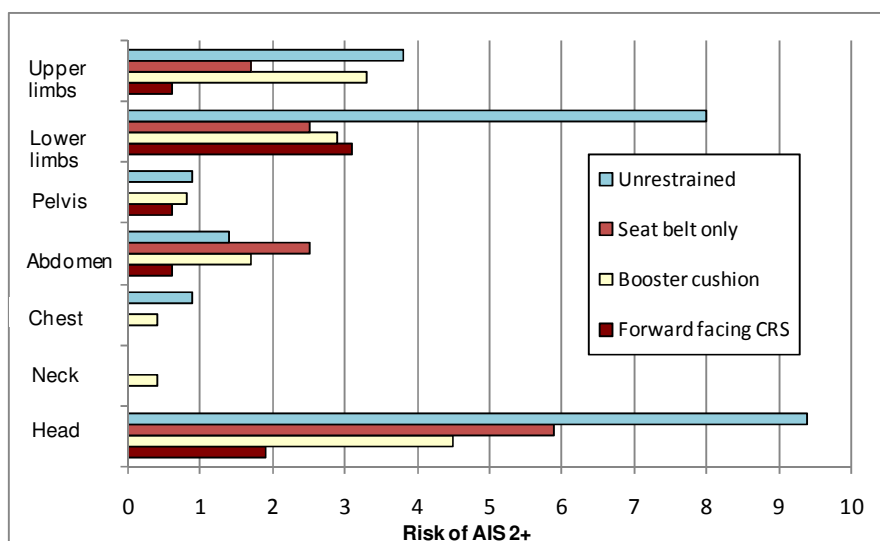


**Figure 3-72: Comparison of injury risk per body segment for different types of CRS (reproduced from EEVC, 2006)**

Analysis in EEVC (2006) compared the injury risk per body segment for different types of child restraints (Figure 3-72). The children in this sample using different restraint methods are also likely to fall into different age bands. It is reported that the risk of a severe head injury for children restrained in forward facing child seats with a harness in a frontal crash is lower than all other restraint type systems. The risk of a head injury is even lower than the risk of having a lower limb fracture. The risk of injury in the abdominal area is also lower than other restraint systems due to the fact that children are not directly in contact with the seat belt when restrained with restraint systems with a harness.



Children restrained using a booster cushion with the seat belt have a risk of 4.5 out of 100 of having a severe head injury and 1.7 out of 100 of having an abdominal injury. These injury risks are over double those likely for the child in the harness seat. Children on boosters are likely to be older and therefore taller than the children in harness systems, so they are at more risk of making head contact with the interior of the vehicle. However their risk of injury is much less than when using only the adult seat belt and for children who are not restrained at all.

The use of a booster cushion shows an important decrease in injury risk to the head, chest, pelvis and limbs. The risk of having a severe injury to the neck and abdomen is higher than for unrestrained children, however where there are belt induced injuries, it is likely that other, more serious injuries have been mitigated.

### *Factors affecting injury of children in front impact*

#### Velocity

Cheung and Le Claire (2006) conducted a review of the UK STATS 19 accident data, with particular interest in the distribution of casualties by road speed limit. It was reported that roads with speed limits of 48 km/h (30 mph) and 96 km/h (60 mph) contained the highest number of Killed or Seriously Injured (KSI) casualties (Figure 3-73). This data includes all children under 12 involved in an accident between 1998-2003.

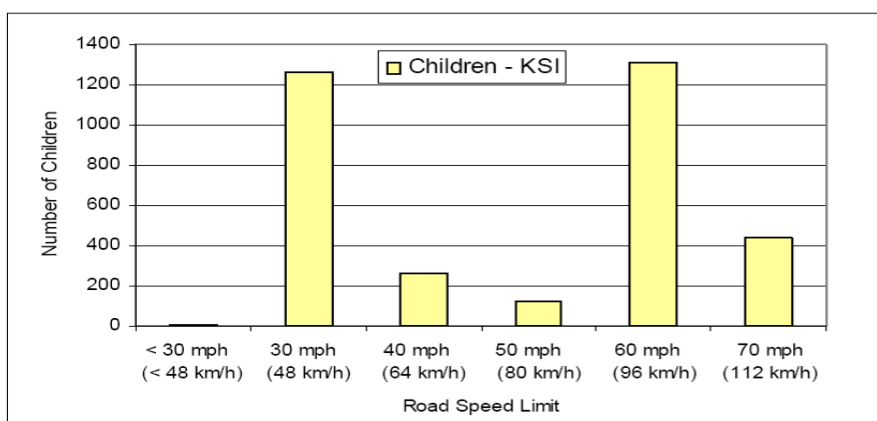


**Figure 3-73: Number of KSI children by road speed limit (reproduced from Cheung and Le Claire, 2006)**

Cheung and Le Claire (2006) also investigated the distribution of front impact severity in the TS97 database. This database contains information for accidents that occurred in 1996-1997, for a region south of Munich in Germany. Figure 3-74 shows the distribution for front impact 'Degree of Damage' for different Energy Equivalent Speeds (EES) from the TS97 database. This shows that around 70% of the accidents occur with an EES of 0-50 km/h, and 50-70 km/h accidents account for the remaining 30%.

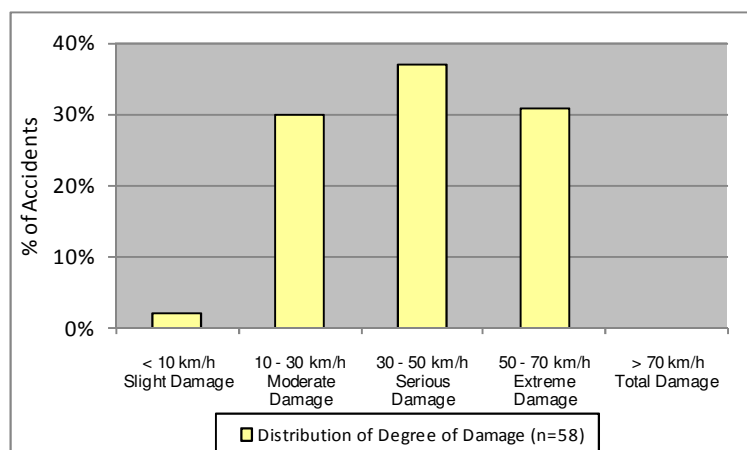


**Figure 3-74: Percentage distribution of front impact accidents at the five Degrees of Damage (reproduced from Cheung and Le Claire, 2006)**

Cheung and Le Claire (2006) concluded that there was a direct collation between the seriousness of injuries to children and the severity of the impact.

Based on all the information for front impacts where the change in velocity was known:

- The majority of accidents involving children occurred with vehicle change in velocity ( $\Delta v$ ) of between 30 and 39 km/h or an EES of 30-50 km/h;
- 50 % of slight child injuries occur below a  $\Delta v$  or EES of about 30 km/h and 95% below of 50 km/h;
- 50 % of serious child injuries occur below a  $\Delta v$  or EES of about 50 km/h and 95% below of 70 km/h.

### Side impact

#### *Injury patterns for children in side impact*

The EEVC Working Group 18 Report: Child Safety - February 2006 (EEVC, 2006) analysed the CREST<sup>1</sup> accident database and concluded that for side impact, the distribution of the injuries according to the different body regions is given in Figure 3-75. Head injuries accounted for 65 percent of all the severe injuries recorded in all restraint types. It was concluded that the current level of protection provided to prevent the occupant's head contacting rigid parts inside the vehicle or an intruding object is at present not sufficient.

Severe injuries also frequently occur in the chest and abdomen body regions. These injuries were mainly observed when the child was sitting on a booster cushion or just using the adult belt and not in CRSs that have side wings for protection. For systems without side wing protection, the chest accounted for 22% of the injuries and the abdomen 16% of injuries.

<sup>1</sup> CREST (Child Restraint System for Cars) was project funded by the European Commission.

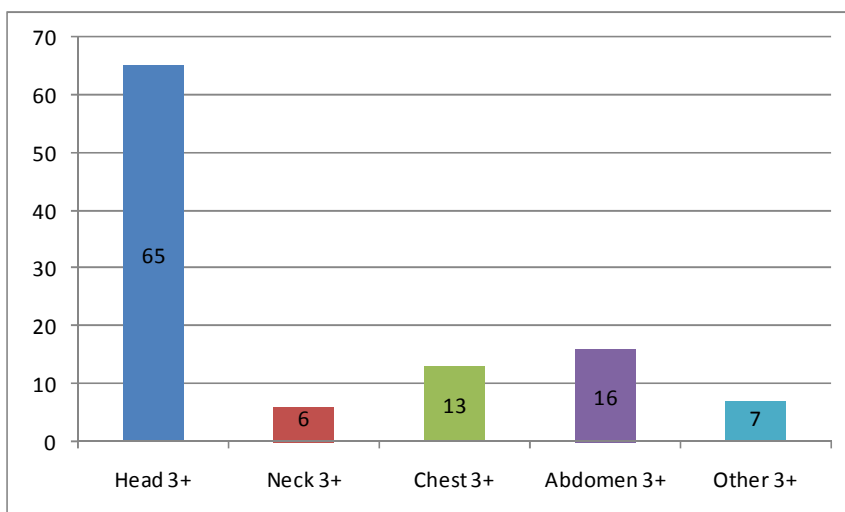


**Figure 3-75: Side Impact AIS 3+ injuries from CREST accident database (reproduced from EEVC, 2006)**

Figure 3-75 shows that the neck is less frequently injured than the other regions. However the neck injuries occurred mainly in young children using forward or rearward facing child restraint systems. Though the number of neck injuries observed was low, in each of the CREST accident cases an AIS3+ injury was observed, and the child was fatally injured. Whether this is a concern for older children is unknown, as the lack of accident data means no trends can be seen.

EEVC (2006) also analysed the CSFC database, where side impact collisions represented 16% of the total accidents. The CSFC database is a record of children of all ages involved in accidents in rural regions in France 1995-96. 206 children were involved in these accidents, of which 37% of children were uninjured, 43% sustained minor injuries and 20% were severely injured.

Further analysis looked at the breakdown of injuries for only the struck side of the vehicle. This showed that the body area most often injured was the head with 42%, with upper limb injuries at 29% and abdominal injuries representing 19% (Figure 3-76).

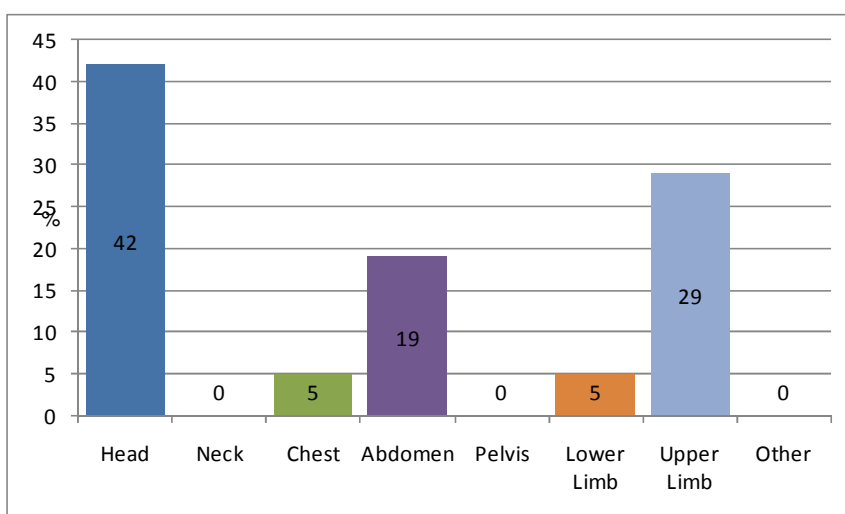


**Figure 3-76: Side impact struck side occupant injury frequency (reproduced from EEVC, 2006)**

EEVC (2006) concluded that there were not enough cases to draw a strong conclusion for severe injuries suffered by children during side impact collisions. However injuries

to the head were very frequent and seemed to account for around 75% of the total body area injured for children involved in side impacts, who were restrained in forward facing child seats on the struck side. For children using booster type restraints head injuries only account for around 50% of the injured body regions and 40% for children only using the adult seat belt.

This difference is not only due to the type of restraint system but also to the difference in height of the children and the corresponding impact areas with the interior of the vehicle. The study was carried out before older children were using child restraint systems so those children restrained are likely to be aged up to 6 years.

Lesire *et al.* (2006) conducted an analysis of CREST and CHILD accident data related to side impacts. They presented a summary of the injury severity for all children under 12 involved in side impact accidents (Figure 3-77). The chart shows that around 50% of the children suffered only slight or no injuries. However this data includes accidents for restrained children of all ages. It is unlikely that many of the children over 6 years old would have been using a CRS.

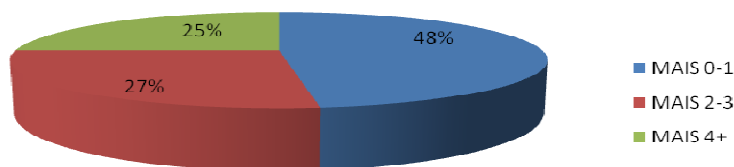


**Figure 3-77: Side impact injury severity (reproduced from Lesire *et al.*, 2006)**

Lesire *et al.* (2006) was however able to identify 35 children in the database that were using booster seats or booster cushions on the struck side of the vehicle. It is most likely that these children will be aged 3-6 years old, as these would be the main users of booster type CRSs at the time. Analysis of the seriously injured showed that head injuries represent over 50% of the injuries (Figure 3-78). The chest is the next largest percentage injured body region with 17% and the abdomen representing 9%. The upper and lower limbs both represent around 10% of the injuries.

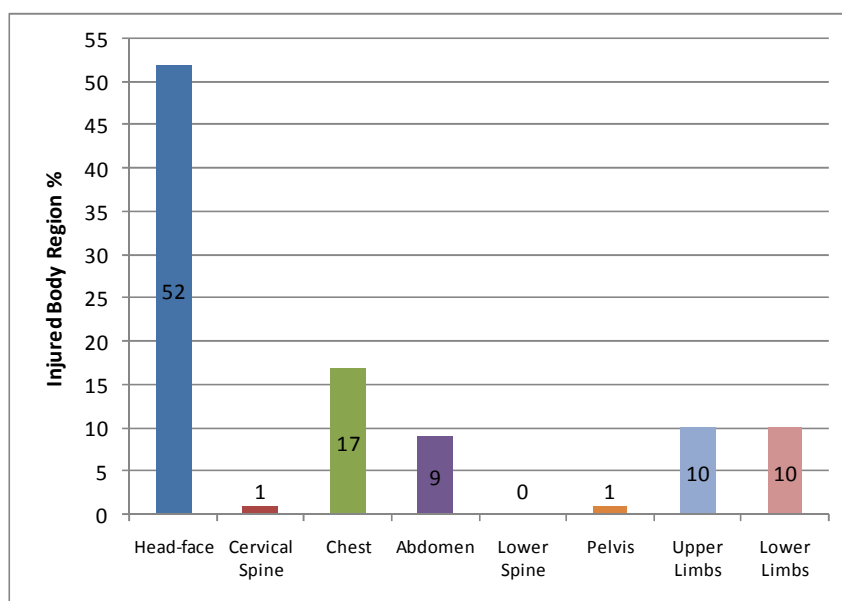


**Figure 3-78: Injured body regions for children using booster type restraints (reproduced from Lesire *et al.*, 2006)**

Lesire *et al.* (2006) also identified 49 children in the CREST and CHILD databases who were only restrained using the adult seat belt. It is most likely that the majority of these children would have been aged over 6 years old, due to restraint use at the time.

The percentage of head injuries is slightly less than for children using booster type restraints, at around 40%. The chest and abdomen injuries are relatively similar in percentage compared to children using the booster type restraints. There is a reduction in upper limb injuries, but an increase in pelvis and lower limb injury percentages (Figure 3-79).

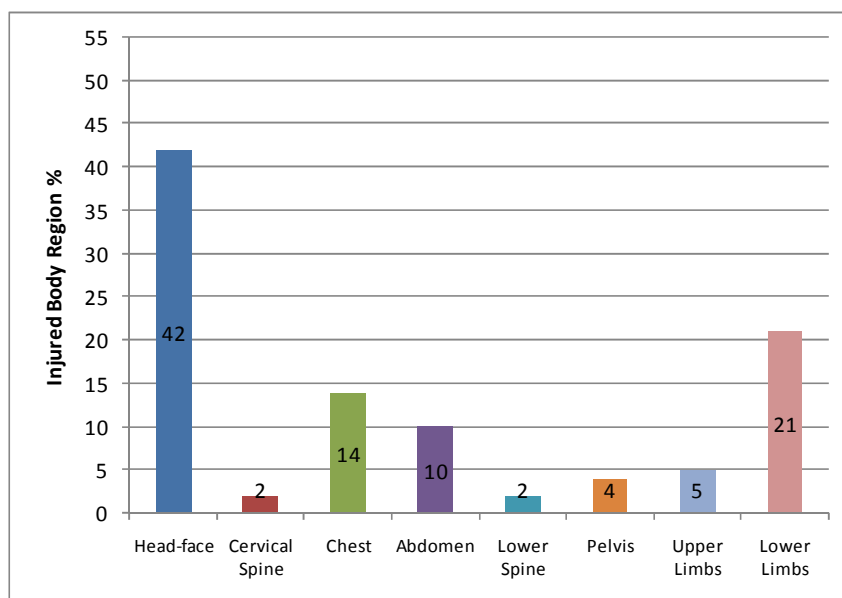


**Figure 3-79: Injured body regions of children using only the adult seat belt (reproduced from Lesire *et al.*, 2006)**

Lesire *et al.* (2006) concluded that in side impact the injury causations for children on the struck side of the vehicle were:

- Head injuries are the most frequent injuries and occur due to head contact with rigid parts of the vehicle interior;
- Chest and abdomen injuries are the next most frequently injured body regions and occur due to compression through door panel contact;
- Upper limb injuries are more frequent for children using booster type restraints and are also usually caused by door panel contact;
- Pelvis and lower limb injuries become sufficiently more frequent for children only restrained by the adult seat belt as there is no protection from intrusion.

#### *Factors affecting injury of children in side impact*

##### *Velocity*

Cheung and Le Claire (2006) analysed several different accident databases which contained side impact collisions. Based on this analysis of these side impact cases where the impact velocity was known, the following conclusions were made:

- The majority of accidents involving children occur with a vehicle change in velocity ( $\Delta v$ ) of 15-25 km/h or an energy equivalent speed (EES) 30-50 km/h;
- 95% of all cases involving children (regardless of restraint) occur with a  $\Delta v$  of less than 50 km/h;
- 50% of slight injuries occur with an EES less than 30 km/h;
- 50% of severe injuries occur with an EES less than 50 km/h;

- 95% for both slight and severe injuries occur with an EES less than 70 km/h.

### Intrusion

Lesire *et al.* (2006) used accident data from the CREST and CHILD databases to investigate the effect of vehicle intrusion on the injury severity of children in side impact. It was found that vehicle intrusion has a direct influence on the injury severity of children.

Eighty-one percent of restrained children seated on the struck side of the vehicle where there was no direct intrusion received no or slight injuries and only less than 14% receive serious injuries. For the cases where direct intrusion was present a 1/3 were uninjured or slightly injured, with a further 1/3 receiving moderate injuries and 1/3 seriously or fatally injured.

The fact that intrusion has a direct influence on injury severity is further corroborated by the breakdown of injury severity compared to maximum intrusion (Figure 3-80). The graph shows that over 300mm intrusion will result in over 50% MAIS 4+ injuries for the occupant. Below 200mm intrusion the MAIS 4+ percentage is less than 20%.

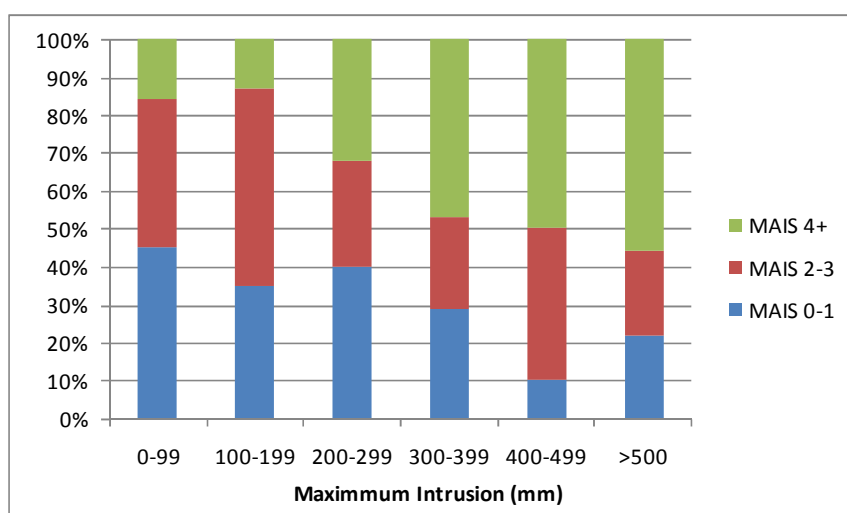


**Figure 3-80: Injury severity percentage for different amounts of side impact intrusion (reproduced from Lesire *et al.*, 2006)**

### Involvement of older children in collisions

The European Road Safety Observatory ([www.erso.eu](http://www.erso.eu)) is a pilot web site established during the SafetyNet project (an integrated project funded by the European Commission). The web site includes basic traffic safety facts, which are delivered in a series of fact sheets. The fact sheets are based on data from the CARE (Community database on Accidents on the Road in Europe) database. Table 3-14 shows that 735 older children were killed in police-reported collisions across the European Union (EU-19) in 2006 (ERSO, 2008).

**Table 3-14: Fatalities by gender and age in EU-19 in 2006 (reproduced from ERSO, 2008)**

Age (years)	Female	Male	Both sexes
5 – 9	102	155	257
10 – 14	164	314	478
<b>Totals</b>	<b>266</b>	<b>469</b>	<b>735</b>

While the CARE data presents European-wide information, more detailed analysis is impossible. The information has therefore been supplemented with data from the UK. Table 3-15 shows that there were 4,193 older child casualties reported to the police in Great Britain in 2007 and the killed or seriously injured casualties amounted to 157. All of these children were car passengers. The data were obtained from Road Casualties Great Britain 2007: Annual Report (DfT, 2008). While it is likely that very few, if any, fatal accidents are not reported to the police, research shows that a significant proportion of non-fatal injury accidents are not reported (Ward *et al.*, 2006). In addition, police may underestimate the severity of injury due to the difficulty in distinguishing severity at the collision scene (DfT, 2008). Nevertheless, Table 3-15 provides an overview of the involvement of older children in personal injury road accidents in a typical country in Western Europe.

**Table 3-15: Older child casualties by age band and severity in 2007**

Age (years)	Killed	Seriously injured	Slight	All severities
5 – 7	6	60	1,443	1,509
8 – 11	6	97	2,581	2,684
<b>Totals</b>	<b>12</b>	<b>157</b>	<b>4,024</b>	<b>4,193</b>

In order to gain more detailed information about older children and their injury patterns, accident cases involving children aged from 6 to 12 years were obtained from the Cooperative Crash Injury Study (CCIS) database<sup>2</sup>. The data span the years from mid-1998 to mid-2008. There were 277 children involved in a front impact collision for all restraint types and injury levels. Figure 3-81 shows the distribution of restraint type for these children.

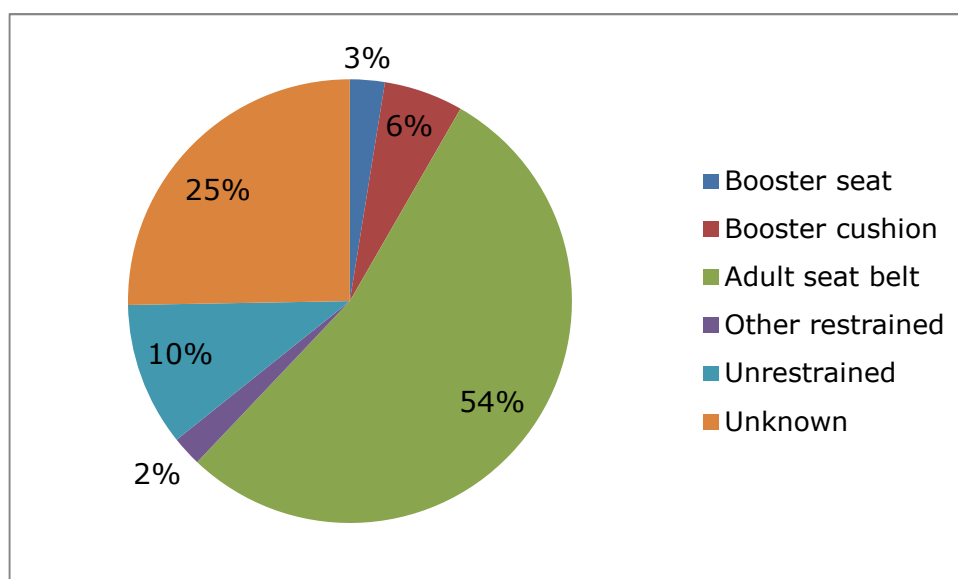


**Figure 3-81: Restraint type for children aged 6 to 12 years in front impacts (n=277)**

There were 127 children involved in a side impact for all restraint types and injury levels. Figure 3-82 shows the distribution of restraint type for these children.

<sup>2</sup> CCIS is one of the world's largest studies of car occupant injury causation. Each year the project investigates more than twelve hundred crashes involving cars or car derived vans ([www.ukccis.org](http://www.ukccis.org)).

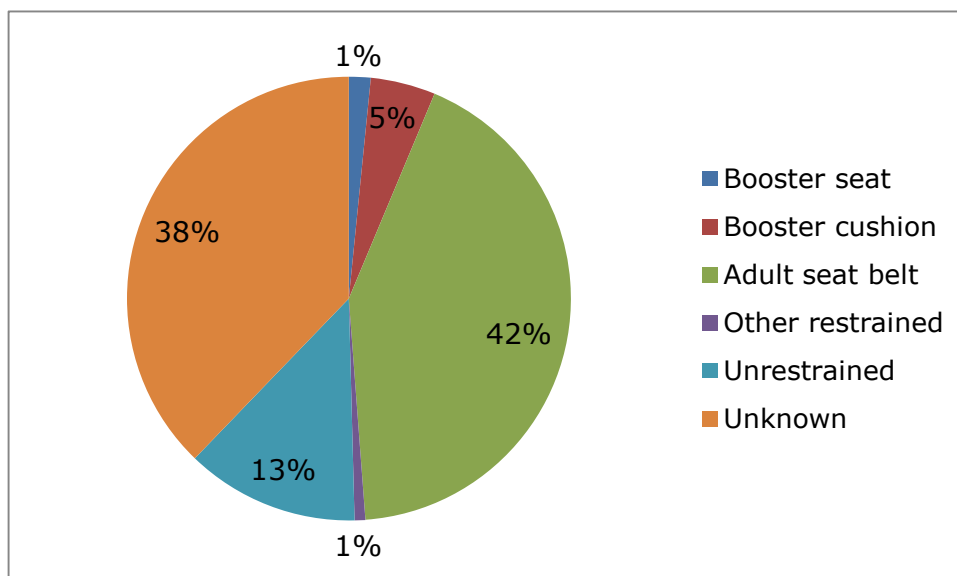


**Figure 3-82: Restraint type for children aged 6 to 12 years in side impacts (n=127)**

There is a large proportion of unknown restraint use in the CCIS database, which could affect any conclusions drawn from these data. Figure 3-81 and Figure 3-82 show that during this ten year period, which was mostly prior to the new seatbelt wearing Directive coming into force in the UK, the adult seat belt was the most common type of restraint for children aged six to twelve years, and there were a greater proportion of children unrestrained than there were using child restraint systems.

### 3.2.3 Overview of collision studies

#### Front impact

##### Injury patterns for older children in front impact

Table 3-16 shows the injury distribution with respect to restraint type for the older children in the CCIS database that were involved in a front impact. The adult seat belt was the most common type of restraint system for these children. Unfortunately, there were too few cases involving children in booster seats and booster cushions to comment on the performance of these devices in comparison with the adult seat belt. It is interesting to note, however that there were no AIS>2 injuries to the children restrained in booster seats.

**Table 3-16: Injury distribution with respect to restraint type for children aged 6 to 12 years**

Restraint type	Total	MAIS0		MAIS1		MAIS2		MAIS≥3		Unknown	
		n	%	n	%	n	%	n	%	n	%
Booster seat	7	1	14.3	5	71.4	0	0.0	0	0.0	1	14.3
Booster cushion	16	1	6.3	8	50.0	1	6.3	2	12.5	4	25.0
Adult seat belt	149	20	13.4	107	71.8	8	5.4	5	2.7	9	6.0
Other restrained	6	1	16.7	2	33.3	0	0.0	1	16.7	2	33.3
Unrestrained	29	6	20.7	15	51.7	4	13.8	3	10.3	1	3.4
Unknown	70	17	24.3	36	51.4	4	5.7	3	4.3	10	14.3
<b>Total</b>	<b>277</b>	<b>46</b>	<b>16.6</b>	<b>173</b>	<b>62.5</b>	<b>17</b>	<b>6.1</b>	<b>14</b>	<b>5.1</b>	<b>27</b>	<b>9.7</b>

Fifteen restrained children (aged 6 to 12 years) received AIS≥2 injuries. Details about these children are shown in Table 3-17. The average age of the injured children was  $9.3 \pm 2.0$  years. Where reported, the average velocity change ( $\Delta v$ ) was 48 km/h,



indicating that the collisions were moderate to severe in severity. Six children were seated in the front passenger seat and 9 children were seated in the rear outboard seats.

**Table 3-17: Cases of AIS≥2 injury in restrained children aged 6 to 12 years**

Case	Age	Restraint type	Seating position	MAIS (Body region)	PDOF/ $\Delta v$ (km/h)	Object hit
1	9	Adult seat belt	Rear nearside	2 (Head)	12/44	Car
2	10	Adult seat belt	Front seat	2 (Head)	12/Unknown	Car
3	7	Adult seat belt	Front seat	2 (Upper extremity)	12/47	Car
4	10	Adult seat belt	Rear offside	2 (Upper extremity)	1/32	Car
5	11	Adult seat belt	Rear nearside	2 (Upper extremity)	1/50	Car
6	12	Adult seat belt	Rear nearside	2 (Abdomen)	12/Severe	Car
7	11	Adult seat belt	Rear nearside	2 (Abdomen)	1/50	Car
8	7	Adult seat belt	Front seat	2 (Abdomen)	12/43	Car
9	10	Adult seat belt	Front seat	3 (Upper extremity, lower extremity)	12/Unknown	MPV or LGV
10	12	Adult seat belt	Front seat	3 (Thorax)	12/Unknown	Car
11	6	Adult seat belt	Rear nearside	3 (Abdomen)	1/53	Car
12	11	Adult seat belt	Front seat	3 (Abdomen)	12/79	Car
13	8	Booster cushion	Rear nearside	2 (Head)	12/31	Car
14	8	Booster cushion	Rear nearside	4 (Head)	12/Unknown	Car
15	7	Booster cushion	Rear nearside	4 (Neck)	12/Unknown	Wide object (>41cm)

There were 18 AIS≥2 injuries among the 15 children. The distribution of injuries is shown in Figure 3-83. Most injuries occurred in the head (n=4), upper extremities (n=4) or the abdomen (n=6).

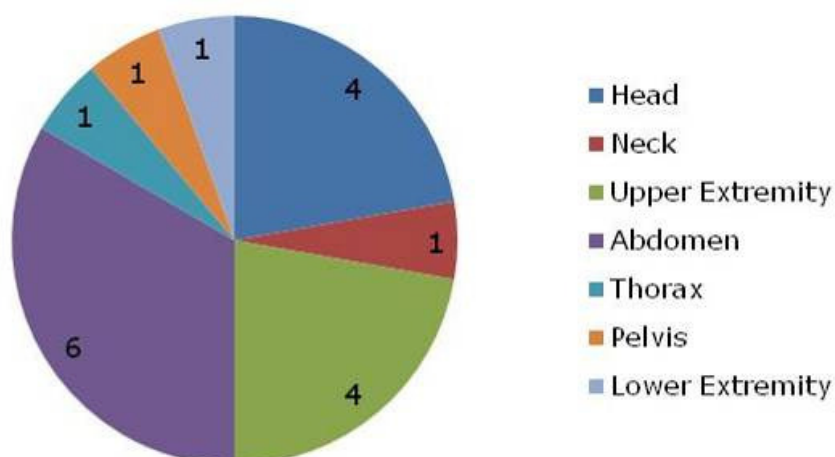


**Figure 3-83: Distribution of AIS≥2 injuries (n=18) among restrained children**

While the number of children receiving an AIS≥2 injury was low in the CCIS sample, similar findings have been reported in the literature. García-España and Durbin (2008) analysed a sample of 761 children aged 8 to 12 years with AIS≥2 injuries. They found

that head injury was the most common injury (60%), followed by injury to the face (9%), upper extremity (9%) and abdomen (9%). However, the study relied on driver reports for information on injury and restraint use, etc, and did not distinguish between front and side impact.

#### Factors affecting injury of older children in front impact

The velocity change of the case vehicle is often associated with a greater injury severity for the occupants. Unfortunately, the velocity change was unknown for most of the children in Table 3-17 with serious injuries and greater (i.e. AIS $\geq$ 3). For example, in Cases 14 and 15, the child received an AIS4 injury but the velocity change of their car was unknown. In Case 15, it seems likely that the collision was severe since their car struck a wide object (>41cm). This could have been a tree, a building or a piece of roadside furniture.

Intrusion into the seating position is also associated with greater injury severity. In Case 9, the child was seated in the front passenger seat of a car involved in a collision with a multi-purpose or light goods vehicle. The child received serious injuries to their extremities, which seem likely to have resulted from intrusion of the fascia and footwell.

Another factor associated with greater injury severity is misuse of the restraint system. Unfortunately, no information was available on the presence of misuse in the sample of cases.

#### Factors affecting the performance of child restraint systems for older children in front impact

The CCIS sample comprised 277 children aged 6 to 12 years and including all restraint types and injury levels. Twenty-three of these children were known to be using a child restraint system: 7 were in a booster seat, while 16 were on a booster cushion. Table 3-17 reveals that none of the children in booster seats received AIS $\geq$ 2 injuries, while three children on booster cushions were injured at that level. Unfortunately, there were too few cases of children using child restraint systems to establish any clear associations or contributory factors related to the performance of the devices.

### Side impact

#### Injury patterns for older children in side impact

Table 3-18 shows the injury distribution with respect to restraint type for the older children in the CCIS database involved in a side impact. The adult seat belt was the most common type of restraint system for these children. Once again, there were too few cases involving children in booster seats and booster cushions to comment on the performance of these devices in comparison with the adult seat belt.

**Table 3-18: Injury distribution with respect to restraint type for children aged 6 to 12 years**

Restraint type	Total	MAIS0		MAIS1		MAIS2		MAIS $\geq$ 3		Unknown	
		n	%	n	%	n	%	n	%	n	%
Booster seat	2	0	0.0	2	100.0	0	0.0	0	0.0	0	0.0
Booster cushion	6	1	16.7	5	83.3	0	0.0	0	0.0	0	0.0
Adult seat belt	54	14	25.9	32	59.3	2	3.7	3	5.6	3	5.6
Other restrained	1	0	0.0	1	0.0	0	0.0	0	0.0	0	0.0
Unrestrained	16	2	12.5	6	37.5	2	12.5	4	25.0	2	12.5
Unknown	48	13	27.1	20	41.7	6	12.5	2	4.2	7	14.6
<b>Total</b>	<b>127</b>	<b>30</b>	<b>23.6</b>	<b>66</b>	<b>52.0</b>	<b>10</b>	<b>7.9</b>	<b>9</b>	<b>7.1</b>	<b>12</b>	<b>9.4</b>

Five restrained children (aged 6 to 12 years) received AIS $\geq$ 2 injuries. Details of the sample are shown in Table 3-19. The average age of the injured children was  $7.8 \pm 2.2$  years. Where reported, the average velocity change ( $\Delta v$ ) was 26 km/h. One child was seated in the front passenger seat and four children were seated in the rear outboard seats.

**Table 3-19: Cases of AIS $\geq$ 2 injury in restrained children aged 6 to 12 years**

Case	Age	Restraint type	Seating position	MAIS (Body region)	PDOF/ $\Delta v$ (km/h)	Object hit
1	11	Adult seat belt	Rear nearside	2 (Head)	1/Unknown	HGV or PSV
2	6	Adult seat belt	Front seat	2 (Head)	11/25	MPV or LGV
3	6	Adult seat belt	Rear offside	4 (Head)	3/17	Car
4	9	Adult seat belt	Rear nearside	3 (Thorax)	10/27	Car
5	7	Adult seat belt	Rear nearside	2 (Lower extremity – left and right)	10/34	Car

There were 8 AIS $\geq$ 2 injuries among the 5 children. The distribution of injuries is shown in Figure 3-84. Half of the injuries occurred in the head (n=4).

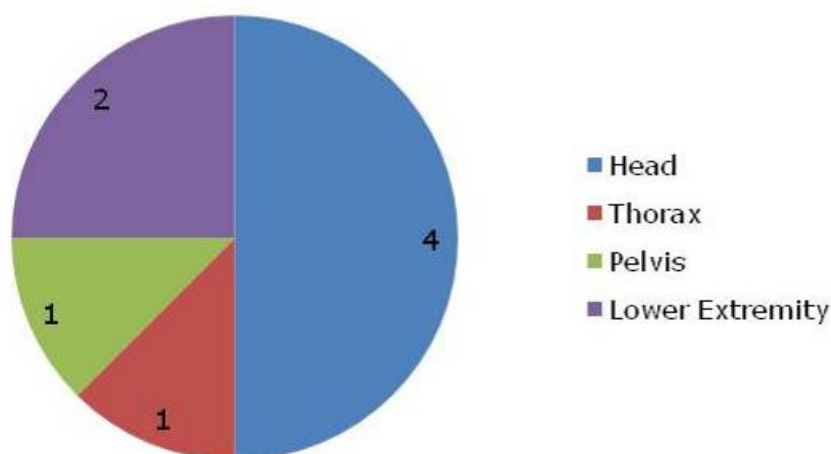


**Figure 3-84: Distribution of AIS $\geq$ 2 injuries (n=5) among restrained children**

Similar findings were reported in the literature, although sample sizes were small. For example, Arbogast *et al.* (2001) described 6 cases involving children with AIS $\geq$ 2 injuries and aged 5 to 9 years. Head injuries were the most common (AIS $\geq$ 2) injuries in this group. In the same study, head injuries were the most common AIS $\geq$ 2 injuries from a sample of 8 10 to 15 year old children; however, extremity injuries occurred more often than in any other age group. Howard *et al.* (2004) also found the head and the extremities to be the most common location for AIS $\geq$ 2 injuries in older children aged 7 years and above.

#### Factors affecting injury of older children in side impact

There were too few cases with AIS $\geq$ 2 injuries to identify any trends associated with the likelihood or severity of injury for older children in side impact. However, in general, the proximity of the child to the intruding side structures, and the level of intrusion into the passenger compartment are important. In four of the five cases in Table 3-19 the child was seated on the struck side of the car. Another consideration is the performance of the car in side impact. At least two of the five cars that the children in Table 3-19 were travelling in were unlikely to have been approved to UN Regulation 95.

### Factors affecting the performance of child restraint systems for older children in side impact

The CCIS sample comprised 127 children aged 6 to 12 years and including all restraint types and injury levels. Eight of these children were known to be using a child restraint system: 2 were in a booster seat, while 6 were in a booster cushion. Table 3-19 reveals that none of the children on booster cushions and booster seats received AIS $\geq$ 2 injuries. It was impossible, therefore, to make any meaningful comments on the performance of the child restraint systems in side impact.

## 3.2.4 Mechanisms of injury in older children

### Front impact

#### Injury mechanisms by body region for older children in front impact

Many studies of child injury mechanisms in front impact collisions include older children in the sample. However, very few studies describe in detail the types of injuries received by older children specifically. Section 3 revealed the importance of head, abdomen and extremity injuries. While the evidence is limited, it appears that most head injuries in older children result from direct contact with the interior of the vehicle (Agran *et al.*, 1987). This causes the skull to deform with the risk of fracture and/or local brain injury. Head contact can also induce relative motion of the brain with respect to the skull. Contact can occur for a variety of reasons. These include vehicle intrusion into the child's seating position or excessive head excursion due to incorrect or inappropriate restraint use. Non-contact head injuries are rare in older children. Nevertheless, in high severity collisions, acceleration (or deceleration) of the head can result in inertial loading that leads to brain injury. Similarly, the risk of basilar skull fracture with neck injury, which has been reported extensively in the literature for younger children, does not seem to be found in older children (Jakobsen *et al.*, 2005).

The most common abdomen injury mechanism in older children is adult seat belt loading directly at the site of the injured organ (Arbogast *et al.*, 2007). This can result from submarining (where the pelvis slips under the lap part of the seat belt) and/or from an initial misplacement of the belt, for instance, due to a slouched posture. Injuries to the lumbar spine seem to be rare in older children, particularly when the diagonal part of the seat belt is used correctly. Individual cases were discussed by Brown and Bilston (2007) and were associated with "high severity" collisions.

Injuries to the extremities of older children are likely to result from interaction with parts of the vehicle interior. Jermakian *et al.* (2007) described the lower extremity injuries in a sample of children in forward facing child restraints. Although the oldest child was only 5 years old, some of the key mechanisms are likely to be the same for older children. Jermakian found that a loose child restraint attachment and/or intrusion of the vehicle seat back in front of the child were important contributing factors. The main injury mechanism is loading applied to the extremity from the vehicle interior resulting in fracture.

### Side impact

#### Injury mechanisms by body region for older children in side impact

The principle mechanism of injury of children in side impact collisions is contact with the vehicle interior, which can occur either with or without significant intrusion (Howard *et al.*, 2007). While the effects of the greater seating height of older children, and their different biomechanical properties, have not been investigated in detail, it is clear that protection of the head is just as important in older children as it is in younger children. Severe head injury can occur, even in cases with no, or minor, intrusion.

While head injury can occur irrespective of the presence or level of intrusion, injuries to other body regions are more likely to occur when the side structure of the car intrudes into the child's seating position. For example, Arbogast *et al.* (2001) described a number of pelvis and femur fractures in children aged 10 to 15 years who were restrained in adult seat belts. The children were seated on the struck side on the vehicle adjacent to the intrusion. Howard *et al.*, (2007) reported similar injuries for children of all ages.

### 3.2.5 Discussion

Children aged between 10 and 12 years old are in the process of puberty and developing into adults. It is therefore important to treat them as specific category of children and not as young adults, which includes protecting them suitably as a passenger in a vehicle. The European Directive 2003/30/EC was designed to do this by stating that all children under 12 years old, or under 150cm must use a child restraint. However this Directive does miss-match with the current child restraint regulation, UN Regulation 44, which specifies that child restraints are designed to accommodate a maximum occupant weight of 36kg, (which is less than the 50<sup>th</sup> percentile mass of a 150cm child).

#### Injury mechanisms

The review of previous literature investigating the main injury mechanisms and injury types has provided some common conclusions for both front and side impact. However, most of the previous studies were conducted before the change in restraint use law, hence children over 6 years of age were unlikely to have been using child restraints at the time. The majority of injury data for children using booster restraints will be for children aged 4-6. However with this in mind common injury trends can still be seen between children using booster restraints and those who only used the adult seat belt.

For the reason that there were very few previous studies involving older children, although it was outside of the project scope, a small investigation into data for older children specifically was conducted. This short study was conducted to analyse recent data in the CCIS database and summary information from CARE database for accidents that only involved 6-12 year old children. Although there were few cases involving older children these databases the main injury body regions identified corroborated the findings of the previously conducted studies.

#### Front impact injuries

For front impact, the main injury body region that was identified by previous studies was the head. Head injuries were also identified in the CCIS database as one of the main injuries. The main injury mechanism for head injury is head contact with rigid parts of the vehicle interior. As a child grows in stature their head excursion will increase. Hence their likelihood of contacting the vehicle interior also increases.

The abdomen is a frequently injured body region and is particularly important to protect as it contains several vital organs. The main injury mechanism is submarining of the child under the lap section of the seat belt. This can be very severe for children who are not using a booster restraint, as the lap belt is not positioned correctly in relation to the child's pelvis. This can also occur due to slouching of the occupant. It is therefore important that the new dummy is capable of mimicking this injury mechanism and has the instrumentation to determine when submarining is occurring.

Protection of the chest was also identified as being important as it contains vital organs. As a child develops more of the vital organs become protected by the ribs, as

the ribcage grows. Chest injuries seem to be less frequent for children using booster restraints with backrests, than booster cushions or only the adult seat belt, which may be due to the backrest positioning the diagonal section of the belt correctly and securely.

Upper and lower limb injuries are also frequently recorded in front impact. These are normally due to contact with rigid parts of the vehicle interior. Previously they have been deemed to be low priority because it would be difficult for the dummy to be able to measure limb loading.

### Side impact injuries

For side impact the main injury body region was also identified by previous studies as the head. The main injury mechanism for head injury is due to the head contacting parts of the vehicle interior or an intruding object.

Chest and abdomen injuries are common for children using booster restraints or just the adult seat belt. These injuries are usually caused by compression of the child through door panel contact. The right hand side of a child is particularly susceptible to injury as that is where the liver is located.

Upper and lower limb injuries and pelvis injuries are also frequently recorded in side impact. These are normally due to contact with the vehicle door panel. Lower limb and pelvis injuries are particularly frequent for children who use only the adult seat belt as there is no side protection provided from the intruding structures.

## Important factors

### Velocity

#### *Front impact*

A review of real world accident severity reported that the majority of front impacts occur between 10km/h and 70km/h. A separate review investigated the road speed limit in accident cases where serious injuries to children occur. This showed that the majority of serious injuries occurred on roads with either a speed limit of 30 mph (48 km/h) or 60 mph (96 km/h).

The current regulation test in UN Regulation 44 is based on a 50 km/h impact and therefore is able to ensure that a child restraint protects children in an accident up to that severity.

The NPACS front impact consumer test was designed to represent an accident with a higher severity ( $\Delta v$  65 km/h) to ensure the child restraints were capable of providing protection for the children at higher severity accidents. It is therefore important that the new dummy can be used at a range of impact speeds in order to be able to assess fully a child restraint's ability to protect a child from the majority of accidents that would cause serious injuries.

#### *Side impact*

A review of real world accident severity reported that half of side impact accidents that result in slight injuries to children have an EES of less than 30 km/h and that half of serious injuries occur at an EES less than 50 km/h. It is therefore important that the new dummy can be used at a range of impact speeds in order to assess fully a child restraint's ability to protect a child from the majority of accidents that would cause injuries in side impact.

### Side impact intrusion

Lesire *et al.* (2006) reported that there was a direct relationship between vehicle intrusion and the injuries sustained by the occupant on the struck side of the vehicle. Below 200mm, the MAIS $\geq$ 4 percentage is less than 20%; however above 300mm intrusion, the percentage of MAIS $\geq$ 4 is approaching 50%. Therefore it is important that the dummy produces realistic kinematics in a side impact test with an intruding door. If the dummy is designed too stiff it will create unrealistic measurements if contacted by the intruding door. The shoulder of the dummy should also have some compliance, and absorb some of the load as a child would and not be too rigid.

### 3.2.6 Conclusions

- The implementation of EU Directive 2003/30/EC means the new dummy needs to be capable of sufficiently assessing a child restraint designed for a child up to 150cm or 12 years old.
- Although the majority of research of injuries sustained by children using booster restraints is limited to children under 6 years old there are comparisons with injuries sustained by children only using the adult seat belt.
- For front and side impact the main injury body region is the head. In both types of accident, injury is caused due to contact with an external rigid object. It is therefore important that the exposure risk of the head is minimised. This would mean a short excursion in front impact and good head containment in side impact.
- The abdomen and chest are the next most significant body regions to protect as this is where the majority of a child's vital organs are located. In a front impact it is important that the child does not submarine under the lap belt. In a side impact it is important that the child restraint provides side protection from the door panel or an intruding object.
- The pelvis has also been identified as an area to protect in side impact, as again it is important the child restraint provides protection from the door panel or an intruding object.
- Limb injuries occur frequently in both front and side impacts; however, they have previously been classed as low priority as they are deemed to be low in severity and difficult for the dummy to measure.

### 3.2.7 Recommendations

Based on the findings from the literature and accident data review the following recommendations are made for the minimum instrumentation that the new dummy should have:

#### Head

- Identified as the most important body region, the head needs to be capable of measuring both linear and angular accelerations.
- The excursion of the head needs to be measured as part of the assessment of a front impact.
- The containment of the head needs to be measured as part of the assessment of a side impact.

#### Abdomen

- The dummy needs to be capable of determining when the abdomen is being loaded and if possible the level of loading.

### Chest

- The chest needs to be capable of measuring both linear accelerations and compression of the ribs (Dx for front impact, Dy for side impact).

### Pelvis

- The pelvis needs to be capable of moving to allow the dummy to reproduce submarining in a front impact sled test. The pelvis could include an angular sensor.
- The pelvis needs to be capable of measuring linear accelerations.

### Neck

- Although not identified a major injury body region for older children, neck forces and moments need to be measured in both the upper and lower neck, to ensure a child restraint is not creating excessive loads in the neck. These measurements are also required for the NPACS assessment.

### Limbs

- Limb injuries occur frequently in front and side impact accidents and therefore consideration should be made as to whether the dummy needs to be capable of measuring loads in the arms and legs, without affecting the kinematics.

### 3.2.8 Acknowledgements

The work described in this report was carried out by the EPOCH consortium. The authors are grateful to the EC, the primary investors in the EPOCH project. We also appreciate the contribution from Kees Waagmeester, Mark Burleigh, Erik Salters, David Hynd, Jolyon Carroll and Costandinos Visvikis for their input to the quality review of this document.

The results of this work were reported at the EPOCH dissemination meeting in Paris, June 2009. Present were representatives from EEVC, CASPER, BAST, Euro NCAP and an informal GRSP group.

### 3.2.9 References

**Agran P F, Dunkle D E and Win D G, (1987).** Injuries to a sample of seatbelted children evaluated and treated in a hospital emergency room (v27(1) p58-64), *The Journal of Trauma*. Baltimore, MD: Lippincott Williams & Wilkins.

**Arbogast K B, Moll E K, Morris S D, Anderko R L, Durbin D R and Winston F K, (2001).** Factors influencing pediatric injury in side impact collisions (v51(3) p469-477), *The Journal of Trauma Injury, Infection and Critical Care*. Baltimore, MD: Lippincott Williams & Wilkins.

**Brant T C S, Parreira V F, Mancini M C, Becker H M G, Reis A F C and Britto R R, (2008).** Breathing pattern and thoracoabdominal motion in mouth-breathing children (v12(n6) p495-501), *Revista Brasileira de Fisioterapia*. Retrieved June 24, 2009, from <http://www.scielo.br/pdf/rbfis/v12n6/aop010.pdf>

**Brown J and Bilston L, (2007).** Spinal injuries in rear seated child occupants aged 8-16 years (paper number 07-0461), *Proceedings of the 20th International Technical Conference on the Enhanced Safety of Vehicles 2007*, June 18-21, 2007, Lyon, France. Washington DC: National Highway Traffic Safety Administration.

**Cheung G and Le Claire M, (2006).** *New programme for the assessment of child restraint systems: Phase 1 final report*. Published Project Report 145. Crowthorne: TRL Limited.



**Department for Transport, (2008).** *Road casualties Great Britain: 2007 annual report*. Retrieved on June 24th, 2009, from <http://www.dft.gov.uk/adobe/pdf/162469/221412/221549/227755/rcgb2007.pdf>

**European Enhanced Vehicle-safety Committee, (2006).** *EEVC working group 18 report: Child safety – February 2006*. Retrieved June 24, 2006, from [http://www.eevc.org/publicdocs/EEVC\\_WG18\\_REPORT\\_Child\\_Safety-February\\_2006-1.pdf](http://www.eevc.org/publicdocs/EEVC_WG18_REPORT_Child_Safety-February_2006-1.pdf)

**European Road Safety Observatory, (2006).** *Traffic safety basic facts 2008: Children aged < 16*. Retrieved June 24, 2009, from [http://ec.europa.eu/transport/wcm/road\\_safety/erso/safetynet/fixe/WP1/2008/BFS2008\\_SN-TRL-1-3-Children.pdf](http://ec.europa.eu/transport/wcm/road_safety/erso/safetynet/fixe/WP1/2008/BFS2008_SN-TRL-1-3-Children.pdf)

**García-España J F and Durbin D R, (2008).** Injuries to belted older children in motor vehicle crashes (v40(6) p2024-2028), *Accident Analysis & Prevention*. Kiddlington, Oxford: Elsevier Science Ltd.

**Howard A, Rothman L, McKeag A M, Pazmino-Canizares J, Monk B, Comeau J L, Mills D, Blazeski S, Hale I and German A, (2004).** Children in side-impact motor vehicle crashes: seating positions and injury mechanisms (v56(6) p1276-1285), *The Journal of Trauma Injury, Infection and Critical Care*. Baltimore, MD: Lippincott Williams & Wilkins.

**Javouhey E, Guérin A-C, Gadegbeku B, Chiron M, and Floret D, (2006).** Are restrained children under 15 years of age in cars as effectively protected as adults? (v91(4) p304-308), *Archives of Disease in Childhood*. London: BMJ Publishing Group Limited.

**Jakobsson L, Isaksson-Hellman I and Lundel B, (2005).** Safety for the growing child – experiences from Swedish accident data (paper number 05-0330), *Proceedings of the 19th International Technical Conference on the Enhanced Safety of Vehicles 2005*, June 6-9, 2005, Washington DC. Washington DC: National Highway Traffic Safety Administration.

**Johannsen H, (2004).** Injury risks of children: possibilities to detect abdomen injuries, *Proceedings of the 2nd International Conference “Protection of Children in Cars” 2004*, September 14-15, 2004, Cologne, Germany. Munich, Germany: TÜV Akademie GmbH.

**Lesire P, Herve V and Kirk A, (2006).** Analysis of CREST and CHILD accident data related to side impacts, *Proceedings of the 4th International Conference “Protection of Children in Cars” 2006*, December 7-8, 2006, Munich, Germany. Munich, Germany: TÜV Akademie GmbH.

**MacGregor J, (2008).** *Introduction to the anatomy and physiology of children: A guide for students of nursing, child care and health*. London: Routledge.

**Nahum A M and Melvin J W (eds.), (2001).** *Accidental injury: biomechanics and prevention*. New York: Springer-Verlag.

**Tanner J M, (1989).** *Foetus into man: physical growth from conception to maturity*. Cambridge, MA: Harvard University Press.

---

**Vesentini L and Willems B, (2007).** Premature graduation of children in child restraint systems: An observational study (v39(5) p867-72), *Accident Analysis & Prevention*. Kidlington, Oxford: Elsevier Science Ltd.

**Ward H, Lyons R and Thoreau R, (2006).** *Under-reporting of road accidents: Phase 1. Road Safety Research Report 69*. London: Department for Transport.

**Wismans J, Waagmeester K, Le Claire M, Hynd D, de Jager K, Palisson A, van Ratingen M and Trosseille X, (2008).** *European enhanced vehicle-safety committee Q-dummies report: Advanced child dummies and injury criteria for frontal impact – working group 12 and 18 report, document no.514*. Retrieved June 24th, 2009, from [http://www.eevc.org/publicdocs/EEVC\\_WG12&18\\_DOC514\\_Q-dummies\\_&Criteria-April\\_2008.pdf](http://www.eevc.org/publicdocs/EEVC_WG12&18_DOC514_Q-dummies_&Criteria-April_2008.pdf)

## 4 Child dummy developments

The P-Series were the most sophisticated child dummies in Europe when UN Regulation 44 was introduced. They have been instrumental in improving the quality of child restraints and have proved extremely durable for regulatory testing. Nevertheless, the dummies are relatively simple load measuring devices. The anatomy and behaviour of the internal structures of the body are not represented, which is one of the fundamental shortcomings of the dummy. In addition, the method it uses to detect abdomen loading (a clay insert) is somewhat subjective and does not allow for a complete assessment of injury risk.

The Q-Series family of child dummies, developed during the CREST and CHILD projects, are thought to represent a considerable improvement over the P-Series and have been evaluated comprehensively by EEVC Working Groups 12 and 18<sup>3</sup>. This chapter draws together the latest research from CASPER and EPOCH on the development of the Q-Series. Section 4.1 describes some potential shortcomings of the dummy before presenting proposals to improve its interaction with the lap part of a seat belt. Section 4.2 provides an update on the development of abdomen sensors for the Q-Series and Section 4.3 presents the results of an assessment of the biofidelity of the Q10. Each section comprises a published report or paper, reproduced here in its entirety. The full references for the reports and papers are:

Beillas, P. and Alonzo, F. (2010). *Auxiliary equipment for Q3 and Q6 to improve belt interaction response - Deliverable D.1.2 of the EC FP7 CASPER project*. Retrieved October 8, 2012 from: <http://www.casper-project.eu/results/>

Beillas, P., Alonzo, F., Chevalier, M-C., Johannsen, H., Renaudin, F. and Lesire, P. (2012). Abdominal pressure twin sensors for the Q dummies: from Q3 to Q10. In: *Proceedings of the International Crashworthiness Conference 2012*, 18-20 July, Milan, Italy. London: Taylor & Francis Group.

Hynd, M., McGrath, M., Waagmeester, K., Salters, E., Longton, A., and Cirovic, S. (2011). EPOCH project dissemination. In: *Proceedings of the 9<sup>th</sup> International Conference Protection of Children in Cars*, 1-2 December, Munich, Germany. Munich, Germany: TÜV SÜD.

### 4.1 Auxiliary equipment for Q3 and Q6 to improve belt interaction response

#### 4.1.1 Introduction: general use of child dummies in the frame of research

##### CRS and car safety equipment improvements

Child ATDs, like adult dummies, are used as human substitutes in regulatory procedures aiming to predict the risk of injuries to the main body regions subjected to loading during the crash. Despite the efforts to develop numerical models of the dummies, physical child dummies are still the tools of choice used by the CRS makers to evaluate the performance of infant carriers, forward and rearward facing seats with harness or shield, and boosters with or without backrest. When considering the road accident epidemiology, it is necessary for crash dummies to have a human-like dynamic response in both frontal and side impacts. Furthermore, since injury risk

---

<sup>3</sup> Wismans, J., Waagmeester, K., Le Claire, M., Hynd, D., de Jager, K., Palisson, A., van Ratingen, M., and Troisseille, X. (2008). Q-dummies report: advanced child dummies and injury criteria for frontal impact. Retrieved November 8, 2012 from: <http://eevc.org/publicdocs/publicdocs.htm>

prediction is based on Physical Parameter Values (PPV) measured during the test, the instrumentation should be comprehensive to cover all important anatomical regions, while being durable and repeatable. It should provide accurate and reliable metrics in the two main crash directions as well as in the oblique direction.

Car makers also have a need of child dummies. Vehicles are designed for adults and advanced safety systems as airbags, pretensioners and force limiters are positioned and calibrated for adults. Such equipment is likely to affect - and sometimes even to decrease - the protection of children in the case of a collision. Airbags for example, represent a specific risk of injury for head, neck, thorax and abdomen so that it is necessary to perform tests with small dummies.

### Accident reconstructions

Biomechanical data with child PMHS is very limited and there are currently no activities such as sled testing on-going in Europe. As a consequence, a specific approach had to be developed for child safety. Therefore, an alternative approach to scaled corridors was developed: accidents reconstructions are used as a basis to better understand child-related injury mechanisms and develop Injury Risk Curves and Injury Assessment Reference Values for approval purpose. In this approach, Physical Parameters Values (PPVs) or other metrics acquired during accident reconstructions are correlated with the type of injuries sustained by the child victim and the associated severity (AIS or Abbreviated Injury Score). These pairs of values are used to plot logistic regressions for body segments exposed to the risk of injury. Furthermore, after setting an acceptable injury severity level (currently AIS 2 at most), a threshold of injury criteria or Injury Assessment Reference Value can be determined for the regulatory testing procedure.

This approach assumes that the biofidelity of the child dummies are sufficient to reproduce or at least approximate the loading modes to the main anatomical regions (e.g. appropriate head trajectory, chest deflection, submarining response, etc). The biofidelity of the dummies is also important in order to be able to evaluate the effects of the misuses of CRS, which is an important issue when real world usage is considered.

## A brief history of European child dummy research and development

### P and Q dummies

P standard dummies were designed by TNO in the seventies. The dummies were not improved until 1995, date of the beginning of the CREST Project (with the exception of a neck sensor for research purpose that was not required for approval). P dummies modifications were carried out in the CREST project for accident reconstructions and parametric tests purpose. The modifications included:

- Abdomen and thigh modifications performed by LAB Peugeot Renault:
  - The shape and stiffness of the abdomen, as well as the stiffness of the upper thighs near the pelvis were modified based on abdominal compliance tests performed on child volunteers [Chamouard *et al.*, 1996];
  - The pelvis shape was modified based on X-Rays of the Debré Hospital in Paris;
  - An abdominal force penetration sensor was developed. The concept includes a rigid metallic plate anterior to the lumbar spine. The plate was instrumented with strain gauges in order to measure a load. The design was initially selected by TNO but the development stopped due to several problems including the stiffening of the lumbar spine and abdomen.

- Thorax modifications performed by INRETS. They consisted in:
  - Removing the inner stiffening membranes of the thorax;
  - Modifying the contours of the “lower ribs” edges based on measurements taken on volunteers [Biard, Alonzo, *et al.*, 1997, + report];
  - Adding a thorax deflection sensor (string potentiometer);
  - Developing a Torso skin providing a better coherence of the torso components;
  - Developing an abdominal penetration pressure sensor. It consisted in a bladder filled;
    - with paraffin oil, fitted with one pressure industrial cell, attached to the acetabulum fossae and the scapula.

Currently, the P dummy series in the original designed without the modifications mentioned above are used in UM Regulation 44. By 1995-1996, the consortium of the CREST EU Project decided to dedicate a significant part of the budget to develop a new generation of child ATD's with an enhanced biofidelity, an improved response to impact, and reliable sensors for body segments exposed to injury risk. All initial specifications, for the frontal impact as well as for the lateral impact, were formulated and agreed upon by the partners involved in the task. This task was particularly difficult due to the lack of child biomechanical data. Nevertheless, it was agreed that the first prototypes - Q3 and then Q6 dummies - would be designed and manufactured on the basis of existing experience and available biomechanical data. In a subsequent phase, the dummies would be evaluated, validated and enhanced based on the results and correlations established in numerous accident reconstructions, complementary parametric sled tests and other tests.

#### Use of Q3 and Q6 in the CHILD programme

During the CHILD programme, new prototypes of abdominal sensors were developed by INRETS (APTS or Abdominal Pressure Twin Sensors) and TU Berlin (FMS Force Matrix Sensor). Details about these sensors are available in Child deliverables and proceedings (IRCOBI, ESV, ISB, Child report D1b, Child Final Workshop: [http://www.casper-project.eu/child\\_web\\_site/workshop\\_output.htm](http://www.casper-project.eu/child_web_site/workshop_output.htm)). No other modification of the Q3 and Q6 dummies were performed as the dummy development effort was focused on the Q0, Q1 and Q1.5. Other testing activities included accident reconstructions, complementary sled tests, and sled tests to evaluate the consequences of misuse.

As explained previously, the knowledge of likely misuses is essential to understand and to assess the real world injury mechanism. It is also essential to quantify the increase in terms of injury severity associated with the misuse.

In this research area, the human-like kinetic response and the performance of the dummy instrumentation used in sled tests are of prime importance. During the sled tests, shortcomings of the Q3 and Q6 (hollow shoulders, lack of continuity of anterior torso surface and groin interstice) were the cause for important limitations in the results (observations made during the CHILD project).

Despite all these limitations, the work to build Injury Risk Curves continued for all regions. At the end of the CHILD project, the Injury Risk Curve based on around 10 to 15 cases at least for each anatomical region.

### 4.1.2 Possible shortcomings in Q3 dummy affecting the dummy response

The purpose of this section is to summarise the possible issues mentioned in the introduction in order to initiate the work on propositions of possible dummy modifications to improve the dummy response. Possible shortcomings are presented hereafter in an anatomical order from top (shoulder) to down (pelvis-thigh).

#### Shoulder

The lack of flesh in the shoulder area, the negative strap-engaging slope, the strap-catching hollow and the hollow armpit can cause the slippage of the thoracic strap. After the slippage, the dummy is restrained by the neck and the clavicle. Such behaviour would be likely to affect the overall kinematics and the neck loads. The high stiffness of the thoracic cage (discussed later) and its geometry may exacerbate this tendency to slippage. An illustration is provided in Figure 4-1.

It must be noted that while CRS manufacturer sometimes have problems keeping belt on the shoulder of the P dummies during tests, this does not seem to be the case for the Q dummies.

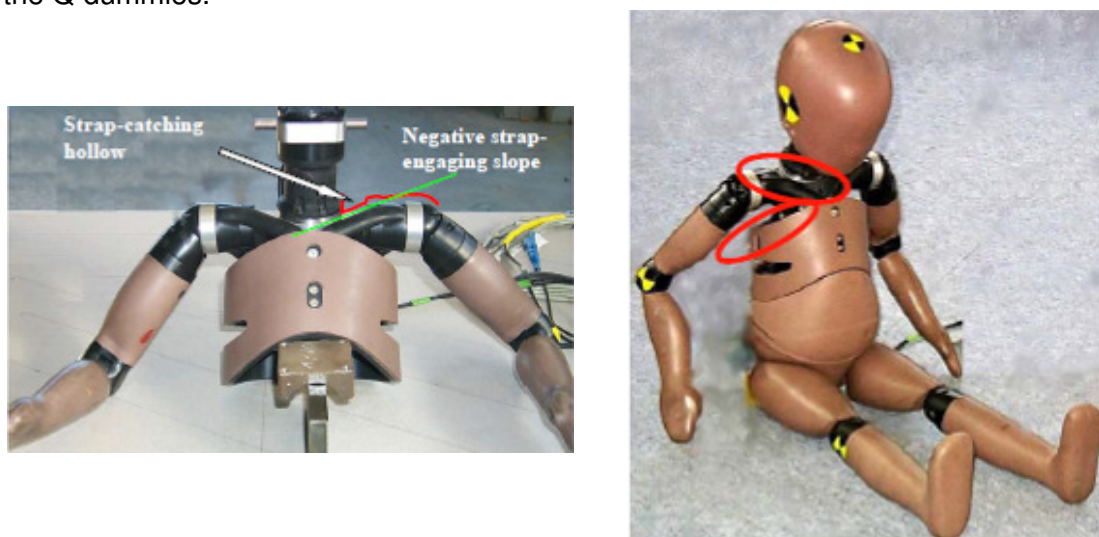


Figure 4-1: Shoulder angle and armpit

#### Thorax

The thoracic cage is made of two polyurethane sheets rolled together. Several sources of information suggest that the ribcages of the current dummies are too stiff:

- When evaluating the response of the dummy (on behalf of the EEVC WG12 and WG18), Kate de Jager, Michiel van Ratingen *et al.*, (2005) found that the dummy response was above the corridors, especially for low speed impact. They stated that overall “Q-biofidelity results are good, except for the (linear scaled) thorax requirement.”. An illustration of the response with the corridors is provided Figure 4-2.
- Recently, Ouyang *et al.* (2006) performed child PMHS testing on the thorax. They found that the response was overall in agreement with the scaled corridors (and therefore not in agreement with the dummy response). Their results also implied that the response against 0.5 (3YO) or 1cm (6 YO) of deflection was linear, which is not the case of the dummy (Figure 4-3).

However, FTSS stated that the initial versions of the Q dummies which matched the corridor shown in Figure 2 suffered from severe, early time, bottoming out in sled tests (TNO Reports, 1997 and 1998). As a consequence the stiffness was adjusted.

It should be noted though that the response of both humans and ATD's depends strongly on the loading type. An example of this is given in Figure 4-4 showing Dummy and PMHS results table top tests for the case of a 50% male. In this case the stiffness characteristics under belt loading are much higher than under hub loading which is used in the corridors of Figure 4-3. For the Q-dummies no efforts were made in CREST nor CHILD to investigate the sensitivity to the loading type. It is recommended to investigate this in future programs.

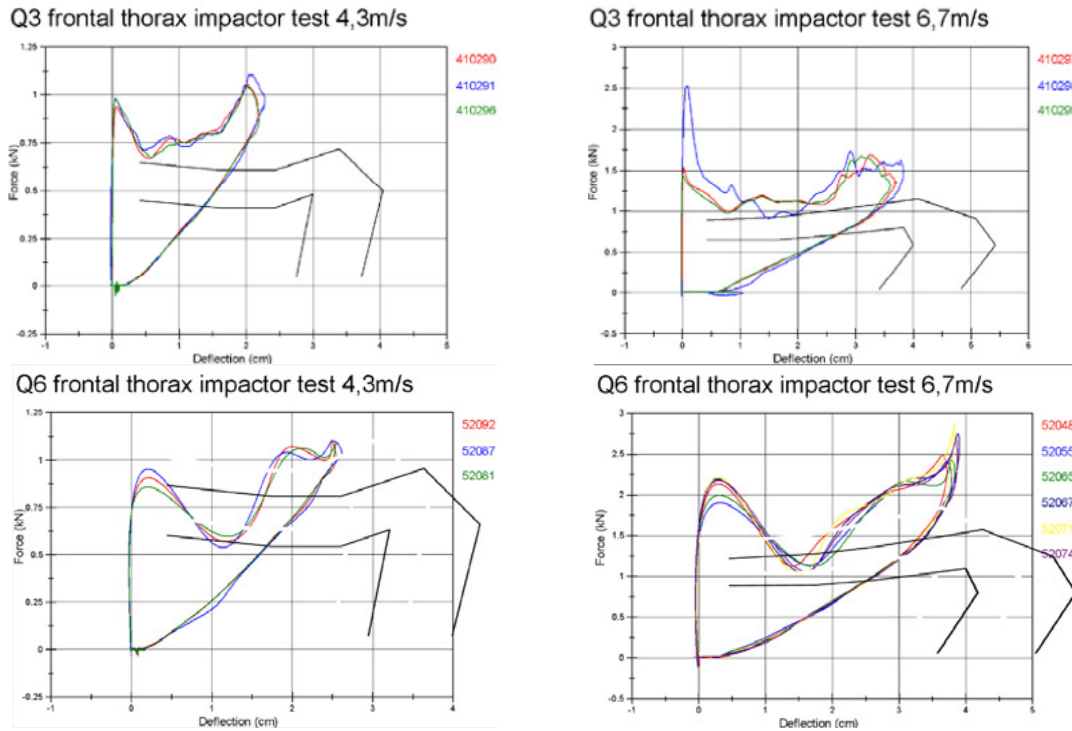


Figure 4-2: Responses of the Q3 and Q6 dummies against scaled corridor data (Wismans *et al.*, 2008)

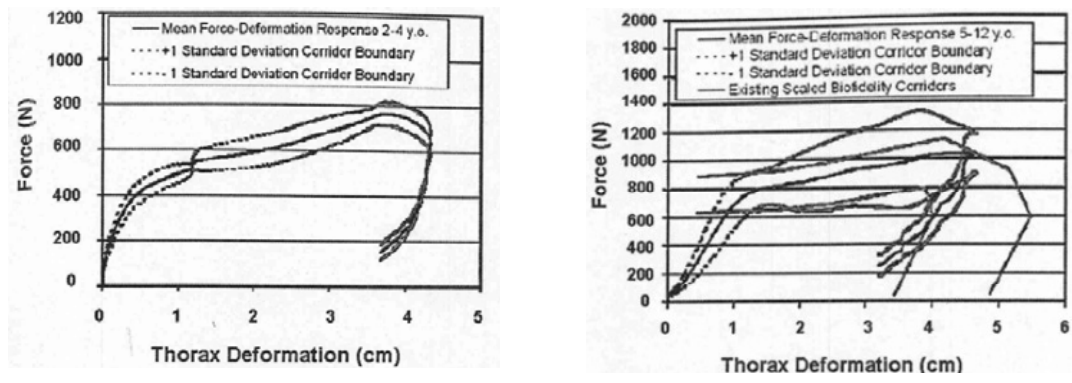
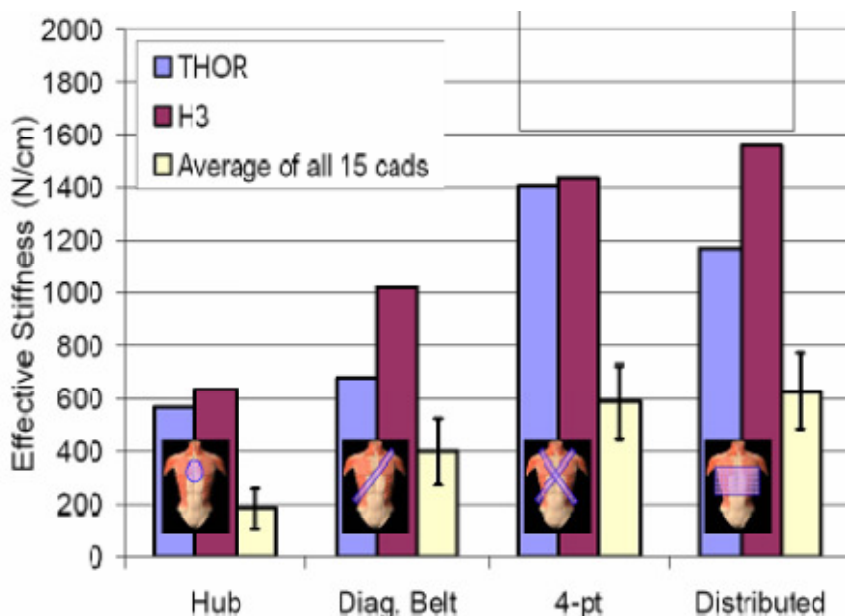


Figure 4-3: Experimental corridors obtained from paediatric PMHS (Ouyang *et al.*, 2006): (right) PMHS tests (impact with a 3.5 kg, 75 mm diameter impactor at 6.0 m/s; includes 4 subjects between 2 and 4 YO, and 5 subjects between 5 and 12 YO).



**Figure 4-4: Dummy and PMHS results table top tests at 0.9m/s with various loading conditions - factors indicate THOR/PMHS stiffness (Kent *et al.*, 2007)**

This has also been confirmed by numerous physicians and physical therapists collaborating with the LBMC of INRETS (see presentation “thoraco-abdominal compliance determined by observation of pulmonary treatments” CHILD Project). Evaluation results of the thoracic compliance from observation of pulmonary treatments will be available in a near future (SECURENFANT Project presentation at ISB 2009, Sandoz *et al.*, 2009). Additional results could also be available from experiments carried out at the Children Hospital of Philadelphia (Maltese *et al.*, 2008).

This stiffness of the thorax may affect the injury risk prediction to the thorax, the interaction with the belt and the overall kinematics.

Another factor to point out is that the upper component of the thorax in the dummy has an orientation that is opposite to the orientation of the ribs in the human. In the case of a thoracic compression induced by the shoulder strap, this tends to create a deformation of the upper thorax in the negative direction along the Z-axis (see picture in Figure 4-5), while in the human, the deformation against the same type of loading would be in the opposite direction.

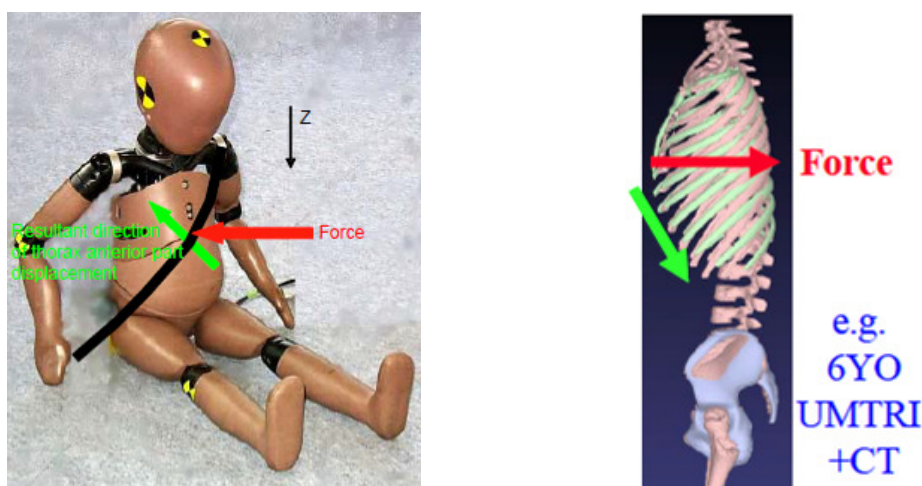


**Figure 4-5: Illustration of belt-thorax interactions**



### Abdominal foam block

Taking into account the results of the study carried out at the LAB (Chamouard *et al.*, 1996) one could conclude that the abdominal foam blocks of the Q3 and Q6 dummies are too stiff. This has been suggested by physicians and physiotherapists collaborating with the LBMC of INRETS (F.Alonzo; C. Goubel; Measurement of thoraco-abdominal mechanical stiffness using regular clinical examinations or Bermond *et al.* WCB 2006). However, the issue needs to be considered carefully considering the rate sensitivity of the abdomen, and the fact that the abdomen was developed using corridors obtained on porcine specimen (Rouhana *et al.*, 1989).

The longitudinal stiffness of the abdominal block is a determinant factor for abdominal deflection in the case of belt penetration while the lateral stiffness will determine the compression magnitude caused by the safety belt, CRS components or car interior accessories as armrests.

The vertical stiffness of the abdominal block is also very important because it can have an influence on the stiffness of the link between the pelvis and the thorax (along with the lumbar spine stiffness). As shown in Figure 4-6, this lumbar region stiffness is a determinant parameter regarding the occurrence of pelvis rotation under the effect of inertial loading due to the legs.

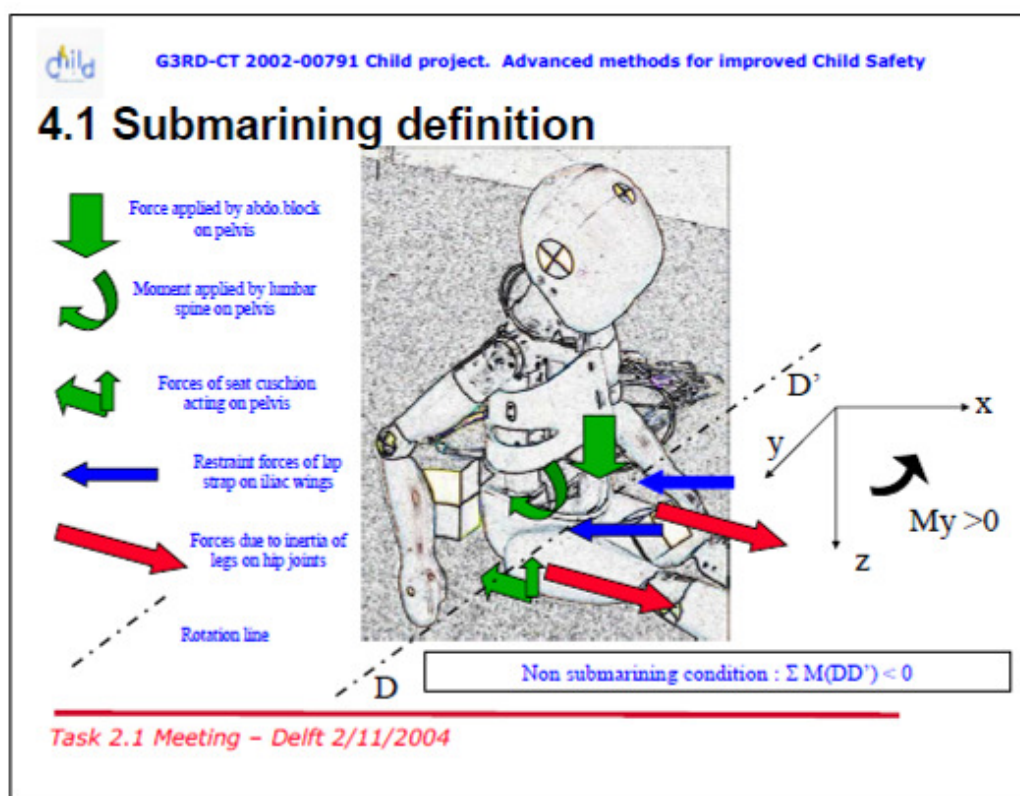


Figure 4-6: Forces acting on pelvis during restraint process and non-submerging condition (Johannsen and Goubel, 2004)

### Lumbar spine

As shown on Figure 6, the stiffness of the lumbar spine is one of the parameters influencing the rotation of the pelvis under the lap strap and its subsequent penetration into the abdominal cavity. Physicians and physiotherapists think that the lumbar stiffness is too high.

It is interesting to note that the lumbar spine stiffness is much lower in the P series than in the Q series. Overall, the spine stiffness (lumbar and thoracic) could affect the kinematics. It has been suggested in several articles (Wismans *et al.*, 1979, Brun-Cassan *et al.*, 1993 and Sherwood *et al.*, 2003) that the spinal stiffness of different dummies other than the Q series could be too high. An illustration is provided Figure 4-7 along with the profiles of P and Q dummies in testing.

This behaviour should be further investigated.

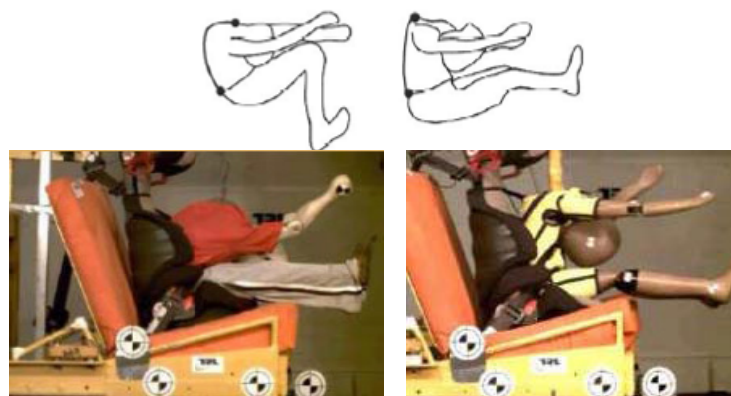


**Figure 4-7: Comparison of PMHS and dummy kinematics**

**Top: 12 YO PMHS (left) and HIII 6 YO dummy (right) kinematics in three point belt tests (Sherwood *et al.* 2003). The highlighted spine segment represents the spine from T1 to mid-lumbar. Bottom: P6 (left) and Q6 (right) tests from Wismans *et al.*, 2008.**

In a study of the performance of child dummies by TRL, Visvikis and Le Claire (2003) stated that "The spine flexion observed with the P3 has been referenced in studies with cadavers (Brun-Cassan *et al.*, 1993), although the limitations of cadaver studies are well known. The Q3 and HIII dummies were designed to conform to more stringent biofidelity targets, but these were based on the scaling of adult data. However, this perhaps explains why the kinematics of these dummies differed so markedly from the P3." However, the authors do not state what the well-known limitations of the cadavers are, and it must be noted that cadaver results are the source for most dummy characteristics (including for children dummies through the use of scaled response corridors). Furthermore, while the authors mention stringent corridors, it is unclear which data they refer to regarding the spine kinematics.

Regarding the shape of the lumbar spine, one may think that a curved lumbar spine for the Qs should be developed in order to get a more realistic posture of the lower torso. This is an important point as the pre-crash posture can affect the likelihood of injury for abdominal organs (submarining).

Reed *et al.* (2005, 2006) measured the actual posture of children in car seats and found that there were more "slouched" than in the standard (imposed) posture. They also proposed adjustments for the HIII seating procedures including the use of a foam pad behind the pelvis of the dummy to improve the posture (Figure 4-8). It is interesting to note that a similar strategy was used in some of the accident reconstructions of CHILD and CREST (proposition to put a tennis ball behind the pelvis in order to get a standard clearance between pelvis and backrest).

Based on these observations, it could be of interest to analyse the reasons for the selection of the current design for the spine and compare it with recent postural data.



**Figure 4-8: Position of the Hill 6YO dummy in a booster seat (Reed *et al.*, 2006)**  
**Left: proposition of padding to help positioning the dummy. Centre: posture without padding. Right: posture with padding**

### Pelvis

It is well-known that the anterior part of the iliac wings (ASIS) is not totally ossified before twelve years. This could be one reason for child vulnerability to lap belt penetration. This has to be checked and modified in the case of a too large protuberance in the area of ASIS. Recent data collected by University of Michigan on the shape of the pelvis could be helpful for this (Reed *et al.*, 2009). The pelvic geometry is one of the parameters believed to affect the risk of submarining.

### Pelvis-thighs junction or groin

The first versions of the Q dummies were developed for “Out Of Position” studies in order to evaluate the risk of injury due to airbag deployment. For this use, a standing dummy was necessary. This led to the use of standing upper thighs and pelvis. While some range of motion around the initial position is expected to be needed at the hip of seated dummies in order to predict correctly the head kinematics, the initial hip flexion angle for standing and seated dummies is obviously different. Head excursion data should therefore be analysed if modifications are performed in this region of the dummy.

For the evaluation of CRS in sitting position, safety straps are located in the area of the lower torso-upper thighs and a standing design does not appear to be appropriate. In some cases, the lap strap can slide into the interstice up to the hip joint where it remains locked (Figure 4-9). This could be very problematic as the belt interaction with the upper thighs and the pelvis is critical for the good simulation of submarining behaviour (e.g. Chamouard *et al.*, 1996, Reed *et al.*, 2008).



**Figure 4-9: Illustration of potential problem with the groin (Johannsen Goubel, 2004) (The neoprene skin is removed for a better visualization of the phenomenon)**

### **Selection of possible shortcomings for further investigation**

Assessing and proposing solutions for all the possible shortcomings is beyond the scope of the task and project. As a consequence, a priority list was established based on discussion between partners during meetings. Possible shortcomings were selected based on the expected interest in terms of dummy response, feasibility and time available. The conclusions of this prioritization are summarized below:

Possible shortcomings to be assessed in the current project:

- 1) Gap at the groin for the Q3 dummy (the problem does not seem as prominent for the Q6);
- 2) Stiffness of the lumbar region.

Both are related to the dummy submarining response and potentially the abdominal injury risk. This selection does not suggest that the other shortcomings are non-existent but only that they were beyond the scope of this project.

It should be noted that all the above mentioned shortcomings come from biomechanical research. When applying dummies in the field for development and regulatory applications other requirements also have to be considered, including Repeatability and Reproducibility. Dummy design needs to take into account these requirements from the beginning and should consider a good balance between biomechanical performance and other requirements.

Moreover a loading type dependency exists in PMHS specimens and ATD's. The effect of this was never investigated on the Q dummies but initial designs that met biomechanical corridors under hub loading suffered from severe bottoming out in sled tests (TNO reports, 1997 and 1998). Unfortunately, this type of phenomena could therefore concern the Q's but was never considered in projects like CREST and CHILD.

#### **4.1.3 Assessment of the lumbar region stiffness in flexion**

The objective of the tests was to evaluate the stiffness of the various components of the lumbar region in flexion and, when possible, to compare them with reference data. The tests were performed on the Q3 dummy only (due to dummy availability at INRETS).

In the Q dummies, the stiffness in flexion of the lumbar region is not only due to the lumbar spine itself but also to the vertical stiffness of the abdominal block: when the flexion occurs, the lower edge of the thorax engages the abdominal block which is then compressed between the thorax and the pelvis. As a consequence, in order to properly evaluate the global stiffness of the dummy, tests cannot be conducted only on the lumbar spine. The tests were therefore performed on the complete dummy with and without the abdominal block. The tests were also performed with the INRETS' Abdominal Pressure Twin Sensor mounted in the abdomen to evaluate their possible contribution to the stiffness.

Due to the limited availability of reference data in the literature, it was decided to compare the Q3 to another dummy representing the same (Hybrid III 3 Y.O.) and for which a calibration procedure exists to characterize the stiffness of the lumbar region. The procedure is described in detail in NHTSA Part 572.145. Since these tests were static, dynamic flexion tests were also performed in a similar setup in order to evaluate the stiffening effects the various components. A total of approximately 20 tests were performed.

## Description of the experimental setup

### Static test setup

In the Hybrid III static test, the dummy is seated on a flat surface with the legs straight and horizontal. It is rigidly held at the pelvis in the back and is pulled forward into flexion using a cable attached at the level of the occipital condyle. The cable is not attached directly to the head (otherwise the neck flexion would affect the results): it is instead linked to the spine box by a rigid extension (Figure 4-10 left). In the initial rest position, the Hybrid III dummy back needs to have an angle of less than 15 degrees with the vertical. The dummy is then pulled down using a cable at a speed between 0.5 and 1.5 degrees until the dummy back angle reaches 45 degrees. The dummy angle and the force applied through the cable are recorded and pass/fail values of the cable force at 45 degrees are provided.

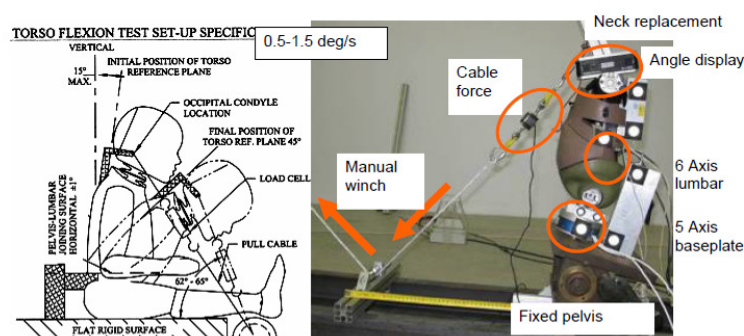


**Figure 4-10: Illustration of the static test setup Left: Hybrid III 3YO calibration procedure from NHTSA Part 572. – Right: simplified fixture developed for the Q3;**

A similar procedure was developed for the characterization of the Q3 dummy (Figure 4-10 right). Only the torso part of the dummy was kept for the test. The aluminium pelvis was attached to a fixed 5 axis load cell using an intermediate aluminium plate, spacers and screws going through the four holes at the bottom of the pelvis. The dummy was oriented such that the back is approximately vertical. A rigid bar was mounted instead of the neck and the cable was attached to it approximately at the level of the occipital condyle. After going around a pulley near the ground, the cable was pulled using a manual winch. A load cell was placed on the cable before the pulley. The forces and moments were also measured in the lumbar spine using the standard 6 axis dummy load cell. The dummy was then pulled down manually at approximately 1 degree per second until it flexed 45 degrees. An electronic inclinometer mounted on the neck replacement was used to provide instantaneous feedback and facilitate the adjustment of the speed. The tests were performed without the abdomen, with the standard abdomen and with the abdomen equipped with the APTS. The tests were captured on video and targets attached rigidly to the spine in the back of the dummy were used to calculate the dummy angle.

### Dynamic test setup

A similar setup was used for the dynamic test. The main difference was the loading method: a rope was passed around the shoulders of the dummy and attached to a heavy rigid pendulum in high position with some slack (Figure 4-11). Then the pendulum was released, pulling the dummy after there was no more slack. In order to protect the dummy from overloading, the pendulum was then stopped using aluminium honeycomb. Two angles of flexion were tested by adjusting the drop height of the pendulum and the slack on the rope: 30 degrees (level1) and 45 degrees (level2). An accelerometer was added to spine instrumentation. The tests were captured on video and targets attached rigidly to the spine in the back of the dummy were used to

calculate the dummy flexion angle. Tests were also performed with and without the abdominal block, and with the APTS.

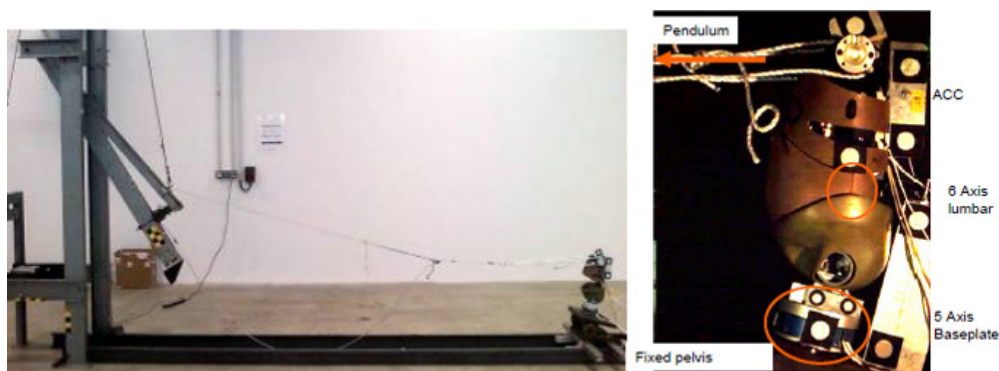


**Figure 4-11: Overview of the dynamic setup Left: overview with the pendulum in high position. Right: Instrumentation of the dummy**

## Results

### Static test results

The flexion was performed successfully until 45 degrees in all tested cases. When the abdomen was present, its compression between thorax and pelvis was very important (Figure 4-12 centre). This compression contributed to approximately half of the cable tension (as illustrated on the Figure 4-12 right). It also resulted in a response that was slightly more non-linear for the spine only tests. The results obtained with APTS were virtually identical to the results with the standard abdomen.

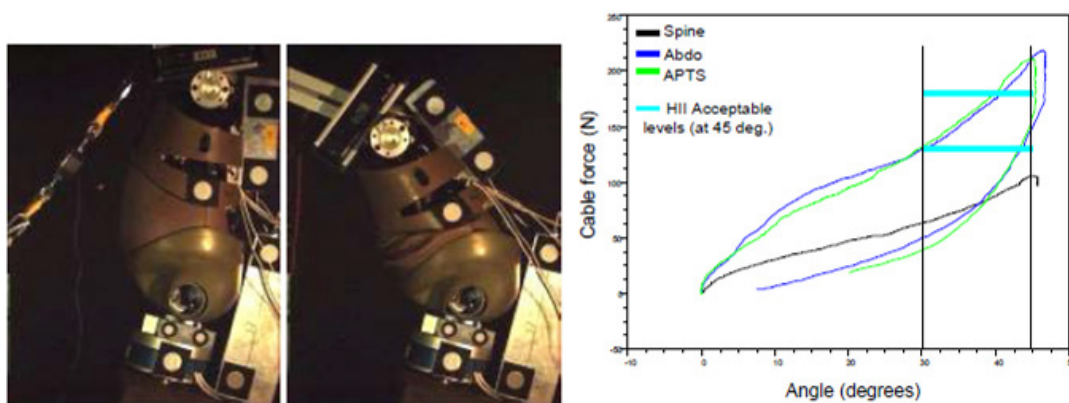


**Figure 4-12: Static test results: initial and final position, cable force vs. dummy angle (From left to right)**

The comparison with the HIII 3 Y.O. requires some interpretation and hypothesis as the geometry of the dummies and their initial positions are different (reference plane etc). If the HIII initial position was at the limit of 15 degrees, then it would need to flex only 30 degrees to reach the final position in the testing. If it was vertical at the beginning then it would flex 45 degrees. This second scenario is however unlikely based on the feedback from a Denton test engineer. The acceptable limits for the cable forces set in Part 572 were therefore added to the plot Figure 4-12 and extended to these two extreme cases. Overall the responses of the dummy with the abdominal block are very close to these limits.

### Dynamic test results and test comparisons

The dynamic tests results were also performed successfully for levels 1 and 2. However, for the case where 30 degrees of motion was targeted, the resistance of the

dummy affected maximum angle reached: the lumbar spine only tests reached approximately 35 degrees while the tests with an abdomen reached a little less than 25 degrees. The motion between 5 degrees and peak typically occurred within 75 ms, which seems a reasonable duration for the current application (crash testing). When an abdomen was present, the moments in the complete section at the lumbar spine were determined by transferring the moment measured the base plate load cell. For the transfer, it was hypothesized that the moment could be transferred using a simple scale factor (constant distance hypothesis). This scale factor was determined using the tests without abdomen. It was found to be approximately 1.6 (Figure 4-13). Overall, the repeatability of the tests was good for the level 1 (Figure 4-13). For the level 2, there were more vibrations visible on the curves due to the higher pendulum velocity (as illustrated on the Figure 4-14). The response of the dummy equipped with APTS was always very close to the response of the dummy with the standard abdominal block.

In all tested cases, the abdominal block was an important contributor to the dummy stiffness in flexion. This contribution also affected the load seen by the lumbar spine load cell (FZ) which was always higher with the block than without for the same flexion angle. In order to evaluate the stiffening effects due to the strain rate and presence of abdominal block, stiffness were computed by linear regression of the moment angle curve prior to the maximum angle. The results are summarized in Figure 4-15. Overall, the presence of the abdominal block approximately doubled the stiffness, for both static and dynamic tests. There is also approximately a factor 2 between the static and dynamic tests. The angular rates increased between level 1 and level 2 but the increase was not sufficient to result in large variations of the stiffness.

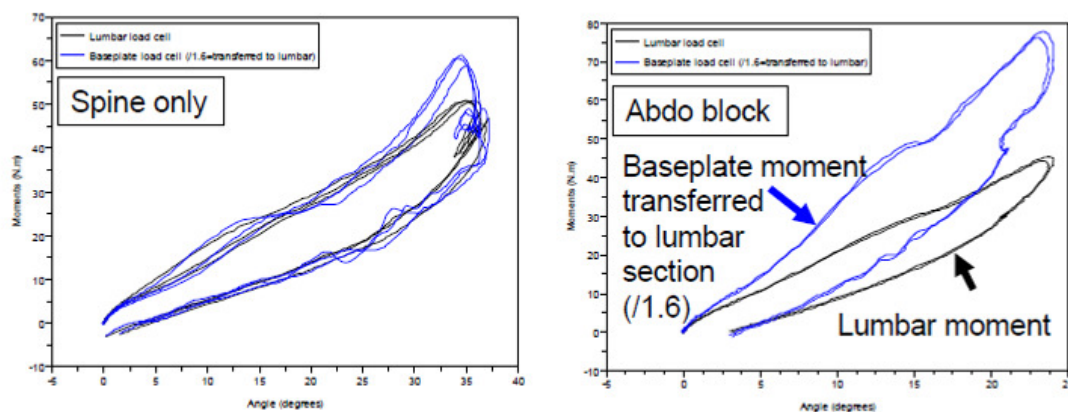


**Figure 4-13: Moment in the lumbar section and moment in the lumbar spine for level 1 tests**

**Left: Three tests with the spine only. Right: two tests with the standard abdominal block. A factor of 1.6 was used to transfer the base plate moment to the lumbar section. The base moment at the lumbar spine corresponds to the moment in the complete lumbar section (including the contribution from the abdominal block) while the results from the lumbar load cell includes only the contribution from the lumbar spine component.**

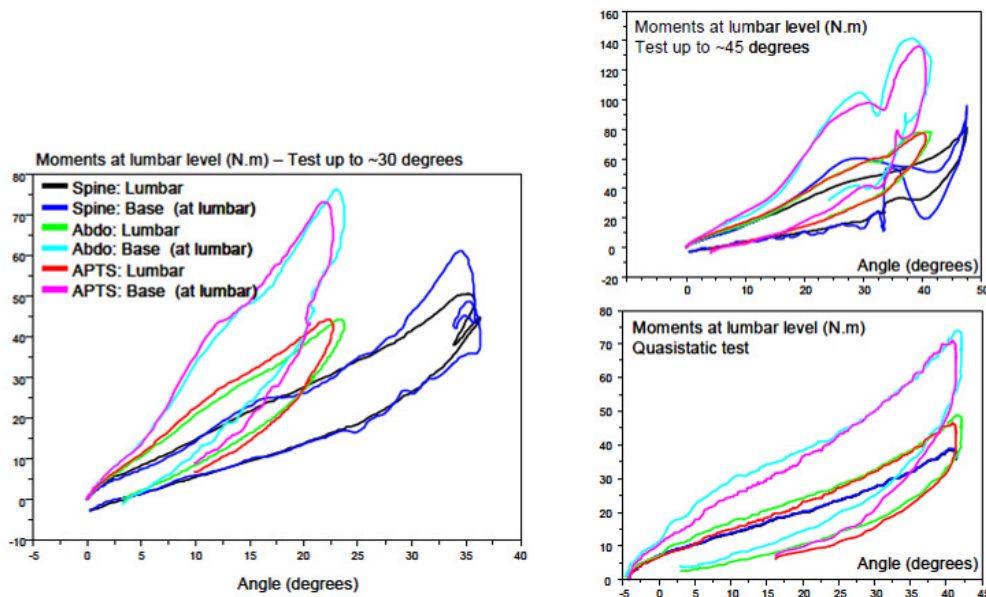


**Figure 4-14: Figure 14: Comparison of the moment vs. angle results for all loading speeds**

**Left: level 1 dynamic; Upper right: level 2 dynamic; Lower right: static calibration test. The Base moment at the lumbar spine corresponds to the moment in the complete lumbar section (including the contribution from the abdominal foam) while the results from the lumbar load cell includes only the contribution from the lumbar spine component.**

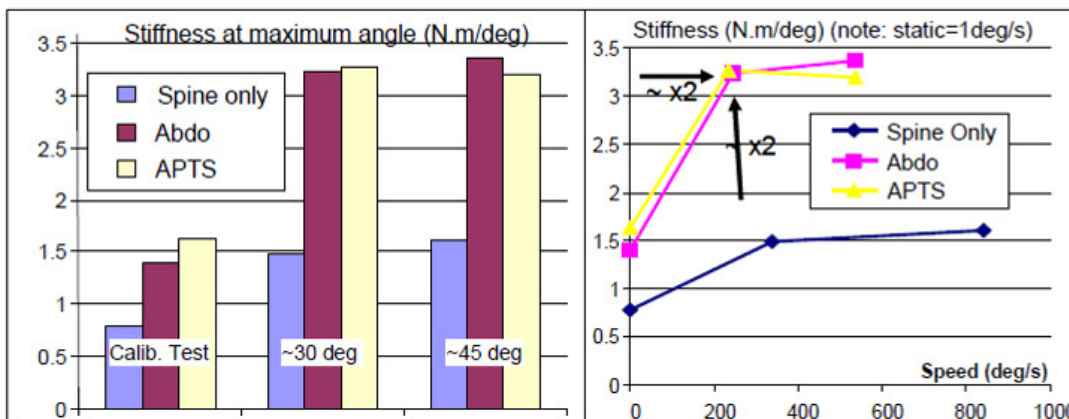


**Figure 4-15: Overall stiffness in the various configurations tested**

**Discussion and conclusion on the lumbar stiffness assessments**

The response of the Q3 dummy in flexion was characterized in static and dynamic tests. The dummy was tested with and without the abdominal insert, and with the insert equipped with the APTS. The contribution of the abdominal foam block to the global dummy response was very important (about 50% of the flexion stiffness, both in static and dynamic), suggesting that the characterization of the lumbar spine component is insufficient to determine or certify the dummy response in flexion. This stiffening, due to the compression of the anterior portion of the back (near the surface) between the thorax and pelvis, was repeatable. While this mechanism is not present (or as prominent) in other dummies families such as the Hybrid III, a similar mechanism could exist in the human (compression of the abdominal content by the floating ribs and by



the diaphragm). However, the amplitude of this contribution to the flexion response is unknown. Also, the use of APTS within the abdominal blocks did not affect the response, perhaps because the sensors are located far enough below the surface not to affect the anterior compression mechanism. The stiffening factor due to the loading speed increase (between static and dynamic) was similar for the tests with and the tests without the abdominal block (factor 2).

Regarding the static tests, the HIII calibration procedure was simplified for the current study. For example, if present, the legs of the Q3 could have contributed to the response at the end of the flexion if the pelvic foam (that is pushed by the abdominal blocks) had contacted the upper thighs. Similarly, it was assumed that the neoprene suit of the Q3 dummy would have negligible effect on the stiffness and the tests were conducted without the suit. Also, the geometrical differences between the dummies make the interpretation difficult (how to define the initial position and the reference planes?). However, beyond these methodological limitations, the results suggested that the flexion stiffness of the Q3 lumbar region (including the abdominal block contribution) was similar to the HIII 3 YO (or at least that the Q3 was not much stiffer than the HIII). In the absence of better biomechanical reference, it was decided that no modification of the lumbar region would be performed at this time.

#### **4.1.4 Proposals to improve the dummy response by removing the gap at the groin**

##### **Description of the gap of the Q3 dummy**

The Q family has a pelvis and hip design corresponding to a standing dummy. Unlike other seated dummy families (e.g. HIII, EuroSID, THOR), it does not have a seated pelvis where the foam covers the pelvis and upper thighs in a single piece. In consequence, in order to leave a sufficient mobility at the hip, the upper thighs and the pelvis are separated by a gap which is clearly non-human like (the femoral neck is not directly visible in humans). This gap, illustrated Figure 4-16, can catch the lap belt after it moves from the upper thighs. The slope of the anterior pelvis foam (overall V shape) would also tend to push the belt towards the bottom into the gap (Figure 4-16 left).

Depending on the belt path, the penetration can also occur on the side gap under the effects of belt tension. Once the belt (in tension) is in the gap, it prevents any anterior rotation of the pelvis making submarining impossible. The presence of the neoprene suit on the dummy could be expected to mitigate the risk of the belt catching mechanism. However the suit is very flexible and has a relatively large fold at the groin in seated position as illustrated Figure 4-17, making that the gap can remain apparent even without loading. Because it is relatively flexible, it cannot prevent the belt penetration if some loading is applied (illustration Figure 4-18). Also, the gap can vary (and increase) as a function of the leg angle (Figure 4-17) and belt load (the tension of the lap belt can compress the foam at the upper thigh and further open the gap).



**Figure 4-16: Illustration of the gap at the pelvis-lumbar junction (groin): dummy without the suit.**



**Figure 4-17: Q3 dummy with suit: effect of hip angle on the fold at the groin**

**Top row: the suit is tensed/straight (no fold) in standing or here supine position but a fold appears and increases with the seating angle. It must be noted that the underlying gap is also affected by the seating angle (the gap reduces from supine to seated). Bottom row: gap when seated (position of third picture from the first row)**



**Figure 4-18: Gap and belt penetration with suit. Under manual tension, the belt seems to be able to penetrate the gap (front and side)**

## Proposals

Several proposals were formulated and discussed. After several iterations two proposals were selected and implemented by INRETS and FTSS within the frame of the CASPER project.

### Proposal 1: seated pelvis (INRETS)

Based on the description of the problem in the previous section, the first proposal from INRETS was to fill completely and permanently the gap to prevent reopening as a function of the leg angle or belt load. This solution would effectively transform the pelvis into a seated pelvis. Illustrations from a proposed implementation are provided in Figure 4-19. It was proposed to fill the gap with a material similar to the one of the pelvis and thighs skin (PVC or polyurethane). The material would be glued to both pelvis and upper thigh foam. However, in order to have space to access and install the hip, no additional material would be added on the bottom of the dummy. Furthermore, the thigh foam would have been cut to make possible the some angular motion of the femur into the thigh foam.

It was proposed to use an angled cut to leave sufficient space for the lap belt on the anterior surface of the thighs (even positioned horizontally on the thighs) while reducing the resistance to the extension of the hip due to the contact of the femur on the posterior surface of the thighs. Also, in order to make possible the assembly of the femoral head into the pelvis, the part of the thigh foam attached to the pelvis would have been cut on the inner face of the thigh and a zipper added to open and close the thigh for installation. It was also proposed to use a PVC plastron to reinforce the neoprene suit in order to improve the continuity of the anterior torso wall. That would have minimized the risk penetration of the shoulder and/or lap strap into the interstices between pelvis and abdominal block, and abdominal block and thorax.

This proposal was not selected because the design change was perceived as too radical for the dummy by other partners. Such a change would have required extensive testing before acceptance, and the limitation of the hip range of motion was also perceived as potentially problematic.



**Figure 4-19: Illustration of “seated pelvis” proposal**

**Top: shape of the material to add in the gap (here with plastiline) and proposed plastron to cover other abdominal gaps. Bottom: position of the zipper (left) and position of the cutting line (right)**

### Proposal 2: shape change using the current Q10 design (FTSS)

FTSS proposed to adapt the design of the Q10 dummy (currently under development). In the Q10, the gap at the groin was minimized by selecting more conforming shapes of the pelvic and thigh foams. The geometrical differences between the two designs are illustrated in Figure 4-20. The flexion beyond the position on the Figure 4-20 would be made possible by the selection of foams that would be soft enough to compress. Also, it can be noticed on the Figure 4-20 that the V shape of the pelvic foam described in a previous section is not present anymore, and that the gap is minimized not only in the front but also on the side of the dummy.

This design could only be adapted to the Q3 once it has been tested in the Q10 (which was not the necessarily compatible with the timeframe of the current task). INRETS also commented that while the gap was removed in the position displayed, different positions (including positions that would better match the actual postures of children in cars) could reopen the gap (Figure 4-21), meaning that the belt could be caught early in the kinematics before any torso flexion occurs. The gap could also reopen under the effect of the lap belt force (that would compress the foam of the thigh).

The use of this design is still considered depending on its performance and the performance of the other proposed solutions. However, its transposition to the Q3 dummy is beyond the frame of the current task (mould change, etc.).

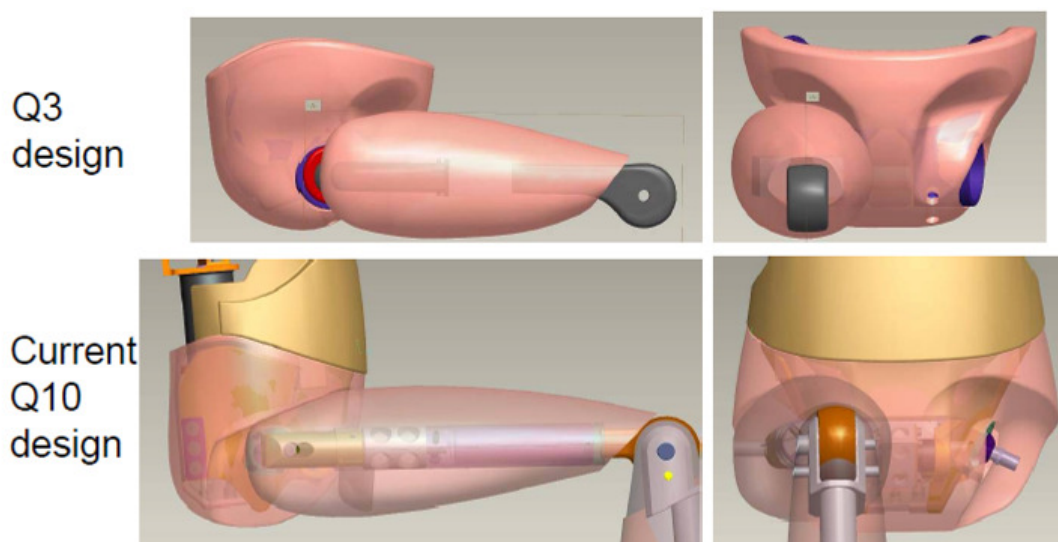


**Figure 4-20: Comparison of the Q3 and Q10 design at the groin**

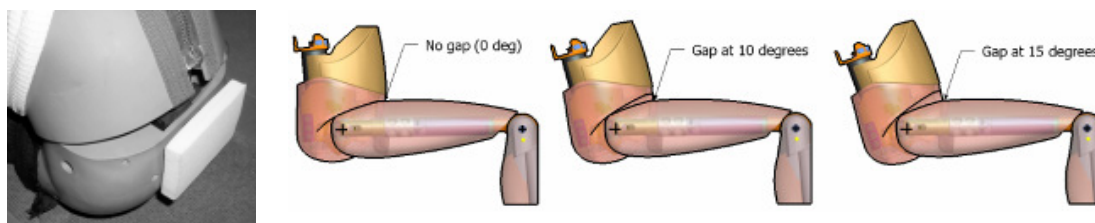


**Figure 4-21: INRETS comment on the proposed Q10 design.**

**Left: relaxed positions with a pelvis tilted forward have been observed by Reed *et al.* (2006) when children were left free to choose their seating position, leading to recommendations to tilt the pelvis forward by adding foam behind it in HILL 6YO seating procedures. Other illustrations: proposed Q10 design and illustrations of the possible gap creation when changing the seating angle (obtained by image editing of the previous)**

### Proposal 3: Soft insert at the pelvis-thigh junction (INRETS)

Following the first proposal, INRETS proposed a different design that would limit the impact on the dummy response. In this solution, an insert made of soft but resistant material would be positioned at the groin and would cover the gap. The insert would not be glued to the pelvis but possibly glued to the thigh. The insert would be an add-on to the dummy. Because of the effect described in the previous figure (Figure 21), the insert geometry would need to be built for a representative position and further flexion would need to be obtained by compression of the material. After preliminary discussions with FTSS and TUB, the design of this solution was continued.

The angle selection for the thighs was performed based on the actual seating of a Q3 in a few child seats. A drawing of the different positions tested is proposed Figure 4-22. Based on this drawing, a reference position was selected and a rigid link between shoulder and knee was built to ensure that the position would be kept for the remainder of the task. It must be noted that the design procedure that followed could be applied to different angles. An insert made of plastiline was modelled manually to fill the gap. The insert (positioned on the right leg) and the reference position are shown in Figure 4-23. Because the insert goes all around the thigh (like a ring), gluing to the thigh may not be necessary. This would make the replacement of the insert relatively easy while still using standard dummy components. It was therefore decided not to glue the insert in its first version (but the option remains available if necessary).

In order to build the prototype without having access to the CAD of the dummy, it was decided by INRETS to mold the insert directly on the dummy in the reference position. A plaster mold was therefore built in small sections around the plastiline insert and the dummy, keeping reservations for an inlet, a vent, and two planes to open the mold. An illustration of the mold is provided Figure 4-24.

The plastiline insert was then removed and a reservation was made with plastiline again to keep some space around the hip and femoral neck (in order to keep a sufficient mobility of the joint).

A polyurethane rubber (Korapur 666) was selected at first for the material of the insert. However, it appeared that it was too rigid and too viscous for the moulding procedure. A softer silicon rubber (Silastic 3481, Dow Corning, stiffness of 24 Shore A) was finally selected. Since the liquid rubber was too viscous for gravity moulding, the insert was moulded by injecting the rubber with a manual pump. After curing, the mold and the insert were removed and the procedure (plastiline insert, plaster mould, etc.) was repeated for the other thigh.

A presentation of the finished prototype is available in the next section.

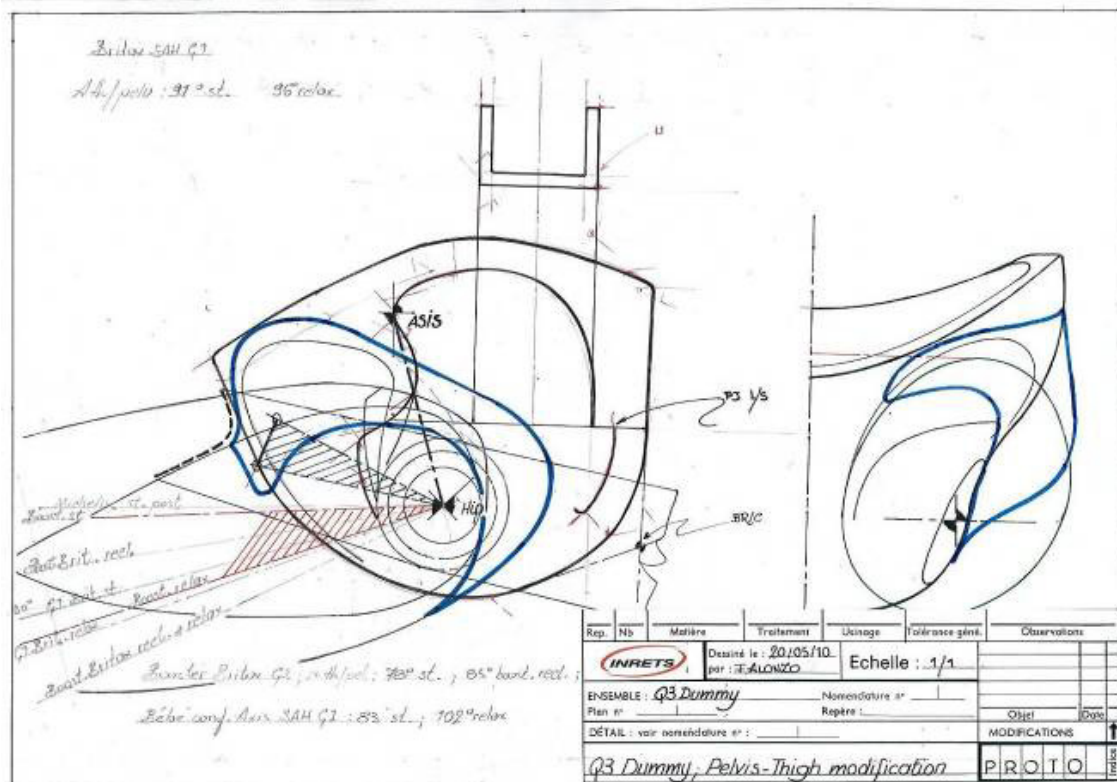


**Figure 4-22: Drawing of the thigh angles obtained when seating the Q3 in actual seats (an outline of the insert position is in blue - front and side views)**



**Figure 4-23: Insert model (in grey plastiline) at the pelvic-thigh junction - the insert was modelled in a reference position that was maintained using a rigid bar  
In this design, the insert goes around the complete thigh while leaving the access to the hip screws (bottom right)**



**Figure 4-24: Illustrations of the plaster mould build around the plastiline insert and the dummy**

#### Proposal 4: Suit reinforcement (FTSS)

Based on the various comments and analysis, FTSS proposed to add reinforcements to the neoprene dummy suit. This solution could be used alone or in combination with other solutions. This proposal was also selected for further work within the task. The prototype corresponding to this proposal is presented in the next section.

#### 4.1.5 Presentation of the prototypes

##### Silicone insert (INRETS)

The silicone inserts filling the gap at the groin that were obtained by moulding are illustrated in Figure 4-25. The silicon rubber matches exactly the shape of the pelvis and thighs. It holds in place on its own and the legs can be easily mounted on the dummy.

The silicon rubber mechanical properties provided by the manufacturer are summarised here below:

- Silastic 3481 with standard curing agent;
- Tensile strength: 4.7 MPa;
- Elongation at break: 544%;
- Tear strength: 26kN/m.

The silicon insert (as well as the pelvis and thigh) was then scanned using a 3D laser scanner. An illustration of the scanned assembly is provided in Figure 4-26. This scan was provided to the task partners for further comments. FTSS comments on the design were overall positive with two remarks:

- 1) The design could result in a stiffening of the dummy response for the hip flexion
- 2) Some parts of the insert seem thin and could be fragile in the long term.

It was commented by FTSS that the insert may affect the dummy response as the interaction between legs and pelvis is affected. The largest the stiffness and hardness of the material applied the larger this effect. On the other hand, the softer the material the less effective it will be. It was also indicated by FTSS that raised ridges on the

insert, as visible on Figure 4-25, could be a long term durability problem. For this reason they are usually avoided in dummy flesh parts.

The above remarks indicate that it is key to find an optimal hardness of the insert material. Also the impact on the repeatability, reproducibility, durability etc. should be evaluated, like for all proposed modifications to the dummy as recommended by FTSS. INRETS agrees with these comments and believes that the inserts need to be tested to answer these questions (the first one in particular since the insert could be inexpensive and replaced often if necessary).

While soft, the silicon is relatively incompressible and is therefore expected to prevent the intrusion of the belt in the gap. However, this incompressibility seems to also result in a stiffening of the hip in flexion past the reference position as illustrated in Figure 4-25. This stiffening is believed to be mainly due to the part of the insert that is directly near the rigid aluminium pelvis. This section could be thinned up if necessary.

If larger numbers of inserts are considered in the future, it is believed that a standalone mold (without the dummy) would be much more practical and repeatable than the current method. Deriving this mould from the 3D scan of the insert would also make possible a perfectly symmetric of the inserts and facilitate small thickness adjustments (or even an adjustment of the reference position).

Also, it may also be possible to integrate the shape of the insert directly in the mold of the thigh, which would allow a better continuity, both for the geometry and the material. However, possible durability issues would have to be evaluated and if needed solved to make this solution practical.

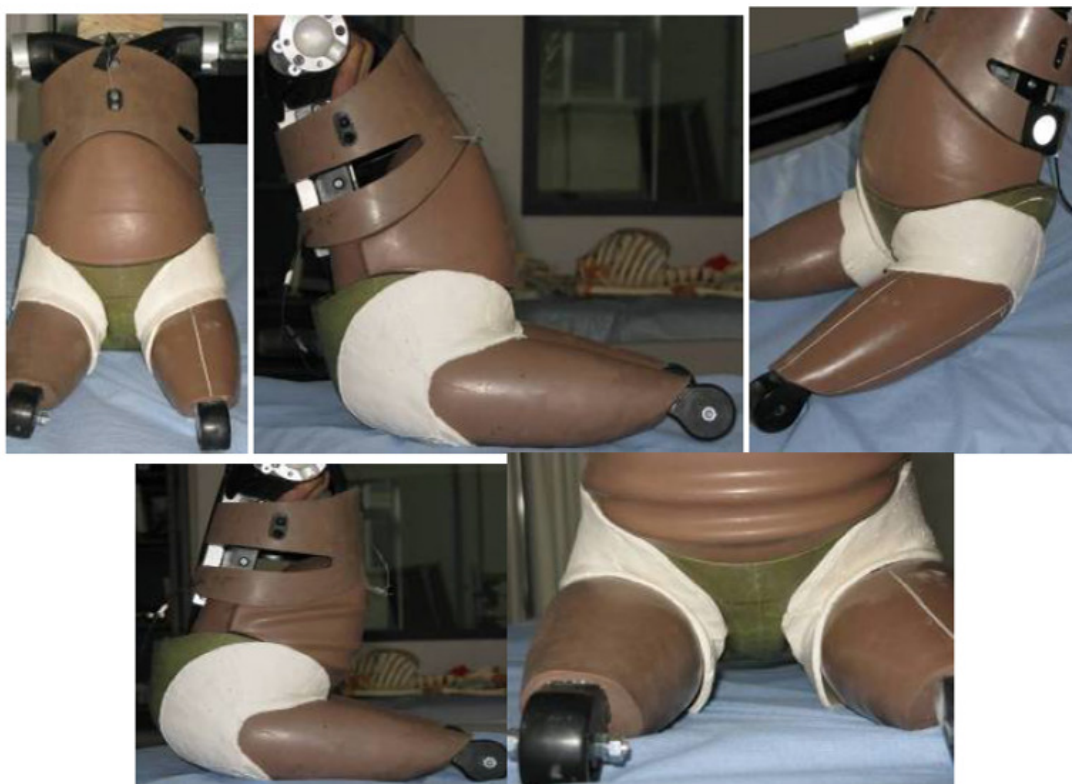


**Figure 4-25: Silicon inserts in position on the Q3 dummy - reference position (top) and dummy in a forward flexed position (bottom)**



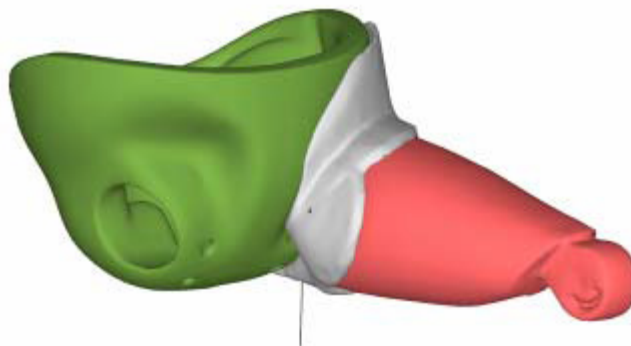


**Figure 4-26: 3D scan of the insert, pelvic foam and thigh**

#### **Modified dummy jacket (FTSS)**

FTSS build a dummy jacket with added reinforcements near the groin. The reinforcement consists in patches of several stiffness/thicknesses with an ellipsoid shape (Figure 4-27). The patches can be attached to the jacket using a Velcro that was sewed onto the jacket near the groin.

The Velcro also allows to orient the patches in an optimal direction. Recommendations on this were made by FTSS to INRETS and will be discussed when defining the sled test series.



**Figure 4-27: Illustration of the Q3 dummy jacket modified by FTSS**

#### **4.1.6 Preliminary evaluation of the prototypes**

The following test was the preliminary evaluation of the prototypes in sled tests. For these tests, the Q3 dummy was seated on a high back booster seat (Graco Junior Maxi, Group 2/3) in test setup similar to the R44 testing (pulse, bench). The tests were performed with the standard dummy, or with auxiliary equipment (silicon insert or Velcro patches). Two postures were tested: standard, with the dummy against the seat back and relaxed, with some space between the pelvis and the seat back.

Two belt paths were also used: normal belt path and an incorrect belt path where the lap belt goes straight to the anchorage points without passing under the armrests. Illustrations of the test setup with the seated dummy are provided in Figure 4-28. The instrumentation included pelvic accelerations, lumbar forces and moments, lap belt force, shoulder belt force, head accelerations and three video cameras (one on-board and two static).

Unfortunately, it was not possible to test all combinations of configurations due to the rupture of the main cable of the sled (that will require several weeks to repair and check). Furthermore and for the same reason, it was not possible to test a configuration where submarining would occur, which is clearly a limitation of this evaluation. Fourteen tests were conducted and a summary of the test matrix is provided in Table 4-1. Visual inspection was performed between each test to ensure that the auxiliary equipment was not damaged.



a) Overview of the setup (no auxiliary equipment) prior to the testing - Notice the fold in the dummy suit



b) From left to right: Softest (not tested), medium (6) and thick (8) patches positioned. The patches tested were painted in red and the belt was highlighted with white



c) From left to right: Medium (6), thick (8) and thick close-up (9) patches with the belt positioned



d) Left: silicon inserts (without the suit); Center and right: close-ups of the area without silicon inserts installed. Notice how the inserts fill the gap and removes the folds



e) Left: Standard position (11) with the back against the seat; Centre: Relaxed position (12) until the knee clears the front of the seat; Right: misuse (the belt does not pass around the armrests)

**Figure 4-28: Postures and auxiliary equipment used in the preliminary sled tests (the test number is in parenthesis)**

**Table 4-1: Summary of test matrix**

Test	Posture	Belt path	Auxiliary equipment	Comment
1	Standard	Correct	None	
2	Standard	Correct	None	Same as 1
3	Relaxed	Correct	None	
4	Relaxed	Correct	None	Same as 3
5	Relaxed	Correct	None	Same as 3; broken forearm
6	Standard	Correct	Patch medium	
7	Relaxed	Correct	Patch medium	
8	Standard	Correct	Patch thick	
9	Relaxed	Correct	Patch thick	
10	Relaxed	Misuse	Patch thick	
11	Standard	Correct	Silicone	
12	Relaxed	Correct	Silicone	
13	Relaxed	Misuse	Silicone	No video
14	Relaxed	Misuse	Silicone	Same as 13; sled cable broken

In the two tests without auxiliary equipment, partial penetration of the belt inside the gap between thigh and pelvis was clearly visible on the videos (Figure 4-29). It was expected to have a larger penetration in the case of misuse however the test could not be conducted due to the sled failure. When the medium stiffness patch was used, partial penetration still seemed visible on the videos and the belt was folded in longitudinally during the flexion of the dummy. Subsequent tests were performed using the stiffer and thicker patch. This thicker patch seemed to reduce the penetration in the standard seating configuration (Figure 4-30). Belt folding was still apparent. There was no belt penetration visible in any of the tests conducted with the silicone insert (Figure 4-31).

The overall kinematics was quite similar for all tests of the same configuration, whether auxiliary equipment was present or not. Results for the standard seating configurations are provided as examples in Figure 4-32. In this preliminary, the effect of the auxiliary equipment on the raw dummy output was limited (as it could be expected based on the similarity of the kinematics). When looking at the target data, it was found that the thigh excursion was affected by the auxiliary equipment: the silicone insert resulted in the shortest excursion, followed by the patches and the dummy without auxiliary equipment (Figure 4-33). However, these results need to be considered as preliminary since no repeatability testing was performed and that minor pulse differences may have affected the maximum excursion. Head excursion data would also be an important output to analyse in order to evaluate the performance of the proposed solution.



**Figure 4-29: Lap belt kinematics in standard position without auxiliary equipment (test 2) - the flexion and the excursion from the abdomen hide temporarily the belt. However, during the extension (rebound, bottom rows), the belt becomes visible again and appears to be in the gap (The images are cropped from the on-board camera with one image every 10ms)**



**Figure 4-30: Lap belt kinematics in standard position with the thick patch (test 8)  
The overall kinematics is similar to the response without auxiliary equipment. Based on the rebound images, the belt does not appear to penetrate the gap (bottom rows). The belt gets folded longitudinally during the dummy flexion and remains folded after the rebound.**



**Figure 4-31: Lap belt kinematics in standard position with the silicon insert (test 11) the overall kinematics is similar to the response without auxiliary equipment. Based on the rebound images, the belt does not appear to penetrate the gap and does not really fold. It remains stable on the pelvis thigh gap during the complete kinematics**

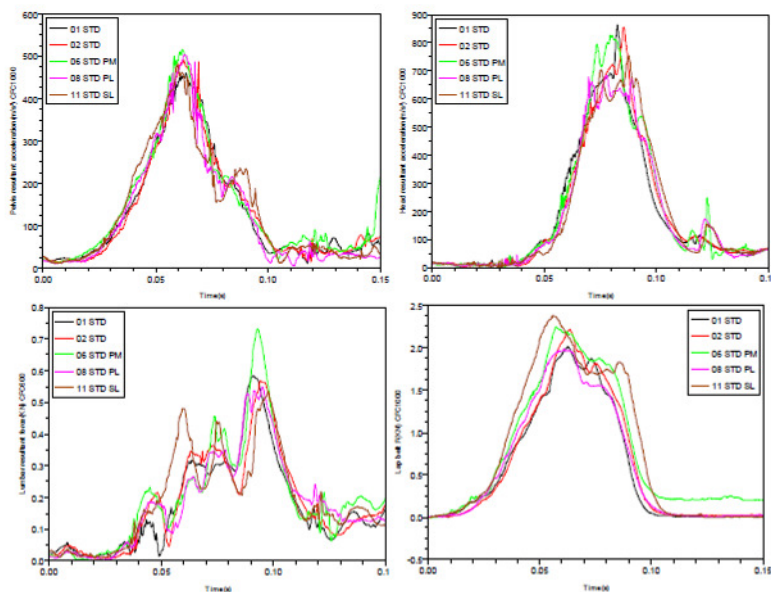


**Figure 4-32: Summary of channel data for the standard configuration, with the medium patch (PM), large patch (PL) and silicon insert (SL)**

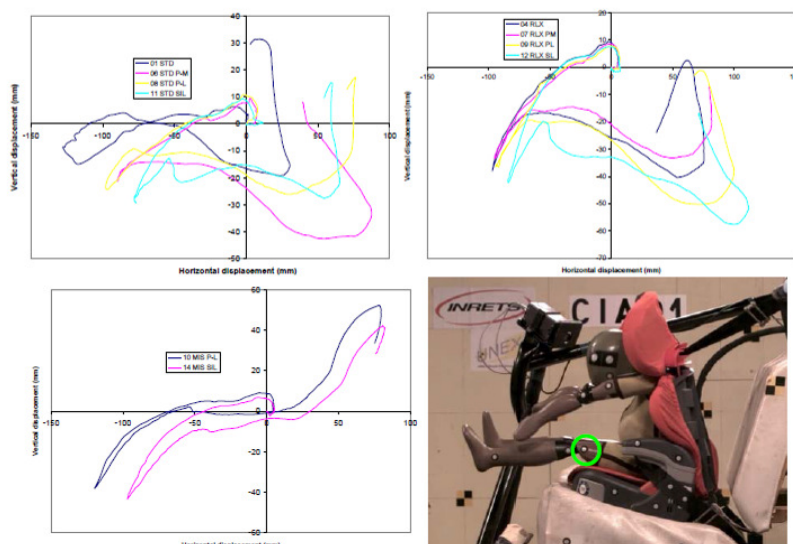


**Figure 4-33: Trajectory of thigh target for the different configurations Legend: STD=standard posture; RLX=relaxed. The thigh target is highlighted by a green circle on the picture**

#### 4.1.7 Conclusions and perspectives

After multiple iterations and discussions, two prototypes for the improvement of the Q3 response in the abdominal region were built. These solutions are relatively generic and could be adapted to the Q6 or the Q10 if needed. A preliminary evaluation of the prototypes in sled tests was performed. It confirmed the interest of the solution to prevent the penetration of the belt in the gap at the groin. However, the testing was limited due to equipment failure and submarining conditions could not be tested. Further data analysis of the current test data (in particular head excursion) could also be performed.

While it is believed that the gap issue should be tackled for the dummy used in future regulation, it must however be noted that in the even in the case of a successful and complete evaluation, more work will be needed to transform the prototypes into an industrial solution.

It should be noted that ultimately, the influence of any dummy modifications proposed in this report should be investigated for repeatability and reproducibility. However, this is beyond the scope of the current task. Good Repeatability and Reproducibility (R&R), as observed with the Q dummies [ref to EEVC WG 12 – 18 report] is key for application in regulatory environment.

#### 4.1.8 References

Bermond, F., Bergeau, J. Alonzo, F., Goubel, C., Bruyère, K., Joffrin, P., Cossalter, B., and Verriest, J-P. Enhanced methods and tools for child thoracic and abdominal compliance assessment, World Congress of the Society of Biomechanics, Munich, August 2006.

Biard, R., Alonzo, F., Muge, A.-C., Dejeammes, M., Chamouard, F., Tarriere, C. (1997) Torso improvements in child dummies used for certification tests in europe. Proc. 2nd Child Occupant Protection Symposium, P-316, pp. 231-242, SAE Technical Paper No. 973315. Society of Automotive Engineers, Warrendale, PA.

Brun-Cassan, F., Page, M., Pincemaille, Y., Kallieris, D., and Tarriere, C. (1993). Comparative study of restrained child dummies and cadavers in experimental crashes. SAE Technical Paper 933105. In *Child Occupant Protection (SP-986)*, 243-260. Warrendale, PA: Society of Automotive Engineers, Inc.

Chamouard, F., Tarriere, C., Baudrit, P. (1996). Protection of children on board vehicles: influence of pelvis design and thigh and abdomen stiffness on the submarining risk for dummies installed on a booster. Proceedings of the 15th International Technical Conference on Enhanced Safety of Vehicles. National Highway Traffic Safety Administration, Washington, DC. pp. 1063-1075.

TNO Report (1997) Prototype Testing Q3 Dummy, 1997.OR.BV.030.1-DT, Dirk Twisk *et al.*

TNO Report (1998) Prototype Testing Q3 Dummy Results, 1998.OR.BV.020.2-DT, Dirk Twisk *et al.*

Johannsen H and Goubel C, (2004) Submarining Research. Task 2.1 Meeting. Delft, 2nd November 2004.

Kate de Jager, Michiel van Ratingen *et al.* (2005) Assessing New Child Dummies And Criteria For Child Occupant Protection In Frontal Impact. On behalf of EEVC WG12 & WG18. Paper no. 05-0157.

Kent *et al.* (2007) Presentation at NHTSA THOR workshop, April 2007.

Maltese, M. R., Castner, T., Niles, D., Nishisaki, A., Balasubramanian, S., Nysaether, J., *et al.* (2008). Methods for determining pediatric thoracic force-deflection characteristics from cardiopulmonary resuscitation. *Stapp Car Crash Journal*, 52, 83-105.

Ouyang, J., Zhao, W., Xu, Y., Chen, W., & Zhong, S. (2006). Thoracic impact testing of pediatric cadaveric subjects. *The Journal of Trauma*, 61(6), 1492-1500. doi: 10.1097/01.ta.0000233711.07823.40.

Reed, M.P., Ebert-Hamilton, S.M., Manary, M.A., Klinich, K.D., and Schneider, L.W. (2005). A new database of child anthropometry and seated posture for automotive safety applications. *SAE Transactions: Journal of Passenger Cars - Mechanical Systems*, 114: 2222-2235.

Reed, M.P., Ebert-Hamilton, S.M., Manary, M.A., Klinich, K.D., and Schneider, L.W. (2006). Improved positioning procedures for 6YO and 10YO ATDs based on child occupant postures. *Stapp Car Crash Journal*, 50: 337-388.

Reed M.P., Ebert-Hamilton S.M., Sherwood C.P., Klinich K.D., Manary M.A. (2008) Evaluation of the Static Belt Fit Provided by Belt-Positioning Booster Seats. September 2008. IIHS report.

Reed M.P., Klinich K.D., Ebert-Hamilton S.M., Manary M.A., Rupp J.D. (2009) Improving Restraints for Older Children: Static and Dynamic Belt Fit Evaluation. SAE Government-Industry 2009. <http://www.sae.org/events/gim/presentations/2009/>.

Rouhana, S.W., Viano D.C., Jedrzejczak E.A. and J.D. McCleary (1989) Assessing Submarining and Abdominal Injury Risk in the Hybrid III Family of Dummies. In

Proceedings of the 33rd Stapp Car Crash Conference, pp 257–279, SAE Paper no. 892440. Warrendale, Pa, Society of Automotive Engineers.

Sandoz B, Vajda E., Alonzo F., Bruyère K. and F. Bermond (2009) Mechanical properties assessment of child trunk. ISB Conference 2009. Cape Town.

Sherwood, C. P., Shaw, C. G., Van Rooij, L., Kent, R. W., Crandall, J. R., Orzechowski, K. M., *et al.* (2003). Prediction of cervical spine injury risk for the 6-year-old child in frontal crashes. *Traffic Injury Prevention*, 4(3), 206-213. doi: 10.1080/15389580309885.

Visvikis and LeClaire (2003) Evaluation of child dummies. TRL Report.

Wismans, Maltha, Melvin and Stalnaker (1979) Child Restraint Evaluation by Experimental and Mathematical Simulation, Twenty-third Stapp Car Crash Conference Proceedings, SAE #791017, 1979.

Wismans J; Waagmeester K, Le Claire M., Hynd D, de Jager K, Palisson A, van Ratingen M, Trosseille X (2008) Q-dummies Report Advanced Child Dummies and Injury Criteria for Frontal Impact, Working Group 12 and 18 Report. Document No. 514, EEVC. April 2008.

## 4.2 Abdominal pressure twin sensors for the Q dummies: from Q3 to Q10

### 4.2.1 Introduction

The abdomen is a relatively common injured region for children transported in cars (e.g. [1]). Children using standard 3-points belts and booster seats seem particularly at risk with injuries thought to be induced by the belt. Recently, the commercial offer and usage of shield CRS seem to be increasing in Europe and the relationship between this CRS type and abdominal injuries is currently not clear.

Child dummies play an important role in the evaluation of the safety of children in cars. They are used in regulatory procedures and consumer testing for the evaluation of Child Restraint Systems (CRS) such as booster seats or cushion, Group 1 seats with harnesses or shields, and infant carriers. They are also used to evaluate the level of protection that vehicles can provide to children. In Europe, P series dummies are currently used in both regulatory and consumer testing of CRS and cars (e.g. EC R44, EuroNCAP).

In the P dummies, the risk of abdominal injury has been assessed by looking at the deformation of a clay block behind the abdominal foam. This assessment can be subjective as it does not provide measurements that could be correlated to the possible injury severity but only information about abdominal penetration. A new generation of child dummies – the Q dummies – is currently being introduced in Europe. These dummies are used in research projects and will likely be introduced in EuroNCAP procedures and EC regulation when these are updated. While they are believed to be an improvement over the current P family of dummies, the risk of injury to the abdomen cannot be assessed directly using these dummies as their abdomen is not instrumented [2].

The implementation of instrumentation to assess the abdominal injury risk in the Q dummies could therefore be useful for the evaluation of the safety of children in cars. Research has been conducted on this issue in the past EC funded projects CREST and CHILD [3, 4] and currently in the CASPER project. CASPER is an EC-funded collaborative project looking at the safety of children in cars using multiple approaches



(sociology, real world misuse and accident data collection, work on Q dummies and human models, accident reconstructions, etc.). Within the CASPER project, several solutions were considered for abdominal instrumentation and the Abdominal Pressure Twin Sensors (APTS) that were previously available for Q3 and Q6 dummies were selected for further evaluation and developments.

Among other requirements, abdominal instrumentation should be able to detect the presence and intensity of abdominal loading in a variety of loading conditions that could be relevant for abdominal injuries, and across age ranges not covered by adult dummies. Conversely, it should have a limited sensitivity to loading modes that are not expected to create serious injuries (e.g. belt loading the pelvis below the anterosuperior iliac spine). Its presence should not affect adversely the biofidelity of the dummy.

The objectives of the current study were to:

- Study abdominal injury patterns as a function of restraint system by analysing the CASPER accident database (in order to isolate relevant scenarios);
- Assess how the APTS affect the dummy biofidelity of the abdominal response, with a focus on the new Q10 dummy in which the APTS were implanted;
- Test the ability of the sensors to detect improper loading to the abdomen across two dummies of very different sizes (Q3 and Q10) and various loading modes (belt, harness or shield CRS, misuse).

## Methods

### CASPER accident database

The database is composed of detailed accident descriptions that were collected during the CASPER, CHILD and CREST EC-funded projects (from 1996 to 2012) in several European countries. It has minimum severity criteria for inclusion (either delta v of at least 40km/h for frontal impact, intrusion of at least 200mm in side impact, or at least one occupant with MAIS2+). The database is therefore not expected to provide an accurate representation of all accidents involving children but it can provide valuable information about the severe accidents leading to injuries. At the time of analysis, the database included a total of 1288 restrained children (aged 0 to 12 years).

Abdominal injuries are ranked from 1 (minor) to 6 (lethal) on the Abbreviated Injury Scale (AIS), with only one injury being rated AIS6 (hepatic) avulsion. The current analysis was performed using the AIS Version 1998 scale.

### Abdominal Pressure Twin Sensors (APTS)

The APTS were developed at Ifsttar (formerly INRETS) during the CHILD project [3, 4]. The APTS are composed of two cylindrical soft polyurethane bladders that are filled with liquids or gels. They are closed by aluminium caps in which miniature sensors measuring the pressure in the fluid are located. The bladders are implanted in holes drilled in the abdominal block of the dummy. The first version of the sensors (APTS V1) was developed during the CHILD project and previously used in Q3 and Q6. A new version (APTS V2), was developed during the CASPER project. It is an evolution that aimed to correct some of the V1 shortcomings (e.g. fragile cable output). It was designed to have similar dimensions and response and to be compatible with Q3, Q6 and Q10 dummies. The APTS V2 was used for the current study. Illustrations of the APTS V2 are provided in Figure 4-34.



**Figure 4-34: Left: APTS V1 (small diameter cap, darker colour) and V2 (large diameter cap, light colour). The APTS are approximately 50mm in diameter. Right: APTS V2 inserted in a Q3 and in a Q10 abdomen. The V2 was used for the current study**

### Test setups

Different test setups were implemented to study the effect of the sensors on the dummy response in the abdominal region, and to evaluate their ability to detect loading.

#### *Abdominal compression tests*

Direct abdominal compression is believed to be an important loading mechanism leading to abdominal injury. For direct belt loading, both belt force and belt penetration have been linked to injuries in animal or post-mortem human subject testing (e.g. Kent et. al [5, 6]). For the Q dummies, belt compression tests are used to define the biofidelity target of the abdomen. The test setup and targeted corridor are described in an EEVC report [2]. They are derived from porcine tests [7] where the specimen is laying supine on a V block and subjected to abdominal loading by a belt mounted on a yoke and moving at 1m/s. For the current study, APTS V2 were implanted in a Q10 dummy and the dummy was tested with standard or instrumented abdomen. After removing limbs, head and neck, the trunk of the dummy was positioned in a supine position on a plateau mounted on top of an Instron testing machine. V blocks were not used as the dummy geometry is sufficiently flat in the back to be stable during testing. The dummy was not coupled to the plateau to avoid over constraining it during the compression. The abdomen was mainly loaded using belts held on a custom yoke mounted on the piston of the testing machine. Different belt strokes and loading locations were tested. In particular, the belt was moved from below the antero superior iliac spine (ASIS) up to the thorax in order to evaluate the sensitivity of the APTS to loading location. For these tests, the stroke was limited to 40mm in order to reduce the risk of ribcage damage. Measurements included the force under the dummy, the displacement of the actuator, and the force at the yoke (mass corrected using a uniaxial accelerometer and called impactor force). Illustrations of the test setup with a Q10 dummy are provided in Figure 4-35.



**Figure 4-35: Belt compression tests: illustration of the test setup for the Q10 dummy**

#### *Detection of loading modes: sled configurations*

Sled tests were performed on instrumented Q3 and Q10 dummies to check the ability of the sensors to detect direct abdominal loading. Different configurations were used for Group 1 and for Group 2/3 CRS:

- Group 2/3: R44 bench and R44 pulse, Q3 (APTS V2) with two boosters CRS, including a configuration with misuse and lap belt anchors raised (to load directly the abdomen);
  - The tests were performed at Ifsttar;
- Group 1 CRS: NPACS bench and accident reconstruction pulse: Q3 (APTS V2) with a 5-point harness CRS and a shield CRS;
  - The tests were performed at TUB.

The accident configuration pulse corresponds to a relatively low speed impact (estimated  $\Delta v$  of 31 km/h) of an older vehicle to a wall with partial overlap. The pulse was found to be similar to a R44 pulse for the beginning of the impact (Figure 4-36) but with a faster acceleration drop. In the accident, a 14 month old child restrained by a shield CRS was located on the front passenger seat. The child suffered from neck injury (AIS 5), serial rib fractures on the right side (AIS 3) and lung contusion (AIS 3). A 29mm chest deflection was measured during the reconstruction performed with a Q1 dummy. The model of shield CRS present in the accident and its reconstruction was also used for the sleds.

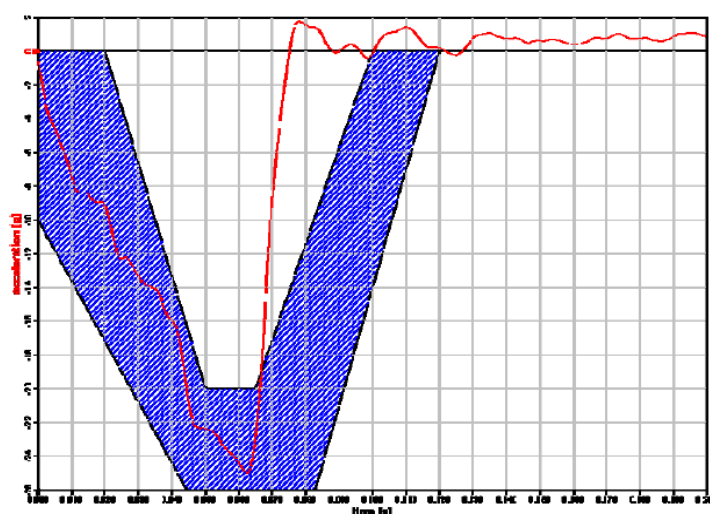
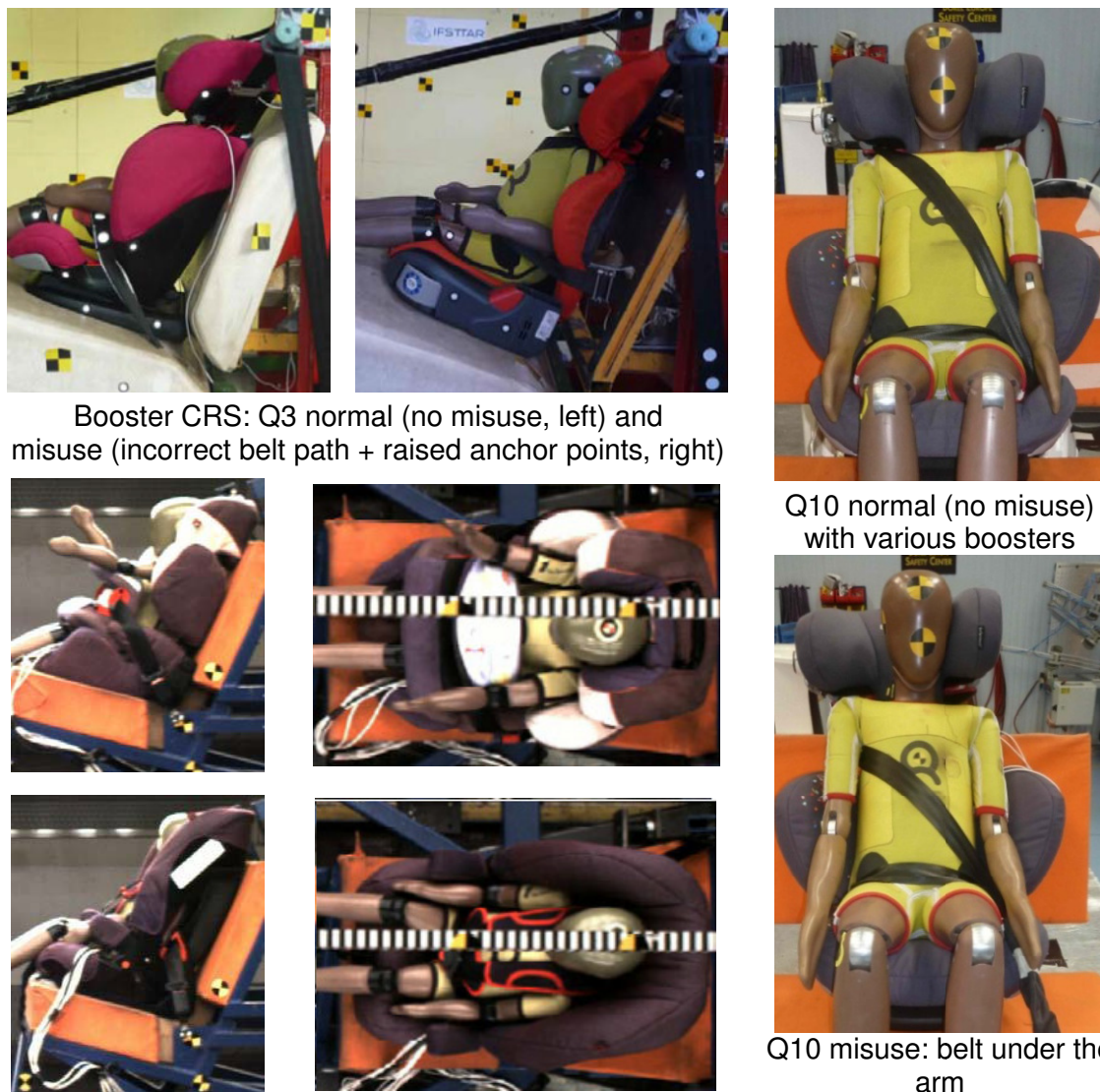


**Figure 4-36: Pulse used for the Group 1 CRS tests (harness and shield).**

Q10 tests were performed at Dorel on an NPACS bench with a R44 pulse (Q10 configuration 1), or in a VW Golf VI body in white with a more severe ADAC pulse, representing a Golf VI EuroNCAP pulse (Q10 configuration 2). The dummy was tested on five different booster seats using normal belt path, and one misuse configuration (shoulder belt under the arm).

Illustrations of the test setups are provided in Figure 4-37. The tests presented were all run with dummy suit reinforcements designed to prevent the lap belt penetration in the space between the pelvis skin and the thigh provided by the dummy manufacturer (Humanetics).



Group 1 CRS: Q3with shield (top) or harness (bottom)

**Figure 4-37: Illustration of sled test setups**

## Results

### Analysis of the accident database

Out of the 1288 restrained children of the database, 21% (n=276) sustained abdominal injuries. About half of these children (n=133) sustained AIS2+ injuries. The distribution of injury severity is provided in Table 4-2. About half of the injuries were AIS2+ (241 out of 457). These AIS2+ injuries occurred mostly in frontal impact (n=207), followed by side impact (n=33) and rear impact (n=1). Overall, the percentage of children that

sustained an injury to the abdomen increased with age, reaching a peak around 8 years old (Figure 4-38). Abdominal injuries were rare for ages lower than 3. When analysing the results as a function of the restraint systems used, the most common configuration in the database was children restrained only by the safety belt (n=455) followed by booster CRS (n=346) and harness CRS (n=333). However, there were disparities among the rate of children with AIS2+ to the abdomen among these restraint types: while the rate of children with AIS2+ to the abdomen was only 4% for children in harness (n=12), it was 14% or more in the two other configurations (n=68 for seatbelt, n=48 for harness). Only 31 cases of shield CRS were present in the database and AIS2+ abdominal injuries were observed in 4 cases or 13%. When analysing in detail the injury patterns for the main restraint types (Table 4-3), abdominal injuries were the second most commonly injured region after the head for AIS2+ and booster or seatbelt configurations, and it was the most commonly injured region for AIS3+ and seatbelt only. In contrast, the abdomen was the least commonly injured region for AIS2+ and AIS3+ when a harness was used. When combined, abdominal and thoracic injuries were more common than head injuries for booster or seatbelt configuration but were still a small fraction of the head injuries (about 1/3) for the harness systems.

Finally, there were differences in injury patterns with CRS usage in frontal impact: the hollow organs of the lower abdomen were more commonly injured when no CRS was used, while the organs of the upper abdomen seemed more common when a CRS was used. More specifically, there were 93 AIS2+ injuries when a CRS was used, including 27% to the liver, 13% to the kidney and 13% to the spleen. When no CRS was used, there were 114 AIS2+ injuries, with 17% to the liver, 16% to the colon and 13% to the spleen. Jejunum and mesentery injuries were also present mostly without CRS, while pancreas and stomach were present with CRS.

**Table 4-2: Distribution of abdominal injuries by severity in the CASPER database**

<b>AIS1</b>	201	44%	<b>241</b> (53%)
<b>AIS2</b>	110	24%	
<b>AIS3</b>	76	17%	
<b>AIS4</b>	45	10%	
<b>AIS5</b>	10	2%	
<b>AIS6</b>	0	0%	
<b>AIS9</b>	15	3%	
	457	100%	

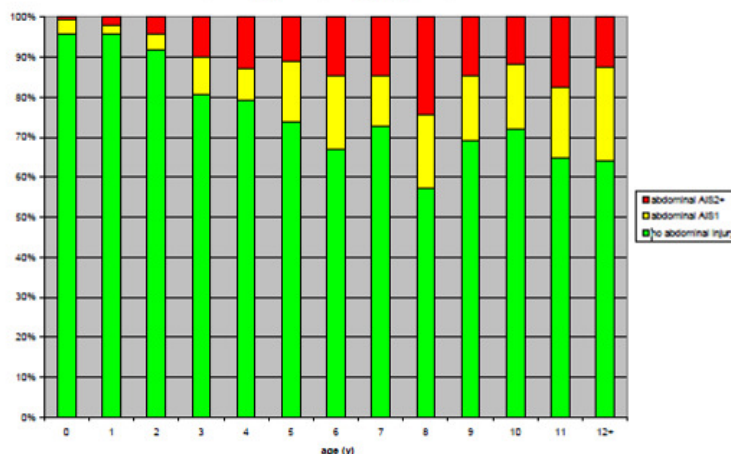


**Figure 4-38: Percentage of the children included in the database that sustained abdominal injuries as a function of age**

**Table 4-3: Injured body regions by main type of restraint configuration. The percentage indicates the ratio between the number of children sustaining at least one injury of the given severity and the number of children in the same restraint configuration**

Body region	Seatbelt (n=355)		Boosters; seat and cushion (n=355)		Harness systems (n=336) G1 or combined 0+/1	
	AIS2+	AIS3+	AIS2+	AIS3+	AIS2+	AIS3+
Head	24.2%	8.8%	24.4%	13.9%	29.2%	18.2%
Neck	2.6%	2.0%	6.0%	3.1%	8.6%	7.7%
Chest	11.6%	8.6%	11.1%	10.5%	6.0%	5.7%
Abdomen	14.9%	10.5%	13.6%	8.0%	3.6%	1.5%
Upper limbs	13.2%	1.3%	12.5%	0.9%	5.7%	/
Lower limbs	13.8%	5.5%	11.9%	5.4%	8.6%	3.3%

#### *Abdominal compression tests Q10*

The APTS v2 had increased the stiffness of the abdomen in compression by as much as 20 to 25% (Figure 4-39). The response was still within the corridor for most of the stroke but it was close to the limit. The stiffening visible at the end of the corridor was not present.

The pressure varied almost linearly with both force and penetration (Figure 4-40). When changing the belt location (Figure 8), the pressure vs. force response remained mostly linear but the slope changed with the position. The highest slope (maximum pressure for a given force) was obtained in the mid abdomen ( $Z=0$  and  $Z=25\text{mm}$  on Figure 8). The slope was then reduced when moving away from this location, with the belt starting to engage the thorax ( $Z=+50\text{mm}$ ) or the pelvis ( $Z=-35\text{mm}$ ). The slopes were even smaller for positions of the belt directly on the thorax ( $Z=+100$ ) or below the ASIS ( $Z=-60$ ).

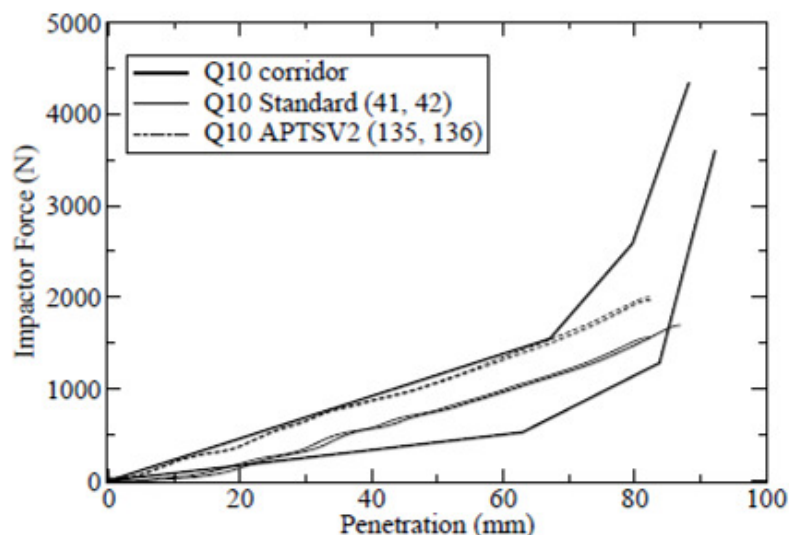


**Figure 4-39: Response to an abdominal compression by a 32mm belt at 1m/s vs. reference corridor.**

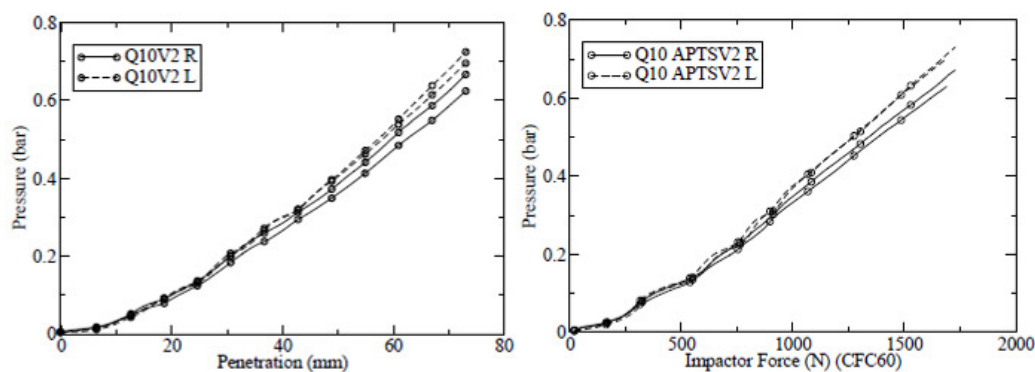


Figure 4-40: Pressure response for the tests shown in the previous figure

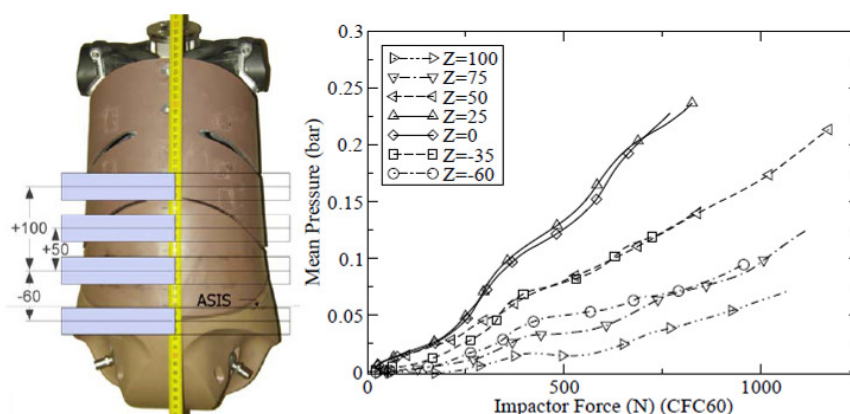


Figure 4-41: Effect of belt loading position on the pressure (32 mm belt, 1 m/s, 40 mm stroke)

Left: dummy and belt position. Right: force vs. pressure responses as a function of location. For clarity, right and left pressure were averaged. Note: Z = 0 mm corresponds to a position just below the ASIS

#### Detection of abdomen loading modes: results from the sled tests

For the Q3 with boosters, tests performed with the 3-point belt in correct position did not lead to visible loading of the abdomen on the video (Figure 4-42 top). The diagonal belt had a tendency to slide towards the neck, thereby limiting the loading to the thorax (also visible on Figure 4-42, top). The lack of direct abdominal loading was associated with peak pressures that were below 0.5 bar. In misuse configuration with belt anchors moved upwards to induce direct abdominal loading, the belt penetration into the soft abdomen was clearly visible on the video (Figure 4-42, top). This penetration was associated with much higher pressures (around 2 bar). When repeating the same belt configuration with misuse three times (Figure 4-42, bottom), the peak pressure varied between 1.93 and 2.28 bar (Difference: 15%), while the thoracic deflection varied from 22 to 25 mm (Difference: 11%).



Booster with normal configuration (01, 02)

Misuse and raised lap belt anchor points leading to visible abdominal loading (29)

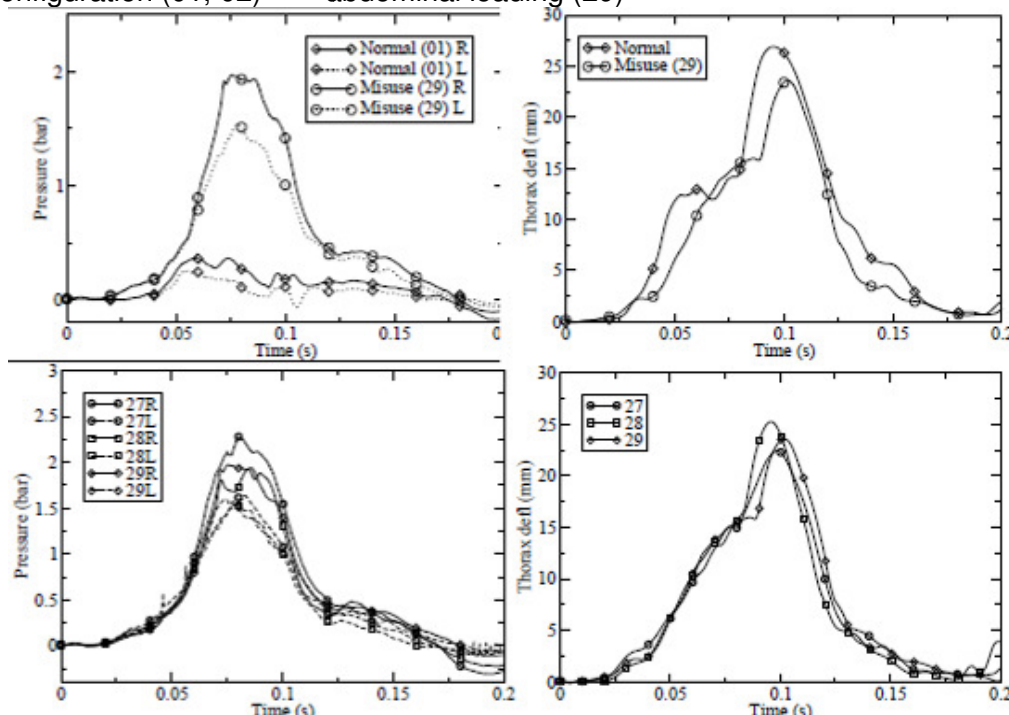


Figure 4-42: Q3 sled testing with boosters

**Top: illustration of the kinematics (at 65ms) in the two test conditions. Centre: Pressure response and thoracic compression for the same tests. Bottom: results from three repetitions of the test 29 (with misuse). L or R indicate the side of the sensor (Left or Right)**

For the Q3 tests with harness CRS (accident reconstruction pulse), there was no visible loading of the abdomen (Figure 4-43, top). The maximum pressure measured during the test was 0.3 bar and the chest deflection was 28 mm. In contrast, when the shield system was used with the same pulse, the thorax and most likely the upper abdomen (which is hidden by the shield on the illustration Figure 4-43) were loaded by the shield, leading to a maximum pressure of 1.5 bar and a chest deflection of 44mm. The test was repeated with a similar CRS model and the pressure and deflections were 1.7 bar and 44 mm, respectively.

The pressure response was not symmetric in most tests and the pressure was typically higher on the side of the buckle, where both diagonal and lap belt push on the dummy or CRS.



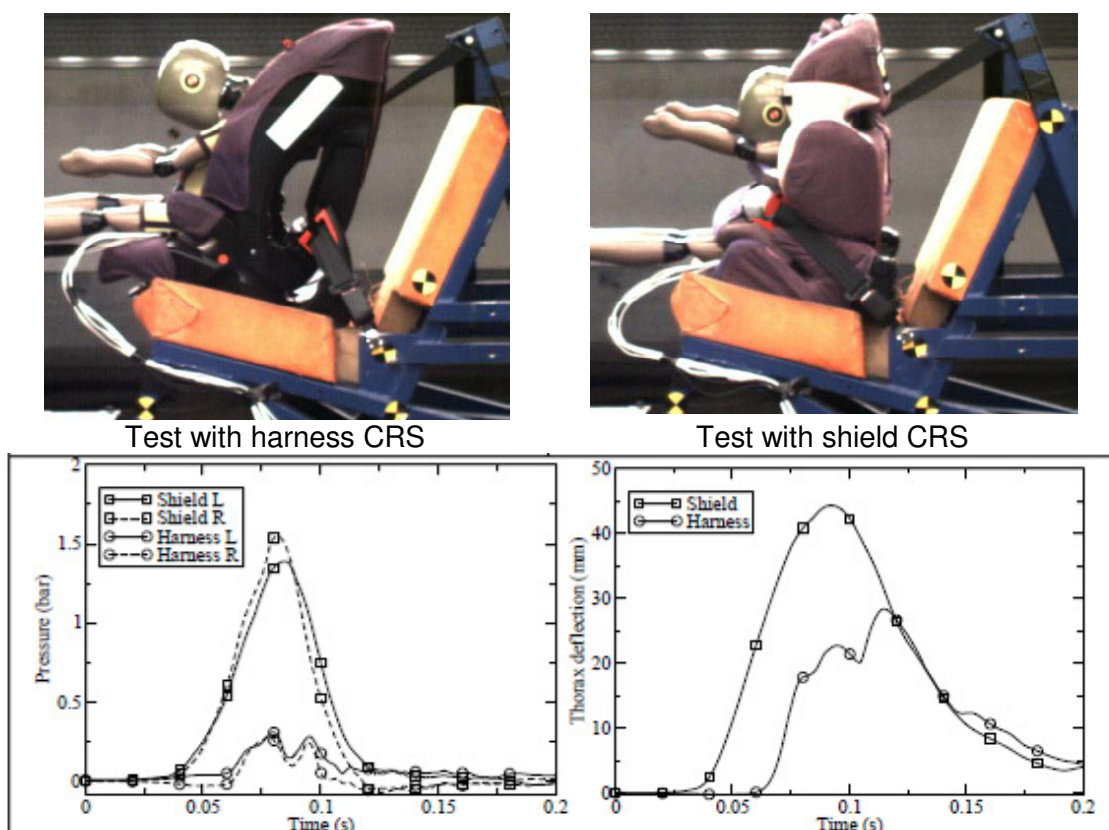


**Figure 4-43: Q3 sled testing with Group 1 CRS**

**Top: illustration of the kinematics in the two test conditions Bottom: Pressure response and thoracic compression for the same tests**

For the Q10, tests performed with three-point belts and normal belt paths did not lead to visible abdominal loading (Figure 4-44, left). This was true for the five booster seats tested in bench or body in white configurations. This was also true for a test performed with the dummy directly on the bench without CRS. The pressures measured during these tests were all at or below 1 bar (Figure 4-44, centre and Table 3). For the test conducted with an incorrect belt path (diagonal belt under the arm), there was visible loading of the upper abdomen by the diagonal belt that slid under the ribcage (Figure 4-44, left). This loading was associated with increased abdominal pressures, with a peak reaching 1.8 bar on the left side. The pressures often were dissymmetric with higher peaks on the buckle side of the dummy where both lap and diagonal belt can contribute to the loading (Table 3). In most tests, the lap belt had a tendency to migrate between pelvis skin and thighs even with the presence of reinforcements of the dummy jacket (Figure 4-44, right).

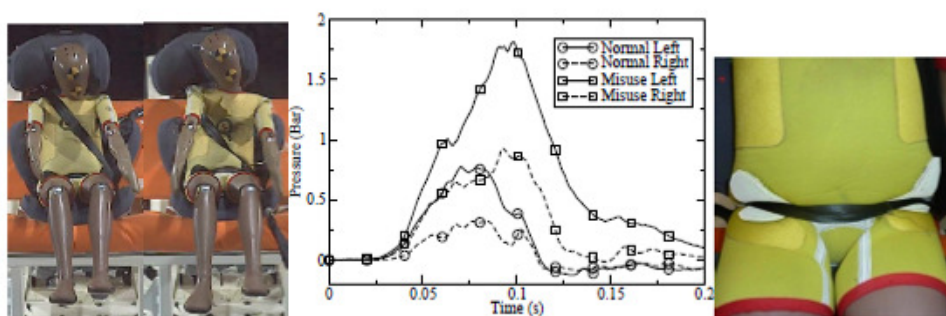


Figure 4-44: Q10 testing in configuration 1

Left: dummy kinematics at 75ms after impact with a normal restraint condition or with misuse (belt under the arm). Centre: pressure curves corresponding to these tests. Right: lap belt position after the test. The colour of the jacket reinforcements was changed to white in the picture so that the belt path can be seen

Table 4-4: Summary of peak pressure results for the Q10 sled testing

Seat	Config.	Test number	Peak pressure		
			Left	Right	Overall
Booster 1 (ISOFIX)	1	1724	0.83	0.29	0.83
Booster 2 (ISOFIX)	1	1725	0.73	0.36	0.73
Booster 3 (inflatable)	1	1726	0.78	0.30	0.78
Booster 4 (Backless)	1	1727	1.02	0.47	1.02
No CRS	1	1728	0.44	0.26	0.44
Booster 1 (ISOFIX, misuse)	1	1729	1.82	0.93	1.82
Booster 5 (ISOFIX)	1	1730	0.65	0.32	0.65
Booster 1 (ISOFIX)	2	1734	0.54	0.50	0.54
Booster 2 (ISOFIX)	2	1735	0.96	0.59	0.96
Booster 5 (ISOFIX)	2	1736	0.45	0.51	0.51
Booster 4 (Backless)	2	1737	0.54	0.57	0.57

#### 4.2.2 Discussion and conclusions

The analysis of the CASPER database confirmed the importance of abdominal injuries for children in specific configurations. In frontal impact, while abdominal injuries were almost non-existent with harness CRS, they were much more common for booster CRS and seatbelt only configurations. They could also be common for shield CRS (13% or 4 out of 31 cases) but the number should be taken with caution as the number of cases in the database is very limited. Some of these configurations (older children with booster or seatbelt only, younger children on boosters) were the focus of the sled tests.

As a first step, the APTS (V2) were implanted in the Q10 dummy. The APTS V2 were found to stiffen the abdominal response of the Q10 in compression. If needed, the design of the bladder could be changed for the Q10 in order to reduce its stiffness, for example by increasing its volume or reducing its thickness. For now, since the response with sensors remained mostly within the reference corridor, it seemed preferable to have a common sensor version for all Q dummies. The APTS were also found to detect abdominal loading on the Q10 with a higher sensitivity in the mid abdomen than in the thoracic and pelvic regions. This was an expected behaviour

considering the geometry of both dummy and sensors. For the pelvic region, it is an important feature to ensure that appropriate restraint conditions with high belt loads transmitted to the pelvis are separated from the loading to the soft abdomen. For the thoracic region, it is also an acceptable result as the thorax instrumentation already provides an assessment of the loading to the region.

For the belted sled tests, the ability of the first version of APTS to detect direct abdominal loading had already been shown in previous studies on the Q3 and Q6 dummies (e.g. [3, 4]). The current tests confirmed this capability for the new version of sensors and extended it to Q10 dummies. Overall, for both Q3 and Q10, pressures at or below 1 bar were obtained for tests with appropriate belt restraint, while values above 1.5 bar were obtained in misuse cases with direct loading to the abdomen. During these tests, there was no visible pelvic rotation under the belt, and more generally, no submarining. This was true even in the case of Q10 test without CRS. It is not known if this behaviour is realistic, due to an excessive stiffness of the lumbar region, to other dummy issues (e.g. belt catching between pelvis and thigh for the Q10), or to test configurations (e.g. anchor point location, bench geometry). This issue should be investigated in the future, for example using modelling approaches with human or dummy models.

For the Q3 tests with Group 1 CRS and the accident reconstruction pulse, the results were very contrasted. For the tests with harness CRS, both abdomen pressure and thorax deflection were relatively small. Pressures were the smallest of any of the tests performed (0.3 bar). This could be in agreement with the very low rate of abdominal injuries observed in the database for this configuration. For the tests with shield CRS and the same pulse, maximum pressures were at or above 1.5 bar. This level is similar to the misuse cases with boosters and belts. However, the loading modes are different between shields and belts, and it is unclear if this means that the two situations could be equally linked with abdominal injuries. The thoracic deflections (44 mm) measured during the tests are similar to deflections (34, 48, 48 and 56mm) measured by Tanaka *et al.* [8] in Q3 testing with a more severe R44 pulse and different shield CRS. These values are close to the scaled Injury Assessment Reference Values (IARV) proposed in [2] for the thorax (46.5mm for the UN Regulation 94 scaled criteria, 36mm and 53mm for 20% and 50% AIS3+ risk estimated by linear regression, respectively). They are higher than harness results from [8] (28 to 31mm) and from this study. From the biomechanical standpoint, large compressions of the lower ribcage could create significant risks for the solid organs of the abdomen and for the soft tissues of the thorax (e.g. lungs) by compressing directly the organs. A similar injury mechanism was recently shown for side impact in the adult [9]. The thorax IARVs proposed in [2] are based only on ribcage properties and aim to assess the risk of rib fractures. Therefore, the IARVs proposed in [2] are larger for smaller children despite smaller ribcages (e.g. Q1 chest deflection of 52mm for the UN Regulation 44 scaled criteria vs. 46.5 for the Q3 and 42 for the Q6). This approach does not take into account the risk of internal organ injuries. Because shield systems are not currently widespread, it could not be established if this possible mechanism corresponds to a real world risk or if it is a dummy artefact. Anecdotal evidence is available from the few cases with shield of the CASPER database (4 abdominal injuries out of 31 cases). Overall, this issue should be further investigated as regulations may not evaluate properly this risk if only chest acceleration is considered.

While no test campaign was specifically performed to evaluate the manufacturing variability, repeatability and reproducibility of the sensors, test results presented in the current study suggest peak pressure variations in the order of 15% in Q3 sled tests, which seems slightly higher than variations observed on thorax deflection (11%). Overall, such variations could be acceptable considering the large increase between

cases with appropriate restraint and misuse observed on the Q3 and Q10 belt tests. However, a testing campaign dedicated to this issue should be performed in the future. In summary, further developments and evaluations were performed on the Abdominal Pressure Twin Sensors for Q dummies. A new sensor version was implanted in the Q10 dummy and tested with the Q3 and Q10. The test results confirm the ability to detect direct abdominal loading for a variety of loading scenarios and also show that the sensor presence has limited effects on the dummy response in abdominal compression.

Work on the sensors continues with further evaluation in the Q3 and Q6 dummies and the consolidation of accidents reconstructions results performed in the CHILD and CASPER projects in order to build an injury risk curve. For future research, this study also highlights the need for further work on shield CRS as they could lead to injury risks that cannot be assessed with the current regulation. The implantation of the sensors in Q1.5 dummies is ongoing for that purpose.

### Acknowledgements

The CASPER project is co-funded by the European Commission under the 7th Framework Programme (Grant Agreement no. 218564). The members of the CASPER consortium are: GIE RE PR - PSA/RENAULT, Technische Universität Berlin, Université de Strasbourg, APPLUS IDIADA Automotive SA, IFSTTAR, Loughborough University, FIAT Group Automobiles Spa, Medizinische Hochschule Hannover, Chalmers tekniska högskola AB, Bundesanstalt für Straßenwesen, TNO, Verein für Fahrzeugsicherheit Berlin e.V., Ludwigs Maximilian Universität, Centre Européen d'Etudes de Sécurité et d'Analyse des Risques, Humanetics Europe GmbH. Further information is available at the CASPER web sites: [www.childincarsafety.eu](http://www.childincarsafety.eu) and [www.casper-project.eu](http://www.casper-project.eu). The partners wish to acknowledge all the CREST/CHILD and CASPER data collection teams and their sponsors from all the countries involved in this work.

Part of the work presented in the current study was supported by French Ministry of Industry and Pays de la Loire Regional Council through the ProEtech Competitive Cluster project.

UK Loughborough cases, collected during the EC CREST/CHILD projects, include accident data from the United Kingdom Co-operative Crash Injury Study, collected up to 2006. CCIS was managed by TRL Ltd on behalf of the Department for Transport (Transport Technology and Standards Division) who funded the project with Autoliv, Ford Motor Company, Nissan Motor Europe and Toyota Motor Europe. The data were collected by teams from the Birmingham Automotive Safety Centre of the University of Birmingham, the Vehicle Safety Research Centre at Loughborough University, and the Vehicle & Operator Services Agency of the Department for Transport. The views expressed in this work are those of the authors and not necessarily those of the UK CCIS sponsors.

### References

1. Khaewpong, N., Nguyen, T., Bents, F., Eichelberger, M., Gotschall C.S. and Morrissey R., (1995) Injury Severity in Restrained Children in Motor Vehicle Crashes, SAE Technical Paper 952711, 1995.
2. EEVC (2008) Q-dummies Report: Advanced Child Dummies and Injury Criteria for Frontal Impact. Working Group 12 and 18 Report, Document No. 514. April 2008. Available online at: [http://eevc.net/publicdocs/EEVC\\_WG12&18\\_DOC514\\_Q-dummies\\_&Criteria-April\\_2008.pdf](http://eevc.net/publicdocs/EEVC_WG12&18_DOC514_Q-dummies_&Criteria-April_2008.pdf), accessed June 3, 2012.

3. Johannsen H., Alonzo F., Goubel C., Schindler V., 2005, Abdominal injuries, injury criteria, injury severity levels and abdominal sensors for child dummies of the Q family. Proceedings of IRCOBI Conference 2005, p. 201.
4. Johannsen J., Alonzo F., Schindler V., 2007; Abdominal sensors for child dummies of the Q family, injury criteria and injury risk curves. Proceedings of the IRCOBI Conference, Sept 2007, Maastricht, The Netherlands, p389.
5. Kent, R., Stacey, S., Kindig, M., Forman, J., Woods, W., Rouhana, S. W., *et al.* (2006). Biomechanical response of the pediatric abdomen, part 1: development of an experimental model and quantification of structural response to dynamic belt loading. *Stapp Car Crash Journal*, 50, 1-26.
6. Kent, R., Stacey, S., Kindig, M., Woods, W., Evans, J., Rouhana, S. W., *et al.* (2008). Biomechanical response of the pediatric abdomen, Part 2: injuries and their correlation with engineering parameters. *Stapp Car Crash Journal*, 52, 135-166.
7. Rouhana, S.W., Viano D.C., Jedrzejczak E.A. and J.D. McCleary (1989) Assessing Submarining and Abdominal Injury Risk in the Hybrid III Family of Dummies. In Proceedings of the 33rd Stapp Car Crash Conference, pp 257–279, SAE Paper no. 892440. Warrendale, Pa, Society of Automotive Engineers.
8. Tanaka Y., Yonezawa H., Hosokawa N., Matsui Y., Mizuno K., Yamaguchi M., Yoshida R. (2009) Responses of Hybrid III 3YO and Q3 Dummies in Various CRSs Tested Using ECE R44 Impact Conditions. ESV Conference 2009, Paper number 09-0242.
9. Kremer, M.A. Gustafson, HM, Bolte, J.H., Stammen J., Donnelly B., (2011). Pressure-based abdominal injury criteria using isolated liver and full-body post-mortem human subject impact test. *Stapp Car Crash Journal*, 55, p.317-350.

### **4.3 Q10 biofidelity – dummy validation in certification-type loading**

#### **4.3.1 Introduction**

In 2009 EPOCH disseminated the specifications for the Q10 dummy and presented the prototype Q10 dummy in 2010. This section presents results of the dummy evaluation, it includes component and full body level evaluations using standard certification test equipment like head drop table, neck pendulum and full body pendulum for thorax. The following is a report on the dummy compliance with requirements on anthropometry, biofidelity, sensitivity to impact conditions, repeatability and reproducibility, handling and durability. Results for front and side impact are presented.

#### **4.3.2 Method**

The Q10 dummy performance will be compared to the requirement definition specified in the Q10 Design Brief (Waagmeester 2009) to show level of compliance. A summary of the requirements definition was presented in the Conference Protection of Children in Cars, Munich 2009 (Waagmeester 2009). Before the first two prototype Q10 dummies were released for evaluation within the EPOCH consortium in November 2010 their performance was tuned to obtain the best possible compliance with the requirements. This work was reported in the Conference Protection of Children in Cars (Waagmeester 2009).

The Q10 dummy performance was tested with standard dummy test equipment: Head Drop Table, Neck Pendulum and Full-body Pendulum (mass 8.76 kg, diameter 112 mm, six-wire suspended). The test matrix executed at Humanetics in Watering, The Netherlands (Head drop and full-body pendulum tests) and in Heidelberg, Germany (Neck pendulum tests) comprised in total of 254 tests:

58 Head drop tests (frontal and lateral)	21 Shoulder lateral tests	29 Lumbar spine tests (15 Flexion, 14 Lateral flexion)
64 Neck tests (23 Flexion, 21 Extension, 20 Lateral flexion)	55 Thorax tests (33 Frontal, 22 Lateral)	27 Pelvis lateral tests

The test matrix was developed to examine the dummy biofidelity, research the dummy sensitivity for impact speed and offsets, to assess the repeatability and to establish provisional certification test procedures.

### 4.3.3 Anthropometry

For the anthropometry validation the overall dimension as shown in Figure 4-45 are used. A comparison of the drawing dimensions with the requirements specified in the Q10 Design Brief (Waagmeester 2009) is given in Table 4-5. In Table 4-6 the actual mass distribution is compared with the requirements specified in the Q10 Design Brief (Waagmeester 2009).

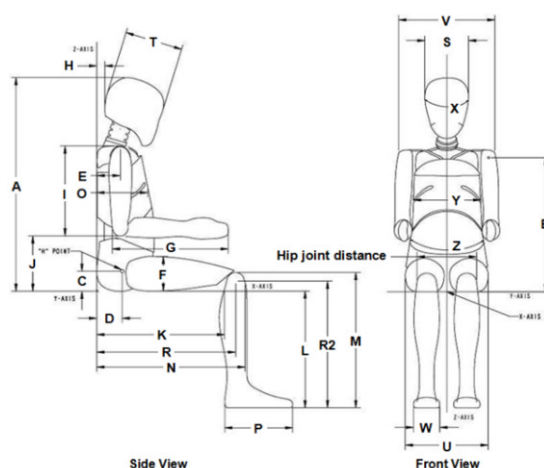


**Figure 4-45: Q10 Overall dimensions**

**Table 4-5: Q10 dimensions drawing versus requirement**

Description	Requirement in [mm]	Drawing dimensioning [mm]
A1 - Sitting Height (head tilt)	747.6	733.7
A2 - Sitting Height (via T1)	747.6	748.4
B - Shoulder Height (top of arm)	473	472.5
C - Hip Pivot Height	65.9	65.9
D - Hip Pivot from Back Plane	90.4 (1)	90.4
- Hip Joint Distance	130.0 (1)	132.0
F - Thigh Height	114.0	114.0
G - Lower Arm & Hand Length	374.7	374.2
I - Shoulder to Elbow Length	292.9	291.6
J - Elbow Rest Height	189.6	181.0
K - Buttock Popliteal Length	417.5	414.9
L - Popliteal Height	405.7	405.7
M - Floor to Top of Knee	445.6	446.0
N - Buttock to Knee Length	488.4	485.4
O - Chest Depth at Nipples	171.2	171.0
P - Foot Length	220.0	220.0
- Standing Height (head tilt)	1442.5	1441.2
- Standing Height (via T1)	1442.5	1455.5
R - Buttock to Knee Joint	(none)	445.7
R2 - Floor to Knee Joint	(none)	414.0
S - Head Breadth	143.9	144.0
T - Head Depth	187.4	186.5
U - Hip Breadth	270.4	271.5
V - Shoulder Breadth	337.8	337.8
W - Foot Breadth	86.0	86.0
X - Head Circumference	534.5	534.0
Y - Chest Circum at Axilla	687.3	604.6
- Chest Circum at Nipples	684.9	633.6
Z - Waist Circumference	593.5	664.6

Note 1: The data of M.P. Reed (2009) are transformed from standing to sitting and scaled from 10 YO stature 1374 to 1442.5 for Q10.

**Table 4-6: Q10 mass actual versus requirement**

Description	Requirement in [kg]	Actual Mass in [kg]
Head	3.59	3.59
Neck	0.60	0.63
Upper torso	5.15	5.14
Lower torso	9.70	$8.05+0.98=9.03$
Upper arm (each)	1.09	$1.05+0.04=1.09$
Lower arm + Hand (each)	0.90	$0.83+0.07=0.90$
Upper leg (each)	3.71	3.70
Lower leg + Foot (each)	2.52	2.44
Total body mass	35.5	34.7

## Discussion and conclusion

From Table 4-5 and Table 4-6 it can be seen that dimensions and masses in general correlate well with design brief specifications that are based on the CANDAT database used for all Q-dummies ref. (Waagmeester 2009) and a publication of UMTRI (Reed 2009).

### Dimensions

The deviation in Sitting and Standing Height is explained by the fact that these dimensions are measured in full erected posture while the dummy is assembled with the head-neck system 27 degrees tilted forward. To enable comparison with erected posture the dimensions measured via T1 is given, in which case good correlation is obtained. Also it should be noted that for the Standing Height an extra deviation is introduced by the pin-joint knee. In the human it is a synovial joint that produces series of involute midpoints and transverse axes. The leading dimensions for the optimum knee joint location were K, L, M and N (Waagmeester 2009). In addition to the sitting and standing height the chest circumferences show deviations. Actual dimensions are smaller than specified values because the soft muscle tissue at nipple and axilla level is not represented in the dummy. Also the ribcage is made as a single curved conic part to prevent complex secondary bending stresses that would occur in a double curved rib cage. This geometry assumption restricts the possibilities to comply with all chest dimensions.

### Mass distribution

The mass of the prototype dummies revealed to be too small, especially for the upper and lower arms and the pelvis. With an addition of some ballast items to the upper arms: 40 gram each, lower arms 70 gram each and the sacrum block 970 gram the dummy mass was increased towards an acceptable level. The dummy design will be reconsidered to incorporate the additional mass in the regular dummy parts.

## 4.3.4 Biofidelity

In this chapter the Q10 dummy biofidelity performance information for frontal and lateral impacts is presented per body region top down from head to pelvis.

### Head

For the head biofidelity two criteria for head drops on a rigid plate can be evaluated (Waagmeester 2009):

- Frontal 130 mm drop height: Biofidelity corridor limits based on EEVC scaling are: 113.1 – 194.2 g;
  - The average measured value is 120.0 g;
- Lateral 130 mm drop height: Biofidelity corridor limits based on EEVC scaling are: 116.1 – 200.0 g;
  - The average measured value is 133.7 g.

The head drops were performed with a half upper neck load cell replacement attached to the head base plate. In Figure 4-46 the resultant head accelerations versus time are shown.



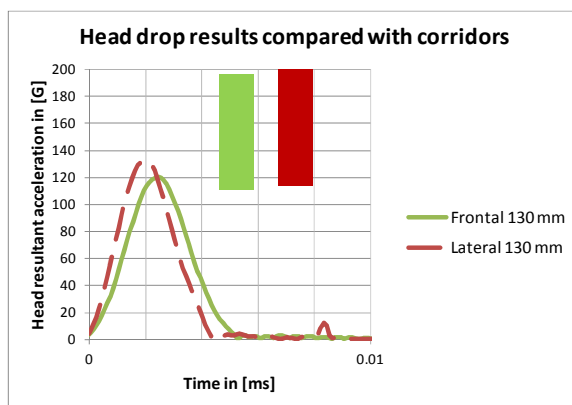


**Figure 4-46: Head drop biofidelity results**

### Discussion and conclusion

It can be concluded that the head meets the frontal (130 mm) and lateral (130 mm) low in the EEVC corridors. This is in accordance with the results in Waagmeester (2010). In general the head stiffness will increase when the product ages. Therefore it is recommended to slightly increase the stiffness of the head such that its performance is at the lower side close to the middle corridor.

### Neck

For the neck biofidelity requirements in flexion, extension and lateral flexion are evaluated below.

#### Flexion

In Figure 4-47 the neck flexion bending performance in a Part 572 neck pendulum test is given in comparison with the flexion biofidelity corridor (Waagmeester 2009). The flexion response is in the lower range of the corridor and the stiffness increase that should occur round about 30 to 35 degrees of head rotation is slightly late; actually it occurs round 45 degrees head rotation. The stiffness raise is correct. An improved performance could be obtained by increasing the rubber stiffness but that would affect the fracture toughness and therefore the durability of the part. Another possibility is to change the neck mould, but this may affect the response in other directions. The performance is considered to be adequate for the evaluation phase in the EPOCH project. A mould change will be considered later base on final EPOCH recommendations.

#### Extension

In Figure 4-48 the neck extension bending performance in a Part 572 neck pendulum test is given in comparison with the extension biofidelity corridor (Waagmeester 2009). It can be concluded that the extension performance fits the corridor very well. No further adjustments are necessary and there is some room to allow changes as a result of the recommended mould change to improve flexion performance.

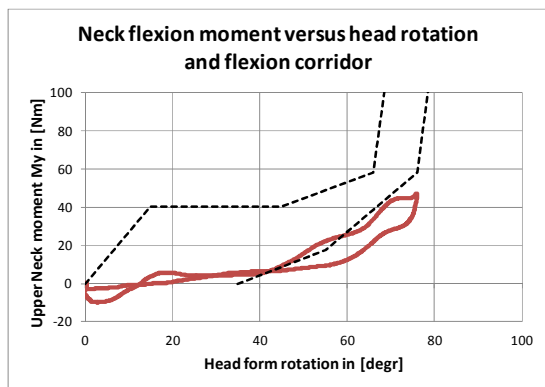


**Figure 4-47: Neck flexion moment versus head rotation**

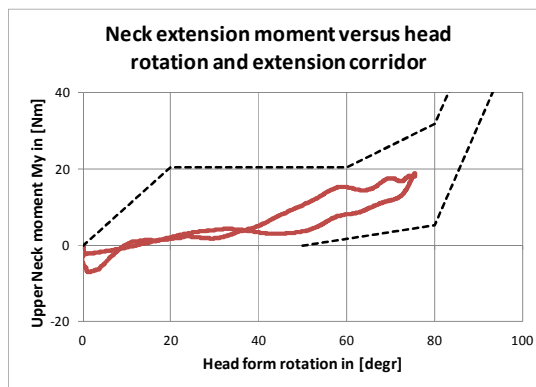


**Figure 4-48: Neck extension moment versus head rotation**

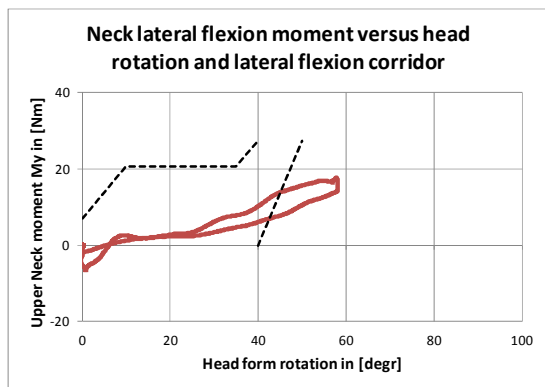
**Lateral flexion**

Figure 4-49 shows the neck lateral flexion bending performance in a Part 572 neck pendulum test in comparison with the lateral flexion biofidelity corridor (Waagmeester 2009). The Q10 development in the EPOCH project so far did not consider side impact performance tuning. It can be concluded that up to 45 degrees of head lateral flexion the performance is in the right order of magnitude.

**Shoulder**

**Lateral impact**

For the shoulder a lateral impact there was no requirement defined in the EPOCH project. The shoulder full body biofidelity test is done at a speed of 4.5 m/s with a full body pendulum (mass = 8.74 kg, diameter = 112 mm, six wire suspended). Figure 5 6 shows the pendulum force versus time in comparison with and scaled biofidelity corridor. The corridor of Figure 4-50 is based on scaling factors estimated by interpolation, using the shoulder impact corridor specified in the Q6 design brief and the corridor for adults.



**Figure 4-49: Neck lateral flexion moment versus head rotation**

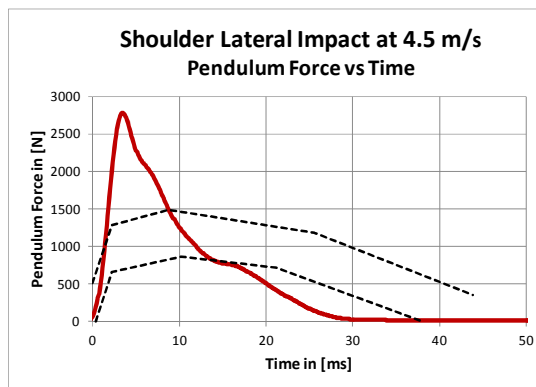


**Figure 4-50: Lateral Shoulder impact force versus time**

**Discussion and conclusion**

It can be observed that the initial response of the shoulder overestimates the stiffness whereas the response at later times gives lower stiffness. However, the Q10 is an omni-directional dummy and performance tuning in either direction will affect the performance in the other direction. In the EPOCH project, an optimal balance was sought for the Q10 performance in both directions with the focus on frontal impact.

As will be shown below similar trends with regards to lateral impact performance are observed for thorax and pelvis region. Hence the stiffness distribution in lateral impact is balanced between these body regions avoiding dominance of a single body segment in absorbing loads.

## Thorax

### Frontal impact

For the frontal biofidelity two pendulum test impact speeds are specified: 4.31 and 6.71 m/s. In Figure 4-51 and Figure 4-52 the pendulum test results for these two impact speeds are shown in terms of pendulum force versus average rib displacement in impact direction. The results are compared with the scaled biofidelity corridors (Waagmeester 2009). Three slightly different dummy postures are explored:

- Thoracic spine vertical with upper arms down along the thorax and the hand adjacent to the thighs (This posture is commonly used for Q-dummies thorax impact (certification) tests so far and standard in this test series;
- Thoracic spine vertical with arms forward, supported with rods under the elbows;
- Thoracic spine tilted forward about 12 degrees so that the sternum is parallel to the pendulum impactor face with upper arms down along the thorax and the hand adjacent to the thighs.

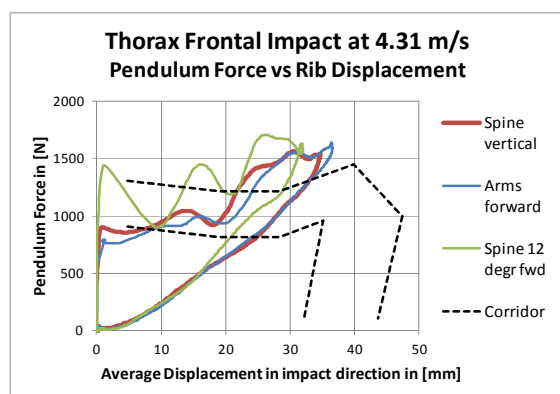


**Figure 4-51: Thorax frontal pendulum impact 4.31 m/s**

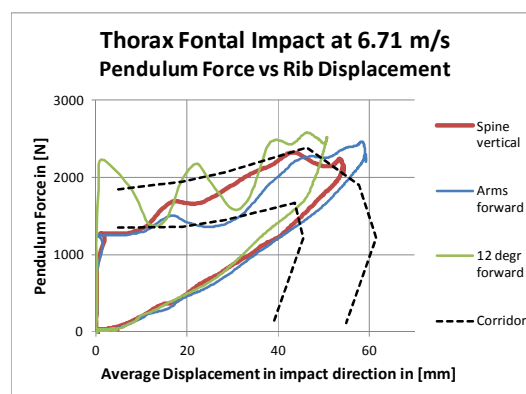


**Figure 4-52: Thorax frontal pendulum impact 6.71 m/s**

### Discussion and conclusion

From Figure 4-51 (impact 4.31 m/s) and Figure 4-52 (impact 6.71 m/s) it can be observed that the rib cage response in general meets the corridors reasonably well, especially for 6.71 m/s. For the lower impact speed at 4.31 m/s the response is somewhat above the corridor, this is in line with the performance of the other Q dummies that have been made stiffer to prevent early bottoming out of the rib cage to the thoracic spine. Q10, however, having more room for displacements in the chest, has in comparison to other members of the Q family a better compliance with the corridors (Waagmeester 2010). The different postures explored show that there is sensitivity in the dummy response to this variable. This phenomenon is also observed in other dummies like the THOR currently under development in the THORAX project. However, there is no reason to deviate for the biofidelity test from the commonly used for Q-dummies thorax impact (certification) tests posture.

### Lateral impact

For the lateral biofidelity two pendulum test impact speeds are specified: 4.31 and 6.71 m/s. In Figure 4-53 and Figure 4-54 the pendulum test results for these two impact

speeds are shown in terms of pendulum force versus time. The results are compared with the biofidelity corridors as specified in the Q10 design brief (Waagmeester 2009).

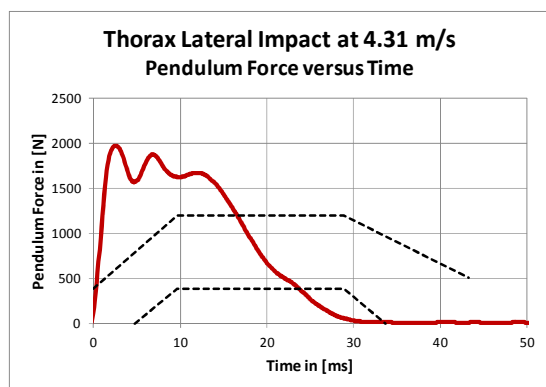


**Figure 4-53: Thorax lateral pendulum impact 4.31 m/s**

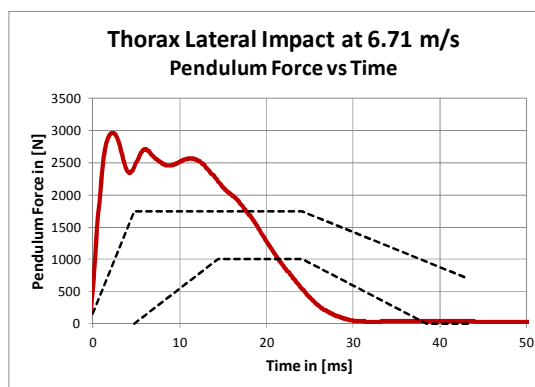


**Figure 4-54: Thorax lateral pendulum impact 6.71 m/s**

### Discussion and conclusion

As for the shoulder, the initial response of the thorax overestimates the stiffness whereas the response at later times gives lower stiffness. This is true for both impact speeds. Although performance tuning might be applied, this would affect the frontal performance and introduce an imbalance with the shoulder and pelvis (result shown below) under lateral loadings.

### Lumbar spine

The lumbar spine is made of a cylindrical rubber column therefore is the flexion and lateral flexion performance approximately the same. In Figure 4-55, test results obtained in dynamic and quasi-static tests are presented. The dynamic tests seem to show a slightly higher stiffness than the static tests:

- Dynamic: 80 Nm/58 degr = 1.38 Nm/deg or 79.0 Nm/radial;
- Static: 80 Nm/74 degr = 1.08 Nm/deg or 61.9 Nm/radial.

### Discussion and conclusion

These stiffness values are significantly smaller than the scaled requirements (Waagmeester 2009); that is 137.1 Nm/rad for flexion and 142.8 Nm/rad for lateral flexion. The actual stiffness of a Q6 lumbar spine is about 50% of its scaled requirement (103 Nm/rad). During the performance tuning phase in October 2010 it was decided by the EPOCh consortium to set the target stiffness of the Q10 lumbar spine to 50% of the scaled requirements (68.6 Nm/rad for flexion and 71.4 Nm/rad for lateral flexion). The Lumbar spine tested in this test series complies with the requirement.

### Pelvis

#### Lateral impact

For the pelvis lateral impact there is a biofidelity corridor specified in the Q6 design brief. The pelvis lateral full body biofidelity test should be done at a speed of 5.2 m/s. However in the test series there are tests available at 4.5 and 5.5 m/s. To estimate the response at 5.2 m/s the signals are linear interpolated. This is allowed because the pendulum force is found to be about linear with the impact speed in this interval (see Figure 4-75). In Figure 4-56, the lateral pelvis impact performance in terms of

pendulum force versus time is shown in comparison with and the scaled biofidelity corridor. The biofidelity corridor shown in Figure 4-56 is based on scaling factors estimated by interpolation using the pelvis impact corridor specified in the Q6 design brief and the corridor for adults.

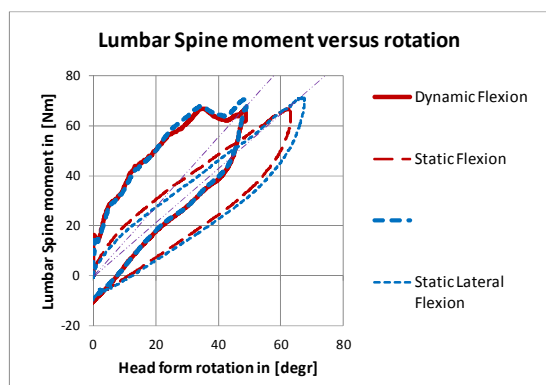


**Figure 4-55: Lumbar spine stiffness (dynamic and static)**

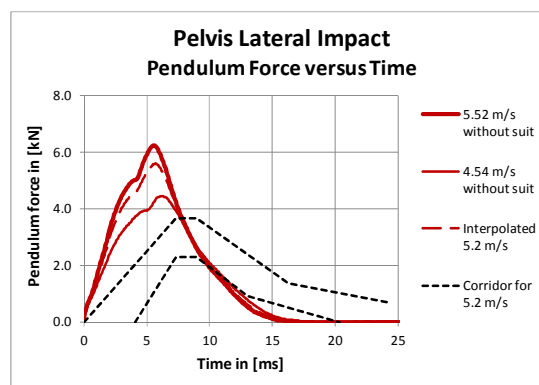


**Figure 4-56: Pelvis lateral pendulum impact at 5.2 m/s**

### Discussion and conclusion

The pelvis response is in line with the lateral shoulder and thorax responses showing an initial response that overestimates the stiffness whereas the response at later times gives lower stiffness. Known side impact dummies like EuroSID-2 and WorldSID show a similar response character.

With regards to lateral impact it can be concluded that all three important body regions (shoulder thorax and pelvis) show initially an overestimated stiffness with a relative low stiffness at later times. This balances out the load distribution over the dummy torso in lateral impact. As a consequence none of these body regions will be overexposed to the load in the lateral pulse.

### 4.3.5 Sensitivity

In this chapter the Q10 dummy sensitivity performance information for frontal and lateral impacts is presented per body region top down from head to pelvis.

#### Head

For the head the sensitivity for impact angle variation was investigated. In two impact conditions the impact angle was varied  $\pm 10$  degrees. In Figure 4-57 and Figure 4-58, the results are presented as the average measured peak resultant acceleration together with the maximum and minimum measured values. For the nominal impact direction five (5) tests were completed and for the  $\pm 10$  degrees impacts three (3) tests were done.

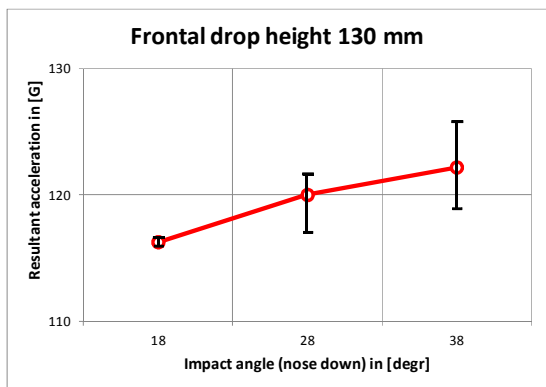


**Figure 4-57: Frontal angle variation, 130 mm drop height**

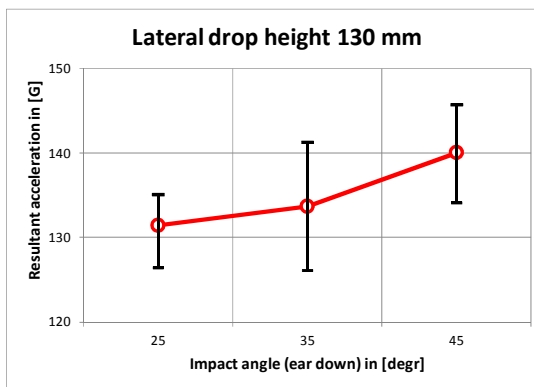


**Figure 4-58: Lateral angle variation, 130 mm drop height**

**Discussion and conclusion**

From Figure 4-57 and Figure 4-58 it can be seen that head is not sensitive for angle variation. The sensitivity found for ±10 degrees impacts is in the same order as the variation that can be expected for the impact tests in a single test conditions. This means that the head response is, as desired, not significantly sensitive for the small variations of the impact location.

**Neck**

For the neck no sensitivity assessment can be reported.

**Shoulder**

**Lateral impact**

For the lateral shoulder impact the sensitivity for speed, impact alignment offset and impact angular offset variation was investigated considering the peak pendulum force and T1 peak acceleration (measured on lower neck interface plane level). Figure 4-59 shows the sensitivity for the impact speed. Figure 4-60 and Figure 4-61 give the sensitivity for the angular offsets ±10 degrees from pure lateral impact in the horizontal plane. In Figure 4-62 and Figure 4-63 show the sensitivity for the impact alignment offsets ±15 mm from the lateral impact aligned with the centre of shoulder joint in the horizontal plane.

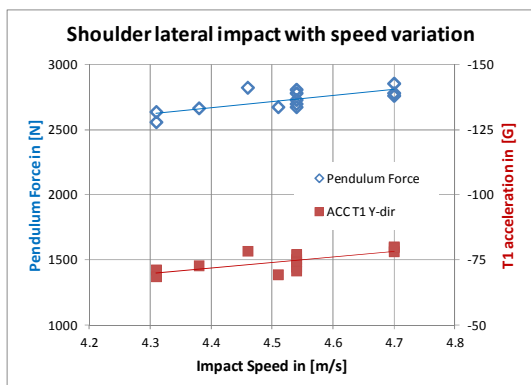


**Figure 4-59: Shoulder lateral impact results versus speed**

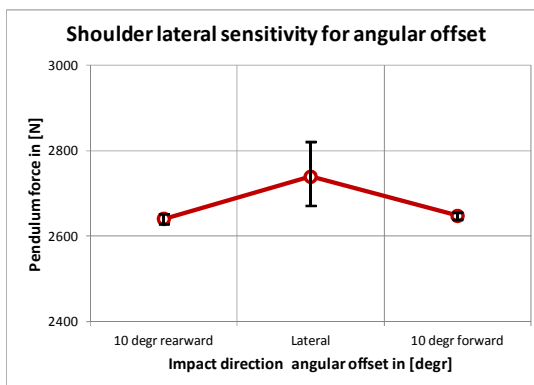


**Figure 4-60: Impact force sensitivity for angular offset**

*Discussion and conclusion*

As can be seen from Figure 4-59 both pendulum force and T1 lateral acceleration increase with impact speed as one might expect. Variations in impact angle (compared to pure lateral impact) and location (compared to impacts at centreline) result in a decrease of the pendulum force (see Figure 4-60 and Figure 4-61). This can be contributed to the introduction of rotation in the dummy. It appears though that the T1 lateral accelerations are insensitive to variations in the impactor alignment (Figure 4-63) while showing a large sensitivity to impact angle (Figure 4-61). The latter can be explained by the fact that the shoulder rubber is loaded in flexible bending mode when impacted from the rear, whereas for forward angle impacts the shoulder rubber becomes loaded in a compression mode which stiffens the load path in the dummy.

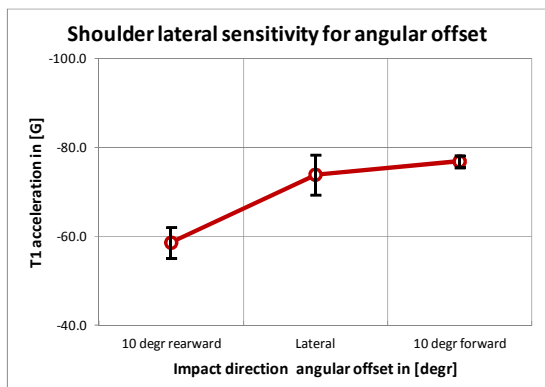


**Figure 4-61: T1 acceleration sensitivity for angular offset**

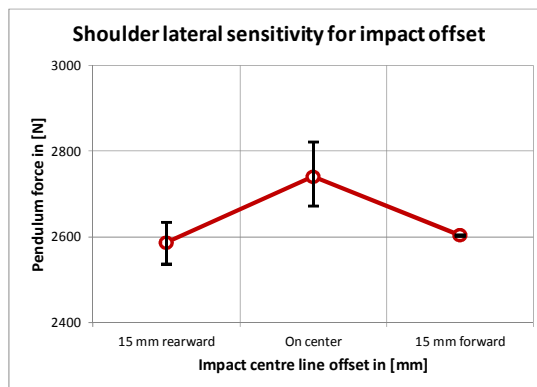


**Figure 4-62: Impact force sensitivity for alignment offset**

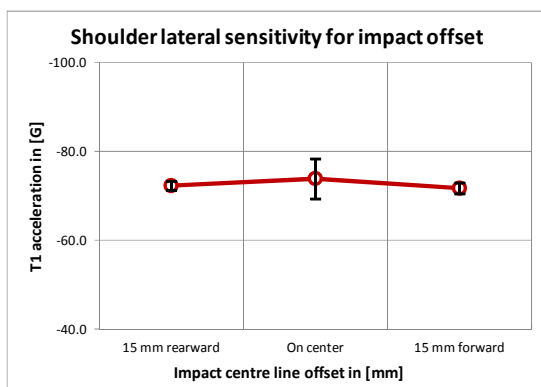


**Figure 4-63: T1 acceleration sensitivity for alignment offset**

**Thorax**

**Frontal impact**

For the thorax, frontal impact the sensitivity for impact speed and angular offset from the pure frontal was investigated. In Figure 4-64, the sensitivity of pendulum force and chest displacement (Dx) for impact speed is shown for impact speeds of 4.3, 5.5 and 6.7 m/s. For the angular offset sensitivity, the pure frontal impact test results at 4.3 m/s are compared with the results of impacts at the same speed with an angular off-set of 10, 20 and 30 degrees to the left hand side (two tests for each offset direction). It is assumed that the sensitivity will be symmetrical for both sides. In Figure 4-65, the results for the pendulum force are shown. In Figure 4-66, the results for the chest deflection are given. For the chest deflection the resultant displacement has been taken to allow for the combined X- (longitudinal) and Y- (lateral) displacement that can be calculated from the IR-TRACC and potentiometer signals. In Figure 4-67, the

average 2-dimensional deflection trajectory of the sternum in X and Y direction is plotted for all four impact directions.

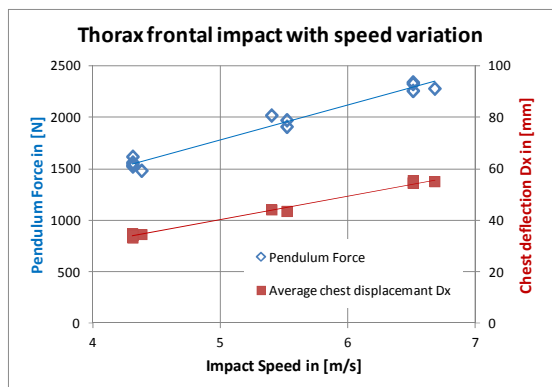


Figure 4-64: Thorax frontal impact results versus speed

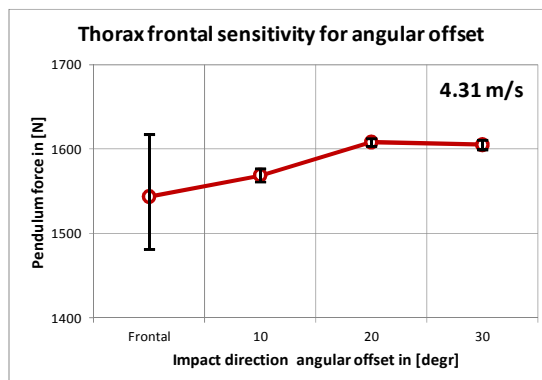


Figure 4-65: Pendulum force sensitivity for angular offset

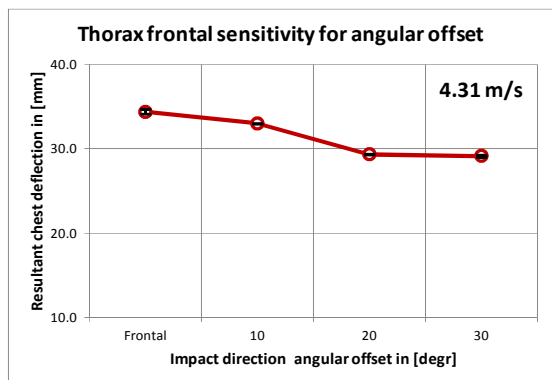


Figure 4-66: Chest deflection sensitivity for angular offset

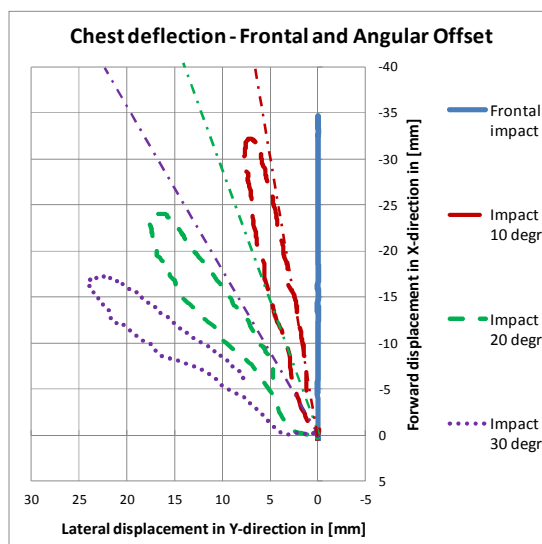


Figure 4-67: Chest deflection - frontal and angular offset

*Discussion and conclusion*

In Figure 4-64, the pendulum force and chest deflection show sensitivity for the impact speed as expected. For the angular offset sensitivity the pendulum force increases slightly up to about 4% (Figure 4-65) whereas the resultant chest deflection decreases significantly up to about 15% (Figure 4-66). This may be contributed to the fact that the 2D-IRTRACC measures the displacement of the forward point of the chest which is not optimal in case of impacts with an angular offset. The X-Y displacement plots given in Figure 4-67 clearly show that the pure frontal impact results in a pure longitudinal chest deflection. However in case of impact with angular offsets the lateral displacement measured at the forward 2D-IRTRACC attachment points show an over proportional increase of the lateral chest deflection. For 20 and 30 degrees angular offset the 2D-IRTRACC records initially even a pure lateral chest deflection, later the deflection becomes an X-Y displacement. It is recommended to always assess the X-Y displacement to get the best possible indication of the chest deformation and to use the resultant deflection for injury assessment.



### Lateral impact

For the thorax lateral impact the sensitivity for impact speed and angular offset from the pure frontal was investigated. In Figure 4-68, the sensitivity of pendulum force and chest displacement ( $D_y$ ) for impact speed is shown for impact speeds of 4.3, 5.5 and 6.7 m/s. For the angular offset sensitivity the pure lateral impact tests at 4.3 and 6.7 m/s are compared with the results of impacts at the same speed with an angular off-set of 15 degrees rearward and 15 degrees forward from lateral (two tests for each offset direction). In Figure 4-69 and Figure 4-70 the results for the pendulum force are shown and in Figure 4-71 and Figure 4-72 the results for the chest deflection are given. For the chest deflection it should be noted that the lateral line on the rib cage will always deflect in lateral and forward direction. In the graphs Figure 4-71 and Figure 4-72 the displacement in lateral directions ( $D_y$ ) has been used. In Figure 4-73 and Figure 4-74, the average 2-dimensional deflection trajectory of the lateral rib cage line in lateral (Y) and forward (X) direction are plotted for all three impact directions.

### Discussion and conclusion

The pendulum force and chest deflection ( $D_y$ ) in Figure 4-68 increase with impact speed as expected. For the angular offset sensitivity at 4.31 m/s the pendulum force increases about 10% relative to pure lateral in case of rearward angular offset while decreasing about 11% in case of forward angular offset (see Figure 4-69). At 6.71 m/s impact speed the pendulum force increases up to about 12% in case of rearward angular offset and decreases about 7% in case of forward angular (see Figure 4-70). The chest deflection in lateral direction ( $D_y$ ) decreases significantly in case of rearward angular offset: 42% relative to pure lateral at 4.3 m/s impact speed (Figure 4-71) and 49% at 6.7 m/s impact speed (Figure 4-72). In case of forward angular offset the measured lateral chest deflection remains almost the same as in pure lateral impact. This means that the dummy behaves stiffer for rearward direction impacts, which is due to the attachment of the rib cage to the thoracic spine.

The X-Y displacement plots given in Figure 4-73 (4.31 m/s impacts) and Figure 4-74 (6.71 m/s impacts) clearly show that the pure lateral impact results in a combined lateral and forward deflection of the lateral 2D-IRTRACC to rib cage attachment points. This is a well-known phenomenon in side impact dummies and resulted in the introduction of the 2-D IRTRACCs in the WorldSID dummies (for the small female WorldSID (Waagmeester, 2010)). The pronounced 2-D response in case of lateral impact is induced by the fixation of the ribcage at the thoracic spine. For pure lateral and forward angular offset impacts the lateral inward deflection of the rib is obvious. For the rearward angular offset impacts, however, the rib cage deflects initially mainly forward. The 2D-IRTRACC lateral rib attachment points seem to rotate around the rib attachment to the thoracic spine. It is recommended to always assess the X-Y displacement to get the best possible insight in the chest deformation. For the injury assessment the lateral deflection ( $D_y$ ) might be used as common in side impact dummies or, once available for other dummies, like the WorldSID dummies, two criteria using X and Y displacements might be introduced. Though, this will need further biomechanical research.

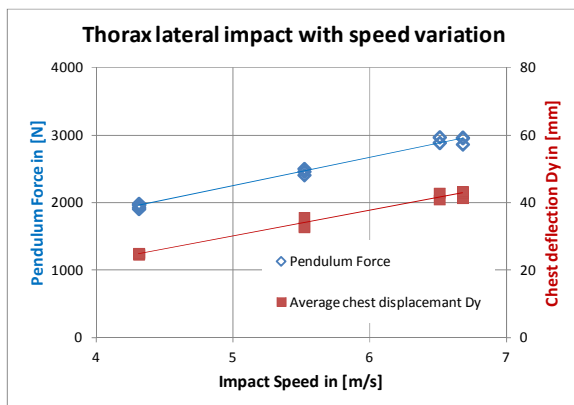


Figure 4-68: Thorax lateral impact results versus speed

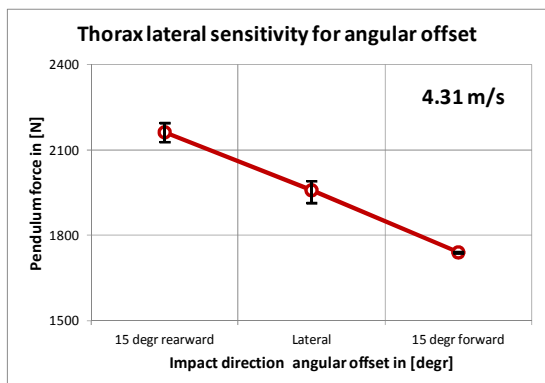


Figure 4-69: Pendulum force sensitivity for angular offset

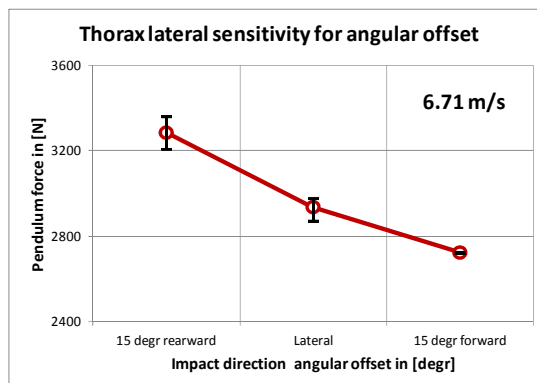


Figure 4-70: Pendulum force sensitivity for angular offset

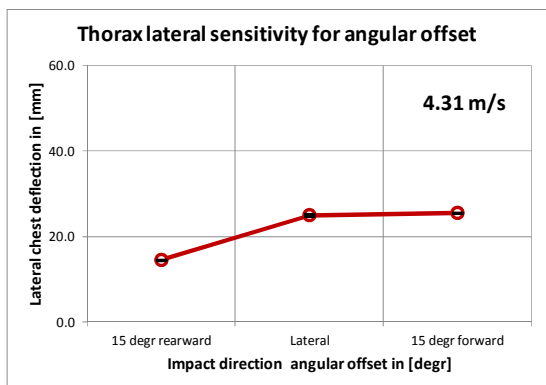


Figure 4-71: Chest deflection sensitivity for angular offset

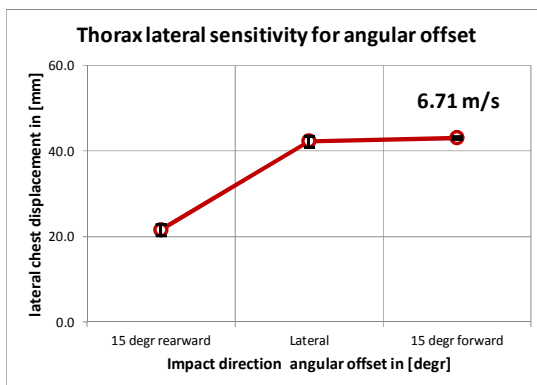
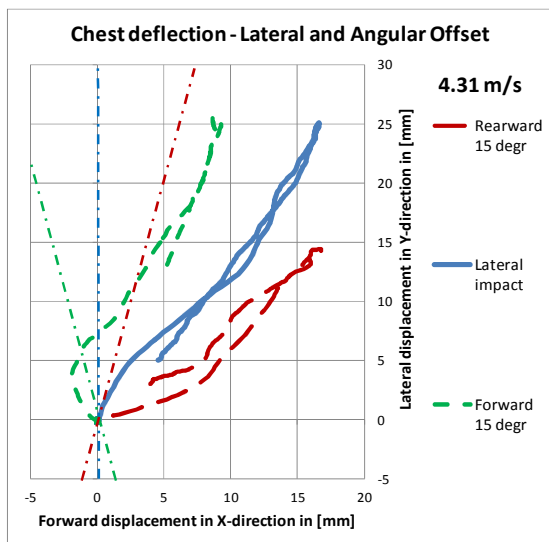
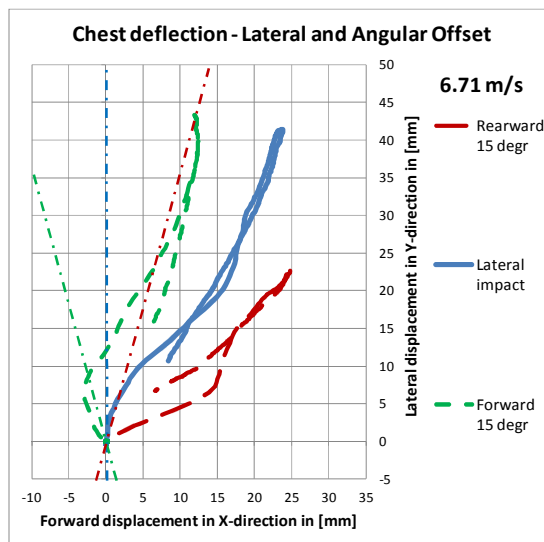


Figure 4-72: Chest deflection sensitivity for angular offset



**Figure 4-73: Chest deflection - lateral and angular offset**



**Figure 4-74: Chest deflection - lateral and angular offset**

**Lumbar spine**

For the lumbar spine no sensitivity assessment can be reported.

**Pelvis**

For the pelvis lateral impact the sensitivity for impact speed and alignment offset was investigated. Figure 4-75 shows results for the pendulum force and pubic symphysis loads as function of impact speed. Figure 4-76 and Figure 4-77 show sensitivities of parameters to the impactor alignment. The offsets considered in these tests are 30mm above the H-point and 30 mm forward of the H-point. The impact speed is 4.5 m/s in all these offset sensitivity cases.

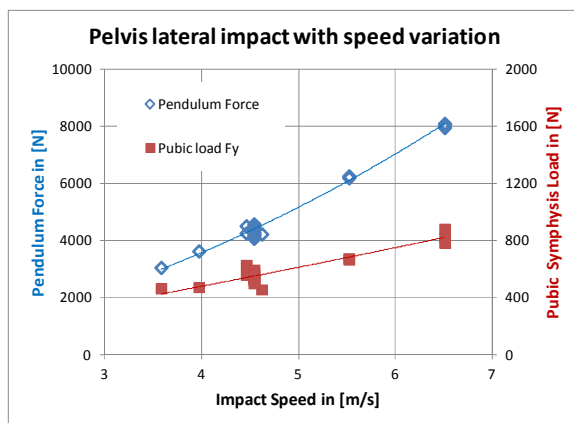


**Figure 4-75: Pelvis impact results versus impact speed**

*Discussion and conclusion*

In Figure 4-75, the pendulum force and pubic symphysis force show sensitivity for the impact speed as expected. Trend lines quadratic with the impact speed gives the best fit through the data points. When impacted 30mm above the H-point the pendulum force increases about 7% (Figure 4-76) and the pubic symphysis load drops with about 5% (Figure 4-77). This can be explained because this case not only the upper leg thigh is exposed to the impact, but also the pelvis flesh part above the thigh and behind that the most lateral upper margin of the iliac wing. In an impact 30mm forward of the H-

point the pendulum force is the same as in an impact aligned with the H-point (Figure 4-76). In that case the pubic symphysis load rises with 4% (Figure 4-77). It should be note pubic symphysis loads most likely are influenced by the bottoming out of the hip joint hardware against the sacrum block. This occurs in the current dummy at pendulum impact with speed larger than 4.0 m/s. This bottoming out will be considered in a pelvis redesign that should provide more clearance between the iliac wings and the sacrum block and more stiffness in the iliac wings.

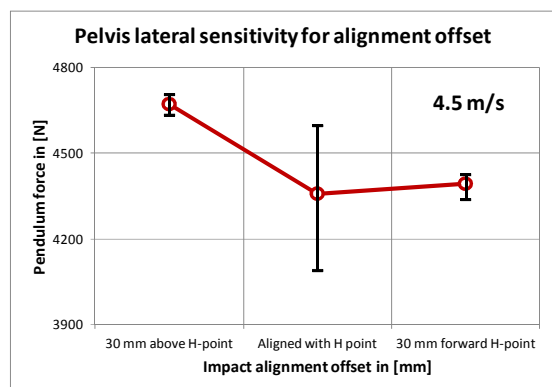


**Figure 4-76: Impact force sensitivity for alignment offset**

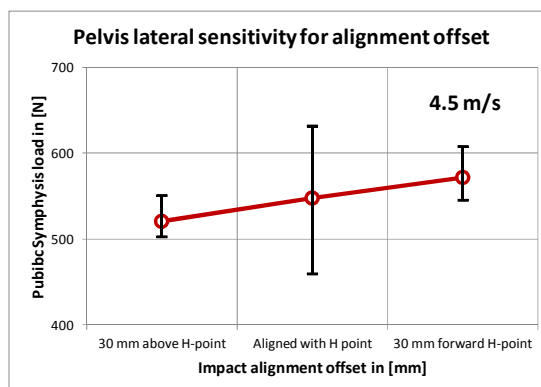


**Figure 4-77: Pubic load sensitivity for alignment offset**

#### 4.3.6 Repeatability

The level of repeatability of dummy responses is often expressed in the Coefficient of Variation ( $CoV = \text{Standard Deviation} / \text{Mean value}$ ). In component and full body impactor tests, that are considered to be highly repeatable the number of variables involved is small. In those tests the dummy, the impact pulse and the temperature of the setup are the main variables and a CoV of maximum 5% is considered to be acceptable. For a proper statistically valid CoV the minimum number of tests is seven (7), the test series performed in this dummy validation exercise comprises in general maximum five (5) and minimum two (2) tests of the same test configuration. Therefore an alternative approach is used: for each test result the relative deviation is calculated by: Deviation from the mean value of the group divided by the mean value of the group. Taking the standard deviation of the relative deviations of a number tests over group boundaries results in a statistical significant CoV values. Below per body region, top down from head to pelvis, tables are presented that show the test configuration considered and the CoV values obtained per composed group. Between brackets the associated number of tests in the (composed) group is given. Tests that deviate more than 7% from the mean result of the group are excluded from the calculation.

**Table 4-7: Head impact repeatability**

Test configuration	Head acc
Frontal impact 130 mm	1.59% (11)
18 degrees	2.83% (3)
28 degrees	1.53% (5)
38 degrees	0.31% (3)
Lateral impact 130 mm	2.50% (22)
25 degrees LH- and RH- side	1.29% (6)
35 degrees LH- and RH- side	3.59% (10)
45 degrees LH- and RH- side	1.19% (6)
Lateral impact 200 mm	2.65% (20)
25 degrees LH- and RH- side	2.11% (5)
35 degrees LH- and RH- side	2.24% (10)
45 degrees LH- and RH- side	4.21% (5)
<b>All tests together</b>	<b>2.35% (53)</b>

**Table 4-8: Neck bending repeatability**

Test configuration	Upper neck moment	Head form rotation
Flexion	2.04% (11)	0.67% (11)
4.7 m/s	1.62% (3)	0.27% (3)
4.8 m/s	2.46% (5)	0.99% (5)
4.9 m/s	2.47% (3)	0.48% (3)
Extension	4.03% (11)	0.80% (11)
3.6 m/s	4.81% (3)	0.75% (3)
3.7 m/s	5.31% (5)	1.11% (5)
3.8 m/s	1.79% (3)	0.43% (3)
Lateral Flexion	1.59% (11)	1.10% (11)
3.6 m/s	1.71% (3)	1.01% (3)
3.7 m/s	2.15% (5)	1.36% (5)
3.8 m/s	0.67% (3)	0.48% (3)
<b>All tests together</b>	<b>2.67% (33)</b>	<b>0.87% (33)</b>

**Table 4-9: Shoulder impact repeatability (lateral impact)**

Test configuration	Pendulum force	T1 Y- acceleration
Lateral impact		
4.3 m/s	2.10% (3)	3.03% (3)
4.5 m/s	2.30% (7)	3.90% (7)
4.7 m/s	1.76% (3)	1.29% (3)
4.5 m/s 15 mm rearward	2.66% (2)	2.01% (2)
4.5 m/s 15 mm forward	0.10% (2)	2.36% (2)
4.5 m/s 10 degr rearward	0.64% (2)	<i>Excluded &gt;7%</i>
4.5 m/s 10 degr forward	0.44% (2)	2.47% (2)
<b>All tests together</b>	<b>1.97% (21)</b>	<b>3.23% (19)</b>

**Table 4-10: Thorax impact repeatability**

Test configuration	Pendulum force	Rib deflection
Frontal impact	1.90% (24)	1.50% (24)
4.3 m/s	3.26% (5)	0.66% (5)
5.5 m/s	2.79% (3)	0.80% (3)
6.7 m/s	1.67% (4)	0.84% (4)
4.3 m/s, forward 10 degr	0.70% (2)	0.54% (2)
4.3 m/s, forward 20 degr	0.40% (2)	2.58% (2)
4.3 m/s, forward 30 degr	0.50% (2)	5.10% (2)
6.7 m/s, forward 10 degr	1.01% (2)	2.21% (2)
4.3 m/s, tilt 12 degr	0.80% (2)	1.04% (2)
6.7 m/s tilt 12 degr	1.03% (2)	1.97% (2)
Lateral impact	1.49% (21)	2.16% (19)
4.3 m/s	1.62% (5)	0.97% (5)
5.5 m/s	1.89% (3)	5.07% (3)
6.7 m/s	1.69% (5)	2.61% (5)
4.3 m/s, rearward 15 degr	2.18% (2)	0.60% (2)
6.7 m/s, rearward 15 degr	3.28% (2)	<i>Excluded &gt;7%</i>
4.3 m/s, forward 15 degr	0.17% (2)	0.35% (2)
6.7 m/s, forward 15 degr	0.14% (2)	1.04% (2)
<b>All tests together</b>	<b>1.61% (45)</b>	<b>1.77 (43)</b>

**Table 4-11: Lumbar spine bending repeatability**

Test configuration	Lower lumbar moment	Head form rotation
Flexion	1.15% (11)	2.52% (11)
4.3 m/s	1.20% (3)	0.49% (3)
4.4 m/s	0.52% (3)	1.00% (3)
4.5 m/s	1.57% (5)	3.76% (5)
Lateral Flexion	1.68% (11)	1.69% (11)
4.3 m/s	2.45% (3)	0.21% (3)
4.4 m/s	1.55% (5)	2.63% (5)
4.5 m/s	1.81% (3)	0.55% (3)
<b>All tests together</b>	<b>1.40% (22)</b>	<b>2.11% (22)</b>

**Table 4-12: Lumbar spine bending repeatability**

Test configuration	Lower lumbar moment	Head form rotation
Flexion	1.15% (11)	2.52% (11)
4.3 m/s	1.20% (3)	0.49% (3)
4.4 m/s	0.52% (3)	1.00% (3)
4.5 m/s	1.57% (5)	3.76% (5)
Lateral Flexion	1.68% (11)	1.69% (11)
4.3 m/s	2.45% (3)	0.21% (3)
4.4 m/s	1.55% (5)	2.63% (5)
4.5 m/s	1.81% (3)	0.55% (3)
<b>All tests together</b>	<b>1.40% (22)</b>	<b>2.11% (22)</b>

**Table 4-13: Pelvis impact repeatability (lateral impact)**

Test configuration	Pendulum force	Pubic symphysis load
Aligned with H-point	1.70%(19)	4.62%(14)
4.5 m/s	2.04% (13)	4.99% (8)
5.5 m/s	0.55% (3)	0.85% (3)
6.5 m/s	0.91% (3)	5.95% (3)
30mm above H-point		
4.5 m/s	0.77% (3)	5.07% (3)
30mm forward H-point		
4.5 m/s	1.08% (3)	5.67% (3)
<b>All tests together</b>	<b>1.52% (25)</b>	<b>4.62% (20)</b>

#### Discussion and conclusion

The results presented in Table 4-7 to Table 4-13 show a good repeatability all over the dummy. Nearly all values remain below 2.5% except the T1 Y-acceleration in the shoulder lateral impact tests and the pubic symphysis load in pelvis lateral impacts tests. The T1 acceleration (CoV=3.2%) is obtained with an provisionally mounted accelerometer, may be the double sided mounting tape on the slightly curved lower neck load cell flange was not very consistent. The relatively large variation of the pubic symphysis load (CoV=4.6%) may be contributed to the fact that the iliac wing and hip joint hardware bottoms out against the sacrum block in impact with a speed larger than 4.0 m/s. Overall it is concluded that the Q10 dummy can be used as a repeatable tool in crash test environments.

#### 4.3.7 Durability

The 254 tests of the validation test program were performed on the dummy also used for the EPOCh project dynamic evaluation test program at TRL. For the neck tests a new neck was used. The validation tests on the dummy did not lead to damage to the dummy. It is concluded that the dummy is durable for the load levels reached in the biofidelity and certification tests.

The evaluation of the Q10 dummy under UN Regulation 44 and NPACS test conditions performed by DOREL, IDIADA and TRL revealed some durability related issues on the neck, torso, lower legs and suit. A separate paper dealing with these evaluation tests

will address the durability issues in detail (Waagmeester 2009). During the EPOCH evaluation some improvements were implemented straight away, others based on EPOCH recommendation may be implemented later in a dummy update.

#### 4.3.8 Certification procedures

In this chapter the provisional certification procedures are specified per body region top down from head to pelvis. Certification corridors are not specified in this paper because some parts may change in performance as a result of EPOCH project recommendations and the results of several batches of products and of different test laboratories should be considered before corridors can be established.

##### Head

The head certification test set-up consists of a complete head including the accelerometer mounting hardware. Additional to the head a half steel upper neck load cell replacement (mass 0.15 kg, part number TE-010-1007) should be mounted to the lower side of the head base plate. The head should be equipped to record the X, Y and Z accelerations filtered at CFC1000. From these results the resultant head acceleration should be calculated. The following certification test impacts should be performed:

##### Frontal

With the head tilted  $28 \pm 2$  degrees nose down (from pure facial impact) and a drop height of 130 mm. (as standard for Q-dummies).

##### Lateral

With the head tilted  $35 \pm 2$  degrees ear down (from pure lateral impact) and a drop height of 130 mm. (as standard for Q-dummies).

##### Neck

The necks must be certified with the standard Part 572 neck pendulum with a head form that replaces the actual head. Between the pendulum base and the neck lower plate a special interface ring should be used (part number TE-010-2015). Between the upper neck plate and the head form the high capacity upper neck load cell (IF-217-HC) should be mounted. In the tests the pendulum acceleration (CFC180), the head form rotation obtained with the pendulum and head potentiometers (CFC600) and the upper neck moments  $M_x$  (side bending) and  $M_y$  (forward bending) (CFC600) should be recorded. For the deceleration of the pendulum 6 inch honeycomb is used. The certification test procedures to be followed are:

##### Flexion

For the neck certification flexion test the pulse should be between the following boundaries:

- Pendulum speed: between 4.7 and 4.9 m/s
  - @ 10 ms: 1.0 – 2.0 m/s;
  - @ 20 ms: 2.3 – 3.4 m/s; and
  - @ 30 ms: 3.6 – 4.8 m/s.

The pulse corridor and the pulses of the tests performed are shown in Figure 4-78.

##### Extension

For the neck certification extension test the pulse should be between the following boundaries:

- Pendulum speed: between 3.6 and 3.8 m/s
  - @ 10 ms: 0.7 – 1.7 m/s;
  - @ 20 ms: 1.7 – 2.8 m/s; and

- @ 30 ms: 2.8 – 4.0 m/s.

The pulse corridor and the pulses of the tests performed are shown in Figure 4-79.

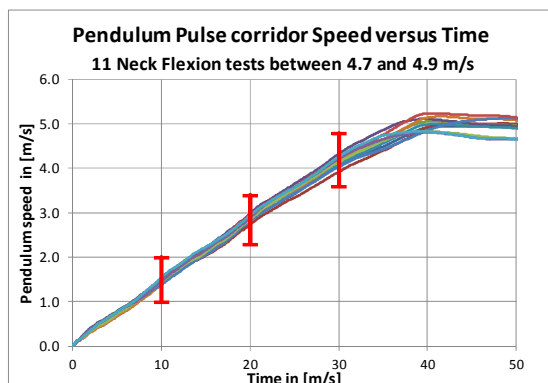


**Figure 4-78: Pendulum pulse for neck flexion test**

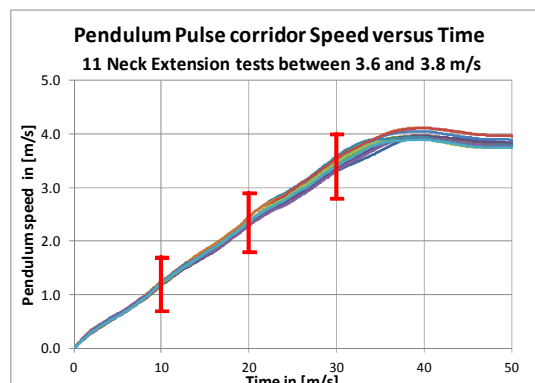


**Figure 4-79: Pendulum pulse for neck extension test**

### Lateral flexion

For the neck certification lateral flexion test the pulse should be between the following boundaries:

- Pendulum speed: between 3.6 and 3.8 m/s
  - @ 10 ms: 0.7 – 1.7 m/s;
  - @ 20 ms: 1.7 – 2.8 m/s; and
  - @ 30 ms: 2.8 – 4.0 m/s.

The pulse corridor and the pulses of the tests performed are shown in Figure 4-80.

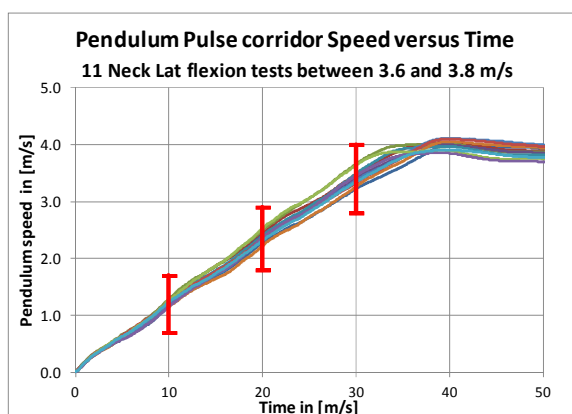


**Figure 4-80: Pendulum pulse for neck lateral flexion test**

#### 4.3.8.1 Shoulder (lateral impact)

For the shoulder certification a full body lateral impact test should be done with a six wire, suspended pendulum (mass of 8.76 kg and a diameter of 112 mm). The pendulum speed should be between 4.2 and 4.4 m/s. The impact should be pure lateral with the pendulum aligned with shoulder joint. The dummy should be sitting with the thoracic spine vertical, the upper arms along the thorax and the legs stretched forward on two sheets of PTFE (Teflon) to minimize the friction. In the tests the pendulum acceleration (CFC180) should be recorded.



## Thorax

For the thorax certification a full body frontal and lateral impact test should be done with a six wire suspended pendulum (mass of 8.76 kg and a diameter of 112 mm). The pendulum speed should be between 4.2 and 4.4 m/s. The impact should be pure frontal or lateral with the pendulum centerline in the middle between the IR-TRACC to ribcage attachment screws. The dummy should be sitting with the thoracic spine vertical and the legs stretched forward on two sheets of PTFE (Teflon) to minimize the friction. In the frontal test the upper arms should be along the thorax sides. In the lateral test the arm at the impact side should be taped to the head to enable free impact exposure to the side of the rib cage. In the tests the pendulum acceleration (CFC180) and both 2D IR-TRACCs (IR-TRACCs and potentiometers at CFC600) should be recorded.

## Lumbar spine

The lumbar spine must be certified with the standard Part 572 neck pendulum with a head form mounted to the upper lumbar spine interface. A special head form central block (part number TE-2651-14) that allows for the offset in the upper lumbar spine mount should be used. Between the pendulum and the lumbar spine lower mount a steel load cell replacement of high capacity load cell (IF-217-HC) should be used. In the tests the pendulum acceleration (CFC180) and the head form rotation with the pendulum and head potentiometers (CFC600) should be recorded. The certification test procedures to be followed are:

## Flexion

For the lumbar spine certification flexion test the pulse should be between the following boundaries:

- Pendulum speed: between 4.3 and 4.5 m/s
  - @ 10 ms: 0.9 – 1.9 m/s;
  - @ 20 ms: 2.3 – 3.4 m/s; and
  - @ 30 ms: 3.4 – 4.6 m/s.

The pulse corridor and the pulses of the 11 flexion tests performed are shown in Figure 5 37.

## Lateral Flexion

For the certification neck lateral flexion test the pulse should be between the following boundaries:

- Pendulum speed: between 4.3 and 4.5 m/s
  - @ 10 ms: 0.9 – 1.9 m/s;
  - @ 20 ms: 2.3 – 3.4 m/s; and
  - @ 30 ms: 3.4 – 4.6 m/s.

The pulse corridor and the pulses of the 11 lateral flexion tests performed are shown in Figure 5 38.

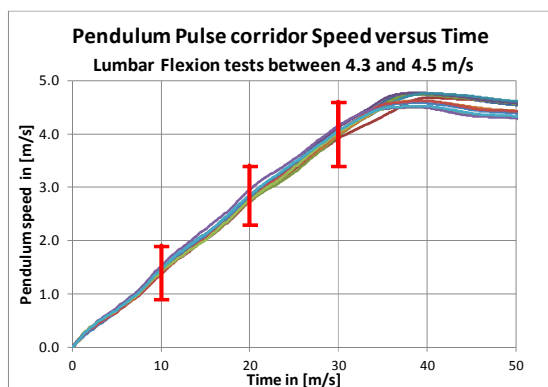


**Figure 4-81: Pendulum pulse for lumbar flexion**

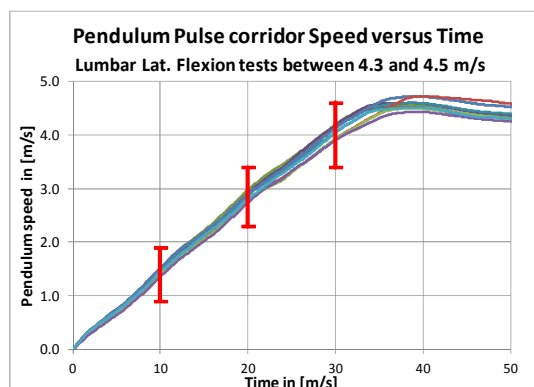


**Figure 4-82: Pendulum pulse for lumbar lateral flexion**

### Pelvis (lateral impact)

For the pelvis certification a full body lateral impact test should be done with a six wire suspended pendulum (mass of 8.76 kg and a diameter of 112 mm). The pendulum speed should be between 4.2 and 4.4 m/s. The impact should be pure lateral with the pendulum aligned with the hip joint (65.9 mm above the seating plane and 90.4 mm forward of the back plane). The dummy should be sitting with the thoracic spine vertical, the upper arms along the thorax with the hands on the lap and the legs stretched forward on two sheets of PTFE (Teflon) to minimize the friction. In the tests the pendulum acceleration (CFC180) and the pubic symphysis load (CFC600) should be recorded.

### 4.3.9 Summary and conclusions

The Q10 dummy was extensively evaluated on biomechanical performance, sensitivity, repeatability and durability to impact loading in head drop, neck pendulum and full body wire pendulum tests. Moreover certification procedures were developed.

#### Biofidelity

For frontal loading conditions it can be stated that the dummy correlates well with biomechanical targets specified in the Q10 design brief. For lateral impacts the dummy shows a response which is initially too stiff and at later stages too soft relative to side impact biofidelity corridors. Identical trends are found though for shoulders, thorax and pelvis meaning that the load distribution over the dummy is such that none of the regions is overexposed in case of distributed side impact loading.

#### Sensitivity

Sensitivity studies show obvious trends to variations in impact speeds, impact direction and alignments.

#### Repeatability

Repeated tests show generally small variations in response of less than 2.5%. Only the T1- acceleration in the lateral shoulder impact test and the pubic symphysis load in the lateral pelvis impact tests show larger variations: 3.2% and 4.6% respectively. All the coefficients of variation are with the required 5%. It is concluded that the Q10 dummy can be used as a repeatable tool.

#### Durability

The durability of the dummy meets requirements as specified. Separate reports describe the durability shown in sled test according to UN Regulation 44 and NPACS tests in detail.

---

#### 4.3.10 References

Reed, M.P., Sochor, M.M., Rupp, J.D., Klinich, K.D., Manary, M.M. (2009). *Anthropometric Specification of Child Crash Dummy Pelves through Statistical Analysis of the Skeletal Geometry*, Journal of Biomechanics 42 (2009) 1143-1145.

Waagmeester, C.D. *et al.* (2009). *Q10 Design Brief*, European Commission, EPOCH Project, Work Package 1, Task 1.2, EPOCH Deliverable D1.2, September 15, 2009.

Waagmeester, C.D. *et al.* (2010). *Q10 Dummy Status Review – Biofidelity Performance Validation*, Protection of Children in Cars Conference, Munich, December 2010.

## 5 Injury criteria and performance limits

With any new test tool, dummy or series of dummies, it is necessary to specify injury risk functions and acceptable thresholds or criteria for the appropriate age and size of occupant and the application. The dummy measurements represent an opportunity to relate performance in tests to the likelihood of injuries occurring in real-world accidents. Therefore, by selecting relevant measurement thresholds it is hoped that product safety can be driven to improve protection in priority areas. This is the intention for specifying performance thresholds for use with the Q-Series dummies and their use in testing child restraint systems.

Injury risk curves have been developed for adult occupants, typically by matching dummy tests with the outcome from equivalent tests with PMHS (post-mortem human subjects). However, there is little biomechanical data from which specific injury risk functions for children can be derived. Therefore two alternative approaches tend to be used:

- Perform accident reconstructions using the child dummy under development;
- Scale adult injury risk functions and/or criteria to be relevant to the child size (dummy) being investigated.

This section presents research undertaken in the CASPER and EPOCH projects to develop injury criteria for the Q-Series. Section 5.1 comprises the principal findings from CASPER, in which the injuries observed in the real-world accidents were paired with Q dummy measurements from around 60 validated reconstruction tests. Accident reconstructions with the newly-developed Q10 were beyond the scope of EPOCH and hence Section 5.2 describes the development of injury risk curves using scaling techniques. Each section comprises a published paper, reproduced here in its entirety. The full references for papers are:

Johannsen H, Trosseille X, Lesire P and Beillas P (2012). Estimating Q-dummy injury criteria using the CASPER Project results and scaling adult reference values. In: *IRCOBI Conference Proceedings*, 12-14 September 2012, Dublin, Ireland. Zurich, Switzerland: International Research Council on Biomechanics of Injury (IRCOBI).

Hynd, M., McGrath, M., Waagmeester, K., Salters, E., Longton, A., and Cirovic, S. (2011). EPOCH project dissemination. In: *Proceedings of the 9<sup>th</sup> International Conference Protection of Children in Cars*, 1-2 December, Munich, Germany. Munich, Germany: TÜV SÜD.

### 5.1 Estimating Q-dummy injury criteria using the CASPER project results and scaling adult reference values

#### 5.1.1 Introduction

The EC CASPER (Child Advanced Safety Project for European Roads) project aims at decreasing injuries and fatalities of child occupants. This goal represents a major social and economic benefit for the whole European Community.

CASPER involves a consortium of 15 European partners representing a good balance between industries, medical and technical universities, road state institutes and organisations that specialise in road safety issues for a 38-month project. This project was established under the GA n°218564 of the FP7-SST-2007-RTD-1-program of the

European Commission that is partially funding the project. Data from previous European projects CREST and CHILD were used as a basis.

This project has two main objectives that are complementary to improve the real level of protection of children in cars. The first one is the improvement of the rate of correctly restrained children in cars, and the effect of this can be seen in a short-term. This is done through the analysis of the reasons and the consequences of the conditions of transportation of children. The second one is the improvement of the efficiency of child protection which includes tools and test procedures that are used to evaluate the protection of children in cars for regulatory approval and consumer information tests. This second point – even if taking longer before any improvement can be observed in the field – is a necessary and continuous work. It consists of improving existing tools used for the evaluation of protection of children and in the development of the missing ones. Finite element models have been developed for child dummies and for human child bodies and proposals for improvements of the Q-series crash test dummies have been made. The CASPER project has also been evaluating a selection of existing solutions that could be applied to improve child safety in cars, although experts have found that it is sometimes difficult to have solutions that are at the same time scientifically based, approved, acceptable by both parents and children and that improve the ease of use of the restraint system. One major outcome of the CASPER project is the development of missing injury risk functions for Q-dummies. The CASPER project is continuing the earlier research of the CREST and CHILD projects that were reported by Palisson *et al.* [1].

Injury risk functions reported by Palisson *et al.* [1] were based on accident reconstructions and scaled adult data. While reliable risk curves for the head in frontal impact conditions were computed (see Figure 5-1), neck injury risk curves were based on scaled adult data only and for the chest compression both data sources were combined.

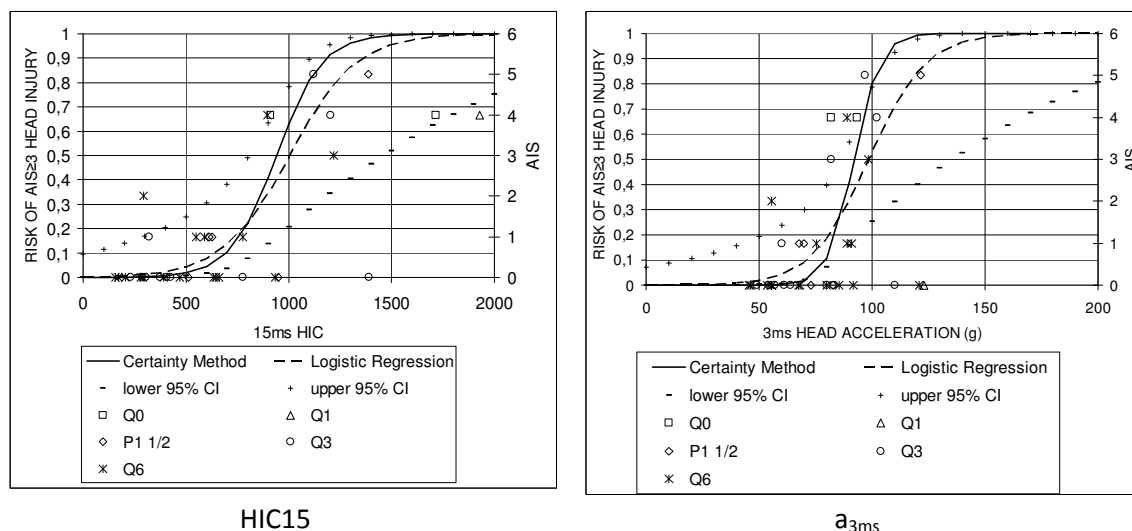


Figure 5-1: Q3 head injury risk curves and data dots resulting from CHILD project [1]

### 5.1.2 Methods

In order to focus the accident reconstruction on body regions that are considered to be most important for future regulation and consumer information, the injury risks of specific body regions for specific age groups were compared with the number of existing data points. Data from accidentology are used to identify the priorities in terms of protection of children and to evaluate the level of confidence of the existing tools

used for the evaluation of CRS and criteria available to predict injuries on the different body segments, see Table 5-1.

Taking into account the specific injury risks and the available data points, it was decided to aim for being able to compute injury risk functions for the following body regions, impact conditions and age groups:

- Neck injuries for frontal impact for Q1, Q1.5 and Q3 in forward facing CRS;
- Chest for frontal impact;
- Abdomen for frontal impact for booster type CRS;
- Head for lateral impact.




The method used in CASPER is similar to the one used in the previous EC research project in order to be able to integrate data previously obtained in the development of injury risk curves for the Q-series dummies. As there are very few biomechanical data available for children and because post-mortem tests on children are rare and ethically limited in Europe, the methodology is based on injuries sustained by restrained children in cars involved in real accidents and the physical reconstruction of real accidents in crash test laboratories in order to compare injuries with dummy readings.

**Table 5-1: Injury risks for different body regions dependent on age for frontal and lateral impact**

Frontal Impact							
	Head	Neck	Chest	Abdomen	Pelvis	Upper Limbs	Lower Limbs
New-born							
1 YO							
1,5 YO							
3 YO							
6 YO							
10 YO							
Remarks / Injury pattern	Skull and brain injuries, concussion, diffuse axonal injuries and subdural hematomas	Neck injuries mainly for upper cervical spine (C1 to C4), Injury pattern: fraction, dislocation (w. & wo. cord injury) and cord injury.	Flexibility of thoracic spine to be considered. 1-3YO organ injuries wo rib fracture, 6-10 YO organ injuries with rib fracture	Damage of soft organs (liver, spleen & kidneys) due to penetration of the belt (submarining & oop). No information for 0-1,5YO	No severe injuries were observed	Fractures, especially in rebound. No data for 3-10YO available	Fractures, especially in rebound. No data for 3-10YO available

## Lateral Impact

	Head	Neck	Chest	Abdomen	Pelvis	Upper Limbs	Lower Limbs
New-born							
1 YO							
1,5 YO							
3 YO							
6 YO							
10 YO							
Remarks / Injury pattern		Unclear but seems to be connected with head injuries.	1-3YO organ injuries without rib fracture, 6-10YO organ injuries with rib fracture	Abdominal penetration of side structure or booster base.	Injuries caused by contacts with penetrating structure	Shoulder and arm fractures due to intrusion. No information for 0-1,5YO.	Tibia fractures for 0-1,5YO. Tibia and femur fractures for 3-10YO.

	No severe injuries
	High risk of injury / high severity
	No sufficient information available / see remarks

From detailed accident data, including medical reports, restraint conditions and in depth investigation of cars, experts define the causes of injuries and accident scenarios. It is then necessary to determine if the accident conditions can be properly reproduced in crash-test laboratories using similar vehicles and CRS and child dummies of a size as close as possible to the children involved in the accident. It should be noted that the accidents are selected to be relevant for the development of injury risk functions and therefore are not necessarily representative of European accidents involving children. Selection criteria are that at least one restrained child suffered at least one MAIS 2+ injury or the delta-v exceeded 40 km/h for a frontal impact or the crush exceeded 200 mm in a lateral impact, respectively.

The reconstruction test results are discussed and validated on a case-by-case basis by experts both from accidentology (e.g. similar deformations of the cars, expected structural behaviour) and from biomechanics (e.g. study of the global kinematics of the child dummy and focus on the repetition of the injury mechanisms in the child dummy). A correlation is then made between the level of injury severity of the child and the dummy readings on different body segments. In case of positive result, one point is added to the cloud of existing ones for each body segment. It was necessary to have a large number of reconstructions performed before having injury risk curves for the different sizes of dummies and for different types of impacts. Currently the accident reconstruction database includes 76 valid reconstructions using Q-dummies. The distribution on the different dummy sizes is shown in Table 5-2.

**Table 5-2: No. of available reconstructions by dummy size and impact type**  
**Note: the number of cases exceeds the number of reconstructed accidents**

Dummy	Valid no. of cases frontal impact	Valid no. of cases lateral impact
Q0	3	0
Q1	8	4
Q1.5	5	1
Q3	26	10
Q6	27	8
Q10	1	0

Unfortunately injury severity levels were not always known for all body regions. In addition, dummies were not always equipped with all sensors or measurement failures occurred. Therefore the number of existing cases is lower when looking into individual body regions. In addition, this methodology is only valid for injury mechanisms observed in car accidents for restrained children that can be properly reproduced by existing child dummies and in configurations for which their response is sufficiently biofidelic.

A tentative programme of using more simple accident configurations than the one of children in cars has been explored through the analysis and reproduction of domestic accidents such as falls but it seems that dummy response to this kind of impact condition is different to what is known from car occupant conditions. Results of tests from this kind of accident were therefore not included in the risk curves presented in this paper.

**Scaling**

Reconstructions were performed on dummies from birth to 6 years old. As a consequence, the number of cases for each dummy age is very small and cannot be processed as it is. In order to consolidate these data, it was proposed to scale all results to a given age. This was done using the method proposed by Mertz [2] and applied to the Q dummies by Palisson [1].

**Table 5-3: Used scaling factors [1], [2]**

Scaling factor	$\lambda_{\sigma f}$	Head			Neck			
		$\lambda_{\sigma L}$	$\lambda_{+HIC}$	$\lambda_A$	$\lambda_x$	$\lambda_y$	$\lambda_F$	$\lambda_M$
Formula			$\lambda_{\sigma f}^{2,5} \lambda_L^{-1,5}$	$\lambda_{\sigma f} \lambda_L^{-1}$			$\lambda_{\sigma f} \lambda_x \lambda_y$	$\lambda_{\sigma f} \lambda_x^2 \lambda_y$
Q0	0,73	0,69	0,79	1,06	0,65	0,67	0,32	0,21
Q1	0,82	0,92	0,69	0,89	0,95	0,91	0,71	0,67
Q1.5	0,88	0,95	0,78	0,93	0,96	0,95	0,80	0,77
Q3	1	1	1,00	1,00	1	1	1,00	1,00
Q6	1,13	1,03	1,30	1,10	1,11	1,07	1,34	1,49

Scaling factor	$\lambda_{\sigma f}$	$\lambda_{Eb}$	$\lambda_{ET}$	Chest Frontal		Chest Lateral			Abdomen
				$\lambda_x$	$\lambda_y$	$\lambda_d$	$\lambda_{VC}$	$\lambda_{Acc}$	$\lambda_{Pression}$
Formula						$\lambda_x \lambda_{\sigma f} \lambda_{Eb}^{-1}$	$\lambda_{\sigma f} \lambda_{ET}^{-1/2}$	$\lambda_{\sigma f} \lambda_y^{-1}$	$\lambda_{\sigma f}$
Q0	0,73	0,51	0,62	0,63	0,66	0,94	0,92	1,15178	0,73
Q1	0,82	0,68	0,75	0,80	0,89	1,07	0,94	1,0214	0,82
Q1.5	0,88	0,77	0,79	0,80	0,93	1,06	0,99	1,10584	0,88
Q3	1	1,00	1,00	1,00	1,00	1,00	1,00	1	1,00
Q6	1,13	1,43	1,14	0,99	1,12	0,89	1,06	1,13801	1,13

This method takes into account geometrical parameters but also material variation through the ages. Table 5-3 gives the scaling factors corresponding to head and neck



injury criteria. For instance, if a HIC=1000 is acceptable for a 3 year old child, the acceptable limit for a 1 year old child will be HIC=690.

As a consequence, each individual result has to be divided by the corresponding scaling factor for the 3 year old equivalent value. For instance, if a 1 year old child sustains a given head injury with HIC=690, it is assumed that a 3 year old child would have sustained the same level of injury with a HIC=1000.

### **Injury risk curve construction**

Several methods can be used for drawing injury risk curves. However, it was demonstrated by Petitjean [3] that the survival analysis generally provided the best estimate. Therefore, guidelines for the construction of the injury risk curves were developed and agreed on among ISO experts. These guidelines include several steps:

Step 1: collect the relevant data.

According to the methodology developed in this paper, the relevant data correspond to the real accident case injuries and the dummy measurements from the paired reconstruction.

Step 2: assign the censoring status (left, right, interval censored, exact). Here, all the cases are censored.

Step 3: build the injury risk curve with the Consistent Threshold Estimate (CTE) [4] and check for dual injury mechanism.

Step 4:

If there is evidence of dual injury mechanism, separate the sample into samples with single injury mechanism and return to Step 1.

If there is no evidence of dual injury mechanism, build the injury risk curve with the survival analysis according to the following steps.

Step 5: estimate the parameters of the Weibull, log-normal, log-logistic distribution with the survival analysis method.

Step 6: identify overly influential observations using the dfbetas statistics. The dfbetas statistic gives an indication on the change of each parameter estimate when deleting one observation of the sample after another. An absolute value of the dfbetas statistic higher than 0.3 indicates that the associated observation was possibly overly influential. These observations are checked for any specificity. If there is no evidence of difference between these observations and the others included in the sample, these observations are kept in the construction of the injury risk curve.

Step 7: check the distribution assumption graphically using a qq-plot or the CTE method.

Step 8: choose the distribution with the best fit, based on the Akaike information criterion (AIC). The AIC criterion is calculated based on the likelihood of the model taking into account the number of variables used in the model ( $AIC = -2 \cdot \log \text{likelihood} + 2 \cdot \text{number of variables}$ ). The lowest AIC indicates the best fit of the model with the test data.

Step 9: check the validity of the predictions against existing results (such as accidentology outcome), if available.

**Step 10:**

- Step 10.1: calculate the 95% confidence intervals of the injury risk curve with the normal approximation of the error.
- Step 10.2: calculate the relative sample size of the confidence interval (width of the confidence intervals at 5%, 25% and 50% relative to the value of the stimulus at 5%, 25% and 50% of risk respectively).

**Step 11:** Provide the injury risk curve associated with the quality index based on the relative sample size of the 95% confidence interval. A scale was defined with four categories (“good” from 0 to 0.5, “fair” from 0.5 to 1, “marginal” from 1 to 1.5, “unacceptable” over 1.5).

**Step 12:** recommend one curve per body region, injury type and injury level.

- Step 12.1: If several injury risk curves can be compared with AIC and if the difference of AIC is greater than 2, then the curve with the lowest AIC is recommended over the others.
- Step 12.2: If an injury risk curve had an “unacceptable” quality index, it should not be recommended.
- Step 12.3: if several injury risk curves were still available for a given injury type and level, engineering judgment is used to recommend one curve over another.
- Step 12.4: The recommended injury thresholds should be provided associated with their quality indexes.

### 5.1.3 Results

#### Injury mechanisms and injury criteria

The Q dummies can be equipped with the following sensors:

- Head - three axial acceleration;
- Head - three axial angular velocity;
- Upper neck - six axial forces and moments;
- Lower neck - six axial forces and moments (only Q3 and Q6);
- Chest - three axial acceleration (approximately at T4 level);
- Chest - sternal deflection or lateral deflection at sternum level;
- Lumbar spine - six axial forces and moments (except Q0);
- Pelvis - three axial acceleration.

In order to assess abdominal injury risk in Q dummies, absent from the above, two different sets of abdominal sensors were developed within the CHILD project [5] [6] and then evaluated for future use in the CASPER project. Due to technical shortcomings of the Force Matrix Sensor (FMS) that were impossible to solve, the Abdominal Pressure Twin Sensor system was selected to be proposed as the abdominal sensor system for Q-dummies. After this decision was taken, the sensor was optimised to make it more robust.

Based on previous research head  $a_{3ms}$  and HIC are suitable criteria for the head in head contact cases. This was also confirmed by Palisson *et al.* [1] for children. For the cases without head contact, it is currently debated whether or not head  $a_{3ms}$  and/or HIC can be used. This discussion is important as the frontal impact assessment of CRS normally takes place without any surrounding interior that the head could contact. Another option could be the rotational acceleration of the head as proposed e.g. by Newman *et al.* [7] in combination with linear acceleration. For children it is proposed that angular acceleration could be used as an injury criterion for non-contact cases. For contact cases it is believed that the accuracy in accident reconstruction does not allow

valid assessment of the loads as the angular velocity is highly dependent on the lever arm (i.e. the correct impact point).

For the neck it is also important to distinguish between head contact and non-head contact cases. Neck tension and flexion are the most promising injury criteria for the injuries sustained by children in the database. For lateral impact cases in addition to neck tension, lateral bending moments can be used as well as the combination of neck bending moments and neck Z forces by using the NIJ criterion as used in FMVSS 208. As the main risk for neck injuries was reported for the youngest children in forward-facing CRS (i.e., Q1, Q1.5 and Q3) and no lower neck load cells exist for Q1 and Q1.5, only upper neck was taken into account.

For the thorax in current regulation, UN Regulation 44,  $a_{3ms}$  is used. For the new regulation proposal it is planned to keep this criterion with the current limit. In addition, sternal deflection (frontal impact), lateral chest deflection at sternum level (side impact) and the viscous criterion (VC) derived from chest deflection are in discussion. While chest deflection mainly aims at rib fracture risks, VC addresses injury risks for internal organs. Finally, peak abdominal pressure correlated best with injury risk given the selected abdominal sensor based on previous research [6].

### Injury risk curves for frontal impact

The raw data for the head obtained from the reconstructions are presented in Figure 5-2. The head accelerations were then scaled to a 3 year old (Figure 5-3) and a survival analysis was conducted. The circled data points were found to be overly influential. They were checked for any inconsistency, but nothing was found to be wrong. Therefore, only the red circled data point was removed from the analysis because it was really different from the cloud. Finally, the injury risk curve with its confidence intervals was plotted (Figure 5-4). The relative sizes of the confidence interval at 5%, 25% and 50 % of risk were calculated. They were 129%, 47% and 46% respectively. Therefore the error was considered as marginal at 5%, while it was considered as good at 25% and 50%. The values are summarized in Table 5-4.

The HIC values were processed in the same way. However, the AIC were higher and the confidence intervals larger. It should be noted that the HIC should be calculated only in case of impact, which should not happen in a certification test. Therefore, the HIC was not recommended as a criterion for the assessment of child restraining systems in frontal impact.

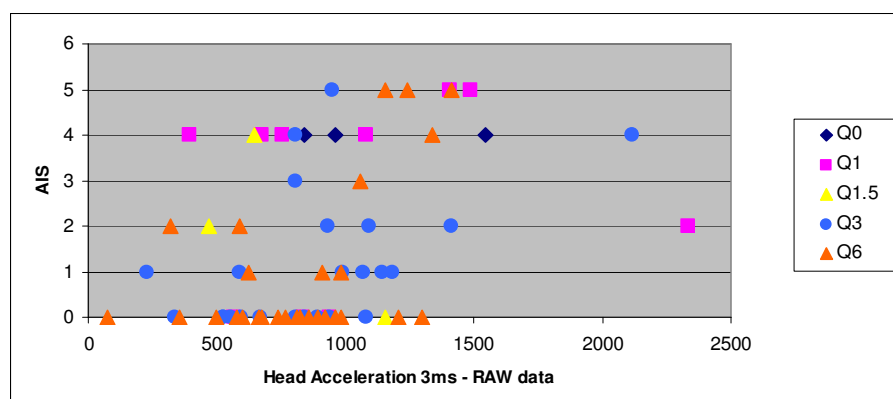


**Figure 5-2: Head AIS as a function of head linear acceleration 3ms for frontal reconstructions**

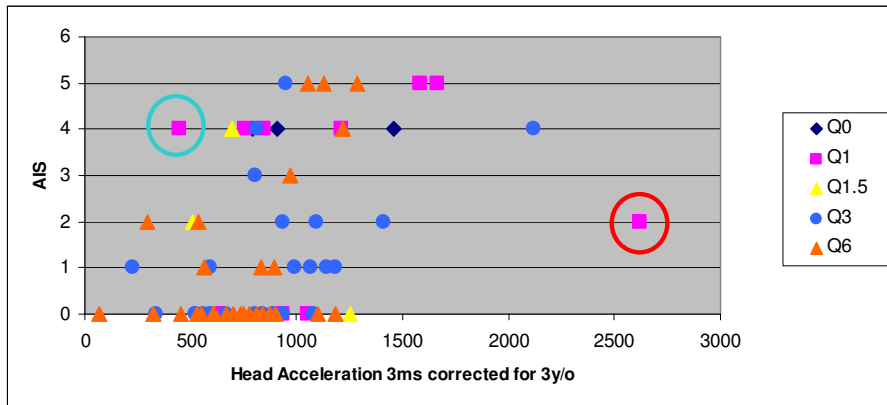


Figure 5-3: Head AIS as a function of scaled head accelerations

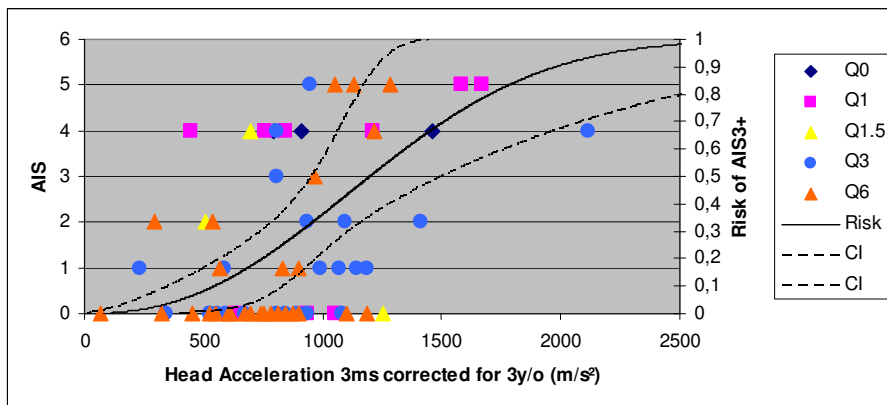


Figure 5-4: Head injury risk curve as a function of head acceleration 3ms for 3 year old

The neck data points were plotted separately for Q1/Q1.5 and Q3/Q6 dummies since younger children are at particular risk for neck injury in frontal loading. The data points were plotted in Figure 5-5 for the Q1 and Q1.5 dummies after scaling at 1 year old. The injury risk curve was constructed. The relative sizes of the confidence interval at 5%, 25% and 50 % of risk were 265%, 130% and 83% respectively. Therefore the error was considered as unacceptable at 5%, while it was considered as marginal at 25% and fair at 50%. It can be observed that no severe injury appeared below 1 kN and that all children sustained a severe injury above 1.3 kN. Neck My data points for cases without head impact do not allow the development of an injury risk curve, see Figure 5-6.

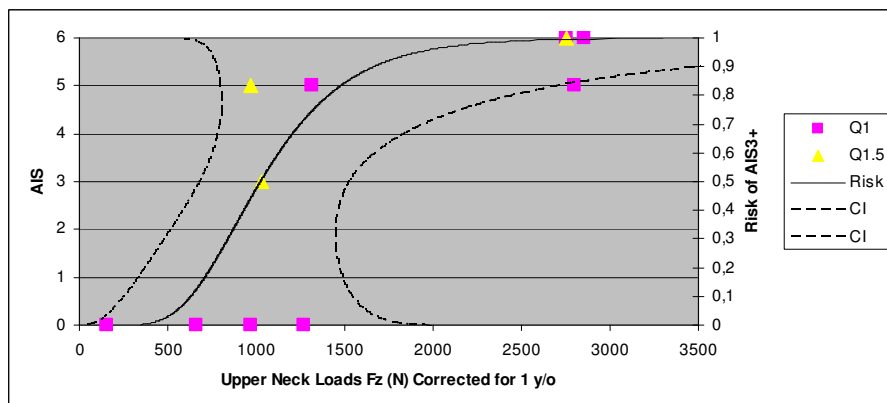
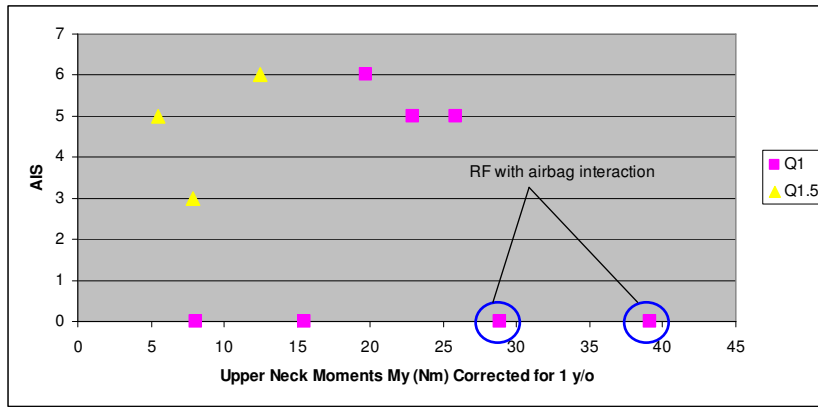
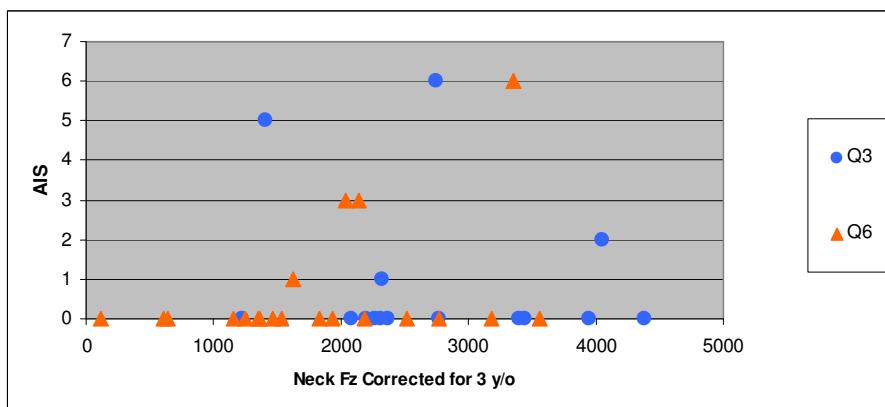


Figure 5-5: Neck AIS as a function of vertical upper neck loads (Fz) corrected for 1 year old



**Figure 5-6: Neck AIS as a function of Upper Neck bending moments (My) corrected for 1 year old**

For Q3 and Q6 dummies, only the cases without head impact were kept. Figure 5-7 shows the AIS as a function of the scaled Fz and Figure 5-8 the AIS as a function of the scaled My. None of the parameters allowed for the construction of a relevant injury risk curve. A combination of Fz and My was investigated, but did not lead to a more relevant parameter.



**Figure 5-7: Neck AIS as a function of Neck Fz corrected for 3 year old**

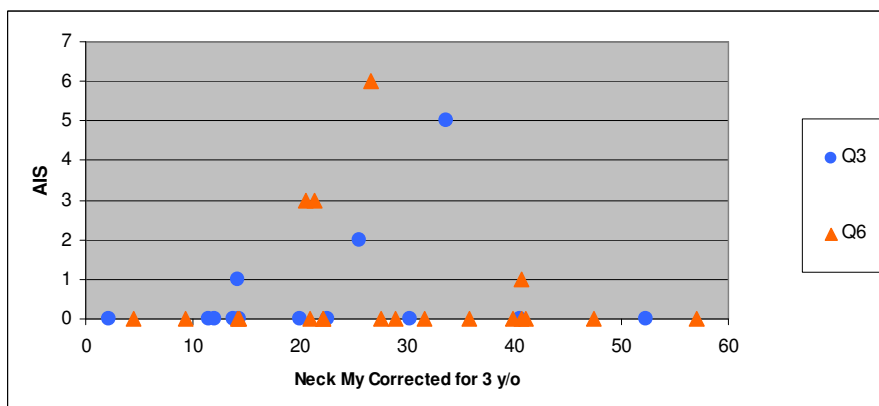


**Figure 5-8: Neck AIS as a function of Neck My corrected for 3 year old**

Chest AIS were plotted as a function of chest deflections (Figure 5-9) and accelerations (Figure 5-10) corrected for a 3 year old. Cases where the children were restrained by harnesses were separated from cases where the children were restrained by the 3-point belt, with or without boosters, because the response of the chest may differ with the two systems. It can be observed that neither the deflection nor the acceleration was

able to predict the risk of AIS3+ injury. The statistical regressions confirm this observation.

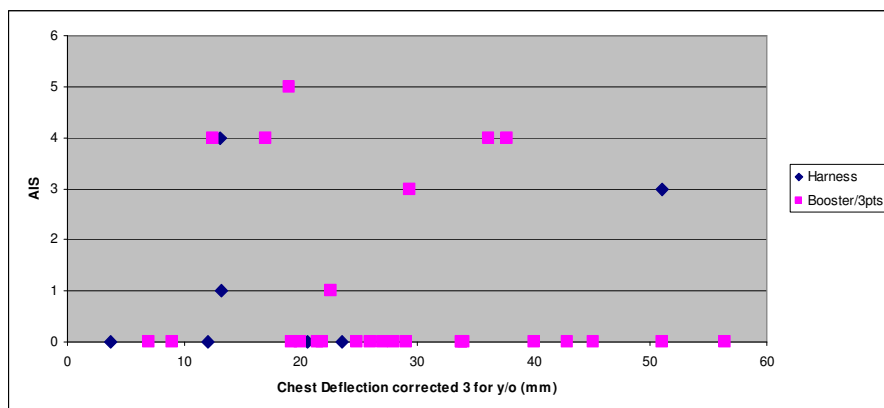


**Figure 5-9: Chest AIS as a function of chest deflection corrected for 3 year old**

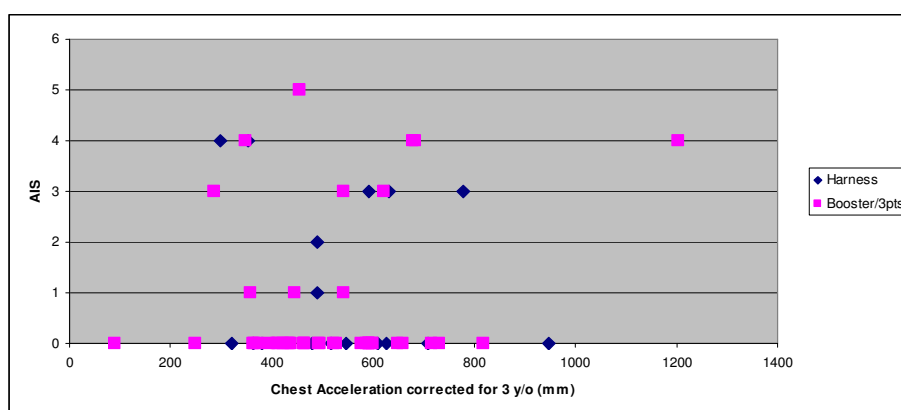
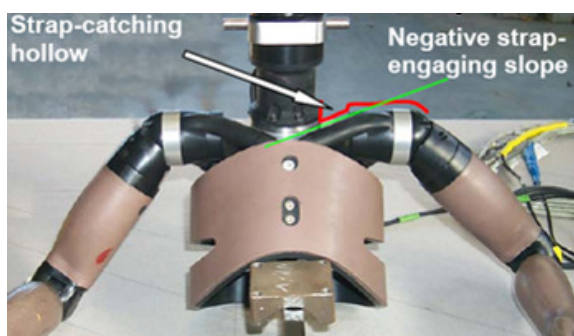
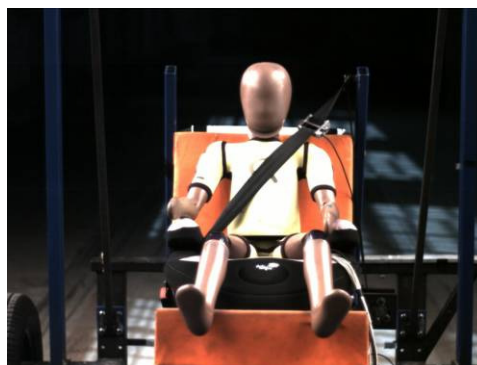


**Figure 5-10: Chest AIS as a function of chest acceleration corrected for 3 year old**

The basis for chest peak deflection and chest VC is the chest displacement measurement using a string potentiometer or an IR-TRACC. It is well known that the accuracy of chest deflection assessment is highly dependent on the positioning of the belt with respect to the location of the chest deflection sensor in Hybrid III adult dummies. In principle the same is true for Q-dummies. Following on that, chest deflection measurement seems to be meaningless for CRS with harness systems as none of the straps will directly interact with the sensor. Furthermore, the problems identified for adult dummies and belt use are more dominant for Q dummies as the shape of the shoulder and thorax leads the shoulder belt to slip away from the sternum, see Figure 5-11. In general this leads to an underestimation of the true deflection, which is likely linear, to the measured deflection. However, under specific circumstances which are not yet understood the belt does not move upwards. In addition, in a large number of cases the measured chest deflection was judged to be invalid. In most of the cases it was possible to prove incorrect use of the sensor (e.g., wrong installation direction, incorrect use of IR-TRACC etc.). If chest deflection load limits are to be applied, countermeasures against incorrect use of the sensors are necessary.



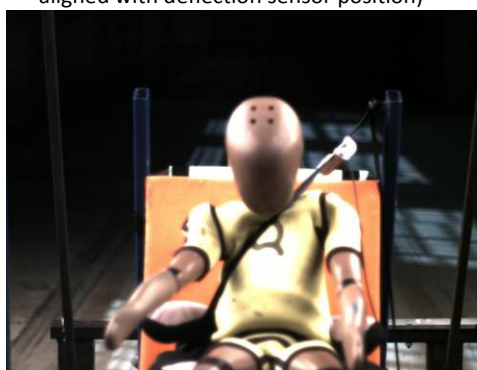
Negative slope towards neck in shoulder shape



Typical shoulder belt routing before impact (belt is aligned with deflection sensor position)



Thorax shape from lateral view, slope of the thorax facilitates in addition to the shoulder design upwards movement of the shoulder belt



Belt position observed in most of the cases after initial loading (belt moved upwards and is not aligned with deflection sensor)

**Figure 5-11: Problems with frontal impact chest deflection measurement in Q dummies**

The abdominal raw data (CFC60) obtained from the reconstructions are presented in Figure 5-12 and the data points scaled to a 3 year old are plotted in Figure 5-13 together with the injury risk curve. Several data points were found to be overly influential. However since no reason was found to remove them, they were kept in the analysis. However, harness-type CRS cases were removed from the sample. The relative sizes of the confidence interval at 5%, 25% and 50 % of risk were 99%, 60% and 51% respectively. Therefore, the error was considered as fair at 5%, 25% and 50% of risk. The values are summarised in Table 5-4.

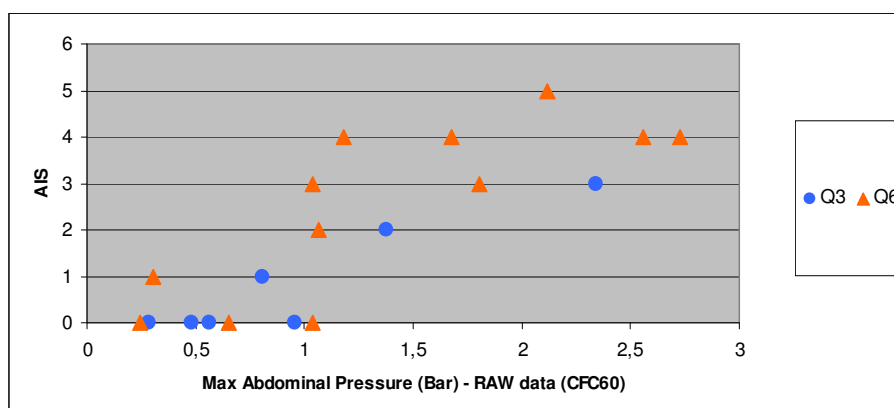


**Figure 5-12: Abdominal AIS as a function of abdominal pressure CFC60**

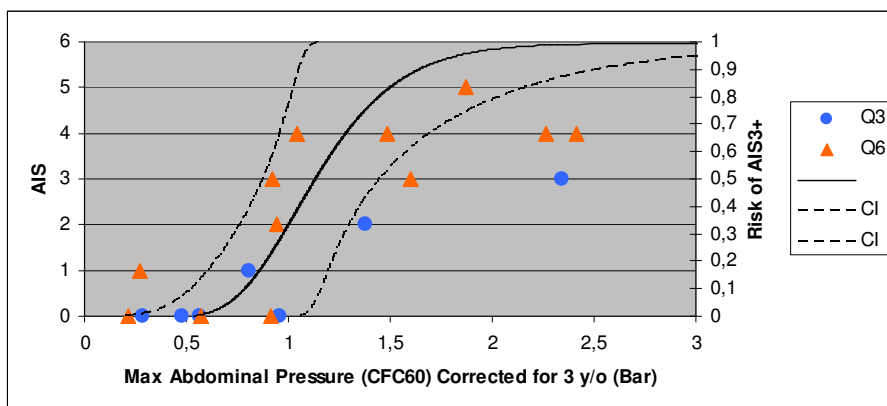


**Figure 5-13: Abdominal AIS as a function of abdominal pressure CFC60, corrected for 3 year old**

**Injury risk curves for lateral impact**

The head raw data obtained from the reconstructions are presented in Figure 5-14 as a function of head acceleration and the data points scaled to a 3 year old are plotted in Figure 5-15 together with the injury risk curve. Several data points were found to be overly influential. However since no reason was found to remove them, they were kept in the analysis. The relative sizes of the confidence interval at 5%, 25% and 50 % of risk were 298%, 123% and 64% respectively. Therefore the error was considered as unacceptable at 5%, while it was considered as marginal at 25% and fair at 50%. The values are summarised in Table 5-4. The same process was done with the HIC36ms and HIC15ms. The AIS values were not comparable since some data points were missing for the HIC. However, the sizes of the confidence intervals were higher, leading to unacceptable curves. It was then recommended to use the linear acceleration 3ms and not the HIC. Based on testing experience with the new GRSP IG CRS side impact test procedure GRSP concluded to concentrate on head  $a_{3ms}$  instead of HIC because the latter was shown to be less reproducible in this test procedure.

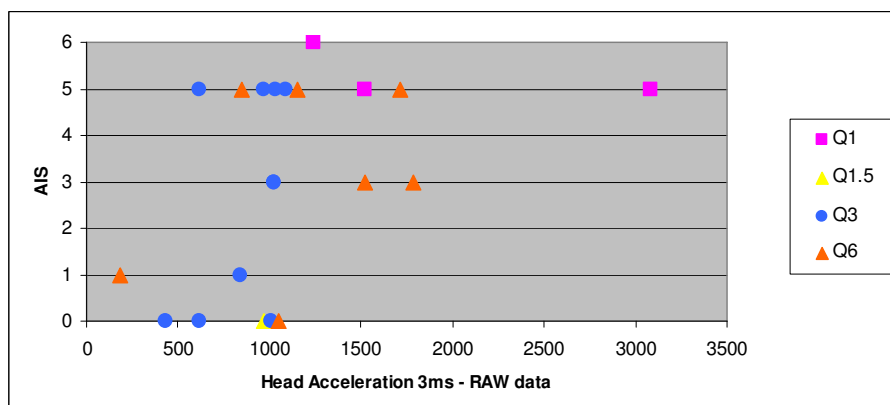


**Figure 5-14: Head AIS as a function of head linear acceleration 3ms for lateral reconstructions**



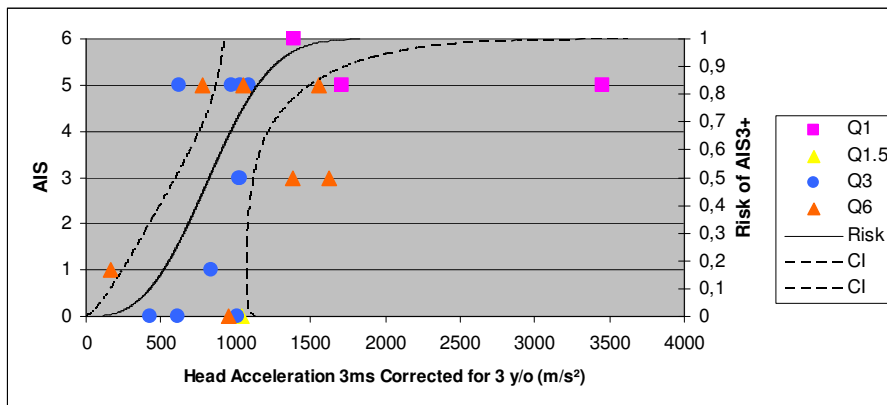


**Figure 5-15: Head injury risk curve as a function of head acceleration 3ms for 3 year old**

Chest AIS values were plotted as a function of chest accelerations corrected for a 3 year old (Figure 5-16). The number of reconstructed accident cases with severe chest injuries in side impact was too small to allow for the definition of thresholds.

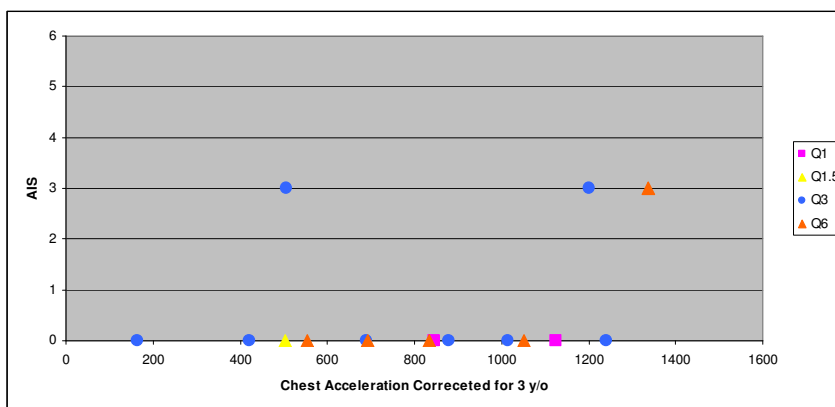


**Figure 5-16: Chest AIS as a function of chest acceleration corrected for 3 years old in side impact**

**Table 5-4: Summary of injury assessment values**

			5%	25%	50%
Frontal	Head Acc 3ms	Q3	402	827	1196
	Neck Fz	Q1		791	1022
	Abdominal Pressure	Q3	0.70	0.93	1.13
Lateral	Head Acc 3ms	Q3		604	821
good	fair	marginal	unacceptable		
0-50%	51-100%	101-150%	>151%		

**Proposed load limits**

Based on the injury risk curves and the data points for the neck presented above, the following load limits are proposed taking into account the 50% risk for an AIS 3+ injury.

**Table 5-5: Proposed load limits**

Body region	Head (frontal)	Head (lateral)	Neck	Chest	Abdomen
Reference dummy	Q3	Q3	Q1	Q3	Q3
Criterion	$a_{3ms}$ [m/s <sup>2</sup> ]	$a_{3ms}$ [m/s <sup>2</sup> ]	FZ [N]	no proposal	pressure [bar]
Proposed limit	1,000	835	1,200	no proposal	1.13

### 5.1.4 Discussion

First of all it is important to state that the injury risk curves shown above are based on comparing Q dummy readings with injury severity and are therefore only applicable to Q dummies. However, the advantage of this approach is that no scaling between human and dummy is necessary because the curves have been derived using the most appropriate tools available.

One important limitation of the study is the relative small number of cases to be analysed. In order to make up for the small number of cases results of different dummy sizes were scaled to one size, normally the Q3. The used scaling factors were the same that were used to develop the dummy therefore it is reasonable to apply the same assumptions for the development of injury risk functions. It is clear that scaling methods for children rely mainly on assumptions and cannot be accepted as completely validated. In order to address this limitation several approaches were used: for the neck, Q1 and Q1.5 were analysed separately from the other dummy sizes as scaling problems for neck forces were discussed before. In addition data points for different dummy sizes were plotted in different styles in order to allow visual checks of scaling validity and finally statistical analysis supported the indication mentioned above.

**Table 5-6: Comparison of load limits proposed by EEVC [8], GRSP IG CRS [9] and CASPER**

	Head $a_{3ms}$	HIC	Neck FZ	Neck MY	Chest $a_{3ms}$	Chest DS	Abdomen	Head lateral $a_{3ms}$
Reference Dummy	Q3	Q3	Q1	Q1	Q3	Q3	Q3	Q3
Unit	g	-	kN	Nm	g	mm	bar	g
UN R1XX	80	800	-	-	55	-	-	80
EEVC	75	780 - 1000	1.2	64	55	36	-	-
CASPER 20 % risk	75	Not recommended	1 (no injuries observed below)	No sufficient data	Generally not recommended but any limit for chest necessary	No sufficient data	0.88	55
CASPER 50% risk	120	Not recommended	1.3 (only children with AIS 3+ injuries above)	No sufficient data	Generally not recommended but any limit for chest necessary	No sufficient data	1.13	85

Table 5-6 shows a comparison between the load limits proposed by EEVC, used by the new regulation for the homologation of CRS and the CASPER results. The comparison shows that in general the EEVC proposals can be confirmed. However, within the EEVC data set for head risk curves the injury cases were mainly based on head contact cases and the risk curve was not valid for injury prediction without contact. With

the new data the situation changed as the injury cases were almost equally distributed amongst contact and non-contact cases. The neck load limits proposed by EEVC were based on scaling of adult data. With the CASPER data it is possible to confirm the scaled data at least for Q1 and Q1.5. For Q3 and Q6 it is recommended that limits be defined based on the state of the art of CRS performance in order not to allow worsening of the situation compared to today.

Chest measurement is an issue. Biomechanically, chest deflection is the criteria to be considered but the sensors and the dummy response do not provide results that can be used with confidence.

Except for the head in frontal impact conditions, the risk curves still suffer from a lack of data points. Therefore, further research is necessary to improve the confidence level. This is in particular true for lateral impact.

### 5.1.5 Conclusion

Based on accident reconstructions from CREST, CHILD and CASPER projects injury severity levels were paired with dummy reading results. Especially for the head in frontal impact conditions, a reliable number of data points is available to derive solid injury risk curves using the survival method. For the neck in frontal impact conditions, a trend for the Q1 and Q1.5 dummies can be observed derived from scaled adult data which seem to describe the injury risk quite well. For the chest neither resultant acceleration nor the chest deflection seem to be injury risk predictive; for the chest compression this is likely caused by belt interaction problems of the Q dummies for 3-point belts. The improved APTS abdominal sensor shows good prediction of injury risk although the number of cases is still low. For lateral impact only an injury risk curve for head  $a_{3ms}$  was derived. For the other body regions the number of cases with injuries is too low.

### 5.1.6 Acknowledgement

The authors want to acknowledge EC for funding the research works and CASPER partners for all efforts done to contribute to the construction of injury risk curves.

### 5.1.7 References

- [1] Palisson A, Cassan F, Trosseille X, Lesire P, Alonzo, F, Estimating Q3 dummy injury criteria for frontal impacts using the CHILD project results and scaling reference values, *Proceedings of the IRCOBI Conference*, Maastricht, pp. 263-276, 2007.
- [2] Mertz HJ, Prasad P, Improved neck injury risk curves for tension and extension moment measurements of crash dummies, *Proceeding of the 44<sup>th</sup> Stapp Car Crash Conference*, Atlanta, Georgia, 2000.
- [3] Petitjean A, Trosseille X, Statistical Simulations to Evaluate the Methods of the Construction of Injury Risk Curves, *Stapp Car Crash Journal 55*, pp 411-440, 2011.
- [4] Nusholtz G, Mosier R, Consistent threshold estimate for doubly censored biomechanical data, SAE1999-01-0714, 1999.
- [5] Johannsen H, Alonzo F, Goubel C, Schindler V, Abdominal injuries, injury criteria, injury severity levels and abdominal sensors for child dummies of the Q family, *Proceedings of IRCOBI Conference*, Prague, pp. 201-212, 2005.
- [6] Johannsen, H.; Alonzo, F.; Schindler, V.: "Abdominal sensors for child dummies of the Q family, injury criteria and injury risk curves, *Proceedings of the IRCOBI Conference*, Maastricht, pp. 389-392, 2007.

- [7] Newman JA, Shewchenkow N, Welbourne E, A proposed new biomechanical head injury assessment function - the maximum power index, Proceedings of the 44<sup>th</sup> Stapp Car Crash Conference, Atlanta, Georgia, 2000.
- [8] Wismans J, Waagmeester K, LeClaire M, Hynd D, de Jager K, Palisson A, van Ratingen M, Trosseille X, Q-dummies report – advanced child dummies and injury criteria for frontal impact, EEVC Document No. 514, 2008
- [9] GRSP, Draft new regulation on uniform provisions concerning the approval of enhanced child restraint systems used onboard of motor vehicles, ECE/TRANS/WP.29/GRSP/2011/21, 2011

## 5.1.8 Appendices

Table A1. Frontal head sample

Test Number	Dummy	Head AIS	Lin acc (m/s <sup>2</sup> )	HIC 36	head contact
CCN 1005 / 1	Q0	4	960.4	673	yes
CCN 1211 / 1	Q0	4	838.6	1149	airbag deployment
CCN 2012 / 1	Q0	4	1542.9	2540	yes
CCN 1185 / 1	Q1	4	1079.2	1215	yes
CCN 2014 / 2	Q1	5	1408.4	5103	yes
CCN 2015 / 1	Q1	5	1487.18	3128	no
CCN 2017 / 1	Q1	4	395.9	204	no
CCN 2053 / 1	Q1	0	568.8	339	soft impact with shield
CCN 2062 / 3	Q1	4	675.4	657	yes airbag deployment
CCN 2094 / 1	Q1	4	752.4	882	yes airbag deployment
CCN ITF-CRS Case E 2 / 1	Q1	2	2334.8	3391	no
CCT 0038 2 / 1	Q1	0	835.1	1254	no
CCT 0038 2 / 2	Q1	0	939.7	1197	no
CCN 2016 1 / 1	Q1.5	4	646	494	yes
CCT 0011 / 1	Q1.5	2	471.2	343	no
CCT 0068 / 1	Q1.5	0	1158.4	2087	no
CCN0352	Q3	4	808.56	985	no
CCN2059	Q3	2	1410.75	3024	yes
CCN 0002 / 2	Q3	1	588.6	456	chin-chest
CCN 0056 / 2	Q3	0	804.4	637	head-foot
CCN 0123 / 1	Q3	1	229.5	59	likely not, no video
CCN 0182 / 1	Q3	0	523.8	460	likely not, no video
CCN 0323 / 1	Q3	0	557.1	476	no
CCN 0329 / 1	Q3	0	594.5	560	chin-chest
CCN 1067 / 1	Q3	0	937.1		no
CCN 1082 / 1	Q3	0	524.9		chin-chest?
CCN 1119 / 1	Q3	0	1082.6	1522	no
CCN 1148 / 1	Q3	1	1186.6	3067	chin-chest
CCN 1199 / 1	Q3	0	840.6	821	no
CCN 1207-2 / 1	Q3	2	1094.4	2109	no
CCN 2001 / 1	Q3	2	933	1661	yes
CCN 2001 / 1	Q3	1	988.8	1670	no
CCN 2012 / 1	Q3	4	2116.6	7540	yes
CCN 2015 / 2	Q3	1	1142	1837	no
CCN 2016 1 / 1	Q3	0	340.2	167	likely
CCN 2058 / 1	Q3	5	949.8	1380	no
CCN ITF-CRS Case E / 1	Q3	3	804.4	1107	no
CCT 0022 / 3	Q3	1	1069.3	1693	yes
CCT 1029-sled / 2	Q3	0	890.9	1329	no
CCT 1081 / 3	Q3	0	669.9	719	no
CCN 0002 / 2	Q6	0	578.8	562	chin-chest
CCN2043	Q6	5	1410.75	4233	no
CCN 0089 / 1	Q6	2	321.4	83	likely not, no video
CCN 0225 / 1	Q6	0	1206.6	1028	chin-chest
CCN 0391 / 1	Q6	3	1061.1	2433	chin-chest
CCN 1043 / 1	Q6	1	985	1561	chin-chest?
CCN 1079 / 1	Q6	0	498.2	389	chin-chest
CCN 1104 / 1	Q6	0	1301.1	1755	chin-chest?
CCN 1104 / 1	Q6	0	986.7	1767	chin-chest?
CCN 1148 / 1	Q6	1	912	1924	chin-chest
CCN 1149 / 1	Q6	0	855.7	1306	no
CCN 1215 / 1	Q6	0	602.5	631	chin-chest
CCN 1229 / 1	Q6	0	959.8	2425	no
CCN 2003 / 1	Q6	4	1336.7	3604	no
CCN 2017 / 1	Q6	0	352.4	152	no
CCN 2023 / 1	Q6	5	1239.4	4278	no
CCN 2032 / 1	Q6	0	809.6	1124	no
CCN 2032 / 1	Q6	1	621.5	754	no
CCN 2061 / 1	Q6	0	673.5	1124	no
CCN 2062 / 3	Q6	0	76.5	5	no
CCN 2103 / 1	Q6	0	665	497	no
CCN ITF-CRS Case E / 1	Q6	2	588.6	785	no
CCT 0022 / 2	Q6	0	824	1129	no
CCT 0038 / 3	Q6	0	922.1	1280	no
CCT 0038 2 / 1	Q6	0	767.6	1167	no
CCT 0038 2 / 2	Q6	0	892.1	1413	no
CCT 0095 / 2	Q6	5	1156.6	2023	yes
CCT 0249 sled tests / 1	Q6	0	735.8	1034	no

Table A2. Frontal neck sample

Test Number	Dummy	Neck AIS	Upper Neck (loads) Z [N]	Upper Neck Moments Y [Nm]	head contact
CCN 1185 / 1	Q1	0	662,18	15,45	yes
CCT 0038 2 / 1	Q1	5	2800,855	25,85	no
CCN 2015 / 1	Q1	6	2855,56	19,67	likely not
CCN 2014 / 2	Q1	6	2756,27		yes
CCN 2017 / 1	Q1	0	1268,35	8,1	no
CCN 2062 / 3	Q1	0	151,21	39,14	airbag and RF
CCN 2094 / 1	Q1	0	970,4	28,9	airbag and RF
CCN 2053 / 1	Q1	5	1317,49	22,93	slight contact to shield
CCT 0068 / 1	Q1,5	6	3120,23	14,15	no
CCN 2016 / 1	Q1,5	3	1163,78	8,94	no
CCT 0011 / 1	Q1,5	5	1101,27	6,18	no
CCN 0123 / 1	Q3	0	1225	40,6	no
CCN 0182 / 1	Q3	0	2080	14,3	no
CCN 0329 / 1	Q3	0	2200	2,1	chin - chest
CCN 0002 / 2	Q3	0	2310	14,22	no
CCN 1067 / 1	Q3	1	2328	33,7	no
CCN 0323 / 1	Q3	5	1404	12	no
CCN 1102 / 1	Q3	0	2365	30,32	no
CCT 1081 / 3	Q3	0	2268	11,54	no
CCN 1119 / 1	Q3	0	3446	13,82	no
CCN 1148 / 1	Q3	0	4385,65	22,5	no
CCN 1199 / 1	Q3	0	2768,06	52,35	no
CCT 1029-sled / 2	Q3	0	3949,76	19,96	no
CCN 2001 / 1	Q3	0	3398,72	25,52	in rebound
CCN 0352 / 1	Q3	2	4046	61,2	no
CCN 2058 / 1	Q3	6	2742,87	21,4	no
CCN 0089 / 1	Q6	0	2059	33	no
CCN 0225 / 1	Q6	0	1827	6,7	chin - chest
CCN 0225 / 1	Q6	0	1680	70,71	chin - chest
CCN 0002 / 2	Q6	0	820	84,9	chin - chest
CCN 0391 / 1	Q6	0	4770,2	33,1	no
CCN 1043 / 1	Q6	0	3715,09	59,32	no
CCN 1079 / 1	Q6	0	1553	53,37	no
CCN 1104 / 1	Q6	0	2930	41,05	no
CCN 1104 / 1	Q6	0	4262	31,71	no
CCN 1229 / 1	Q6	0	3373,67	30,67	no
CCT 0038 2 / 1	Q6	3	2725,84	43	no
CCT 0038 2 / 2	Q6	3	2875,87	13,95	no
CCN 2061 / 1	Q6	0	1968,78	47,02	no
CCN 2062 / 3	Q6	0	154	60,63	no
CCN 2029 / 1	Q6	0	2596,24	31,22	no
CCN 2103 / 1	Q6	1	2181,73	60,63	no
CCN 2017 / 1	Q6	0	853,82	39,72	no
CCN 2032 / 1	Q6	0	2453,83	21,1	no
CCN 2043 / 1	Q6	6	4502		no
CCN 2032 / 1	Q6	0	1817,37		no

Table A3. Frontal chest sample

Test Number	Dummy	Chest AIS	Lin. acc. [m/s <sup>2</sup> ]	Chest deflection front [mm]	CRS
CCN 1185 / 1	Q1	0	389.2		4 5-point harness
CCN 2017 / 1	Q1	4	361.8		14 5-point harness
CCT 0038 2 / 1	Q1	0	723.5		4-point harness
CCT 0038 2 / 2	Q1	0	639.1		4-point harness
CCN 2016 1 / 1	Q1,5	4	331.1		5-point harness
CCT 0011 / 1	Q1,5	1	540.7		14 5-point harness
CCT 0068 / 1	Q1,5	0	572		25 4-point harness
CCN 0002 / 2	Q3	0	480.7		4-point harness
CCN 0056 / 2	Q3	0	598.4		backless booster
CCN 0123 / 1	Q3	0	436.7		7 backless booster
CCN 0182 / 1	Q3	0	373.3		highback booster
CCN 0323 / 1	Q3	0	462.8		20 backless booster
CCN 0329 / 1	Q3	0	319.8		20,55 4-point harness
CCN 1067 / 1	Q3	0	422.8		26 backless booster
CCN 1082 / 1	Q3	0	465.9		34 highback booster
CCN 1102 / 1	Q3	0	494		51 backless booster
CCN 1119 / 1	Q3	3	592.9		51 4-point harness
CCN 1148 / 1	Q3	0	717.3		40 highback booster
CCN 1199 / 1	Q3	0	546.6		5-point harness
CCN 2001 / 1	Q3	2	490.1		5-point harness, harness below arms
CCN 2001 / 1	Q3	0	591		27 highback booster
CCN 2012 / 1	Q3	0	948.4		5-point harness, harness below arms
CCN 2015 / 1	Q3	0	609.31		12 5-point harness
CCN 2016 1 / 1	Q3	4	349.1		17 backless booster
CCN 2058 / 1	Q3	3	631.2		5-point harness
CCN ITF-CRS Case E / 1	Q3	0	412		highback booster
CCN0352	Q3	0	731		28 highback booster
CCN2059	Q3	3	778.83		5-point harness
CCT 1029-sled / 2	Q3	0	658.5		29 highback booster
CCT 1081 / 3	Q3	5	454.1		19 backless booster
CCN 0002 / 2	Q6	0	559.2		adult three-point
CCN 0225 / 1	Q6	0	414		5-point harness
CCN 0225 / 1	Q6	1	505.7		backless booster
CCN 0391 / 1	Q6	3	707		adult three-point
CCN 1006 / 1	Q6	0	674.2		30 highback booster
CCN 1043 / 1	Q6	0	599.2		19,37 adult three-point
CCN 1079 / 1	Q6	3	324.3		backless booster
CCN 1104 / 1	Q6	0	495.2		30 backless booster
CCN 1104 / 1	Q6	0	465.8		50 backless booster
CCN 1148 / 1	Q6	0	102		22 adult three-point
CCN 1149 / 1	Q6	0	593.8		19 backless booster
CCN 1171 / 1	Q6	3	617.2		26 pillow
CCN 1215 / 1	Q6	0	417.2		highback booster
CCN 1229 / 1	Q6	0	674.3		8 backless booster
CCN 2003 / 1	Q6	4	771.4		32 backless booster
CCN 2017 / 1	Q6	0	283.9		17 backless booster
CCN 2023 / 1	Q6	4	1368.6		33 highback booster
CCN 2029 / 1	Q6	0	738.8		38 adult three-point
CCN 2032 / 1	Q6	0	528.9		40 backless booster
CCN 2061 / 1	Q6	0	491.5		highback booster
CCN 2103 / 1	Q6	1	408.3		20 backless booster
CCN ITF-CRS Case E / 1	Q6	0	451.3		backless booster
CCN2043	Q6	4	778.83		11 highback booster
CCT 0022 / 2	Q6	1	618		adult three-point
CCT 0038 / 3	Q6	0	932		backless booster
CCT 0038 2 / 1	Q6	0	667.2		backless booster
CCT 0038 2 / 2	Q6	0	682.6		backless booster
CCT 0095 / 2	Q6	0	413		backless booster
CCT 0249 sled tests / 1	Q6	0	657.3		highback booster

Table A4. Frontal abdomen sample

Test number	Dummy	Abdomen MAIS	Max Pressure (CFC60)	CRS	Misuse
CCN_0352 / 1	Q3	2	1.38	highback booster	no but shoulder belt guide released during crash
CCN_0323 / 1	Q3	0	0.96	backless booster	shoulder belt under arm
CCN_1102 / 1	Q3	0	0.29	backless booster	no
CCN_1148 / 1	Q3	1	0.81	highback booster	no
CCN_1082 / 1	Q3	3	2.34	highback booster	shoulder belt under arm
CCN_1067 / 1	Q3	0	0.56	backless booster	no
CCN_1207 / 2	Q3	0	0.48	backless booster	no
CCN_0391 / 1	Q6	4	1.68	adult belt only	no CRS
CCN_1171 / 1	Q6	3	1.8	pillow	not a CRS
CCN_1043 / 1	Q6	0	1.04	adult belt only	no CRS
CCN_1149 / 1	Q6	1	0.31	backless booster	no
CCN_1215 / 1	Q6	2	1.07	highback booster	no
CCN_1148 / 1	Q6	0	0.65	adult belt only	no CRS
CCN_2041 / 1	Q6	4	2.56	highback booster	no
CCN_2003 / 1	Q6	4	1.18	backless booster	no
CCN_2017 / 1	Q6	0	0.24	backless booster	no
CCN_2043 / 1	Q6	5	2.12	highback booster	no
CCN_2032 / 1	Q6	3	1.04	adult belt only	no CRS
CCN_2032 / 1	Q6	4	2.73	backless booster	shoulder belt under arm

Table A4. Lateral head sample

Test Number	Dummy	Head AIS	Lin. acc. [m/s <sup>2</sup> ]	HIC36	HIC15
CCN_0405 / 1	Q1	5	3080,3	9977	9977
CCN_1048 / 1	Q1	5	1525,5	2065	2065
CCN_1255 / 1	Q1	6	1241,6	9211	3886
CCN_2051 / 2	Q1.5	0	967,3	613	613
CCN_0165 / 1	Q3	0	615,3	37	20
CCN_0196 / 1	Q3	5	1090,9	2300	
CCN_0235 / 1	Q3	0	431,6		
CCN_0255 / 1	Q3	5	620,1	530	388
CCN_1033 / 1	Q3	5	1036,3	826	818
CCN_1037 / 1	Q3	5	972,8	573	541
CCN_1236 / 1	Q3	3	1021,4	669	669
CCN_2006 / 1	Q3	3	1027,2	1011	1011
CCN_2030 / 1	Q3	1	839	385	385
CCN_2095 / 1	Q3	0	1008,8	1351	1316
CCN_0165 / 1	Q6	1	185,2	318	318
CCN_0166 / 1	Q6	3	1785,4	2710	2705
CCN_0168 / 1	Q6	3	1520,5	2044	2043
CCN_0263 / 1	Q6	5	1151,7	1415	1413
CCN_2052 / 1	Q6	5	850,8	1646	921
CCN_2095 / 1	Q6	5	1710,4	18480	18480
CCN_2095 / 1	Q6	0	1046,2	1048	1048

## 5.2 Development of injury risk curves for the Q10 dummy

### 5.2.1 Introduction

The concept of the EPOCh project is to drive the improvement of safety for older children travelling in vehicles. To enable this, the EPOCh project has produced a 10.5 year old dummy, the Q10.

It is necessary to specify injury risk functions and accepted thresholds or criteria for use with this new dummy, which are appropriate to this age and size of occupant. With adult humans the conventional approach taken to derive injury risk functions has been to conduct representative tests around the injury threshold with Post-Mortem Human Subjects (PMHSs). These tests are then repeated with the dummy and the relevant dummy output compared against the observed risk of injury for the PMHS. By following this process, dummy-specific injury risk functions are defined directly relating a dummy measurement with the risk of injury for a human.

Unlike the adult situation, there is very little biomechanical data from which specific injury risk functions for children can be derived. As alternatives, two approaches have been used recently (Wismans *et al.*, 2008):

- Perform accident reconstructions using the child dummy under development;
- Scale adult injury risk functions and/or criteria to be relevant to the child size (dummy) being investigated.

According to the first of these approaches, The European Enhanced Vehicle-safety Committee (EEVC) Working Groups 12 and 18 used the accident reconstruction data developed within the European Commission (EC) CREST and CHILD projects to help develop risk functions for the Q3 dummy (Wismans *et al.*, 2008).

The CREST (1996-2000) and CHILD (2002-2006) projects included a program of 98 real world accident reconstructions using P- and Q-dummies. Wismans *et al.* used information from these tests to propose injury risk functions for the Q-dummies available at that time. For that purpose, the injuries observed in the real world accidents were paired with Q-dummy measurements from around 70 validated reconstruction tests. As the reconstructions were performed with dummies from 0 to 6 years old, all data were scaled to the Q3 dummy size/age in order to normalise the data for a single age whilst maintaining the size of the dataset to be analysed. Risk curves for injuries with an Abbreviated Injury Scale score of at least 3 ( $AIS \geq 3$ ) for the Q3 were then developed using both the Certainty Method and Logistic Regression. Resulting injury risk curves were drawn for the head, the neck and the thorax.

Accident reconstructions with the newly developed Q10 were beyond the scope of the EPOCH project. As an alternative, the investigation reported here (comprising Task 1.3 of the EPOCH project) has taken the second approach and scaled adult injury risk functions in an attempt to make them relevant for the older child dummy. Consideration has also been given to scaling up the risk functions developed for the Q3 by EEVC WGs 12 and 18.

An earlier report on the scaling approach has been published within the EPOCH Project (Carroll and Pitcher, 2009), available on the EPOCH website, and contains more detailed information on the background, supporting information and discussions than can be reported within the constraints of this paper.

### 5.2.2 Scaling approach

Previously, many authors have published techniques for scaling biomechanical measurements to different sizes of subject. While the general principle behind the scaling remains consistent, each of the publications seems to adopt different specific detail. For instance, slight differences in the formulae used by each author can be observed alongside differences in the material properties considered to be the most



appropriate. Also different authors may be considering slightly different injury priorities, when developing their scaling strategy.

The equations used in the following precedents were considered and compared throughout this work:

- van Ratingen *et al.* (1997) in the development of biofidelity requirements for the Q3 dummy;
- NHTSA (1996) in the development of injury assessment values for child dummies;
- Irwin and Mertz (1997) in their biomechanical basis for the CRABI and Hybrid III child dummy families;
- Mertz *et al.* (2003) in the development of injury assessment reference values for frontal and side impacts;

These approaches include both behaviour scaling and injury risk scaling. In general, the behaviour scaling factors include stiffness (Young's modulus) and characteristic length scaling factors, whereas the injury risk scaling factors include maximum failure stress or strain and length scaling factors. For some criteria the Young's modulus factor also contributes to the injury risk scaling factor. As such one could consider that the behaviour scaling approaches could be equated to an injury risk scaling approach which includes stiffness scaling but where the failure stress factor was set to one.

In the following sections of the paper all of the available scaling methods have been reviewed for each body region and dummy measurement, regardless of their original application. The review considered whether there are any new material property data available to aid the scaling process and if the output is reasonable for injury risk scaling.

### 5.2.3 Head acceleration

The scaling ratio used for head acceleration differs between that published by van Ratingen *et al.* (1997) that used by Irwin and Mertz (1997) and the EEVC WG12 and 18 (Wismans *et al.*, 2008). van Ratingen *et al.* assumed that the head impact test condition could be represented as a single spring-mass system, whereas the EEVC equated the force applied to the head in terms of Newton's second law ( $F=ma$ ) and the failure stress ( $F=\sigma S$ , where  $\sigma$  is the failure stress and  $S$  is the cross-sectional area). Both of these approaches seem reasonable in principle; noting that one would need to consider the failure stress behaviour under dynamic conditions, rather than quasi-static, to match with the motion implied by the head acceleration. However, the approaches will give different scaling values.

van Ratingen <i>et al.</i>	Irwin and Mertz	EEVC WG12&18
$R_a = \frac{a}{A} = \left( \frac{R_K}{R_M} \right)^{\frac{1}{2}}$	$R_a = \frac{\lambda_E}{\lambda_x}$	$R_a = \frac{\lambda_{\sigma t}}{\lambda_x}$
Where $R_a$ is the scaling ratio for the head acceleration; $R_K$ is the ratio of head linear stiffness; and $R_M$ is the ratio of head mass.	Where $\lambda_E$ is the ratio of the elastic moduli of bone; and $\lambda_x$ is the ratio of head length.	Where $\lambda_{\sigma t}$ is the ratio of calcaneal tendon failure stress; and $\lambda_x$ is the ratio of head length.

Also, there is the issue as to from where the head compression stiffness data will come. Irwin and Mertz (1997) and van Ratingen *et al.* (1997) used cranial bone

bending stiffness data. However, Irwin and Mertz demonstrated that head stiffness was dominated by the bulk modulus of the brain. This agrees with the finding from the modelling work conducted by Coats *et al.* (2007), which identified that the compressibility of the brain significantly affected bulk modulus and varied the principal stress in the skull. Ideally, the ratio of head compression stiffness would, therefore, reflect the bulk modulus of the brain. The bulk modulus for adult brain tissue has been reported in the literature; however, an appropriate value for children has not been determined empirically, as far as could be determined at the time of this study. In the absence of a bulk modulus scaling ratio, Mertz *et al.* (2003) and the EEVC (Wismans *et al.*, 2008) both used calcaneal tendon failure stress as a proxy for the brain failure property. The appropriateness of using either the elastic modulus of cranial bone or tendon failure stress is not clear and alternatives were sought from the literature.

Post-mortem human paediatric specimens were used by Prange *et al.* (2004) to determine the static and dynamic properties of the whole infant head. The biomechanical tests were conducted using three unembalmed fresh-frozen human infant specimens of ages one, three, and eleven days after birth. By comparing the stiffness value of the new-born child with the adult stiffness reported by Hodgson *et al.* (1967) a new stiffness ratio was obtained. Using this new stiffness ratio in the van Ratingen *et al.* head acceleration scaling formula, a good agreement was obtained between scaled down adult head accelerations and the new-born drop test data.

To determine the head stiffness for a 10.5 year-old, it was necessary to interpolate between the adult and new-born. The curve applied for this interpolation was that used with bone elastic bending modulus (Mertz, 2001).

The head anthropometry measurements related to the heads of children, six years old and Q10 age (10.5 year-old), and adults are shown in Table 5-7. These values have been taken from the EPOCH Task 1.2, Deliverable 1.2 (Waagmeester *et al.*, 2009) and are based on measurements in the CANDAT anthropometry database.

**Table 5-7: Geometric (anthropometric) measurements relating to the head**

Measurement	6 year old	Q10 (10.5 year old)	Adult
Head mass (kg)	3.38	3.59	4.55
Head length (mm)	183.0	187.4	195.6
Head width (mm)	138.0	143.9	155.0
Head depth (mm)	189.0	202.2	221.0

As implied above, the head stiffness and anthropometry information was used in the van Ratingen *et al.* calculation for the head risk curve factor. This calculation using interpolated stiffness from an adult and newborn (Prange *et al.*, 2004), produced a scaling ratio that was very close to 1 (0.991 for the Q10). Even with the EEVC approach the ratio was 0.913.

The implication of this is that the tolerance of the older child's head is very close to that for the adult. Based on this information, the adult head injury risk function could be used without incurring a significant error. The probability of skull fracture for an adult, based on average acceleration, drawn using survival analysis and a log-logistic distribution assumption, is shown in Figure 5-17. The data supporting this function are those as used by Prasad and Mertz (1985), in the development of the HIC. The scaled Q10 risk curve estimate based on the EEVC scaling is also shown in this figure.

It should be noted that this is not the same function as was proposed by Prasad and Mertz. Therefore, adopting this injury risk function (as shown in Figure 5-17) would be a deviation from what has been adopted for use with other dummies. Despite the statistical validity of this function, for consistency with previous dummy limits it would be more appropriate to adopt the existing adult head acceleration limit(s).

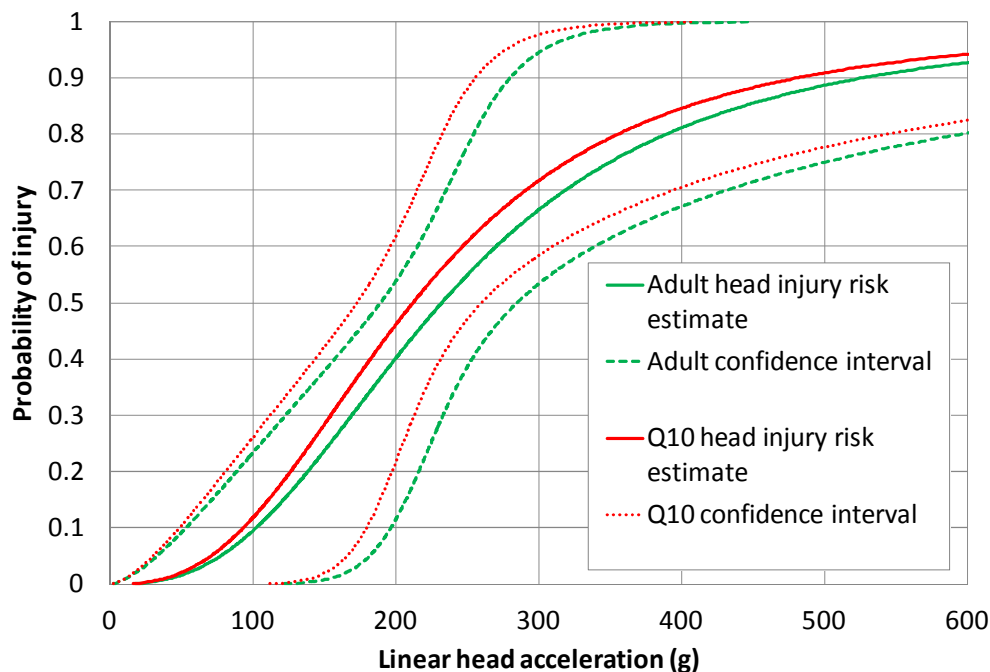


**Figure 5-17: Head injury risk curve for an adult and the Q10 (scaled using the EEVC formula) based on peak acceleration**

This first method used to calculate head injury thresholds for the Q10 scaled down the peak acceleration injury risk from adult data. For comparison, an alternative method was used, which involved scaling up from the 3 year old (Q3) 3 ms head acceleration threshold values reported by the EEVC (Wismans *et al.*, 2008). The van Ratingen scaling method using the stiffness values from Prange *et al.* (2004) and Hodgson *et al.* (1967) (interpolated with a curve of the shape reported by Mertz *et al.* {2001}) was used again to calculate the head acceleration ratio for the Q3 to Q10 (Table 5-8). These ratios were then used to scale the EEVC 3 year old head injury thresholds to obtain values for the Q10.

**Table 5-8: Q10 head data**

	3 year old	Q10
Stiffness (N.mm <sup>-1</sup> )	516	1332
Head Mass (kg)	2.84	3.59
Head length (mm)	177	187
Ratio	1	1.43 (van Ratingen scaling) 1.71 (EEVC scaling)

The resulting head injury (AIS 3+) values from scaling up the EEVC Q3 thresholds are not directly comparable with the values derived from scaling down the adult peak head acceleration injury risk curve. The adult head injury risk is for an unspecified severity of injury and relates to the peak acceleration value rather than the value exceeded for 3 ms. The EEVC 20 percent risk of AIS 3+ head injury coincides with a 116 g, 3 ms

exceedence; whereas the adult risk curve suggests a peak value of 138 g for a 20 percent risk of head injury.

The 3 ms head acceleration values scaled up from the three year old (as shown in Table 5-9) could be compared with the adult value of 80 g, used in Regulation (R94). However, the risk of injury associated with the adult 80 g limit is not known.

**Table 5-9: Head injury data scaled from 3 year old, 3 ms exceedence values**

	3 year old	Q10 (van Ratingen scaling)	Q10 (EEVC scaling)
20% Head Injury Risk (g)	81	116	138
50% Head Injury Risk (g)	99	141	169

It is known from sled tests with the Q10, carried out within the EPOCH Project (Task 3.2), that modern booster seats and cushions should be able to limit the measured 3 ms exceedence to within 80 g, under UN Regulation 44 conditions. As 80 g would be a more conservative criterion than suggested from the scaling work, it is recommended that this is taken forward for use with the Q10. This would promote consistency between the older child and adult criteria.

#### 5.2.4 Head excursion

Within the Q10 testing evaluation reported by EPOCH Task 3.2 head excursion limits were proposed (Table 5-10). The proposal was based on back-to-back testing of CRS with the P10 and Q10; changing the limits to achieve an equivalent assessment with the Q dummy, compared to that of the P. The limits used currently in UN Regulation 44 with the P10 were adjusted by a factor accounting for the difference in mean excursion between P10 and Q10 dummies. The calculated head horizontal excursion limit for the Q10 is shorter than the current Regulation 44 limit for the P10, whereas the vertical limit is larger than the current limit. These changes reflect the differences in dummy kinematics observed with the two dummies.

While these excursion limits are not linked directly with any particular risk of injury, they are an obvious way to manage the likelihood of a head contact through CRS design. It seems sensible to keep such a limit for use with the new Q10 dummy in order to at least maintain the status-quo relating to product performance.

**Table 5-10: Head excursion limits proposed for use with the Q10 for equivalence with P10 limits in the current Regulation 44**

Criterion	Q10 limits
Head horizontal excursion (mm)	465 mm
Head vertical excursion (mm)	885 mm

#### 5.2.5 Neck

As noted earlier, the scaling formulae used by van Ratingen *et al.* (1997), Irwin and Mertz (1997), Mertz *et al.* (2003), and the EEVC WGs 12 and 18 (Wismans *et al.*, 2008) are being considered as previous examples of scaling relationships within this report. The formulae published by these authors with regard to neck loading measurements are shown below.

For the neck, the authors of previous scaling studies agree on the terms to be used in the formulae for neck tension and bending. The tensile strength of the neck is governed by a ratio of soft tissue tensile strength (e.g. tendon failure strength) and the ratio of

cross-sectional area. For the bending moment, an additional term is added to reflect the ratio of the moment arms.

The neck anthropometry measurements related to the necks of six year old children, Q10 and adults are shown in Table 5-11. As with the head anthropometry, these values have been taken from the EPOCH Deliverable 1.2 (Waagmeester *et al.*, 2009). The data for the child sizes are taken from the CANDAT anthropometry study (for the six and ten year olds). The adult measurements are taken from the Hybrid III 50<sup>th</sup> percentile adult dummy.

van Ratingen <i>et al.</i>	Irwin and Mertz	EEVC WG12&18
<p><math>R_T</math> is the scale factor for bending moment about the x- or y-axis.</p> $R_T = \frac{t_x}{T_x} = R_E \lambda_x \lambda_y^2$ $R_T = \frac{t_y}{T_y} = R_E \lambda_y \lambda_x^2$ <p>Where <math>t_x</math> and <math>T_x</math>, or <math>t_y</math> and <math>T_y</math> are the resistive moment to neck bending for the adult (upper case) or child (lower case) about the x- or y-axis;  <math>R_E</math> is the scaling factor for the elastic modulus;  <math>\lambda_x</math> or <math>\lambda_y</math> are the length scale factors in the x- or y- axis.</p>	<p><math>R_M</math> is the ratio of neck bending moments.</p> $R_M = \lambda_x^3$ <p>Where <math>\lambda_x</math> is the scale factor of the necks.</p> <p>Mertz <i>et al.</i></p> $\lambda_F = \lambda_\sigma \lambda_C^2$ <p>Where <math>\lambda_F</math> is the ratio of neck force, either compression or shear;  <math>\lambda_\sigma</math> is the ratio of calcaneal tendon failure stress; and  <math>\lambda_C</math> is the ratio of neck circumferences.</p>	<p>EEVC WG12&amp;18</p> $\lambda_F = \lambda_{\sigma t} \lambda_x \lambda_y$ $\lambda_M = \lambda_{\sigma t} \lambda_x^2 \lambda_y$ <p>Where <math>\lambda_M</math> is the ratio of peak neck flexion moment;  <math>\lambda_{\sigma t}</math> is the ratio of calcaneal tendon failure stress; and  <math>\lambda_x</math> or <math>\lambda_y</math> are the length scale factors in the x- or y- axis.</p>

**Table 5-11: Geometric (anthropometric) measurements relating to the neck**

Measurement	6 year old	Q10	Adult
Neck circumference (mm)	260.0	288.4	383.0
Neck length (mm)	95.0	110.0	142.0
Neck width (mm)	78.0	85.6	118.0
Neck depth (mm)	75.0	81.0	84.8

The work of Ouyang *et al.* (2005) provides an important source of information concerning the scaling of cervical spine tolerance to tensile loading. This ought to be incorporated in the tensile force criterion, and is used in the following analyses of scaling techniques. However, the limited dataset of Ouyang *et al.* did not have the statistical power to derive tensile stiffness changes with age (only failure force). Therefore, other sources of cervical spine stiffness ought to be used in setting biofidelity response requirements. For compressive properties, the stiffness data of Nuckley and Ching (2006) could be incorporated.

The different approaches for calculating neck injury thresholds were evaluated. The Irwin and Mertz (1997) formula uses the ratio of neck circumference to calculate the neck force scaling ratio. The bending moment scaling ratio is calculated using the cross-sectional area of the neck and the neck depth perpendicular to the axis about which the bending is defined. The EEVC WGs 12 & 18 refined the Irwin and Mertz method to include the calcaneal tendon failure strength in both the force and moment scaling calculations (Wismans *et al.*, 2008).

For comparative purposes, the equations for the force and moment modulus were also calculated using the stiffness data reported by Nuckley and Ching (2006) derived directly from experimental testing. Table 5-12 shows a comparison of the equation results. The formulae used to derive the scaling factors are shown in each case. The values used to derive the geometrical scaling ratios are taken from Table 5-11. For the Nuckley and Ching equation it should be noted that the equation only provides the stiffness value for a particular age. The scaling factor will be that result divided by the stiffness value for the age from which the response is being scaled. In preparing these values, an adult age of 25 has been used.

**Table 5-12: Neck force and moment scaling factors (or ratios)**

Method	Formula	Q10 factor
Force		
Mertz <i>et al.</i>	$\lambda_F = \lambda_\sigma \lambda_C^2$	0.556
WG 12 & 18	$\lambda_F = \lambda_{\sigma t} \lambda_x \lambda_y$	0.679
Nuckley and Ching	$-0.0032 (Age)^2 + 0.304 Age + 3.452$	0.695
Ouyang <i>et al.</i>	Failure = 372.7 ln (Age+1) + 72.9	0.763
Moment		
Irwin & Mertz	$R_M = \lambda_y \lambda_x^2$	0.662
WG 12 & 18	$\lambda_M = \lambda_{\sigma t} \lambda_x^2 \lambda_y$	0.649
Nuckley and Ching	$-0.010 (Age)^2 - 0.599 Age - 2.702$	0.422

These calculated ratios were then used to scale the EEVC adult injury limits for neck tension and shearing force and extension and flexion moment. The calculated values are shown in Table 5-13.

**Table 5-13: Neck injury values**

Method	Q10	Adult
Tension (N)		
Mertz <i>et al.</i>	1834	3300
WG 12 & 18	2241	3300
Nuckley and Ching	2294	3300
Ouyang	2521	3300
Shear (N)		
Mertz <i>et al.</i>	1723	3100
WG 12 & 18	2105	3100
Nuckley and Ching	2155	3100
Extension (Nm)		
Irwin & Mertz	38	57
WG 12 & 18	37	57
Nuckley and Ching	24	57
Flexion (Nm)		
Irwin & Mertz	126	190
WG 12 & 18	123	190
Nuckley and Ching	80	190

The injury thresholds calculated for the Q10 have been scaled down from adult data. To validate this approach an alternative method was used, involving scaling up from the 3 year old. The EEVC WG 12 & 18 method was used to calculate the ratio of the Q10 to the 3 year old (Table 5-14). These ratios were then used to scale the EEVC (Wismans *et al.*, 2008) accident reconstruction 3 year old injury thresholds data, to calculate neck injury values for the Q10 (Table 5-15).

**Table 5-14: Q10 data**

	3 year old	Q10
$\lambda_x$	67.7	81.0
$\lambda_y$	72.6	85.6
$\lambda_{\sigma t}$	0.83	0.98
$\lambda_F$	1	1.67
$\lambda_M$	1	1.99

**Table 5-15: Neck injury data scaled from 3 year old**

Risk percentage and neck load parameter	3 year old	Q10
20% Neck Tension Force (N)	1555	2590
50% Neck Tension Force (N)	1705	2840
20% Neck Flexion Moment (Nm)	79	157
50% Neck Flexion Moment (Nm)	96	191

Comparing the values between Table 5-13 and Table 5-15 indicates that the 20 percent risk of injury values scaled up from the three year old are greater than the values scaled down from the adult, using any method. The level of injury risk associated with the adult threshold values are between 3 and 5 percent or correspond to IARVs (Injury Assessment Reference Values). Therefore it was to be expected that the scaled up values are greater.

In the EPOCH Task 3.2 tests with the Q10 the results for the upper neck force on the Q10 ranged between 2,055 and 2,932 N for the booster cushions, where all but one booster seat produced a larger result up to 4,239 N. These results suggest that the neck force thresholds derived above are not feasible for modern CRS to meet under Regulation 44 test conditions.

The Regulation 44 test conditions are intended to represent the typical severity for frontal impact accidents, in cars from the 1970s. Therefore if scaled injury threshold values are being exceeded regularly in this test, one might expect to see neck injuries (relating to a tension mechanism) in the child accident data. However, the neck has not been identified as a frequently injured body region for older children when restrained (Visvikis *et al.*, 2009).

On the basis that the accident data would not support the need for a substantial improvement in tensile loading to the neck, a pragmatic threshold could be chosen to prevent any future degradation of safety in this area. The adult neck tension threshold is 3,300 N. Adopting this limit would lead to a failure for three of the five booster seats tested for EPOCH Task 3.2. As such a stringent threshold is not desired it is recommended that further testing should be carried out before defining the exact neck tension limit.

Accompanying any tensile value, a neck extension limit of 37 Nm and a flexion limit of about 125 Nm seem feasible and can be supported by the scaling approach.

### 5.2.6 Thorax

The scaling relationships used before, for the thoracic body region, specifically chest deflection, are reproduced below.

Further scaling formulae have been reported for impactor type testing of the shoulder, thorax, abdomen, and pelvis. Based on the expected use of the older child dummy developed within EPOCH, it is not likely that impactor type events will be used in evaluating injury risk. Therefore, based on relevance, only the chest deflection scaling formulae are reproduced. The EEVC approach seems most appropriate to this study as it includes terms accounting for geometric, stiffness, and failure ratios.

<p>Irwin and Mertz</p> $R_D = \lambda_x$ <p>Where <math>R_D</math> is the ratio of chest deflections; and <math>\lambda_x</math> is the ratio of chest depth.</p>	<p>WG12&amp;18</p> $\lambda_\sigma = \frac{\lambda_y \lambda_{\sigma t}}{\lambda_{Eb}}$ <p>Where <math>\lambda_\sigma</math> is the ratio of peak sternal deflection; <math>\lambda_y</math> is the ratio of rib length; <math>\lambda_{\sigma t}</math> is the ratio of calcaneal tendon failure stress; and <math>\lambda_{Eb}</math> is the ratio of bone modulus. Assuming the thoracic organ modulus ratio, <math>\lambda_E</math>, is equal to 1, then; <math display="block">\lambda_\sigma = \lambda_y \lambda_{\sigma t}</math></p>
---	--

The thoracic anthropometry measurements related to six-year-old children, the Q10, and adults are shown in Table 5-16. As with the head and neck anthropometry, these values have been taken from the EPOCH Deliverable 1.2 (Waagmeester *et al.*, 2009).

**Table 5-16: Geometric (anthropometric) measurements relating to the thorax**

	6 year old	Q10	Adult
Shoulder width (mm)	282.0	337.8	429.0
Thorax width (mm)	180.0	217.4	305.5
Thorax depth (mm)	134.8	153.9	230.0
Thorax Circumference (mm)	570.0	687.3	950.0

Regarding material properties for the thorax, Mertz *et al.* (2003) used both the parietal bone elastic modulus and calcaneal tendon failure stress in scaling the Injury Assessment Reference Values for the shoulder, thorax, abdomen, and pelvis. The reason for using material property scaling values from other body regions is likely to be due to the absence of scaling properties from the correct region. However, there was some, limited, information available with which to try and validate the scaling proposed by Mertz *et al.* and this has been added to in recent years. This has provided some interesting and novel areas of paediatric research, such as quantitative chest compression data from cardiopulmonary resuscitation of children.

A relationship between the risk of significant thoracic injury ( $AIS \geq 3$ ) and Hybrid III dummy sternal deflection for shoulder belt loading was developed by Mertz *et al.* (1991). This relationship forms the basis for the thoracic compression criteria in US and European regulation, as well as other regions of the world. Based on the data points underlying this adult risk curve, it has been, and is, possible to scale the relationship for other sizes of occupant.

In the van Ratingen *et al.* (1997) relationship for scaling thoracic response to impactor tests, femoral bone elastic moduli are used. These data are taken from the summary paper of Stürz (1980), although the original source is Currey and Butler (1975). Using the femoral modulus data instead of the skull bone modulus data would have the effect of increasing the scaling rates. It is not known whether the femoral or skull bone moduli are more closely related to the moduli of rib bone. However, adopting the EEVC



---

approach, of not scaling the modulus, will give more conservative tolerance values for children. Therefore this approach is used subsequently in this paper.

The EEVC equation for calculating the chest scale factor incorporates the ultimate tensile strength of the calcaneal tendon for the Q10 and Q12. This was calculated from data provided by Yamada (1970). Having the tendon failure strength values allowed the EEVC equation to be applied, with the thoracic organ modulus ratio ( $\lambda_{Eb}$ ) assumed to be 1. This equation results in a chest scaling factor of 0.653 for the Q10.

These chest injury scaling factors were then applied to data from Mertz *et al.* (1991) to generate injury risk curves for chest AIS 3+ injuries for the Q10. The data from Mertz (1991) measured the average sternal deflection from sled tests (accident reconstructions) using the Hybrid III 50th percentile dummy.

As mentioned in the Introduction, since preparing the original report for Task 1.3, the Q10 dummy has been designed, made and tested within other work packages of the EPOCh Project. It is now known that the design and biofidelity performance of the dummy is in keeping with other dummies in the Q-series. Knowing the relationship to the other dummies in the Q-series, it seems appropriate to try and relate the risk functions to those reported by Wismans *et al.* (2008) in a similar way. This is particularly important where deviations from the scaled biofidelity targets for the Q-series dummies means that effective stiffness would need to be incorporated when scaling down from adult humans. An example of a body region where stiffness may be important would be the thorax, where the Q10 biofidelity performance has the same relative stiffness with respect to the biofidelity corridor as the smaller Q-dummies (e.g. Q6 and Q3).

The data used by Wismans *et al.* to draw up the Q3 injury risk functions are shown in Table 5-17. Here it should be noted that all of the test data have been scaled to make them appropriate for the Q3 dummy.

**Table 5-17: Q3 Chest deflection and injury data (as used by Wismans *et al.*, 2008)**

Case identification	Dummy	AIS	Deflection (mm)	Scaling ratio	Deflection corrected (mm)	AIS 3+
ITF-VTI	Q3	0	37	1	37.0	0
225/1	Q3	1	31.4	1	31.4	0
329/1	Q3	3	20.6	1	20.6	1
297	Q3	3	44	1	44.0	1
56	Q3	0	7	1	7.0	0
1079	Q3	3	55.6	1	55.6	1
1102	Q3	0	51	1	51.0	0
1081	Q3	0	19	1	19.0	0
1082	Q3	0	33	1	33.0	0
1067	Q3	0	26	1	26.0	0
1119	Q3	3	51	1	51.0	1
132	Q3	0	6	1	6.0	0
089/1	Q6	0	20	1.1	22.2	0
113/2	Q6	0	34	1.1	37.8	0
038/1	Q6	0	48	1.1	53.3	0
177/1	Q6	3	50	1.1	55.6	1
182/1	Q6	0	27	1.1	30.0	0
95	Q6	0	6	1.1	6.7	0
1104	Q6	0	30	1.1	33.3	0
1149	Q6	0	19	1.1	21.1	0
1006	Q6	0	30	1.1	33.3	0
1104	Q6	0	50	1.1	55.6	0

Based on these data Wismans *et al.* (2008) drew injury risk functions for the Q3 dummy. Those authors used the Certainty Method and logistic regression to derive the functions.

Since publication of the EEVC Q-dummy document, ISO WG5 has issued advice that injury risk functions should be developed primarily using survival analysis. The following figure (Figure 5-18) presents a risk curve generated using these data and survival analysis. The survival analysis shown assumes a Weibull distribution for the underlying data. As shown in Figure 5-18 the survival and logistic regression curves are similar, but not the same, up to about 50 mm of deflection and a 40 % risk of AIS  $\geq$  3 injury. From this point onwards, the curves diverge slightly with the survival function predicting a lower risk of injury for a given chest deflection.

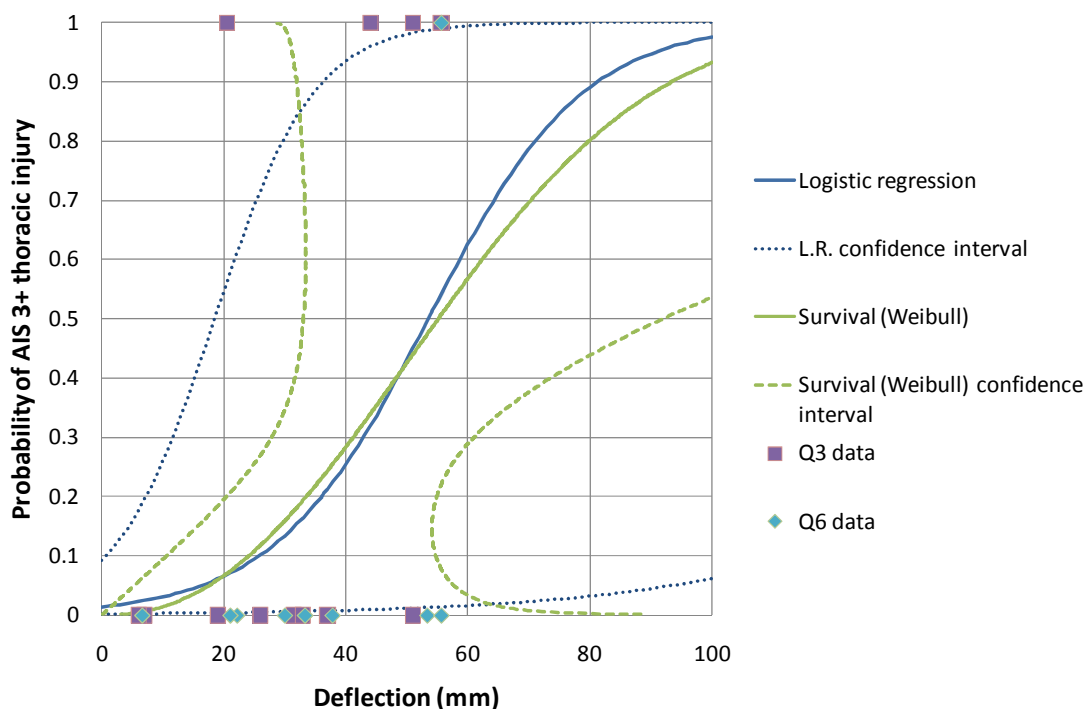


**Figure 5-18: CREST and CHILD data points and AIS  $\geq 3$  logistic regression and survival analysis injury risk curves for Q3 chest deflection.**

Based on the scaling values provided by XT, it is possible to scale the injury risk curves to make them relevant for the Q10 dummy. In practice this means multiplying the Q3 data by 0.67 and the Q6 data by 0.75. The survival analysis injury risk curve based on the CREST and CHILD data scaled for the Q10 dummy is shown in Figure 5-18, “Survival (Q10)”, again a Weibull distribution is assumed for the analysis.

In order to compare the function developed by scaling up from the Q3 with the other approach of scaling information down from the adult size, scaling factors are needed for the Q10. As described above, using the rationale of Wismans *et al.* and some further interpretation of the available material property data, scaling factors have been developed. Using the Q10 scaling ratio as proposed earlier in this section, the Hybrid III 50th percentile adult sternal deflection injury risk function was scaled down to make it appropriate for the Q10. The resulting curve is also shown in the following figure (Figure 5-19). A log-normal distribution assumption was used in the survival function.

It can be seen from Figure 5-19 that the scaled down adult risk function predicts a lower risk of injury for a given chest deflection. The two curves diverge with increasing deflection. This means that the difference between the scaled up CREST and CHILD data and the scaled down Hybrid III data for a 20 percent risk of an AIS  $\geq 3$  thoracic injury is between 23 and 28 mm. Whereas the difference is greater for a 50 % risk of injury, and is between 37 and 56 mm.

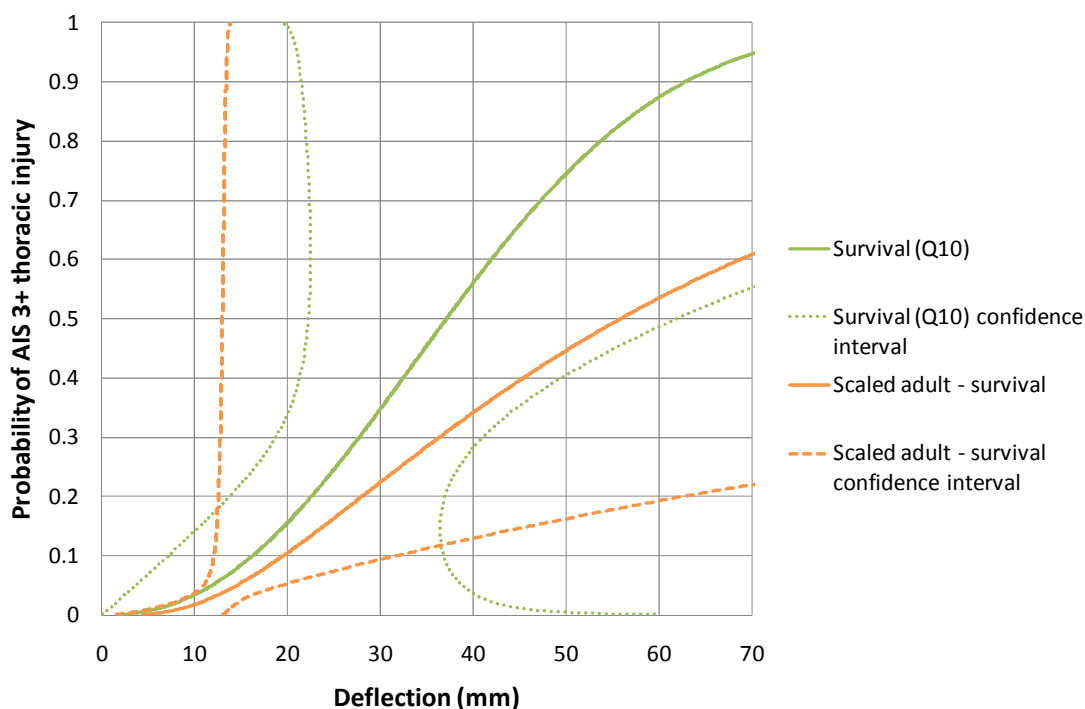


**Figure 5-19: AIS  $\geq 3$  survival analysis injury risk curves for Q10 chest deflection derived from the CREST and CHILD data or from scaling of the adult 50<sup>th</sup> percentile Hybrid III sternal deflection.**

From the EPOCH tests with the Q10, results for the upper and lower chest compression measurement points have been obtained. The smallest peak value from either IR-TRACC was 44 mm and the highest value was 60 mm.

Based on these results all of the CRSs would have exceeded a 50 percent risk of AIS  $\geq 3$  thoracic injury using the risk function scaled from the CREST and CHILD data. Some CRSs would also have exceeded the 50 percent risk level based on the function scaled down from the adult (Hybrid III) data.

As with the neck tension values described in the previous chapter, the high estimates of potential injury risk call into question the relationship between the dummy values measured in laboratory tests and real world injury rates. Again thoracic injuries have not been identified as a priority for prevention for restrained older children in frontal impact accidents. Therefore, it may not be necessary (or perhaps even advantageous) to implement a stringent chest deflection criterion. It is important that child restraints that position the 3-point belt across the torso of the dummy, thus to engage the belt correctly, are not penalised by a chest compression criterion. Instead it seems appropriate to maintain a similar level of performance for future restraint systems. On this basis it is suggested that a chest deflection threshold of about 56 mm is used with the Q10 initially.

With a multi-point chest deflection measurement system there is some scope for combining data from the two sensors to give more information about potential injury risk. For instance, it may be that loading one part of the chest in isolation is more injurious than distributed loading over the whole chest. In this case, there may be benefit to using an advanced criterion which accounts for force distribution somehow. The appropriateness of such a proposal would need further research and validation than has been possible within the EPOCH Project. However, work has been carried out investigating the response of the Q10 thorax to hub or diagonal seat belt loading in

table-top test conditions. This work should help understanding of the regional stiffness of the Q10 thorax and perhaps inform later discussions on the balance of importance given to either the upper or lower chest deflection measurement. In the meantime it is suggested that the deflection limit is applied to either sensor.

### 5.2.7 Thorax acceleration

Real world accidents involving both child car occupants (seated in Römer-Peggy I or II restraints) and pedestrians were recreated by Stürtz (1980) using VIP 3c and 6c dummies. On the basis of nine cases (including six reversible or non-injury cases) Stürtz proposed limits of 105 g for the peak resultant thoracic acceleration and 85 g when exceeded for 3 ms. Apparently these values represented protection criteria covering 75 percent of the reversible injuries and 25 percent of the irreversible injuries. Alternative limits of 55 g for both acceleration measures were also suggested for representing 50 percent of reversible and irreversible cases. The current UN Regulation 44 chest acceleration criteria is also 55 g (3ms exceedence).

It is not known how the biofidelity of the VIP child dummies would compare with the Q-series. It is unlikely that a dummy-specific injury risk function developed for the VIP series could be reliably transferred to the Q-series. However, the use of only nine cases to develop the proposed thresholds for the VIP dummies means that the tolerance values can only really be considered as indicative. On the basis of providing a general guide to a child's tolerance, rather than a specific risk function, the values suggested by Stürtz provide some information.

These values, reported by Stürtz, are around the level proposed for use in US regulation with adult subjects or surrogates of 60 g; although the Stürtz child values are slightly higher than the adult, when looking at the 75:25 risk values. There is no clear basis as to why the child tolerance would be expected to be higher than for adults. Also, if the adult value was maintained it should provide a conservative estimate of injury risk for a child. Therefore it is proposed to maintain the European 55 g limit. The data recorded in EPOCH Task 3.2, for resultant chest accelerations indicate lower values for the Q10 dummy tests compared with those seen in the P10 for all child restraints. Therefore, there is some scope for this value to be reduced for use with the Q10 dummy. A limit of 45 g is suggested based on the EPOCH test results.

### 5.2.8 Summary and discussion

Previously published scaling approaches for use with child biofidelity and the development of injury risk functions have been reviewed. Data needed to be used in these scaling formulae, concerning biomechanical material properties have been sought from previous sources and the latest published literature. These data have been used together with anthropometry information, as reported alongside the design of the Q10 dummy, to provide scaling ratios. These scaling ratios have been set so as to provide a means of relating established injury risk functions from either the adult or Q3 to the Q10 dummy. The scaled injury risk functions have then been compared with initial test results with the Q10 dummy under Regulation 44 conditions. Associated with this comparison has been an assessment of the feasibility for CRS manufacturers to meet prospective criteria. This has also been balanced with pragmatic expectations of how well the criteria may relate to current CRS performance and real world accidental injury incidence. As a result of this work proposals have been made as to the criteria which should be used with the Q10 in regulation 44 type conditions.

As is usual in this area of research, there are several caveats to be taken into consideration:

Each scaling approach makes numerous approximations to keep the formula relatively simple to calculate. As an example geometric similitude is often cited as an assumption, so that the smaller body is the same as the larger in all aspects but size. Such assumptions and approximations will affect the scaling ratios and results. However, it is hoped that those effects are relatively small to the other aspects being taken into consideration.

Material property data for child subjects is limited. This means that alternative, hopefully related, data are often used in scaling and sometimes these data have to be interpolated for the age of interest. From a research perspective, it would be ideal if this lack of information could be resolved in the future.

As with the material property data, it is also uncommon to have child subject test data with which to validate scaling values. It is recognised that there have been recent efforts to address this at least in terms of providing some child related biofidelity information.

Child injury information is certainly not prolific amongst the accident investigation and biomechanics literature. This means that injury risk functions developed for children are usually based upon a small number of data points and therefore have poor robustness (wide confidence intervals). The functions reviewed or derived above certainly fall into that category. This means that care must be taken when using those risk functions to set an injury criterion. The level of confidence offered by the data needs to be kept in mind during any process using such a function.

There has been no direct relationship identified between injury assessment values for child dummies, a particular test severity and real world injury incidence. Any pragmatic decisions based on an expected real world performance of CRS should be considered knowing such a link has not yet been established. However, that is not to say such a link does not exist, only that the exact relationship is unknown to date.

This work has considered frontal test criteria for use with the Q10 dummy. There are only limited biomechanical data on which to base an extension of this work to side impact. Side impact testing is outside the scope of Reg.44 and as such it is not possible to compare P limits to Q response, for the development of equivalent limits. For this reason, the objective of EPOCH was to focus on the development of frontal impact limits for use in Reg.44. However, a similar approach can be taken in future studies, to define limits for side impact testing with the Q10 in newly developed regulations.

It is now known that the Q10 thorax biofidelity responses seem to be slightly closer to the biofidelity corridor than other Q dummies. The consequence of this variation in behaviour could be investigated in the future with respect to its impact on scaled injury risk curves. However, this small behaviour change is unlikely to change the pragmatic threshold level selection suggested above on the grounds of feasibility.

### **5.2.9 Conclusions**

As a result of this injury risk function investigation, it is proposed that the following limits are used with the Q10 under UN Regulation 44 conditions.

**Table 5-18: Proposed injury criteria for use with the Q10 dummy in UN Regulation 44 frontal impact conditions**

Measurement	Threshold
Head acceleration (3 ms exceedence)	80 g
Head horizontal excursion	465 mm
Head vertical excursion	885 mm
Neck tension	†
Neck flexion	125 Nm
Neck extension	37 Nm
Chest deflection (either IR-TRACC)	56 mm
Chest acceleration (resultant 3ms exceedence)	45 g

† It is recommended that a pragmatic neck tension limit is set after further testing with the Q10

### 5.2.10 References

- Carroll, J. A. and Pitcher, M. (2009). *The development of injury risk functions*. European Commission, EPOCh Project, Work Package 1, Task 1.3, Deliverable D1.3
- Coats, B., Margulies, S. S. and Ji, S. (2007). Parametric study of head impact in the infant. *Stapp car crash conference, Volume 51: Papers presented at the 51st Stapp car crash conference, October 2007*, SAE technical paper 2007-22-0001: The Stapp Association, pp.1-15.
- Currey, J. D. and Butler, G. (1975). The mechanical properties of bone tissue in children. *The journal of bone and joint surgery* 1975 (57) 810-814.
- EEVC (2008) Document number 514, *Q-dummies Report, Advanced Child Dummies and Injury Criteria for Frontal Impact*, April 2008.
- Hodgson, V. R., Gurdjian, E. S. and Thomas, L. M. (1967). The development of a model for the study of head injury. *Proceedings of the 11th Stapp car crash conference*, 10-11 October 1967, Anaheim, California, U.S.A., (SAE technical paper 670923). Society of Automotive Engineers, Inc. (SAE): Warrendale, Pennsylvania, U.S.A., pp.432-443.
- Irwin, A. and Mertz, H. J. (1997). Biomechanical basis for the CRABI and Hybrid III child dummies. *Child occupant protection 2nd symposium proceedings*, 12 November 1997 (SAE technical paper 973317), Florida, U.S.A.: Society of Automotive Engineers, Inc., 400 Commonwealth Drive, Warrendale, Pennsylvania, U.S.A.
- Mertz, H., Horsch, J., Horn, G. and Lowne, R. (1991). *Hybrid III sternal deflection associated with thoracic injury severities of occupants restrained with force-limiting shoulder belts* (SAE technical paper 910812). In PT44 - Hybrid III: The First Human-Like Crash Test Dummy. Society of Automotive Engineers, Inc. (SAE): Warrendale, Pennsylvania, U.S.A.
- Mertz, H. J., Jarret, K., Moss, S., Salloum, M. and Zhao, Y. (2001). The Hybrid III 10-year-old dummy. *Stapp car crash journal volume 45: papers presented at the 45th Stapp car crash conference*, 15-17 November 2001 (SAE technical paper 2001-22-0014), San Antonio, Texas, U.S.A.: Society of Automotive Engineers, Inc. (SAE): Warrendale, Pennsylvania, U.S.A.

Mertz, H. J., Irwin, A. L. and Prasad, P. (2003). Biomechanical and scaling basis for frontal and side impact injury assessment reference values. *Stapp car crash journal volume 47: papers presented at the 47th Stapp car crash conference* (SAE technical paper 2003-22-0009): Society of Automotive Engineers, Inc. (SAE): Warrendale, Pennsylvania, U.S.A.

NHTSA (1996). *Technique for developing child dummy protection reference values*. Child injury protection team.

Nuckley, D. J. and Ching, R. P. (2006). Developmental biomechanics of the cervical spine: tension and compression. *Journal of biomechanics*, 39 (2006) 3045-3054.

Ouyang, J., Zhu, Q., Zhao, W., Xu, Y., Chen, W. and Zhong, S. (2005). *Biomechanical assessment of the paediatric cervical spine under bending and tensile loading*. *Spine*, 30 (24) E716-E723.

Palisson, A., Cassan, F., Trosseille, X., Lesire, P. and Alonzo, F. (2007). Estimating Q3 dummy injury criteria for frontal impacts using the child project results and scaling reference values. *Proceedings of the IRCOBI conference*, September 2007, Maastricht, the Netherlands, pp.263-273.

Prange, M. T., Luck, J. F., Dibb, A., van Ee, C. A., Nightingale, R. W. and Myers, B. S. (2004). Mechanical properties and anthropometry of the human infant head. *Stapp car crash journal, Volume 48: papers presented at the 48th Stapp car crash conference*, 1-3 November 2004, Nashville, Tennessee, U.S.A.: The Stapp Association, pp.279-299.

Prasad, P. and Mertz, H. J. (1985). *The position of the United States Delegation to the ISO Working Group 6 on the use of HIC in the automotive environment*. SAE technical paper series 851246, Government/Industry meeting and exposition, 20-23 May 1985, Washington, D.C., U.S.A.: Warrendale, PA, U.S.A.: Society of Automotive Engineers, Inc. (SAE).

Reed, M.P., Sochor, M.M., Rupp, J.D., Klinich, K.D., Manary M.M.,(2009) Anthropometric Specification of Child Crash Dummy Pelves through Statistical Analysis of the Skeletal Geometry, *Journal of Biomechanics* 42 (2009) 1143-1145.

Stürtz, G. (1980). Biomechanical data of children. *Proceedings of the 24th Stapp car crash conference*, 15-17 October 1980, Troy, Michigan, U.S.A., SAE technical paper 801313., Warrendale, Pennsylvania, U.S.A.: Society of Automotive Engineers, Inc. (SAE), pp.513-559.

van Ratingen, M. R., Twisk, D., Schrooten, M., Beusenbergh, M. C., Barnes, A. and Platten, G. (1997). Biomechanically based design and performance targets for a 3-year old child crash dummy for frontal and side impact. *Child occupant protection 2nd symposium proceedings*, 12 November 1997 (SAE technical paper 973316), Orlando, Florida, U.S.A.: Society of Automotive Engineers, Inc. (SAE): Warrendale, PA, U.S.A.

Visvikis, C., Pitcher, M., Girard, B., Longton, A. and Hynd, M. (2009). *Literature review, accident analysis and injury mechanisms*. European Commission, EPOCH Project, Work Package 1, Task 1.1, Deliverable D1.1.

Waagmeester, C.D. and Been, B.W. (2009), *Single rib and 2D rib deflection sensor drop table impact tests; sensitivity to impact load and impact direction*, APROSYS project Deliverable D528, Document AP-SP52-0058, February 04, 2009.



---

Waagmeester, K., Burleigh, M. and Lemmen, P. (2009). *Biomechanical requirements and design brief. EPOCH Project, Work Package 1, Task 1.2, Deliverable D1.2.*

Waagmeester, C.D. *et al.*, (2009) *Q10 Design Brief*, European Commission, EPOCH Project, Work Package 1, Task 1.2, EPOCH Deliverable D1.2, September 15, 2009.

Waagmeester, C.D. *et al.* (2009), *Q10.5 dummy Development Status Report*, Protection of Children in Cars Conference, Munich, December 2009.

Waagmeester, C.D. *et al.* (2010), *Q10 dummy Development Status Review – Biofidelity Performance Validation*, Protection of Children in Cars Conference, Munich, December 2010.

Wismans, J., Waagmeester, K., Claire, M. L., Hynd, D., Jager, K. d., Palisson, A., Ratingen, M. v. and Trosseille, X. (2008). *Q-dummies Report - Advanced child dummies and injury criteria for frontal impact*. EEVC Working Group 12 and 18 report, Document No. 514 (available from the EEVC web site (<http://eevc.org/publicdocs/publicdocs.htm>))

Yamada, H. (1970). *Strength of biological materials*. 428 East Preston Street, Baltimore, Maryland, U.S.A.: The Williams and Wilkins Company, Strength of biological materials.

## 6 Numerical simulation

Simulation techniques, such as finite element analysis and lumped-mass models, are playing an increasing role in vehicle safety research as computer hardware (and software) become more and more powerful. Deployed traditionally as a means of undertaking broad “parameter sweeps” (that are unlikely to be cost-effective for physical crash testing), computer simulation now provides unique opportunities to study injury mechanisms in more detail, particularly with the introduction of human body models.

Finite element models of Q-Series dummies were developed in the CHILD project (2002-2006) and this work continued during CASPER. Similarly, CASPER also further refined finite element models of the child head and neck complex. This chapter draws together the latest research from CASPER on the simulation of child dummies and children. Section 6.1 summarises the development of Q-Series models. Section 6.2 describes the development of a three-year-old child head-neck finite element model, which was used to investigate potential head injury criteria. Section 6.3 presents a similar model for a six-year-old child, which was used to investigate the interaction between children and airbags. Each section comprises a published paper, reproduced here in its entirety. The full references for the papers are:

Lehmann, I., Eisenach, A., and Johannsen, H. (2012). Numerical simulation in the area of child safety using Q-dummy models. In: *Proceedings of the International Crashworthiness Conference 2012*, 18-20 July, Milan, Italy. London: Taylor & Francis Group.

Meyer, F., Deck, C. and Willinger, R. (2012). Development of a 3-year-old child head-neck finite element model and derivation of novel head injury criteria. In *Proceedings of the International Crashworthiness Conference 2012*, 18-20 July, Milan, Italy. London: Taylor & Francis Group.

Meyer, F. and Willinger, R. (2012). Six-years-old child head-neck finite element modelling – application to the interaction with airbag in frontal and lateral impact. In: *Proceedings of the 9<sup>th</sup> International Conference Protection of Children in Cars*, 1-2 December, Munich, Germany. Munich, Germany: TÜV SÜD.

### 6.1 Numerical simulation in the area of child safety using Q dummy models

While numerical simulation is a widely used tool in the development chain of automotive industry for adult safety systems the use of simulation tools just started in the area of child safety. The reasons for this late development step can be seen in low test costs, requirements that can be fulfilled without complex development steps, the relative complex situation compared to adult safety caused by the additional child restraint system and finally because of missing reliable simulation tools such as dummy models.

As additional safety benefits in the child safety domain are expected by using FE simulation tools the development of FE dummy models started during the EC funded research project CHILD with a model of the Q0 new born dummy [1]. Increased requirements and the introduction of more complex and more expensive Q dummies are expected to make simulation more interesting even in this area. Following that in the CASPER project, the successor project of the CHILD project, the remaining models

of the Q-dummy family were developed after FTSS already finalised commercial Q3 dummy model [2].

The aim of this paper is to describe the current status and the experience mainly with Q6 dummy model and for lower extend for other dummy sizes. Furthermore models of the test procedures and generic CRS models have been developed.

### 6.1.1 Q dummy model status

#### Complete FE dummy family

One aim of the CASPER project was to complete the whole Q dummy family in order to facilitate the use of modern development tools for the improvement of CRS. As Q0 model was already developed by TU Berlin during the CHILD project and Q3 model was available as commercial model CASPER concentrated on the development of the missing dummy models Q1, Q1.5 and Q6.

#### Model requirements and improvements

The available Q3 FE dummy was used as basis model. Additional requirements were discussed with future users of the models and FTSS<sup>4</sup> in order to provide high-quality usable dummy models. This includes dummy modeling general requirements like the solver version, model naming/numbering, mesh quality criteria for deformable parts, geometry/mass/inertia, control card definition and so on. Also material level tests requirements like detailed testing to develop mathematical material models just as component and sub-assembly level tests (head drop test, neck and lumbar spine pendulum tests and abdomen compression tests) and full dummy level test requirements. Figure 6-1 shows the FE dummy models that were developed within the CASPER project. Q1 and Q1.5 were developed by FTSS and the Q6 model was improved by FTSS.

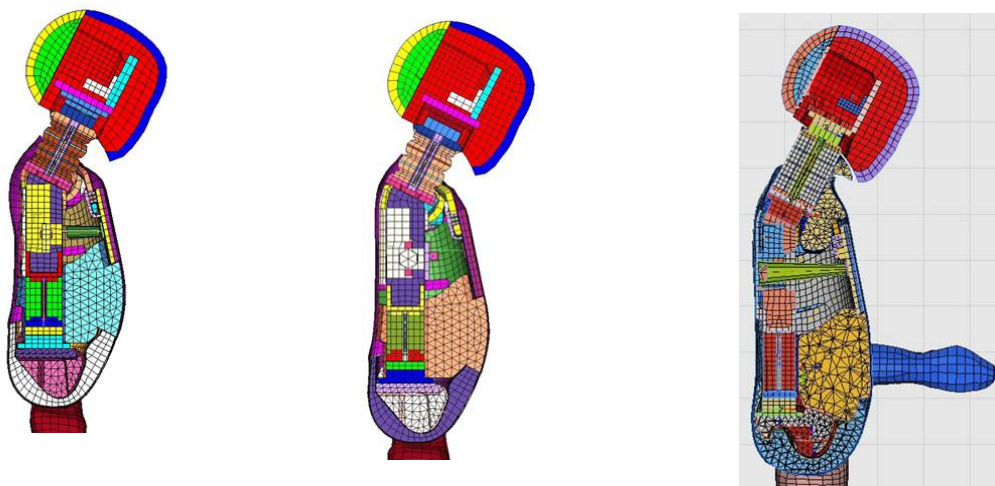


**Figure 6-1: FE dummy models, left Q1, centre Q1.5, right Q6**

With each new dummy model generation the aim is to improve the model and to integrate the knowledge and mesh issues from the previous models. The dummy models should more and more represent the physical properties, e.g., the parts should

---

<sup>4</sup> FTSS – First Technology Safety System, FTSS and Denton ATD became subsidiaries of Humanetics Innovative Solutions in 2010

not been assembled anymore over large-area contact definition but like the hardware dummies with punctual connection at the screw location, Figure 6-2 shows level of detail achieved with current version of Q6 model.

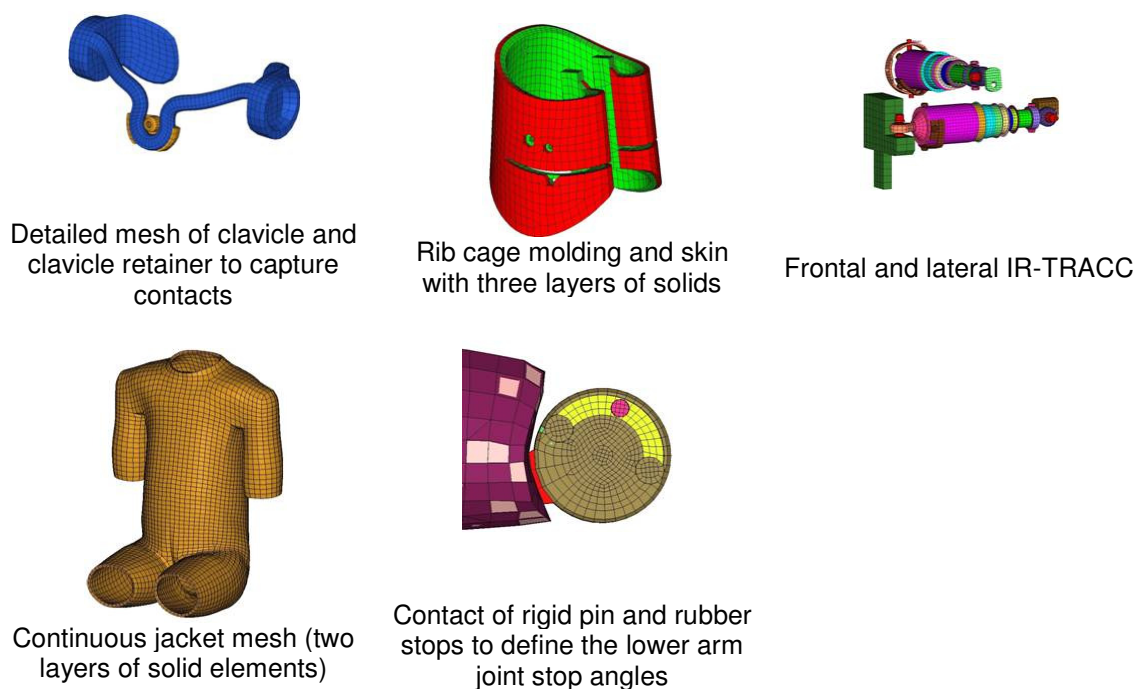


**Figure 6-2: Mesh modifications and improvements**

### 6.1.2 New hardware dummy development – the Q10

In parallel to the CASPER project the Q10 hardware dummy was developed by the EPOCh project. Following the CASPER aim to make available the Q dummy family as FE dummy models the Q10 dummy model development was started in the end of the CASPER project to be completed by Humanetics.

Especially the Q dummies which represent older children, that mean Q6 and Q10, are of interest for car manufacturers because of the planned revision of the Euro NCAP child safety protocol which become effective as of 2015. The new test requirements make use of Q6 and Q10 in the second row for frontal and lateral tests. The aim is to focus more on the safety for older children because based on GIDAS data the injury risk for older children (7 to 12 years old is higher than for younger children (up to and including 6 years old). As the protection of children between 6 and 12 years old is currently not addressed by Euro NCAP the new test protocol should change this [3]. Therefore car and CRS manufacturers are very interested in well validated dummy models to develop and improve their products.

### 6.1.3 Improving Q6 model and validation tests

Currently a consortium of car manufacturers, dummy research and development institutes work together to improve the Q6 model quality. More material, sled and full dummy component tests will enable a high-quality validated model. Following tests were planned to validate the model:

- Simplified frontal sled tests that take into account belt routing resulting from the use of CRS without the need of validating the CRS (by use of a customised rigid “booster”) in 0° and 15° impact angle

- Simplified lateral sled for struck side and non-struck side simulation with CRS and impact surface that requires low validation effort of the environment
- System and subsystem tests extracted from the loading conditions observed in car tests and sled tests, such as modified thorax pendulum impactor test, see Figure 6-3.

Partially the tests were finished and other tests are carried out at the moment.

One important topic of the tests was to analyse vehicle and sled tests to learn more about average force levels and to derived simple component tests. As one example the thorax belt interaction is used. The test analyses showed that the belt impact shape is more like a plane contact surface diagonal over the chest. In contrast the standard chest component test is using a cylindrical impactor which hits the chest punctual in the middle. With this knowledge a test setup was generated by adding a diagonal plane that is attached to the front of the chest pendulum impactor. Impactor speed and weight were adjusted to achieve realistic loading conditions.

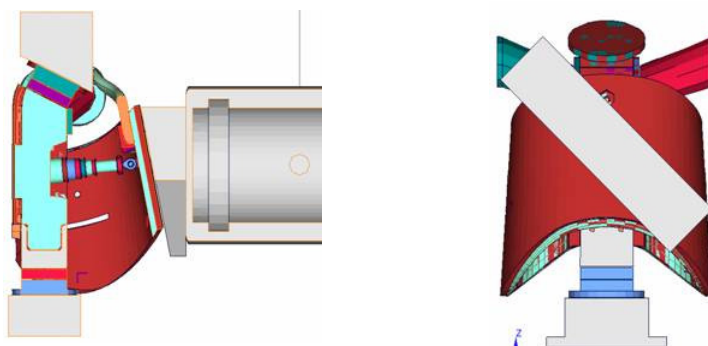


**Figure 6-3: Impactor shape**

The motion of the pendulum was smooth and the impactor shape avoids vertical skidding. The same test procedure was created as FE simulation and the chest materials were modified to achieve good correlation between hardware and simulation tests. Figure 6-4 shows the comparison of test video and simulation animation. Also tests with and without the clavicle were done in hardware and simulation tests to identify the influence of the clavicle to the chest stiffness and to get a better validated model.

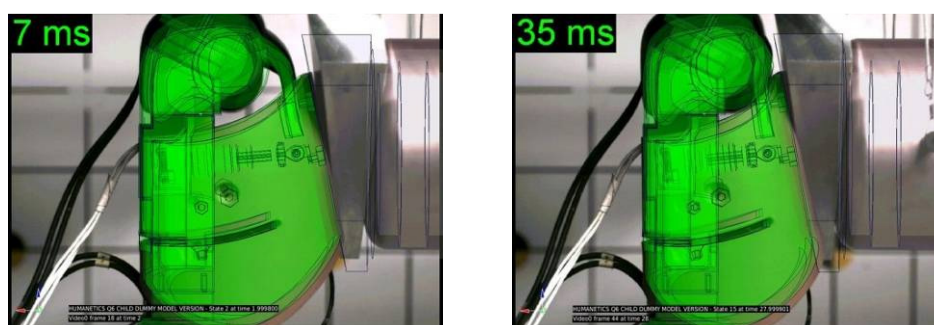


**Figure 6-4: Comparison of chest pendulum test and simulation**

#### 6.1.4 First experience with FE Q-dummies

##### Q0 and Q3

The Q0 dummy model was used to acquire first lateral test procedure analyses. Therefore the Q0 dummy was positioned in a rearward-facing baby shell and the CRS

was adjusted to the test bench. Different initial velocities, velocity profiles, CRS positions (rotation and translation) and ISOFIX use were tested and analysed. The FE Q0 dummy worked numerically stable and the analyses showed that the impact velocity has the major influence to the dummy readings while the velocity profile as minor impact. Also little position variations did not alter dummy readings significantly. No experimental tests were made to compare and ensure the results.

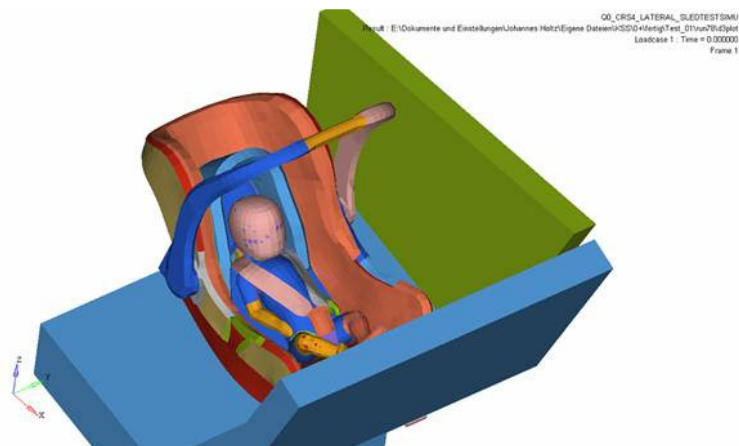


Figure 6.5: Q0 dummy model in lateral sled test environment

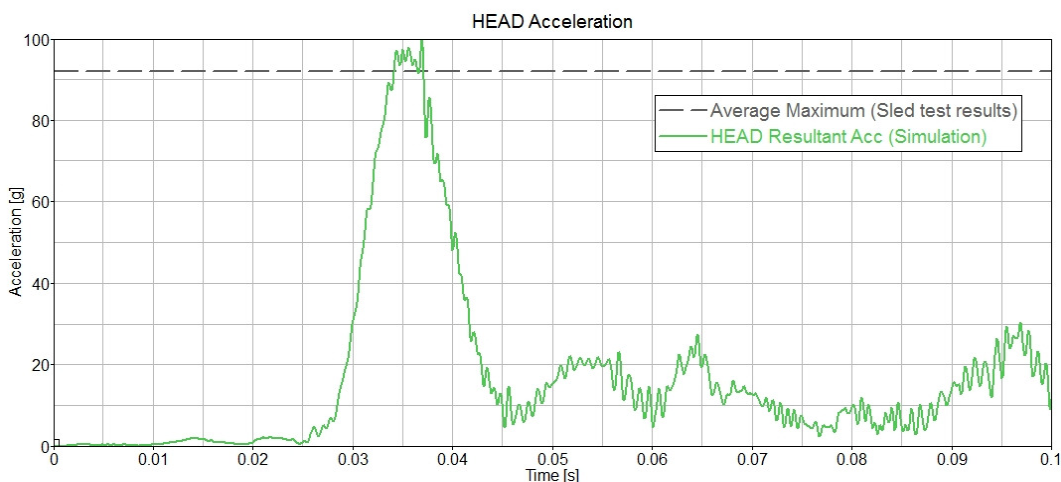


Figure 6.6: Q0 head acceleration (lateral impact)

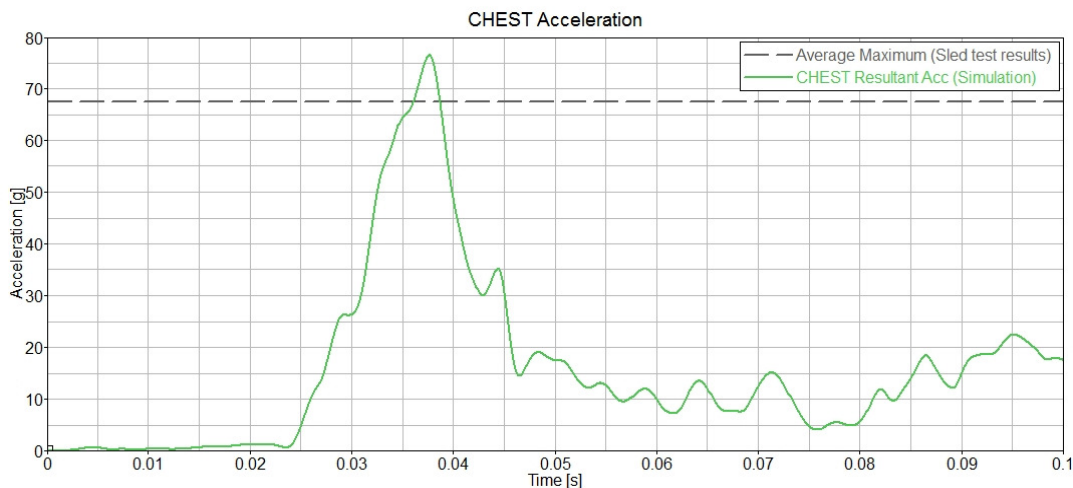
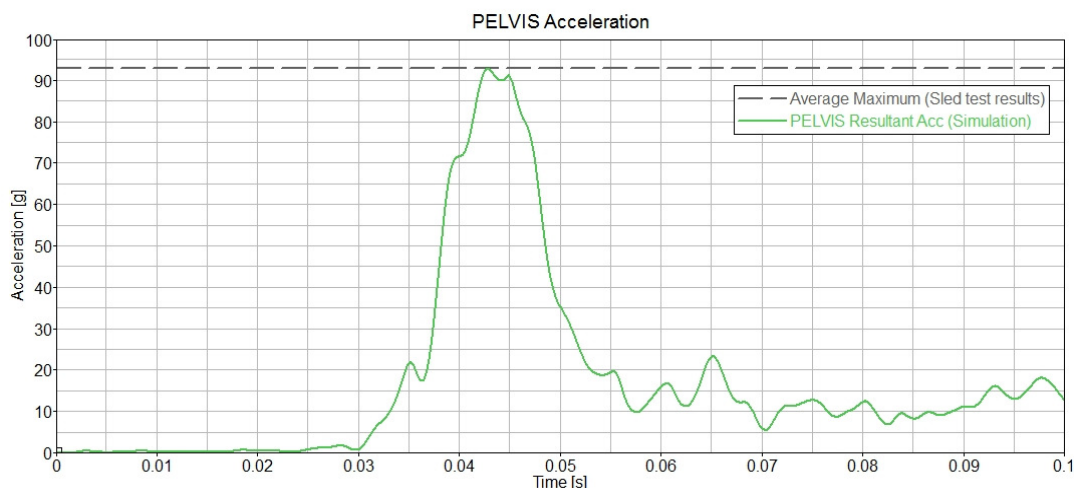
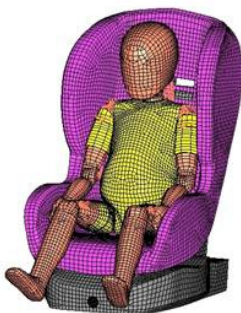


Figure 6.7: Q0 chest acceleration (lateral impact)



**Figure 6.8: Q0 pelvis acceleration (lateral impact)**

The Q3 FE dummy was used to validate a generic group 1 CRS model. The main problem with the Q3 LS-Dyna model is caused by the dummy jacket. It is generated with shell elements and does not generate a stable contact between the dummy parts and the environment (CRS, harness and/or impactor). But at the end the dummy jacket contributes little to the dummy stiffness and could be neglected. Basically analyses and simulations were possible with the FE Q3 dummy model.



**Figure 6.9: Q3 dummy model at a group 1 CRS**

#### **Misuse study with the Q6 dummy**

The Q0 dummy model was used to acquire first lateral test procedure analyses. Therefore the Q0 dummy was positioned in a rearward-facing baby shell and the CRS was adjusted to the test bench. Different initial velocities, velocity profiles, CRS positions (rotation and translation) and ISOFIX use were tested and analysed. The FE Q0 dummy worked numerically stable and the analyses showed that the impact velocity has the major influence to the dummy readings while the velocity profile as minor impact. Also little position variations did not alter dummy readings significantly. No experimental tests were made to compare and ensure the results.

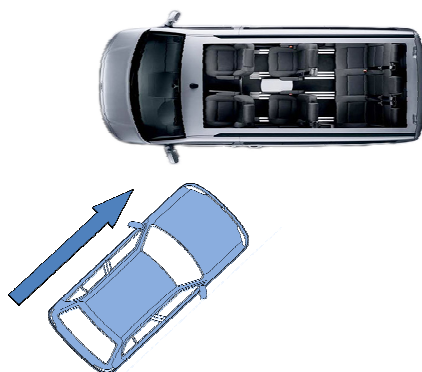


**Figure 6-5: Accident configuration used for belt routing analysis**

#### Accident description

The accident occurred on the crossroad with limited visibility, located on the top of a hill. The driver of the car with a 7 years old child sitting behind the driver stopped at the crossroad and slowly turned left. Another car, coming from the opposite direction could not stop in the short period of time and impacted the car with the child at the level of the front wheel. The child sustained AIS 4 head injuries, probably due to the contact of the head with the side window. Although the dummy displacement was rather high, the shoulder belt has restrained the torso of the dummy.

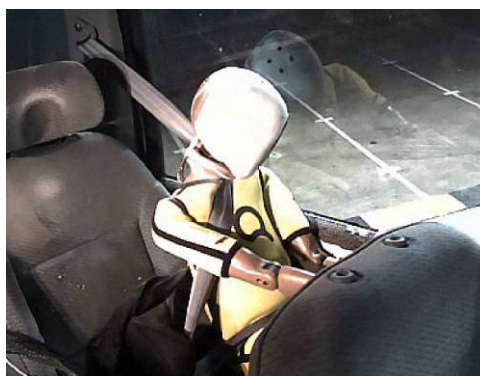


**Figure 6-6: Displacement of the Q6 dummy in the reconstruction**

The deformation of both cars was comparable to the real accident, therefore it was concluded that the belt routing was likely not the standard one.

#### Simulation results

For the simulation, the interior geometry of the accident car was scanned and constructed. The Q6 was restrained in three different ways (below figure). The simulations were conducted by regular restrained, with shoulder belt behind the dummy's torso and one version with the belt under the dummy's shoulder.



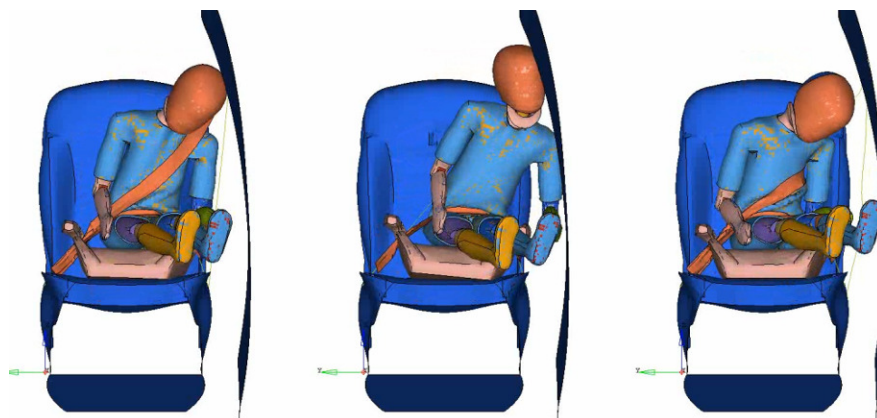


**Figure 6-7: simulation results, different 3-point belt configurations**

As predicted by safety experts the restraint situation with the shoulder belt behind dummy's torso resulted in a heavy impact of the head with the door structure, the other load cases showed no head contact. In addition to the simulation study another real accident reconstruction was performed. The dummy head impacted the side window as expected.

### **CRS validation and test procedures severity investigations**

For a group 2/3 CRS were CAD data made available to configure the seat as FE model. Following the seat should be validated and be usable for simulation analyses, experiences with test procedures and for CRS improvements. The validation and analyses should be done with a Q6 dummy because the FE dummy was developed by the CASPER project and the Q10 FE dummy model (also suitable for group 2/3 CRS) was not available in time.

Frontal and lateral sled tests were conducted with the hardware CRS. Basically the CRS were adjusted to the test bench the Q6 dummy was positioned in the seat and belted. The frontal crash pulse and initial velocity was based on the NPACS test definition. The acceleration output from the sled and all standard output values from the Q6 hardware dummy were selected. Two basis sled tests were made (one repeating test) and one test without ISOFIX anchorage, respectively, one with minor crash pulse and one under an angle of 30 degrees.

The same test environment was configured as FE model and the measured initial velocity as well as the sled pulse from the experimental tests was included in the model. The first simulations to validate the CRS were made with the two basis variants. Therefore the test results from the experimental test procedures were compared with the virtual result. It shows that in the simulation model the belt material definition was too soft. Therefore the dummy was decelerated too late and the result curves did not fit together. After several simulation loops the belt material definition could be adjusted so that the results plus the dummy kinematics from experimental and virtual testing correlated well. For frontal sled test procedures the belt definition is the part with the biggest influence because the interaction between dummy and CRS is not as big as in the lateral test.

With this first validation result a simulation without CRS ISOFIX anchorage and a simulation with lower crash pulse were started. The comparison of simulation results with the test results showed that the validated virtual model allowed good prognoses, Figure 6-8 - Figure 6-10. But with further validations based on all three test procedures (basic, basic without ISOFIX and basic with minor crash pulse) the belt model could be optimised.

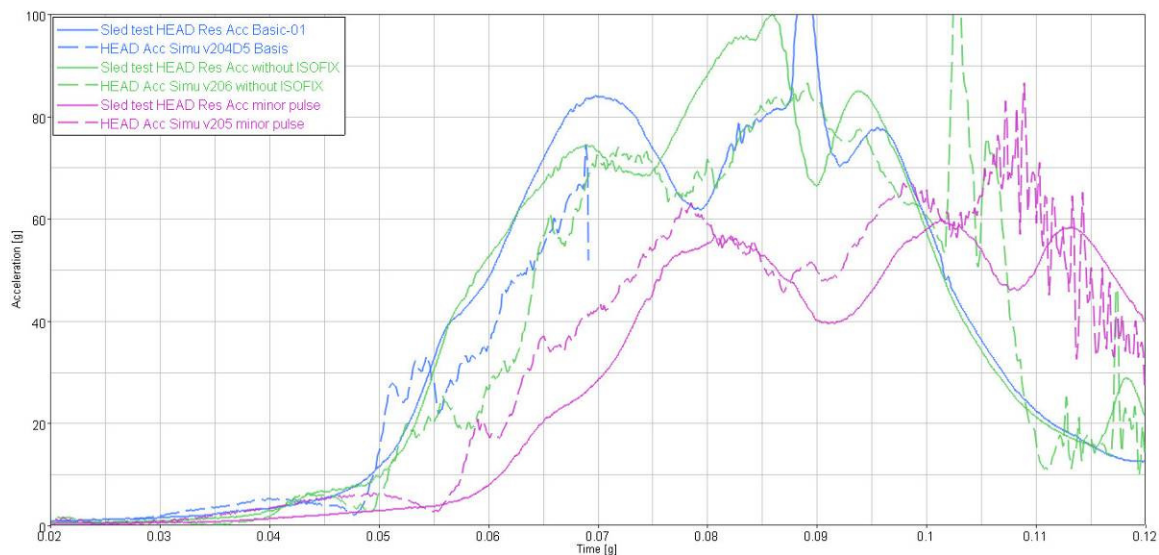


Figure 6-8: Head acceleration

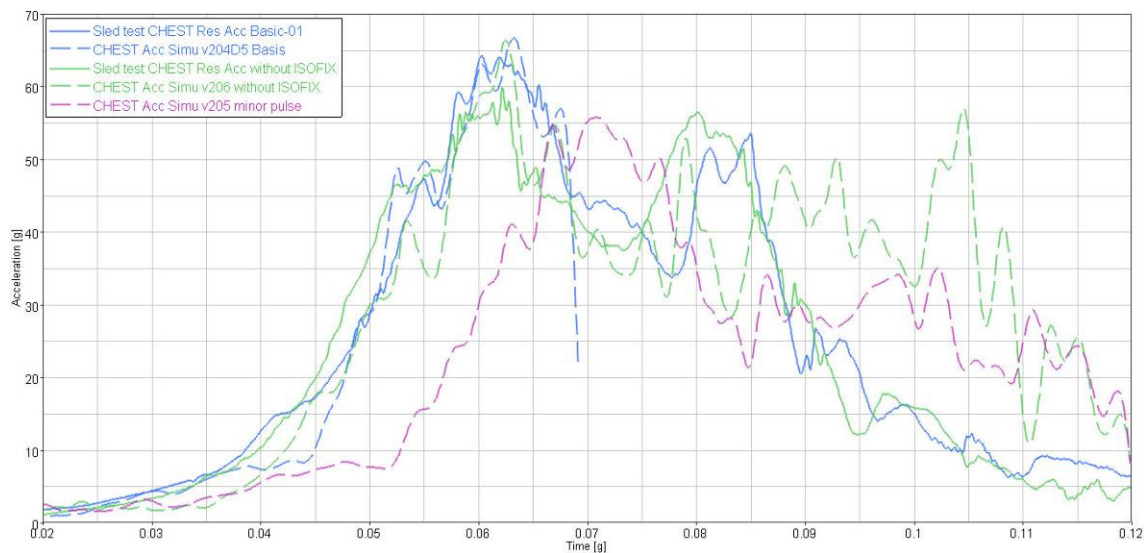


Figure 6-9: Chest acceleration

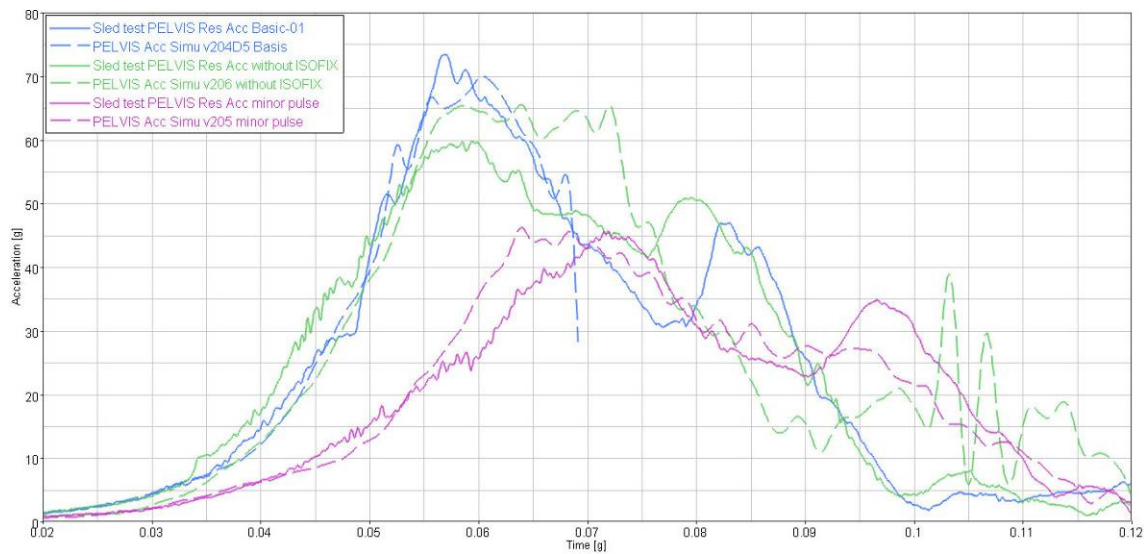


Figure 6-10: Pelvis acceleration

For the interpretation of the frontal test procedure the belt definition has the main influence. Therefore the validation provided the best results as more different test configurations were used.

### Analysis of CRS performances

For the Q6 lateral sled test the same sled environment like for the frontal impact was used but rotated by 90 degrees. In addition the crash pulse based on the new GRSP side impact test proposal for CRS was used. Two basis tests were conducted (with one repeating test). The frontal simulation model was modified respectively.

In the lateral test procedure the interaction between dummy and CRS is more important than in frontal tests. The dummy will interact over the whole side with the CRS structure and the CRS works as buffer between dummy and impactor. First simulation analyses showed that material modifications on the CRS had a big influence to the whole dummy output values. That means that modifications on one CRS area for example in the seating area had influence also in the chest and head acceleration and not only to the pelvis output. Therefore CRS modifications are very sensitive to the whole dummy forces severity and analyses must show which variant of CRS parameters get the best results.

### Influence of dummy positioning

In the lateral simulation the chest and pelvis output acceleration as soon as the IR-TRACC displacement output proved to be very sensitive to the dummy arm position. Depending on whether or not the elbows are hitting the chest more directly a wide difference can be seen. In previous sled tests it was shown that the arm position has a big influence were also detected. Depending on this the dummy arms should be positioned in sled test seen in Figure 6-11.



**Figure 6-11: Arms aligned with sternum**

On the other side small dummy position variation did not result in any significant changes in the dummy readings.

### Detected dummy problems

At the moment following problems with the improved Q6 dummy in the LS-Dyna version were detected:

- LS-Dyna contact definitions are very important and sometimes not stable, therefore penetrations could be appearing (especially with foam contact definitions) and producing different output results.
- The hardware dummy jacket dressed on the dummy with an initial tension and could not be moved off so simple from the body, but this effect is not well presented in the dummy model. For example under the 30 degree impact slides

the jacket from the shoulder by the belt and the dummy could not be restrained. Improvements are necessary.

- The continuous created dummy jacket prevents the belt sliding between pelvis and leg but it makes the dummy positioning more difficult. To position the dummy arm and/or leg is now a pre-simulation needful.

With the Q6 consortium work a better validated and high-quality model can be expected. The CASPER experiences show that a lot of simulations and analysis are necessary to identify all possible problems, to improve the model as good as possible and to transfer the improvements to the other Q dummies.

FE models are sensitive to get productive results but a good validated model (dummy as well as CRS as well as test environment) are precondition to use the whole potential of FE simulation.

### 6.1.5 Human body modelling

#### More detailed investigations with child human model family

The aim of the CASPER project is to improve the safety of children as car passengers. The consortium works on many aspects of child safety, one of the work packages aims at the definition of new numerical human models. Overall five partners are working on the development of different body regions or complete human models, three of them are being developed as finite element models for the age of one, three and six years. The work on the models is split to different body regions, at the end of the project the different body regions were combined to full body models.

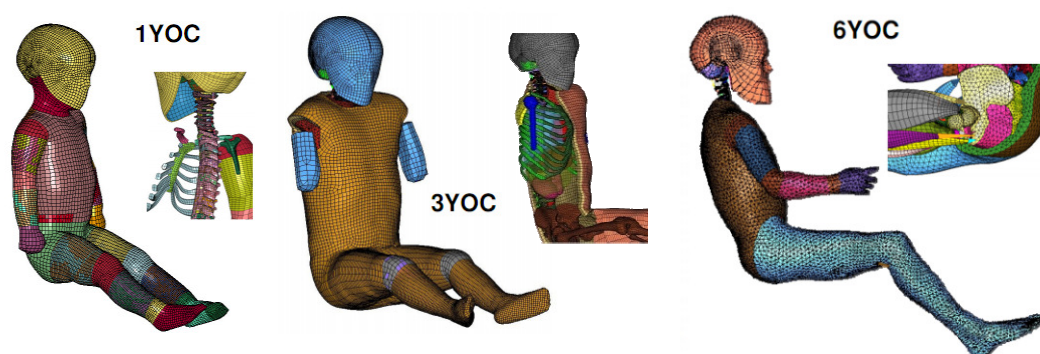


**Figure 6-12: CASPER child FE human models**

Especially in tasks as described above, human models are capable to improve the quality of the researches work. The crash test dummies are well designed but in some cases they lack in biofidelity, it is a difficult task to design a dummy which performs humanlike in every possible situation. With the human model family developed in CASPER an important step towards improvement of the research tools for child safety was created. Although the FE child human models are in an early development stage and need further optimisation, the validation for basic load cases is finished.

### Validation of the three year old child model

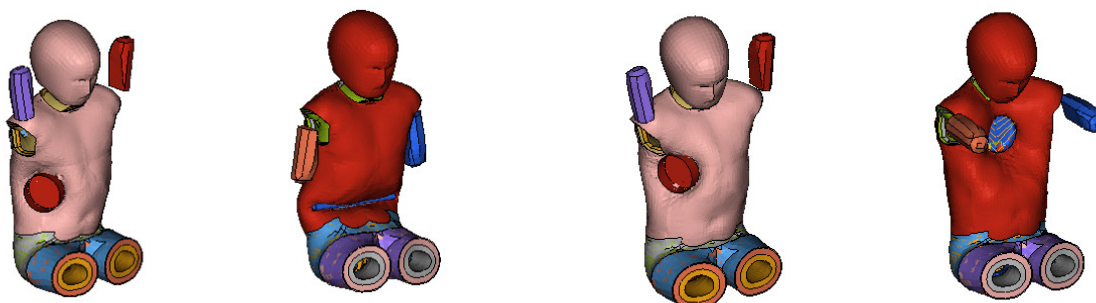


**Figure 6-13: Validation of the three year old child model**

For the three year old model, four impact types were chosen for the validation, two for the thorax (frontal and lateral) and two for the abdomen. The validation of the human model is based on results from cadaver tests which were conducted with adult PMHS. The response curves / corridors were scaled to the appropriate level for the children model. The basis for the scaling are the different geometrical dimensions gathered from literature and by CASPER partners.

#### 6.1.6 Acknowledgements

The research described in this paper is based on results of the CASPER project. The CASPER project is co-funded by the European Commission under the 7th Framework Programme (Grant Agreement no. 218564). The members of the CASPER consortium are: GIE RE PR - PSA/RENAULT, Technische Universität Berlin, Université de Strasbourg, APPLUS IDIADA Automotive SA, Institut Français des Sciences et Technologies des Transports, de l'Aménagement et des Réseaux, Loughborough University, FIAT Group Automobiles Spa, Medizinische Hochschule Hannover, Chalmers tekniska högskola AB, Bundesanstalt für Straßenwesen, TNO, Verein für Fahrzeugsicherheit Berlin e.V., Ludwigs Maximilian Universität, Centre Européen d'Etudes de Sécurité et d'Analyse des Risques, Humanetics Europe GmbH. Further information is available at the CASPER web sites: [www.childincarsafety.eu](http://www.childincarsafety.eu) and [www.casper-project.eu](http://www.casper-project.eu).

#### 6.1.7 References

- [1] Gehre, Christian: „Development of a Model of the New Born Child Dummy Q0”, VDI Verlag, 2007.
- [2] Child Advanced Safety Project for European Roads , [www.casper-project.eu](http://www.casper-project.eu)
- [3] Michiel van Ratingen “An introduction to Euro NCAP’s New Child Occupant Protection Protocol“ Presentation given at the 9th International Conference on "Protection of children in cars", 1-2 December 2011, Munich at <http://prezi.com/dxv2m7mkahdz/an-introduction-to-euro-ncaps-new-child-occupant-protection-protocol/>.

## 6.2 Development of a 3-year-old child head-neck finite element model and derivation of a novel head injury criteria

### 6.2.1 Introduction

The growing demand for greater mobility in Europe has made individual vehicle transportation an essential and perhaps inevitable feature of modern living. Children are increasingly transported in cars or other modes of road transportation. With this increased travel comes the higher risk of children becoming involved in an accident as an occupant. Based on the above accident data, it is obvious that in spite of significant improvements in recent years in vehicle safety, the current number of deaths and casualties in addition to the social and economic costs is still unacceptable. Fatalities and injuries, especially to children, need to be reduced using all available measures: public regulation, prevention/education of road users, road infrastructure, compatibility between vehicles, as well as active, passive, and tertiary safety devices.

Regarding children, it is very difficult to obtain figures relating to child fatalities or severe injuries from the 27 European countries. However, if we consider the 15 countries of the European Union, where the use of child restraints has long been mandatory, approximately 600 children are killed in cars every year on the European roads, while 80,000 are injured (data source: IRTAD). Although there has been a huge effort in developing adult finite element models (FEM). Owing to ethical reasons, there is paucity of experimental data on head characterization in children. In addition, few studies have attempted to quantify the mechanical properties of the child and pediatric skull, brain, and other head structures.

Few studies deal with the influence of age on brain mechanical properties. The first study was conducted in 1998 on developing porcine subjects by [20]. In order to examine variations in the mechanical properties of the developing brain, the authors compared the viscoelastic properties of tissue taken from fully developed 1-year-old pigs (similar to a 4-year-old human child) with those from 2-3-day-old pigs (equivalent to a human newborn <1-month-old). In addition, fresh whole porcine brains were obtained from 2-3-day-old (N=12) and 1-year-old (N=12) domestic pigs. The excised cerebrum and thalamus were stored in refrigerated artificial cerebrospinal fluid, and tests were completed within 3 hours post-mortem. All specimens were removed from the same location in the frontal cerebrum with the same neuroanatomical orientation in order to minimize the possible influence of non-homogeneity or anisotropy. A cylindrical sample of tissue was removed from the cerebrum and sliced perpendicular to its long axis, approximately 5-7 mm from the medial end of the core in order to remove a disc-shaped tissue specimen approximately 1-2 mm thick and 10-12 mm in diameter, free from any penetrating sulci.

Each sample was subjected to oscillatory simple shear strain amplitudes of 2.5-5% (engineering strain) in a sequence over the frequency range of 20-200 Hz in 10 Hz increments. The shear modulus of porcine brain tissue presented significant age dependence. Firstly, regardless of age and strain amplitude,  $G'$  and  $G''$  increased significantly as a function of frequency. Secondly, except for  $G'(\omega)$  at a strain amplitude of 5%, the components of the complex shear modulus demonstrated a significant increase with age, as illustrated in Fig. 1. At 5% strain amplitude,  $G'(\omega)$  of the adult tissue did not significantly differ from the corresponding pediatric  $G'(\omega)$  across all frequencies. Finally, the cross-correlation between age and frequency revealed that the slope of  $G''(\omega)$  increased significantly with age, and that  $G'(\omega)$  only shifted in magnitude, with no significant age-related changes in frequency dependence. In conclusion, these authors showed that storage, loss, and complex shear moduli appear to increase with age, and that the shear modulus of young brain tissue was

independent from the strain level, whereas the shear modulus of adult brain tissue decreased when strain increased.

In order to determine the influence of brain mechanical properties on inertial pediatric brain injury, [17] measured the large deformation material properties of porcine pediatric and adult brain tissues. Pediatric brain tissue samples were obtained from 5-day-old piglets, while adult tissue was obtained from adult farm pigs (~1 year old). Rectangular porcine tissue samples (10x5x1 mm) were excised within 5 hours post-mortem from sections of the frontal lobe and thalamus, while maintaining consistent orientation from animal to animal. Gray (thalamus) and white matter (corona radiata) were tested in the adult tissue specimens. The pediatric tissue was tested only in one region because of the small size of the piglet brains. The pediatric samples were excised from the same location as the white matter samples in the adults, but they approximately comprised an equal distribution of white and gray matter. Using a custom-designed shear-testing apparatus, displacement and force were measured during rapid stress relaxation tests in simple shear up to 50% strain. The mechanical properties of the brain tissue for both infants and adults were found to be significantly different from each other.

In addition to the previous studies, [18] presented data describing the properties of infant and toddler brain tissue at large strains (up to 50%). In order to test the brain tissue for non-homogeneity and anisotropy, rectangular tissue samples (10X5X1mm) were excised from porcine sections of both white matter (corona radiata and corpus callosum) and gray matter (thalamus), while maintaining consistent orientation from animal to animal. The cause of death of the adult animals was rapid exsanguinations, while the pediatric animals were sacrificed using a lethal dose of potassium chloride or pentobarbital. All samples were transported in 4°C mock cerebral spinal fluid (CSF) solution and tested within 5 hours post-mortem. To test brain tissue properties for age-dependency, tissue samples were excised from 5-day-old (N=6) and 4-week-old (N=5) piglets, which present a composition and neurologic development equivalent to a human newborn (<1 month old) and toddler (approximately 1-3 years), respectively. Rectangular samples were taken from the same location as the corona radiata samples of the adult and tested along D1. Due to the smaller brain size, these tissue samples consisted of a mixture of approximately equal amounts of white (corona radiata) and gray matter. This data was then compared with the average white and gray matter properties for the adult porcine data. Each specimen was tested at strain rates ranging between 0.42 and 8.33 s<sup>-1</sup>. The porcine mechanical properties of the brain tissue in infant piglets and adult pigs were found to be significantly different from each other. [20] found significantly stiffer properties in adult tissue compared with pediatric brain tissue when measured at 1.25% shear strain over a frequency range of 20-200 Hz, while no significant differences between adult and pediatric tissue were observed at 2.5% shear strain.

Reference [20] observed that the adult (1-year-old) porcine brain tissue was significantly stiffer compared with immature (2-3-day-old) tissue when measured at 1.25% shear strain, but not at 2.5%, over a frequency range of 20-200 Hz. However, at larger strains (up to 50%), which are relevant to clinical head injury, the immature 5-day-old porcine tissue was about twice as stiff as the adult pig [18]. Indentation tests were also investigated by [8] on a rat brain. All results are superimposed in terms of shear modulus in Figure 6-14. In addition, the human brain undergoes significant alterations over the first 3 years of life. Neurons exhibit more extensive dendritic and axonal branching, which is accompanied by a rise in lipid content as axonal segments become myelinated [5]. However, at 3 years of age, the brain may be considered as mature, meaning that brain mechanical properties could be extracted from adults.

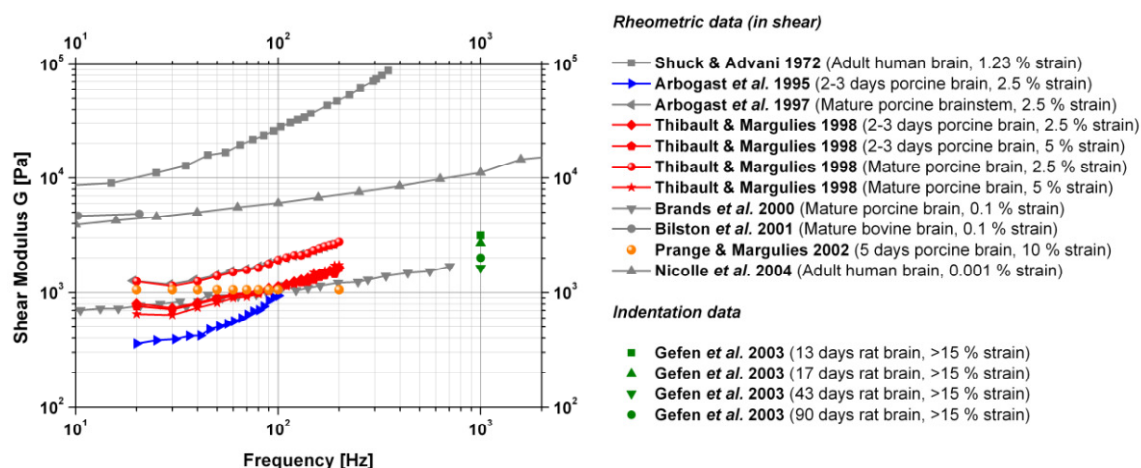


**Figure 6-14: Synthesis of paediatric brain mechanical properties available in the literature**

Concerning child cranial mechanical properties, little information is available for the infant skull. Thus, to determine the age-dependent changes in skull properties, [12] tested human and porcine infant cranial bone in three-point bending. Test specimens were typically 3-5 mm wide and 20-25 mm long, depending on the size of the original donor sample. Neonate pigs (age 2-3 days, N=30) were used in this study, and human infant cranial bone specimens were obtained at autopsy (N=4 subjects). Human subjects ranged from 25 weeks gestation to 6 months of age. Rupture modulus, elastic modulus, and energy absorbed to failure were evaluated for the human infant cranial bone samples in three-point bending subjects (N=4), with a total of 12 samples at “slow” (2.54 mm/min) and “fast” (2540 mm/min) rates. All of the three parameters measured showed an increase in their respective magnitudes as a function of age. This increase appeared to take place between birth and 6 months of age.

More recently, [6] reported material property data for paediatric skull and suture at high rates. Human paediatric cranial bone and suture were collected at autopsy. Subjects ranged in age from pre-term (21 weeks gestation) to 1 year of age. Two cranial specimens were removed and frozen from each subject, notably one occipital bone and one parietal-parasagittal sample containing suture and bone. Human paediatric cranial bone samples (N=46 specimens from 21 infant calveria) were tested in three-point bending using the drop test apparatus. Human paediatric cranial bone-suture-bone specimens (N=14 specimens from 11 calveria) were tested in tension in the drop test apparatus. Test rates for this study were determined by adjusting the height of the free-fall crosshead plate from 0.305 m to 0.914 m, which resulted in average test rates of 1.58 and 2.81 m/sec for the three-point bending tests. A significant influence of both location (parietal/occipital) and donor age on bending modulus and ultimate stress were observed. Parietal bone ultimate stress and modulus were larger than the occipital bone. Ultimate stress and modulus increased with the age of the donor, with a maximum stress of 51.5 MPa at 1 year of age.

To our knowledge, in the scientific literature, there is no available experimental study on the dry cranium of a 3-year-old child (3-year-old child) in terms of both stress and strain at fracture. In addition to this literature review on cranial bone, we recall the study of [10]. These authors proposed a curve fitting of the skull to Young’s modulus value as a function of age, based on the works of [9]-[13]. This evolution is represented in Figure 6-15.



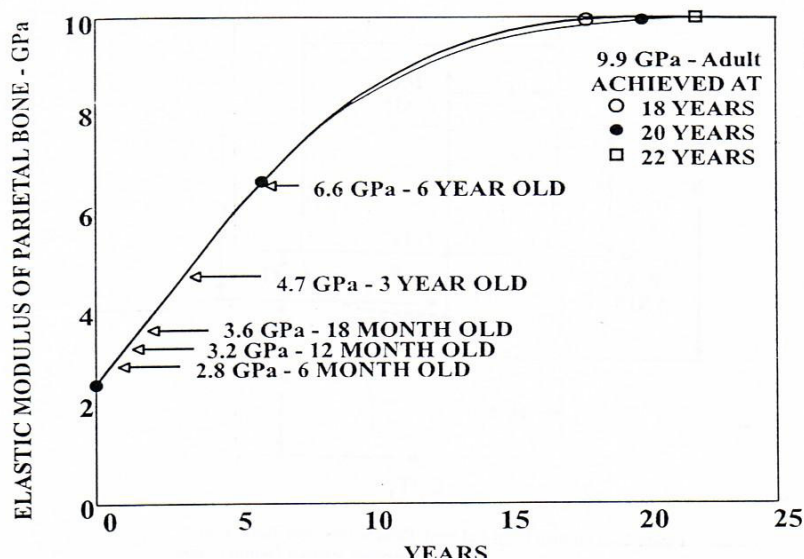


**Figure 6-15: Continue evolution of skull young modulus as a function of age [10]**

To our knowledge, no study to date has provided data on the validation of the human 3-year-old child head. As a consequence, there is a considerable difficulty in validating FEM in children. One way of investigating child head injury criteria using numerical models is to simulate real-world head trauma. Well-documented accidents may help understanding child injuries in comparing numerical mechanical parameters with the actual event, thus distinguishing between the biofidelic behaviour of a child numerical head and the ability to develop an injury predicting tool. Although the biofidelic behaviour of child models cannot be verified, investigations of child injury mechanisms may be performed by developing an injury predicting tool by means of studying the numerical simulation of a large number of real accidents and correlating the mechanical parameter outputs with observed injuries. Frequently, road accidents involve the head of the child impacting different structures in the vehicle, such as the side window, child seat, door handles, or even the front seat. These accidents are often very complex in terms of both the conditions surrounding the head and behaviour modelling of the different structures of the vehicle in question. In order to overcome these difficulties, it would appear that more “straightforward” accidents should be taken into account, that is to say, those involving less approximation for both the circumstances surrounding the accident and the impacted structure. For this reason, domestic accidents were chosen.

In the present study, 13 domestic accident reconstructions involving the fall cases of 3-year-old child were collected from the paediatric emergency departments of different hospitals. The information required for numerical reconstructions, such as age, gender, fall height, head injuries, associated injuries, ground characteristics, impact location, and estimated impact velocity, were extracted from medical files. In parallel, a 3-year-old child head FEM was developed while incorporating the main anatomic structures, notably scalp, brain, brain membranes, cerebellum, and brain stem as well as the bones of the cranium and face. Considering the computed mechanical responses under accident conditions and correlating the mechanical parameters with the occurrence of a given injury, we proposed to reconstruct numerically the collected domestic accidents with the 3-year-old child head model developed and thus, present some of the trends regarding the tolerance limits of skull fractures and neurological injuries in a 3-year-old child head model. Finally, a side road accident case from the CASPER database was selected and reconstructed numerically with the coupled 3-year-old child head-neck FEM. This coupled model was created using a previous 3-year-old child neck FEM developed by [14] along with the head model developed in this

present study. This road accident reconstruction provided an illustration of the methodology in order to predict some of the injuries and verify the capability of our 3-year-old child FEM so that it may be used in the future to optimize child protective systems, such as car seats.

## 6.2.2 Methods

### Development of a three year old child finite element head model

The proposed head FEM was based on the geometrical three-dimensional (3D) reconstruction of slices obtained using a computed tomography (CT) scan. Scanning was performed anonymously on a 3-year-old child for medical purposes without any relation to the present study. No abnormalities were observed by the medical staff. Furthermore, the dimensions and mass of the head corresponded to the 50<sup>th</sup> percentile for a 3-year-old child. The resolution of two-dimensional slices was millimetric, and threshold filtering was applied in order to distinguish the skull from the soft tissue. A 3D triangular mesh was then generated in Standard Tessellation Language (STL) format and imported with the Hypermesh V10.0 software for regular and homogeneous meshing, which was necessary using explicit codes like Ls-Dyna in order to have an acceptable time pitch. This 3-year-old child head model included the main anatomical features, namely the scalp, skull and sutures, face, cerebrospinal fluid (CSF), tentorium and falx membranes, and brain, as represented in Fig. 3. For the age of 3, a bone structure with lambdoid, sagittal, and coronal sutures was considered. Fontanelles were closed. The skull, sutures, and membranes were modelled as shell elements with uniform thickness. The thickness of the skull was 2.5mm based on measurements taken from the CT scan. The brain, CSF, and scalp were modelled as solid elements. The whole model comprised 19,682 solid and 7,640 shell elements.

The mechanical properties applied to the different parts of the head using the Ls-Dyna software are summarized in Table 6-1. An elastoplastic law with the Johnson-Cook damage model was chosen in order to allow for the mechanical component of the child's skull, which at 3 years of age, only contains cortical bone. Regarding the brain, a viscoelastic law was applied.

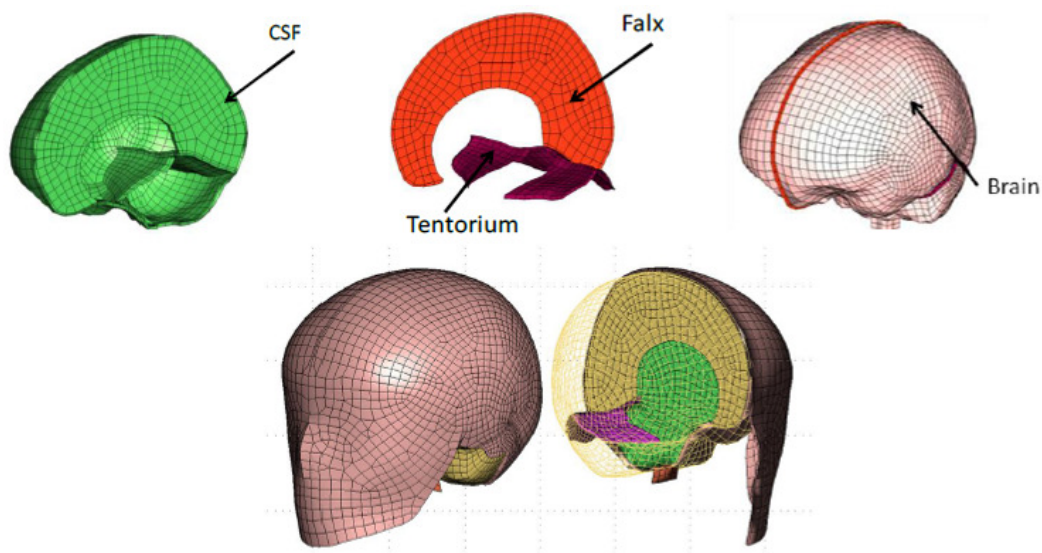


**Figure 6-16: Finite element model of the 3-year old child head**

**Table 6-1: Mechanical properties of the 3-year old child head FE model**

	Young's modulus [MPa]	Poisson's ratio	Density [g/mm <sup>3</sup> ]	Reference
Membranes	31.5	0.45	0.0014	[21]
CSF	0.012	0.499	0.00104	[7]
Scalp	16.7	0.42	0.0012	[7]

	Young's modulus [MPa]	Poisson's ratio	Density [g/mm <sup>3</sup> ]	Yield stress [MPa]	Failure parameter (□) [-]	Reference
Skull	4700	0.2	0.003	75	0.02	[12]

	Young's modulus [MPa]	Poisson's ratio	Density [g/mm <sup>3</sup> ]	Yield stress [MPa]	Failure parameter (□) [-]	Reference
Brain Brainstem	0.00104	1125	0.0167	0.049	0.145	[11]

### Accident database

With aim of reproducing the bone fracture of a 3-year-old child, we collected cases of domestic accidents from several hospitals. These domestic accidents involved free falls from different heights. The scenarios were diverse, but always straightforward, with the aim of approximating less between the numerical simulation and real accident. The scenario may have been a fall from a changing table, a bed, or even from the height of the child. All other scenarios, such as a fall from a shopping cart or stairs were excluded, as it was almost impossible to correctly estimate the height of the fall and thus, the impact speed of the head to the ground. Furthermore, only accidents recorded with the following data were included in the analysis: sex and age of the child, type of flooring, impacted area of the head, in addition to a complete and detailed description of cranial traumas caused by the fall. As regards the clinical descriptions obtained for each patient, injuries were classified in terms of the Abbreviated Injury Scale (AIS) and according to the following parameters: cranial bone fracture, loss of consciousness linked to diffuse axonal injury, and subdural hematomas in the brain. The database of the collected accidents is described in Table 6-2.

**Table 6-2: Domestic database**

	Age [Month]	Sex	Height fall [m]	Type of ground	Head impact location	Subdural hematoma	Injuries		
							Diffuse axonal injury	Skull fracture	AIS
C-72	30	M	0.9	Linoleum	Frontal	No	No	No	1
C-83	33	F	0.9	Concrete	Left Occipital	No	Yes	No	2
C-84	33	M	1.0	Tiling	Frontal	No	No	No	0
C-76	36	M	1.0	Tiling	Left Occipital	No	No	No	0
C-81	36	F	0.9	Gravel	Left frontal	No	Yes	No	2
C-87	36	F	0.9	Concrete	Face	No	No	No	0
C-89	36	M	1.4	Gravel	Left frontal	No	Yes	No	1
C-92	36	M	0.5	Gravel	Right frontal	No	No	No	0
C-93	36	M	1.2	Linoleum	Right temporal	No	No	No	0
C-31	31	M	4.0	Concrete	Right parietal	Yes	Yes	Yes	4
C-65	32	M	1.1	Concrete	Left Occipital	No	No	Yes	2
C-63	36	M	1.1	Concrete	Left Occipital	No	No	Yes	2
C-74	40	M	3.0	Tiling	Right parietal	No	Yes	Yes	2

### Domestic Accidents reconstructions methodology

In order to evaluate the head injury criterion (HIC), all of the accidents were reconstructed numerically using the FEM of a 3-year-old child (i.e., Q3) developed by ALYOTECH. However, to verify the ability of Q3 FEM to calculate HIC for the various configurations of falls to the ground, a trial was first conducted. To this end, a Q3 dummy developed by Humanetics was dropped from a height of 45 cm onto tarmac in order to obtain a first head impact. In parallel, a numerical simulation of the Q3 dummy fall was performed under the same conditions (same head orientation during impact, same flooring, and same impact speed).

The linear accelerations of the Q3 dummy head were recorded during the experimental trials. This fall scenario was reproduced numerically by applying an initial speed to all of the Q3 dummies, with the speed corresponding to a fall height of 2.91 m/s. Table 6-2 shows the linear acceleration of the head FEM compared with the Q3 dummy, showing that the FEM reproduces the head impact exactly in terms of both amplitude and impact duration. This study allowed us to confirm the validity of the HIC calculations, which would be used for all of the numerically reconstructed domestic accidents.

In order to reproduce the free fall cases, four types of surfaces were modelled conforming to the floors noted in the database.

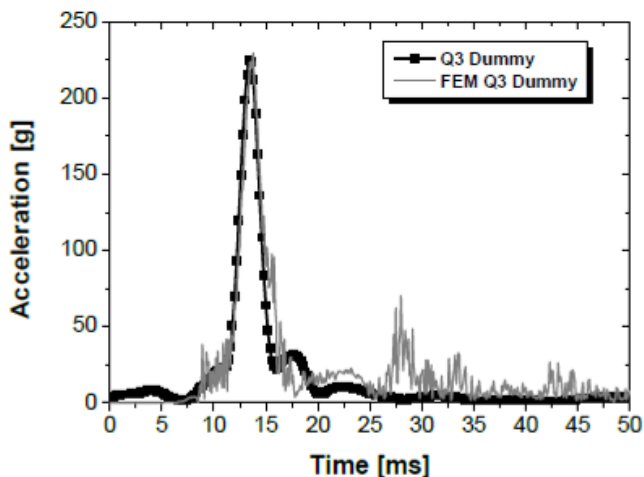


**Figure 6-17: Validation of the Q3 FEM head response in terms of acceleration in comparison with experiment**

For each numerically reconstructed domestic accident, two simulations were conducted. The first consisted of a Q3 FEM impact on the ground in order to calculate HIC, while the second involved a 3-year-old child head FEM to determine the cranial and intracerebral parameters (strain energy of the skull, minimal and maximal pressure,

Von Mises shear stress, strain, etc.). For these two types of simulations, an initial speed was applied to the models. The relation between the fall height and speed impact was calculated using the following formula:

$$V = \sqrt{2gh}$$

Where h is the fall height and g is gravity.

Finally, the impact point of the head was determined in relation to the clinical data reported in each of the 13 cases. The methodology used for reconstructing all of the accident cases is summarized in Figure 6-18. Once the mechanical parameters were calculated for the 13 accidents, a correlation was established between the clinically observed injuries and these parameters (global HIC and local FEM issues) in order to determine the best candidate for predicting injury risk.

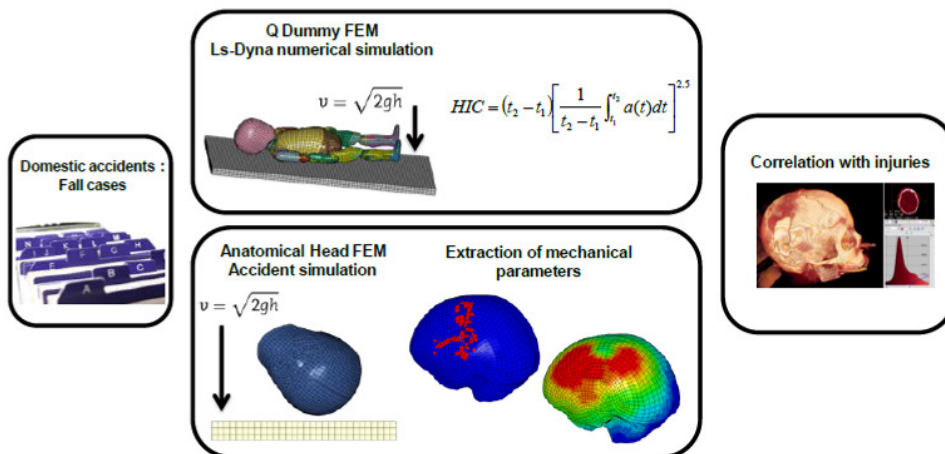


### Figure 6-18: Methodology used to reconstructed domestic accident and injury criteria

#### Illustration of a road accident reconstruction

One of the aims of developing this 3-year-old child head model was to protect the child in the car environment. The majority of cranial fractures occur in a side impact, leading to severe or fatal injuries. In order to verify the predictability of this model for this type of impact, we reconstructed a well-documented case from the CASPER database. This proposed case involved a side impact of a Renault Clio against a tree, with the impact speed estimated at 40 Km/h (case CCN-0196). This accident was reconstructed experimentally with an instrumented Q3 dummy. During the reconstruction, illustrated in Figure 6-19, we observed that the head impacted the side window, leading to a head injury of AIS 5.

To reproduce this impact numerically, the head FEM presented above was coupled with a 3-year-old child neck FEM, which was previously developed and validated by [14]. The coupling of these two models (Fig. 7) was performed by modelling the ligamentous system of the upper spine and creating an interface between the base of the skull and first cervical vertebra.

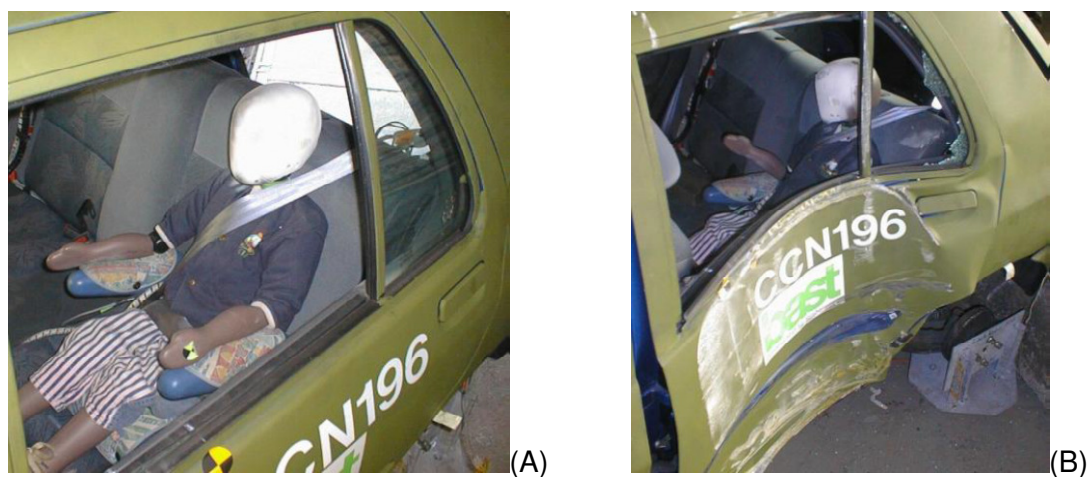


Figure 6-19: Illustration of the initial (A) and final (B) positions of the Q3 dummy during the experimental road accident replication

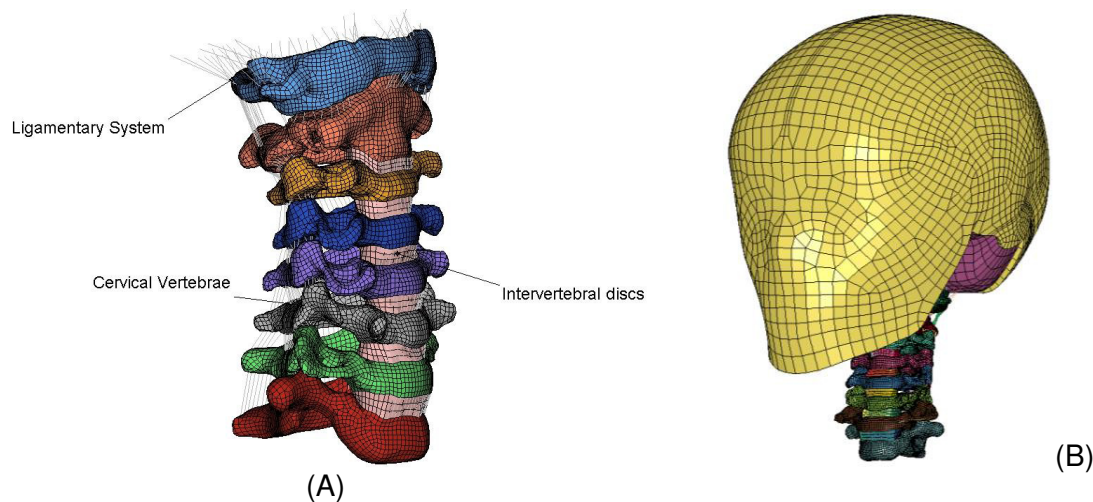


Figure 6-20: (A) Neck FEM of the 3 Year Old Child [Meyer] and (B) the its coupling with the developed 3year-old child head FEM

It should be highlighted that the Q3 dummies were not equipped with accelerometers at the first thoracic vertebra (T1), meaning that no kinematic information was available at this location; in contrast, the chest was equipped with a triaxial accelerometer. These accelerations recorded at the thorax were then implemented into the FEM in T1.

Finally, the side window was modelled by a layer of shell elements, with an elastic law being employed (Young’s glass modulus 72000MPa). The moment of the impact of the head with the side window was calibrated using a video recording during the reconstruction of the accident. The methodology used to reproduce this impact is illustrated in Figure 6-21.

The strain energy of the skull and maximum intracerebral Von Mises stress were calculated in order to evaluate the predictability of this FEM with regard to the clinically observed injuries.

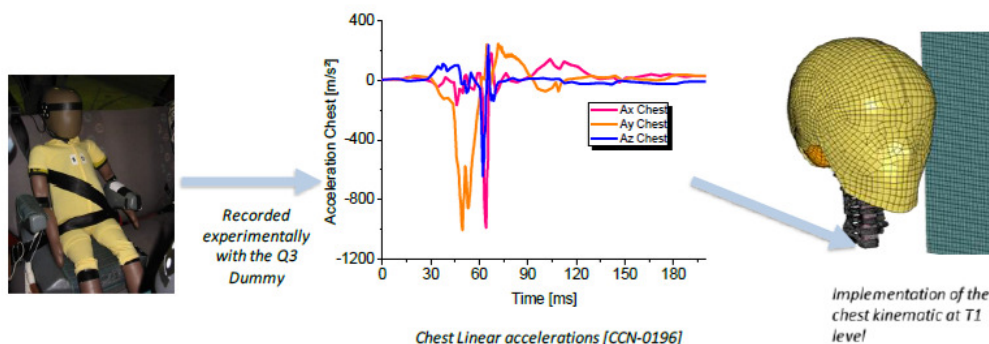


Figure 6-21: Methodology used to reconstruct road accident

6.2.3 Results

Numerical simulations of the collected domestic accidents

For each reconstructed domestic accident, HIC was calculated using the Q3 FEM. The results are presented in Figure 6-22 based on the observed AIS levels, with the different impacted regions being distinguished. The HIC levels ranged from 1,000 to approximately 50,000, with a predominance of high HIC levels for both side impacts. When visualizing the results as a histogram (Figure 6-23), AIS levels tended to correlate with the calculated HIC values, although there was not actually a threshold between AIS 1 and AIS 2 injuries. In addition, the calculated values were markedly higher than those determined by [16] (HIC fixed at 1000 for a risk of AIS >3 injury).

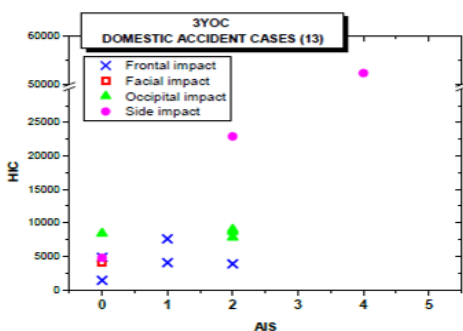


Figure 6-22: HIC calculated with the Q3 FEM for the 13 domestic accidents and classified by AIS level and impact locations

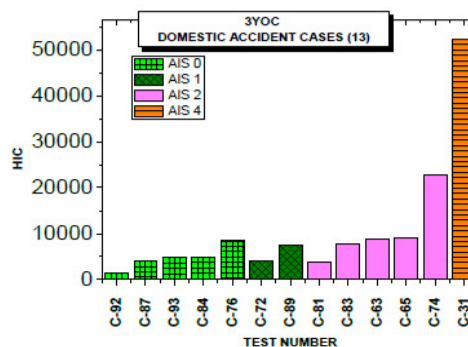
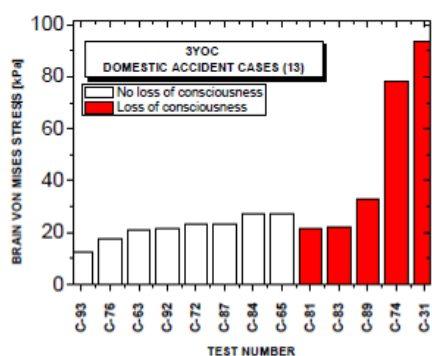


Figure 6-23: HIC values per AIS score obtained for 13 domestic accidents

Concerning the domestic accidents reconstructed with the 3-year-old child head FEM, the following parameters were calculated: intracranial pressure (Pmin and Pmax), Von

Mises stress, Von Mises strain, as well as main strain for predicting the diffuse axonal injury (DAI). For the prediction of skull fracture, only the strain energy of the skull was calculated.

For neurological injuries, the most relevant parameter was Von Mises stress, with pressure and intracerebral strain presented lower levels of correlation. Figure 6-24 illustrates the results as a histogram. Despite the limited number of cases, we nonetheless observed a threshold of around 25 kPa. For predicting skull fracture, Figure 6-25 clearly shows that cranial strain energy was correlated with this type of injury. There was a limit of 7.5 J between the cases presenting bone fracture and those without.



**Figure 6-24: Histogram in terms of intracerebral Von Mises stress for the 13 domestic accident cases**

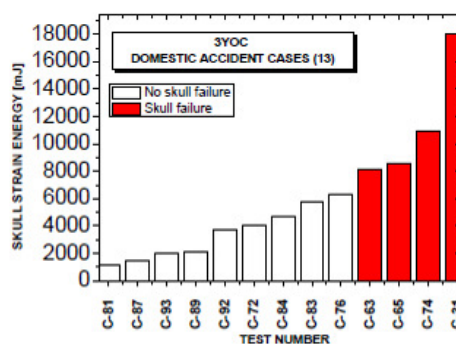


**Figure 6-25: Histogram in terms of skull strain energy for the 13 domestic accident cases**

### Road accident reconstruction

To evaluate the relevance of our 3-year-old child head FEM, a side impact was simulated in a car environment. An illustration of the head impact against the side window is proposed in Figure 7-13). The results are expressed in terms of Von Mises stress as well as strain energy in the brain, which was in line with the study conducted in the setting of domestic accidents. Maximum intracerebral Von Mises stress (Figure 6-27) was calculated at a value of 92 kPa, well above the limit of 25 kPa that was previously established for the loss of consciousness. This result is in accordance with the injuries observed (AIS 5). Regarding the skull, a fracture, as illustrated in Figure 6-28, may be numerically observed, while the strain energy calculated (15J) was two times the estimated limit during the reconstruction of domestic accidents.



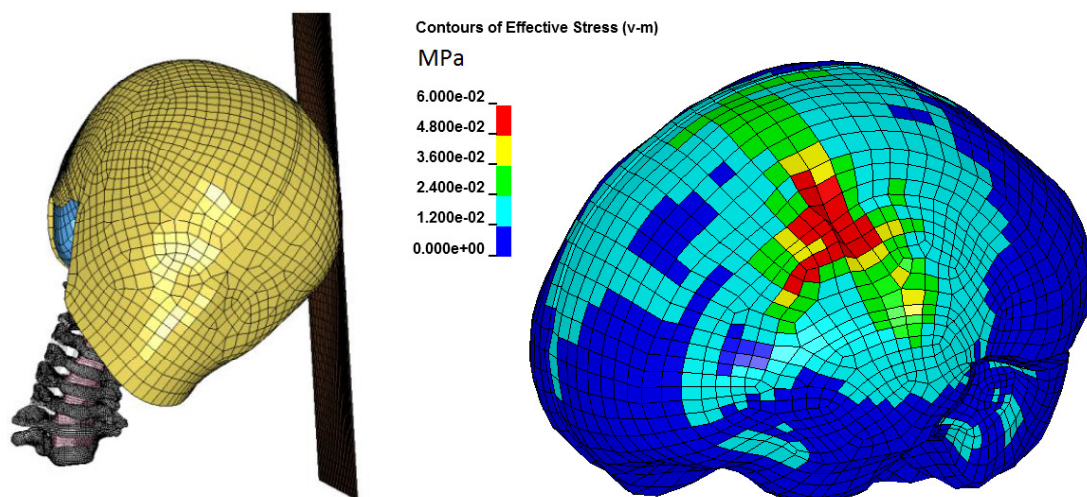


**Figure 6-26: Illustration of the head impact against the side window**

**Figure 6-27: Brain Von Mises stress field calculated**

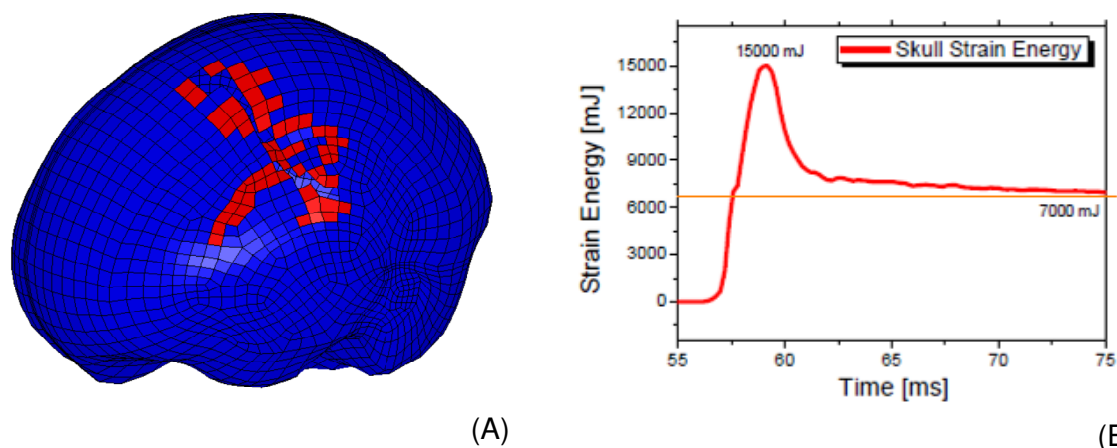


**Figure 6-28: Illustration of a skull fracture obtained numerically by reproducing the road accident case (A) and the skull strain energy calculated (B)**

#### 6.2.4 Discussion

Modelling the head of a child poses numerous difficulties. Firstly, there is little data on the mechanical properties of the different anatomical structures for evident ethical reasons, which poses a real biofidelity problem for FEM. Furthermore, there is no available validation to date for the head of a 3-year-old child. One of the only ways to overcome this lack of data is through the reconstruction of a large number of accidents. In our study, too few domestic accidents were reconstructed to be able to establish the tolerance limits of the craniocerebral system.

During the reconstruction of road accidents, several problems arise:

- The lack of precise data concerning T1 kinematics: during reconstruction of cases, only the linear acceleration of the thorax was recorded, whereas both linear and angular accelerations should be recorded at the T1 level;
- Simulating the mechanical behaviour of the different structures impacted by the head (window, pillars, etc.) is difficult and even more so when this structure was itself impacted and deformed during the accident;
- The experimental reconstruction of this type of accident has its own limitations and approximations (estimating the speed of the vehicle in question, position of the dummy, etc.).

- What about the biofidelity of the dummies used in the experiments?

Despite all of these limitations, the initial results obtained in the framework of this study appear encouraging.

### 6.2.5 Conclusions

This study proposed a detailed FEM of a 3-year-old head involving the principal anatomical structures (scalp, brain, CSF, membranes, and skull). A database pertaining to 13 domestic fall cases was collected from different hospitals, with these accidents being numerically reconstructed. This type of accident has the advantage of being simple to reconstruct numerically, thus minimizing simulation errors. Each accident was first reconstructed using a Q3 FEM, with the aim of obtaining the HIC, which is the criterion mostly used in road safety. Although there is a notable difference between the cases with high AIS and those without any injuries, the HIC reported in our findings, being well above that found in the literature, did not clearly reveal a threshold for moderate injuries. Furthermore, the same accidents were then reconstructed with a 3-year-old head FEM, which was developed in the framework of this study. Several mechanical parameters were extracted from this model, with the aim of identifying the mean criterion able to predict loss of consciousness and bone fracture. This often fatal injury is frequently encountered in the case of side impact during a car accident. Regarding loss of consciousness, Von Mises stress in the brain was a parameter likely to reflect this injury mechanism, with a threshold of around 25 kPa. For bone fracture, the use of the Johnson-Cook model law allowed for cranial fracture to be predicted, while cranial strain energy approached a threshold of around 7.5 J.

With the aim of predicting child head injury in a car environment, this model was reconstructed using a case taken from the CASPER database. This case involved a side impact at a relative speed of 40 Km/h, leading to AIS 5 injury of the head. In order to reproduce this head impact, a 3-year-old child head FEM was coupled with a neck model, previously developed and validated by Meyer *et al.* (2007). In terms of the Von Mises stress for neurological injuries and cranial strain energy, our findings are in line with the preliminary results that we obtained for our domestic accident reconstructions. Despite the difficulties mentioned in the discussion, it would appear that such a tool may be used in the future in order to significantly contribute to the improvement of vehicle protection systems for children.

### 6.2.6 Acknowledgements

The authors would like to thank Dr. Meyer and the paediatric department of the Necker Hospital for their contributions, in addition to the CASPER FP7 project for their financial support.

### 6.2.7 References

- [1] Arbogast, K.B. and Meaney, D.F., Biomechanical characterization of the constitutive relationship of the brainstem. Proc. Of the Society of Automotive Engineers, pp.153-159, 1995.
- [2] Arbogast, K.B. and Margulies, S.S., Material characterization of the brainstem from oscillatory shear tests. Journal of Biomechanics 31, pp.801-807, 1998.
- [3] Brands D.W.A, Bovendeerd P.H, Peters G.W.M, The large shear strain dynamic behaviour of in-vitro porcine brain tissue and a silicone gel model material,

- Proceedings of Stapp Car Crash Conference, paper 2000-01-SC17, 249-260, 2000.
- [4] Bilston L E., Liu Z., Phan-Thien N, Large strain behavior of brain tissue in shear: Some experimental data and differential constitutive model. *Journal of Biorheology*, 38, 335-345, 2001.
- [5] Calder I.M, Hill I, Scholtz C.L, Primary brain trauma in non-accidental injury. *J. Clin. Pathol.*, 37, 1095–1100, 1984.
- [6] Coats B, Margulies S.S, High rate material properties of infant cranial bone and suture. *Proceedings of ASME Summer Bioengineering*, 2005.
- [7] Deck, C., and Willinger, R., Improved head injury criteria based on head FE model. *International Journal of Crashworthiness*, Vol.13, No6, pp.667-678, 2008.
- [8] Gefen A, Gefen N, Zhu Q, Raghupathi R, Margulies S.S, Age-dependent changes in material properties of the brain and braincase of the rat. *J. Neurotrauma*, 20, 1163–1177, 2003.
- [9] Hubbard R. P, Flexure of Layered Cranial Bone, *J. Biomech.*, 4, 251–263, 1971.
- [10] Irwin A, Mertz H.J, Biomechanical Basis for the CRABI and Hybrid III Child Dummies, *Proceedings of Stapp Car Crash Conference*, paper 973317, 261-272, 1997.
- [11] Kruse, S., Rose, G., Glaser, K., Manduca, A., Felmlee, J., Jack Jr., C., Ehman, R., Magnetic resonance elastography of the brain. *NeuroImage* 39 (1), 231–237, 2008.
- [12] Margulies S.S, Thibault K.L, Infant skull and suture properties: measurements and implications for mechanisms of pediatric brain injury. *J. Biomech. Eng.*, 122, 364–371, 2000.
- [13] McPherson G. K, Kriewall T. J, The Elastic Modulus of Fetal Cranial Bone: A First Step Towards an Understanding of the Biomechanics of Fetal Head Molding, *J. Biomech*, 13, 9–16, 1981.
- [14] Meyer F, Bourdet N, Roth S, Willinger R, Three years old child neck FE modelling under automotive accident conditions, *Proceedings of IRCOBI Conference Conf.*, 277- 289,2007.
- [15] Nicolle S, Lounis M, Willinger R, Shear properties of brain tissue over a frequency range relevant for automotive impact situations: new experimental results, *Proceedings of Stapp Car Crash Conference* 48, paper 2004-22-0011, 239–258, 2004.
- [16] Palisson A, Cassan F, Troseille X, Lesire P, Alonzo F, Estimating Q3 Dummy Injury Criteria for Frontal Impact Using the CHILD Project Results and Scaling Reference Values, *Proceedings of the IRCOBI*, 2007.
- [17] Prange M, Kiralyfalvi G, Margulies S, Pediatric rotational inertial brain injury : The relative influence of brain size and mechanical properties, *Proceedings of Stapp Car Crash Conference*, paper 99SC23, 350-360, 1999.

- [18] Prange M.T, Margulies S.S. Regional, directional and age-dependent properties of the brain under-going large deformations. J. Biomech. Eng., 124, 244-252, 2002.
- [19] Shuck L.Z, Advan S.H, Rheological response of human brain tissue in shearing. ASME Journal of Biomechanical Engineering, 905-911, 1972.
- [20] Thibault, K, Margulies S.D, Age-dependent material properties of the porcine cerebrum: effect on pediatric inertial head injury criteria, Journal of Biomechanics, 31, 1119-1126, 1998.
- [21] Zhou C, Kahlil T.B, Dragovic L.J, Head injury assessment of a real world crash by finite element modelling, Proceedings of the AGARD Conference, 1996.

### **6.3 Six-years-old child head-neck finite element modelling application to the Interaction with airbag in frontal and lateral Impact**

#### **6.3.1 Introduction**

The growing demand for greater mobility in Europe has made individual transportation an essential and even inevitable feature of modern living. Children are more and more often conveyed in cars or other modes of road transportations. With this increased travels, the risk for children, of becoming involved in an accident as occupant has consequently increased. Based on the above accident data, it is obvious that in spite of the significant improvements in recent years in vehicle safety, the current number of deaths and casualties added to the social and economic costs is still unacceptable. Fatalities and injuries, especially to children, shall be reduced by all the available ways: public regulation, prevention/education of road users, road infrastructure, compatibility between vehicles, active, passive and tertiary safety devices. As regards children, it is very difficult to obtain figures for fatalities or severely injured children in the 27 European Countries, but if we consider the EU 15 countries, where the use of child restraint is mandatory since a long time, approximately 600 children are killed in cars on the European roads and 80 000 are injured (data source: IRTAD). If there has been a huge effort on human adult FE modelling only very few attempts exist as long as children are concerned.

Due to ethical reasons, there is paucity in experimental data concerning the child's head and neck characterization. As a consequence, there is a considerable difficulty for the validation of children FE models. For the neck validation one solution is to use the Scaling method's established by Irwin's and Mertz 1997. This method permits to calculate a theoretical experimental corridor based on the adult experimental data, in terms of displacement and acceleration. The mechanical properties such as the mass density of the cervical vertebrae, the rigidity both for the intervertebral discs and the ligament are calculated with this scaling method.

One way to investigate child head injury criteria using numerical models is to simulate real world head trauma. Well documented accidents can help to understand child injuries in comparing numerical mechanical parameters with what really happened, distinguishing biofidelic behaviour of a child numerical head and the ability to have an injury predicting tool. Indeed, even if the biofidelic behaviour of child models cannot be checked, based on classical experimental versus numerical validation process, investigations of child injury mechanisms can be performed by developing an injury predicting tool, studying numerical simulation of a large number of real accidents and to correlate mechanical parameters outputs with observed injuries. In the present work these previous published Head and Neck models are coupled to a simplified thorax in order to investigate child head-neck response under frontal and lateral airbag deployment as a function of initial distance between airbag and head.

### 6.3.2 Materials and methods

#### The UdS FE head model

##### Meshing

The UdS Head FE Model Kang *et al.* (1998) was used for this study. The geometry of the inner and outer surfaces of the skull was digitised in the Strasbourg laboratory from a human adult male skull. The data given in an anatomical atlas by Ferner *et al.* (1997) was used to mesh the human head using the Hypermesh code. For this model, the option was chosen to retain a given realistic human adult anatomy rather than trying to find an average geometry, which may not exist. Figure 6-29a below shows the 3D-skull surface obtained by digitising external and internal surfaces of the skull as well as the meshed model (Figure 6-29b).

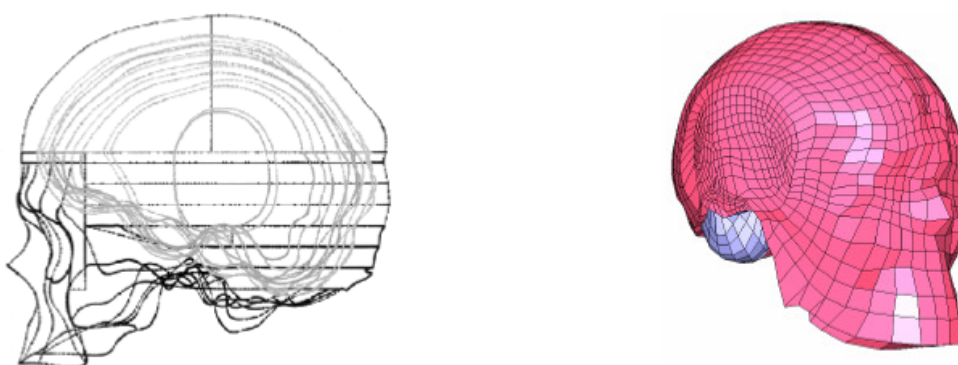


**Figure 6-29: 3D skull surfaces used for the model construction and skull meshing**

The falx and tentorium were simulated with a layer of shell elements, the skull comprised a three layered composite shell and the remaining features were modelled with brick elements. Of particular importance, and rarely modelled, is the subarachnoid space between the brain and the skull, which in this model was represented by one layer of brick elements to simulate the cerebral-spinal fluid. The tentorium separated the cerebrum and the cerebellum, and the falx separated the two hemispheres. Brick elements were used to simulate the cerebral-spinal fluid that surrounds these membranes. A layer of brick elements also modelled the scalp, which surrounds the skull and facial bone. Overall, the current head model, illustrated in Figure 2, consists of 14643 elements and it has a total mass of 4.5 kg.

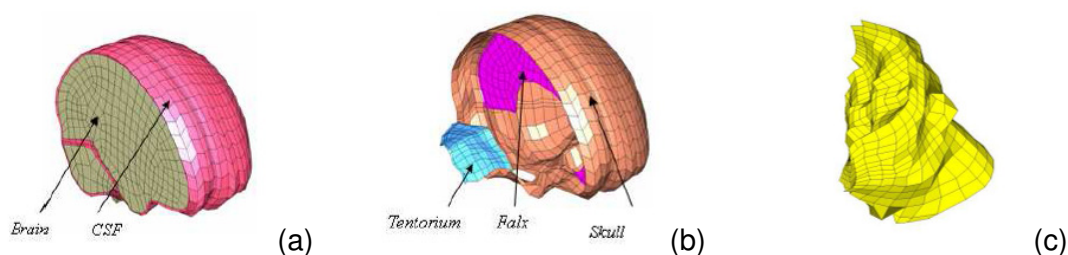


**Figure 6-30: Meshing of the intra-cranial medium brain and CSF (a), falx, tentorium and Skull (b) and face (c)**

##### Mechanical properties

Material properties assigned to the different parts of the UDS Finite Element Head Model are all isotropic and homogenous. The Young's modulus of the subarachnoid space was found by Willinger *et al.* (1995) by modal analysis. The viscoelastic

properties assigned to the brain were scaled from Khalil *et al.* (1977). The behaviour in shear was defined by:

$$G(t) = G_{\infty} + (G_0 - G_{\infty}) \text{Exp}(-\beta t)$$

Where:  $G_0$ : Short term shear modulus,  $G_{\infty}$ : Long term shear modulus and  $\beta$ : Decay constant.

The skull was modelled by a three layered composite shell representing the inner table, the diploë and the external table of human cranial bone. In order to reproduce the overall compliance of cranial bone, a thickness in combination with an elastic brittle law were selected for each layer. In order to model the material discontinuity in the case of fracture, it was necessary to use values for the limiting (ultimate) tensile and compressive stress obtained from Piekarski (1970) and integrated in the Tsai-Wu criterion. All mechanical properties and element characteristics of the Head FEM are summarized in Table 6-3.

**Table 6-3: Mechanical properties and element characteristics of the UDS Head FE model**

Part	Material property	Material parameter	Value	Element type	Shell thickness [mm]
Face	Elastic	Density Young's modulus Poisson's ratio	2500 kg/m <sup>3</sup> 5.0E+03 MPa 0.23	Shell	10.0
Cranium (cortical)	Elastic plastic orthotropic	Density Young's modulus Poisson's ratio Bulk modulus UTS UCS	1900 kg/m <sup>3</sup> 1.5E+04 MPa 0.21 6.2E+03 MPa 90.0 MPa 145.0 MPa	Shell	2.0
Cranium (trabecular)	Elastic plastic orthotropic	Density Young's modulus Poisson's ratio Bulk modulus UTS UCS	1500 kg/m <sup>3</sup> 4.6E+03 MPa 0.05 2.3E+03 MPa 35.0 MPa 28.0 MPa	Shell	3.0
Scalp	Elastic	Density Young's modulus Poisson's ratio	1.0E+03 kg/m <sup>3</sup> 1.67E+01 MPa 0.42	Solid	/
Brain	Viscous elastic	Density Bulk modulus Short shear mod. Long shear mod. Decay constant	1040 kg/m <sup>3</sup> 1.125E+03 MPa 4.9E-02 MPa 1.62E-02 MPa 145 s <sup>-1</sup>	Solid	/
CSF	Elastic	Density Young's modulus Poisson's ratio	1040 kg/m <sup>3</sup> 0.12E-01 MPa 0.49	Solid	/
Falx	Elastic	Density Young's modulus Poisson's ratio	1140 kg/m <sup>3</sup> 3.15E+01 MPa 0.45	Shell	1.0
Tentorium	Elastic	Density Young's modulus Poisson's ratio	1140 kg/m <sup>3</sup> 3.15E+01 MPa 0.45	Shell	2.0

### Head validation and injury criteria

A total of eight instrumented cadaver impacts were reconstructed with the objective of validating the Head FEM under very different impact conditions. The Head FEM has been validated against Nahum's *et al.* 1977 impact in order to validate brain mechanical behaviour and has moreover been validated against other experimental data as those of Trosseille *et al.* 1992 for high damped long impact durations, and those of Yoganandan 1994 for very short impact durations including bone fracture.

In an attempt to develop improved head injury criteria 68 real world head trauma that occurred in motor sport, motorcyclist, American football and pedestrian accidents were reconstructed with UDS Head FEM (Deck *et al.*, 2008). Statistical analysis was then carried out on global head response parameters, such as peak linear and rotational acceleration of the head and HIC, and the intra cerebral parameters computed with the

head FE model, such as the Von Mises Stress or strain and pressure in the brain, in order to determine which of the investigated metrics provided the most accurate predictor of the head injuries sustained in the accidents. Tolerance limits to specific injury were proposed and summarized in Table 6-4 to Table 6-6 for DAI injuries, SDH and skull fracture respectively.

**Table 6-4: Proposed tolerance limits for a 50% risk of mild and severe DAI injuries**

	Mild DAI	Severe DAI
Brain Von Mises strain [%]	25	35
Brain First principal strain [%]	31	40
Brain Von Mises stress [kPa]	26	33

**Table 6-5: Proposed tolerance limits for a 50% risk of subdural haematoma**

	SDH
Minimum of CSF pressure [kPa]	-135

**Table 6-6: Proposed tolerance for a 50% risk of skull fracture**

	Skull fracture injury
Skull strain energy [mJ]	865

## The UoS neck FE model

### Meshing

The UoS Neck FE model (Meyer *et al.* 2004) geometry is based on a living human subject close to 50th percentile male: [Height: 1.72 m, weight: 72 Kg, age: 33 years]. This approach allows us not to make any approximation regarding the geometry of the cervical vertebrae. The principal anatomical parts were taken into account i.e. the cervical vertebrae (shell elements), the intervertebral discs (bricks elements), the upper and lower ligamentary system (springs elements) and the muscles (bricks and spring elements) as illustrated in Figure 3. Figure 6-31 and Figure 6-32 illustrated the continuous meshing between the Head FE model and the Neck FE model.

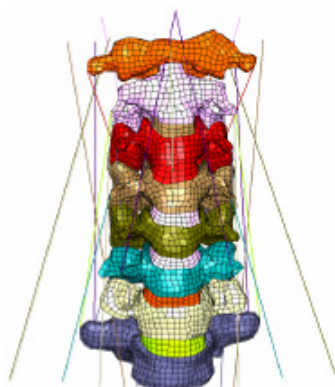


**Figure 6-31: The cervical column**

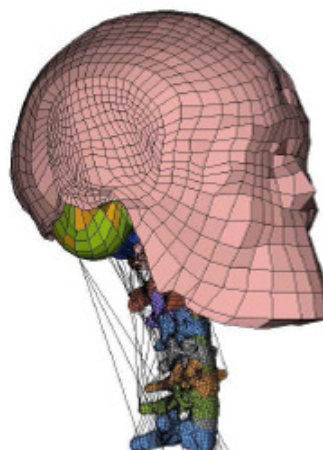


**Figure 6-32: Head-neck FE model**

### Mechanical properties



The ligaments were modelled using non-linear spring elements with a damping coefficient of  $h=900$  Nm/s (De Jager *et al.* 1996,  $h=300$ Nm/s, Dauvilliers 1994,  $h=2000$ Nm/s). To define the behaviour laws of each ligament in both the lower and upper cervical spines, we referred to two complementary studies by Chazal *et al.* (1985) and Yoganandan *et al.* (2001). The Chazal *et al.* study (1985) highlights the non-linear viscoelastic behaviour of ligaments whereas Yoganandan *et al.* (2001) gives information on their failure properties. The overall behaviour of the ligaments can then be characterised by three pairs of coefficients  $a_1$ ,  $a_2$ ,  $a_3$  determining the zone of low rigidity or neutral zone, the linear part, and finally the plastic behaviour. The coefficients used for our model are described in Table 6-7 and a representation of the typical behaviour of the five ligaments of the lower cervical spine is illustrated in Figure 6-33.

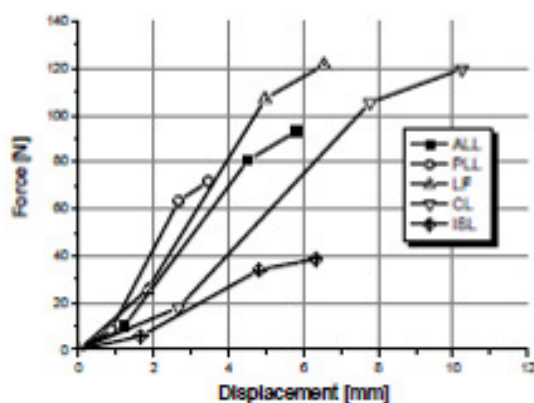


**Figure 6-33: Behaviour laws of the anterior longitudinal ligaments (ALL C2-C5), posterior longitudinal ligament (PLL C2-C5), flaval ligament (FL C2-C5), interspinous ligament (ISL C2-C5), capsular ligament (CL C2-C5) [Yoganandan *et al.* (2001) and Chazal *et al.* (1985)]**

In order to take into account the initial lengths of the ligaments in the model, as well as those measured anatomically by Yoganandan *et al.* (2001) on the lower cervical spine, we calculated the laws as follows:

$$\begin{cases} d_i = \alpha_i * L * \left(\frac{L_m}{L}\right) \\ F_i = \frac{F_s * \alpha_i}{N_{spring}} * \left(\frac{L_m}{L}\right) \end{cases} \quad i=1,2,3$$

Where  $d_i$  is the spring elongation,  $F_i$  the force,  $N_{spring}$  number of springs,  $L$  the experimental ligament length and  $L_m$  the mean length spring in the model.

For the upper ligaments the initial experimental lengths are not given by Yoganandan *et al.* (2001), so the ratio between the initial length of the model and experiment are equal to 1.

**Table 6-7: Coefficients used to define the ligaments constitutive laws (Chazal *et al.* 1985). The rupture strengths are taken from Yoganadan *et al.* (2001)**

Ligament	$\square_1$		$\square_2$		$\square_3$			
	$\square_1/\square_{3max}$ ax	$F_1/F_{3max}$	$\square_2/\square_{max}$	$F_2/F_{3max}$	$\square_{3max}$ C2- C5	$F_{3max}$ C2-C5	$\square_{3max}$ C5-T1	$F_{3max}$ C5-T1
ALL	0.21	0.11	0.78	0.87	0.308	92.8	0.354	145.2
PLL	0.25	0.12	0.77	0.89	0.182	71.1	0.341	188.2
FL	0.28	0.21	0.76	0.88	0.77	121.5	0.884	129.1
ISL	0.30	0.17	0.75	0.87	0.609	38.6	0.681	38.6
CL	0.26	0.15	0.76	0.88	1.41	119.7	1.16	181.1
Average for the upper cervical spine	0.26	0.15	0.76	0.88	1	-	1	-

In our model the hypothesis of a homogeneous linear elastic isotrope material was considered with a Young modulus of 100 MPa and a Poisson's ratio of 0.3. These values are situated between the extreme values related in the literature which represents a global behaviour of this structure (Kleinberger (1993), Dauvilliers (1994)). The cervical vertebrae were declared as rigid bodies. The mechanical characteristics in terms of masse and inertias are taken from the work of Deng *et al.* (1987) and detailed in table 6.

**Table 6-8: Inertial properties of the cervical vertebrae and head applied to the centres of gravity**

Name	Mass [kg]	Ixx [kg/m <sup>2</sup> ]	Iyy [kg/m <sup>2</sup> ]	Izz [kg/m <sup>2</sup> ]
T1	-	-	-	-
C7	0.22	2.2	2.2	4.3
C6	0.24	2.4	2.4	4.7
C5	0.23	2.3	2.3	4.5
C4	0.23	2.3	2.3	4.4
C3	0.24	2.4	2.4	4.6
C2	0.25	2.5	2.5	4.8
C1	0.22	2.2	2.2	4.2
Head	4.69	181	236	173

### Neck validations

This model was validated with the NBDL data in frontal, lateral, oblique and in rear impact with the Prasad (1997) test. Moreover in order to reproduce the “s-shape” a modal validation was perform with the test realize at the Strasbourg University (Willinger *et al.* 2005). The Figure 6-34 illustrated the frequency validation in terms of apparent mass.

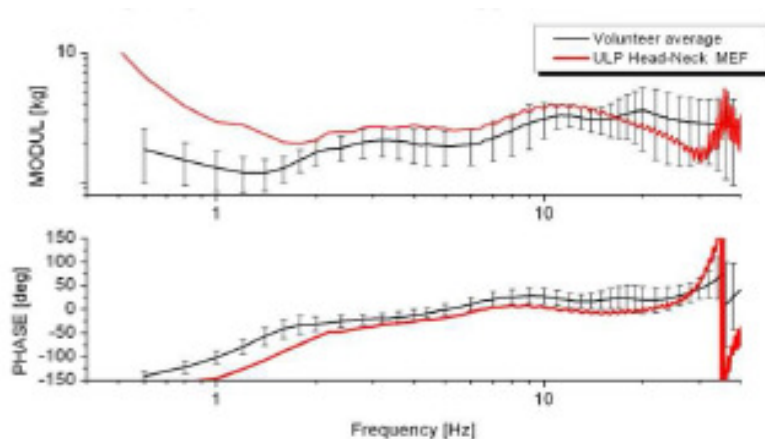


**Figure 6-34: Head-neck system validation in terms of apparent mass at the vertex**

### Six years old child head-neck FE model

In order to develop a 6 year old child head-neck FE model based on the adult one, it was necessary to apply the appropriate scale factors. The reference used to obtain the geometrical factors is Irwin *et al.* 1997 and for the dynamical factor it was referred to Kumaresan *et al.* 2001.

#### Geometrical aspect

The characteristic dimensions were based on the size of children in the United States (Weber *et al.* 1985 and Reynolds *et al.* 1976). With these data the neck scale factor was established at 0.689 in all directions. Concerning the Head the scale factor was established at 0.914. Figure 6-35 summarise the external dimension of the Head and Neck Segment (Irwin *et al.* 1997) and Table 6-9 recapitulate the 6 year old child FE model dimension.

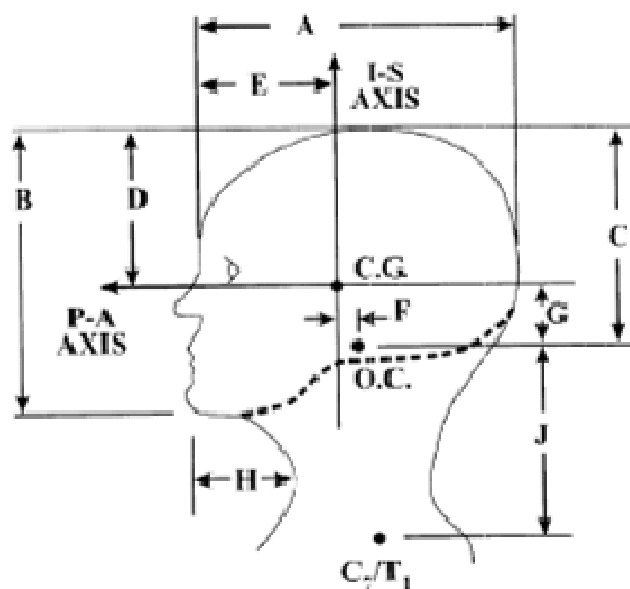


**Figure 6-35: Pertinent head and neck dimensions describe by Irwin *et al.* (1997)**

**Table 6-9: Comparative head and neck dimensions for the 50<sup>th</sup> 6 year-old child (Irwin *et al.* (1997)) and head-neck FE model**

Description	CHILD 50 <sup>th</sup> 6 year-old child (mm)	6 year-old child FE Model (mm)
A	180	177
B	182	185
C	127	138
D	87	83
E	76	87
F	16	11
G	40	51
H	49	-
J	95	94

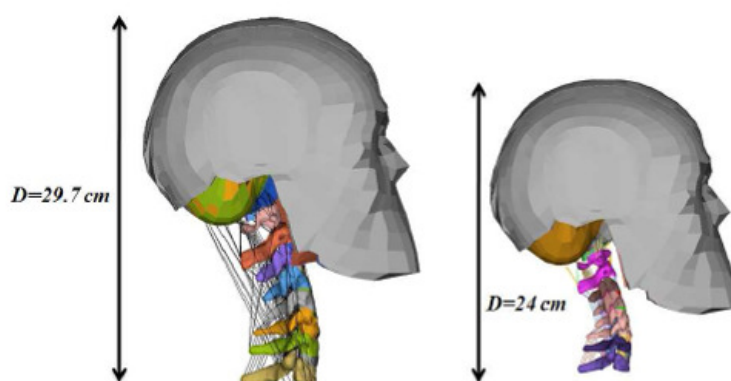


**Figure 6-36: Comparison between the Adult and the scaled 6 year old child head-neck FE model**

If the scaling method can be applied for the head size and shape the bone thickness can however not be scaled as illustrated in Figure 6-37. The skull thickness was therefore fixed at 3 mm for the present 6 year old child skull model.

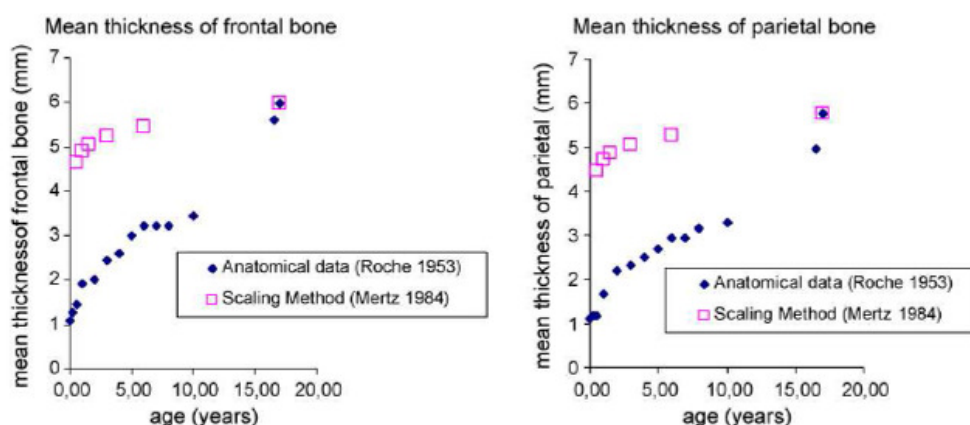


**Figure 6-37: Evolution of skull thickness as a function of age from anatomical study (Roche and scaling method Irwin *et al.* 1997)**

Mechanical properties

Head-FE model

Concerning the skull mechanical properties an elastic law was implemented with a Young modulus set to 6.6 GPa (Irwin *et al.* 1997). The others biomechanical parts have the same mechanical properties as the adult model (table 8). Finally the Head mass was calculated at 3.200 Kg. General evolution of skull elastic modulus as a function of age is recalled at Figure 6-38.

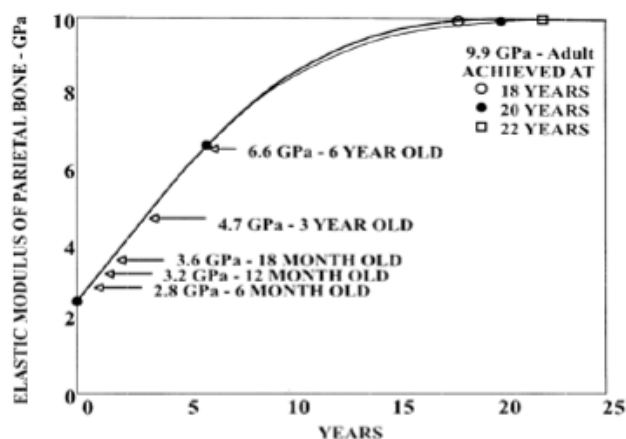


Figure 6-38: Elastic bending modulus of parietal skull bone as a function of age

Table 6-10: Mechanical properties and element characteristics of the UDS 6 year old child head FE model

Part	Material property	Material parameter	Value	Element type	Shell thickness [mm]
Scalp	Elastic	Density	1.0E+03 kg/m <sup>3</sup>	Solid	/
		Young's modulus	1.67E+01 MPa		
		Poisson's ratio	0.42		
Brain	Viscous elastic	Density	1040 kg/m <sup>3</sup>	Solid	/
		Bulk modulus	1.125E+03 MPa		
		Short shear mod.	4.9E-02 MPa		
		Long shear mod.	1.62E-02 MPa		
		Decay constant	145 s <sup>-1</sup>		
CSF	Elastic	Density	1040 kg/m <sup>3</sup>	Solid	/
		Young's modulus	0.12E-01 MPa		
		Poisson's ratio	0.49		
Falx	Elastic	Density	1140 kg/m <sup>3</sup>	Shell	1.0
		Young's modulus	3.15E+01 MPa		
		Poisson's ratio	0.45		
Tentorium	Elastic	Density	1140 kg/m <sup>3</sup>	Shell	2.0
		Young's modulus	3.15E+01 MPa		
		Poisson's ratio	0.45		

Neck FE model

The scaling process affects the mass and inertial properties of each part. Mass and inertia properties were scale down using Irwin *et al.* 1997. Table 6-11 gives the scale factor for head mass, vertebrae mass and the Young modulus of the intervertebral disc.

Concerning the behaviours laws of the ligaments the same methodology was used as for the adult. It means that the scale factor concerns only the failure forces ( $F_{max}$ ).

**Table 6-11: Mechanical scale factors for biomechanical part (Irwin *et al.* 1997)**

$\lambda_m$ Head (Mass)	0.764
$\lambda_m$ Vertebrae (Mass)	0.267
$\lambda$ Intervertebral disc (Young modulus)	0.734
$\lambda$ Ligament (Force Max)	0.861

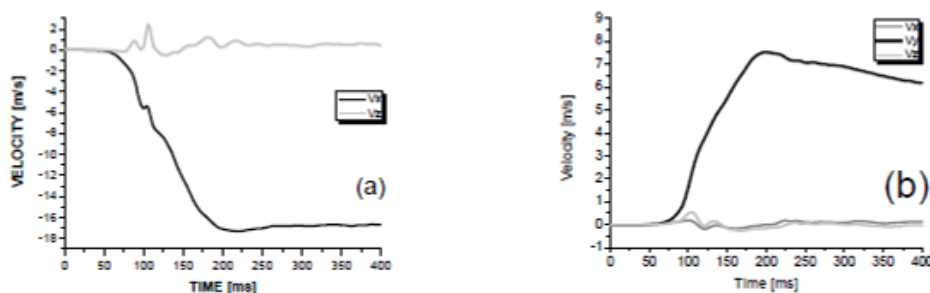
Table 6-12 gives the inertia computed with the 6 year old child Neck FE model. The neck mass was calculated at 1.250 kg.

**Table 6-12: Inertial properties of the cervical vertebrae and head applied to the centres of gravity for the 6 year old child FE model**

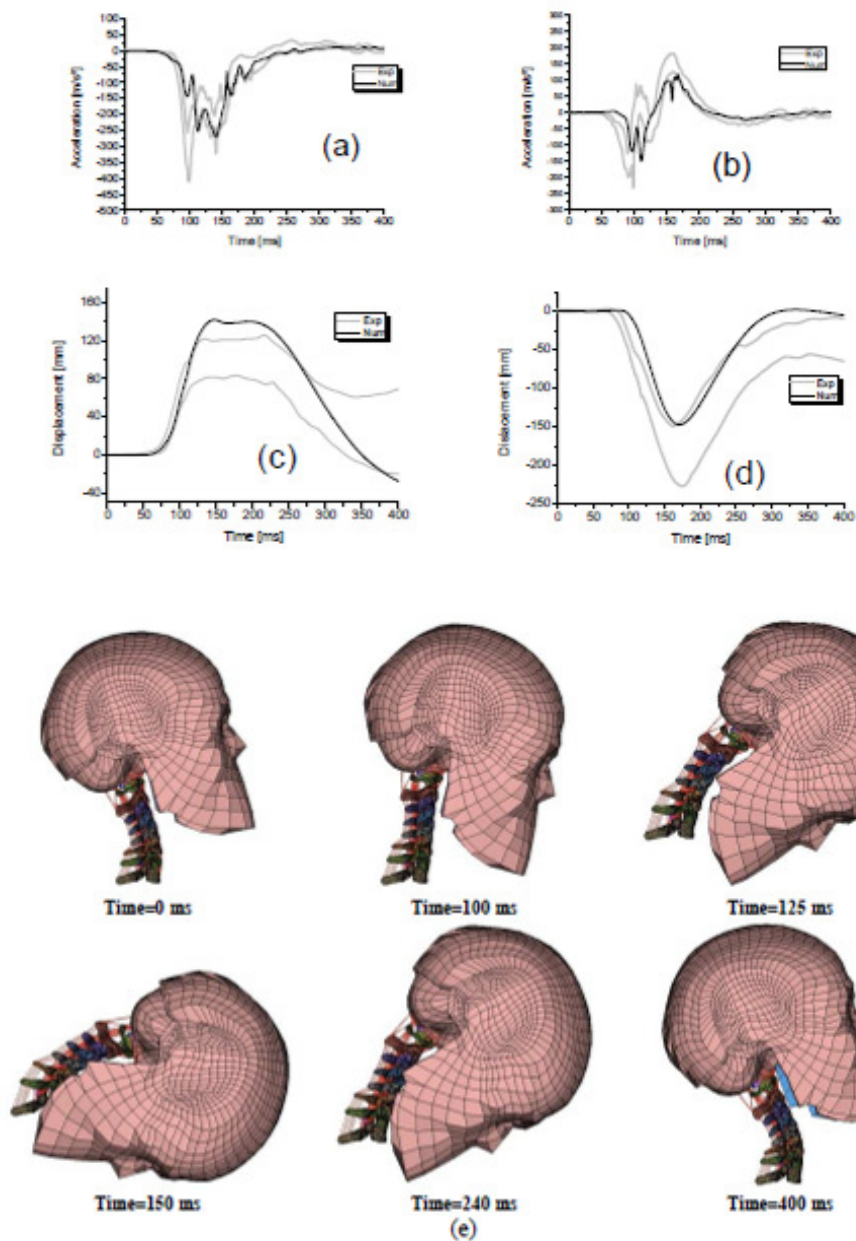
Name	Mass [kg]	Ixx [kg/m <sup>2</sup> ]	Iyy [kg/m <sup>2</sup> ]	Izz [kg/m <sup>2</sup> ]
T1	-	-	-	-
C7	50	0.059	0.046	0.09
C6	50	0.059	0.046	0.09
C5	45	0.057	0.025	0.063
C4	45	0.057	0.025	0.063
C3	45	0.057	0.025	0.063
C2	56	0.077	0.064	0.075
C1	45	0.081	0.031	0.1
Head	3200	88	122	110
Head-neck	4500	217	257	116

### Neck validation

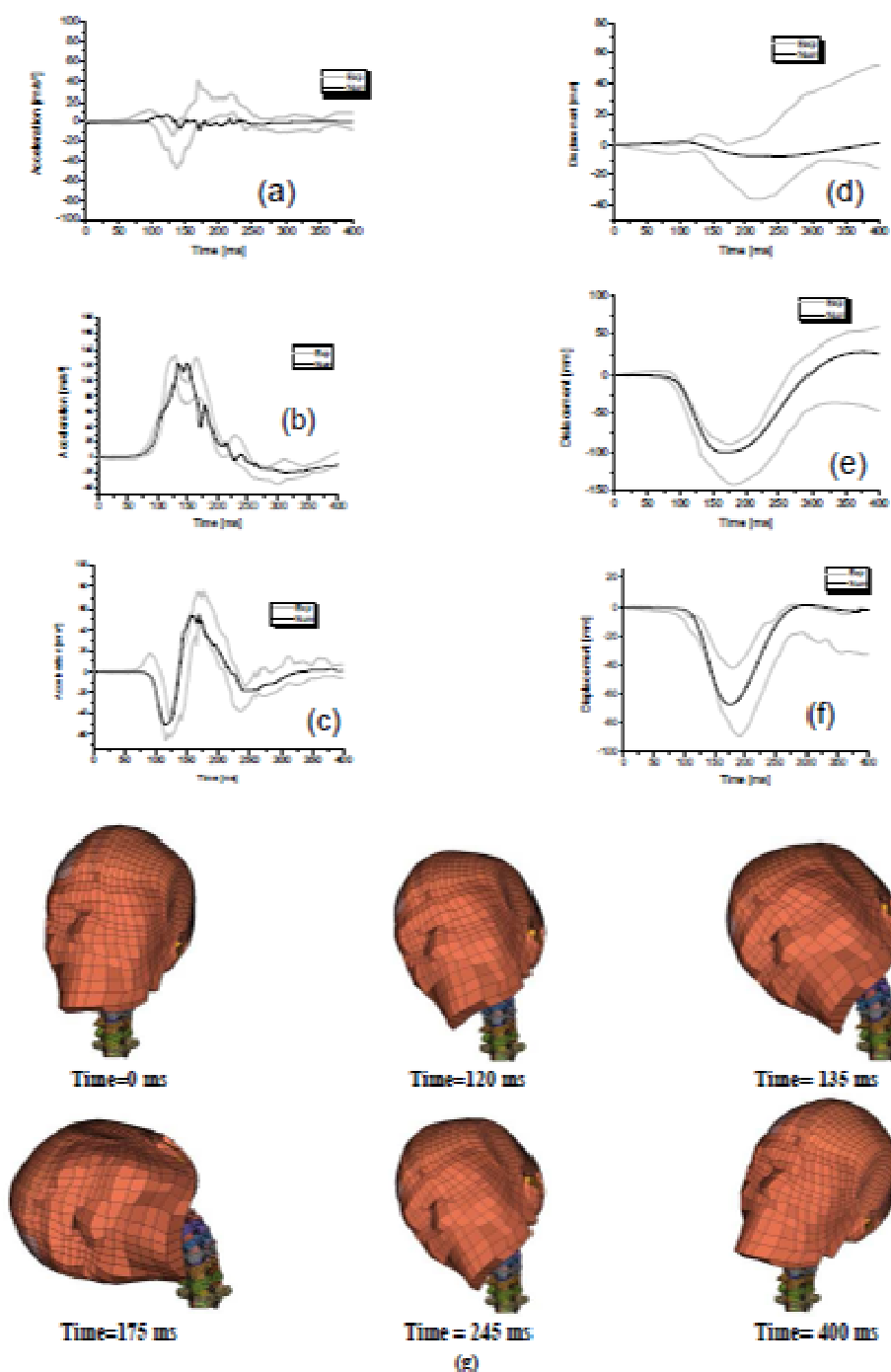
Finite element models of adult neck are typically validated against experimental data carried out by the NBDL, with frontal, lateral, oblique impacts (Ewing *et al.* 1968, Ewing *et al.* 1977). Unfortunately, for ethical reasons, it is not possible to perform similar tests on children so no data exist in the literature for dynamic validation of a paediatric neck models. In the present study, outputs for the six-year-old-child model correspond to those used in the NBDL tests (Frontal, Lateral), i.e., head accelerations and displacements ' corridors, are scaled down in accordance with Irwin's method (1997). An example of the frontal and lateral validation is illustrated in Figure 6-40 and Figure 6-41. In these figures the superimposition of experimental response corridors obtained by the scaling method, with numerical curves obtained with the new finite element model of the child neck is reported.



**Figure 6-39: Impact velocity at T1 for the frontal (a) and the lateral impact (b)**

*Front impact*

**Figure 6-40: Head-neck response under frontal impact: Linear head acceleration, X-axis (a), Z-axis (b), Head displacement X-axis (c), Z-axis (d) and kinematic response of the whole head/neck system (e)**

*Lateral impact*

**Figure 6-41: Head-Neck response under lateral impact: Head acceleration, X-axis (a), Y-axis (b); Z-axis (c) linear, Head displacement ,X-axis (d), Y-axis (e); Y-axis (f); and kinematic response of the whole head/neck system (g)**

### 6.3.3 Results

Two impact conditions are suggested, a frontal and a lateral one. For each case, the child is supposed to be seated statically without seat back, i.e. without any restraint of its thorax and with no initial velocity. For the frontal and lateral impact, five distances between the chin and airbag are proposed, 6, 8, 10, 12 and 13.5 cm and the air bag centre of mass was supposed to be 4.2 cm below the child head centre of mass. The



configuration of the finite element model is shown in Figure 6-42. A global overview of the simulations is given in Figure 6-43.

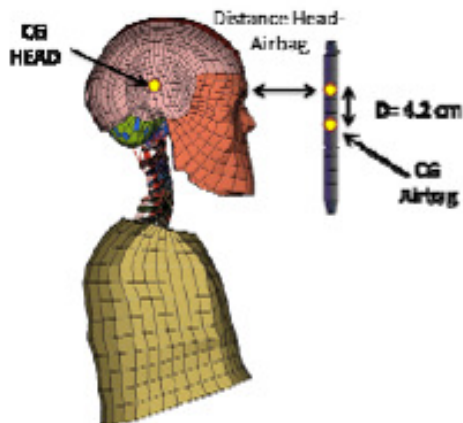


**Figure 6-42: Child under airbag deployment under frontal configuration**

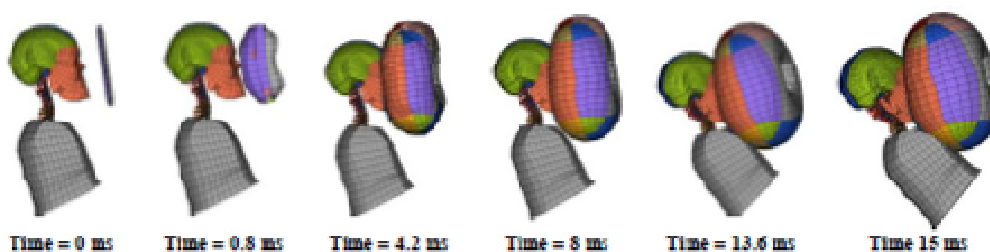


**Figure 6-43: Overall kinematics of the head FEM under frontal airbag deployments (distance 6 cm)**

For each cases the impact forces (Figure 6-44 and Figure 6-45) the intracerebral von Mises stress (Figure 6-46-Figure 6-47) and the elongation of the head-atlas capsular ligament (Figure 6-48) are compared.

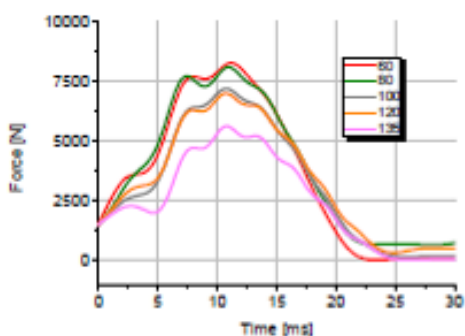


**Figure 6-44: Interaction force calculated between the head and the airbag for each of the 5 distances (d=6 cm; d=8 cm; d=10 cm; d=12 cm; d=13.5 cm)**

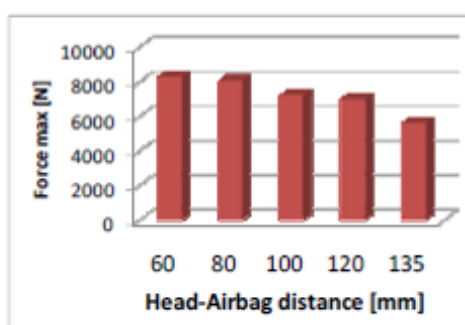


**Figure 6-45: Figure 17. Maximal interaction force calculated for the 5 distances (d=6 cm; d=8 cm; d=10 cm; d=12 cm; d=13,5 cm)**

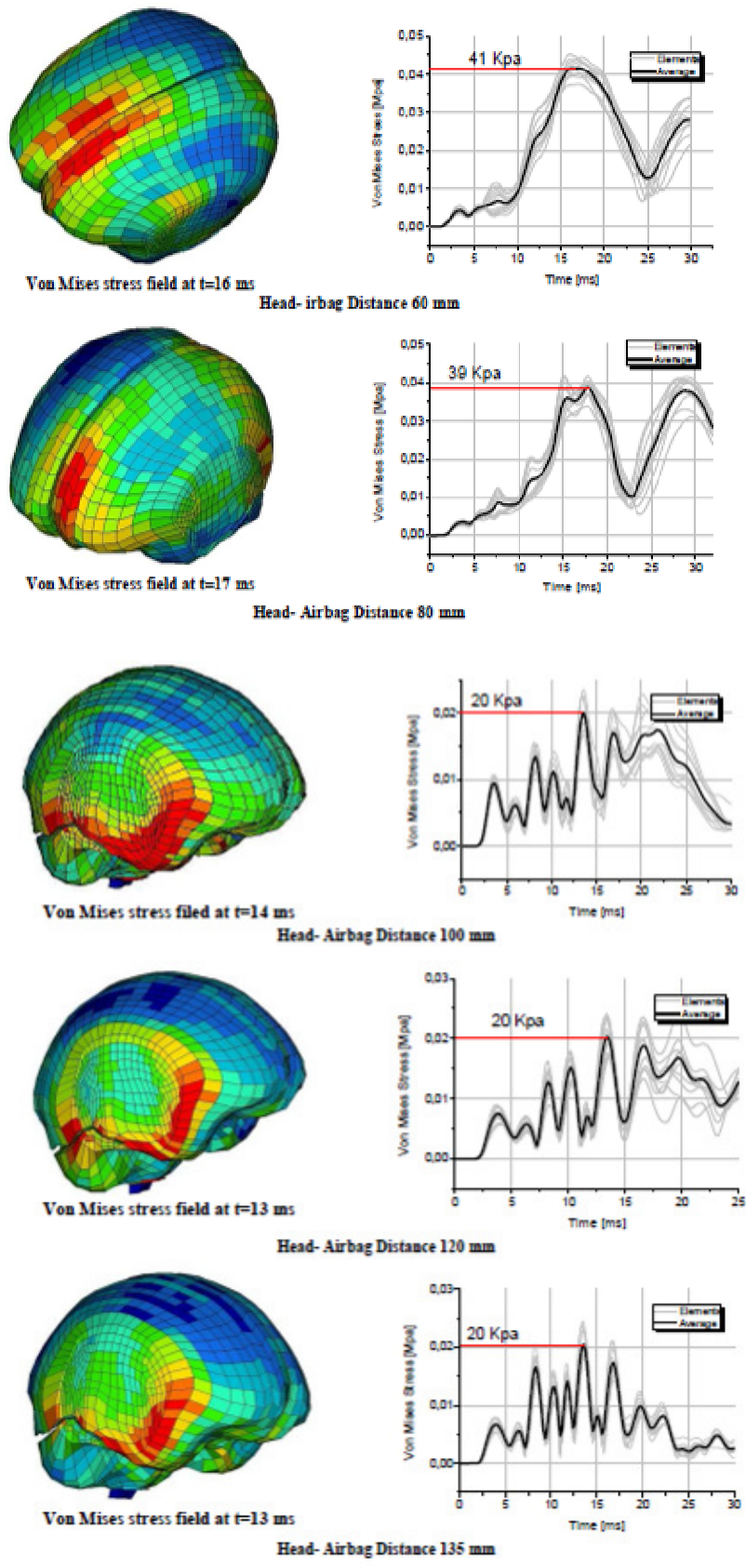
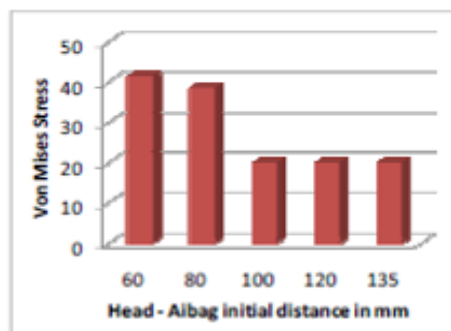
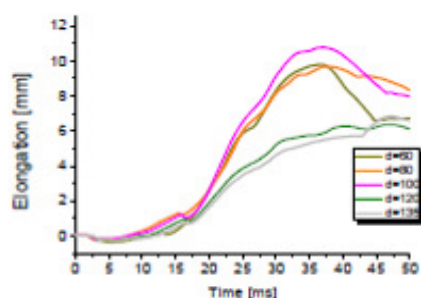


Figure 6-46: Illustration of the intracerebral Von Mises stress calculated for the five head airbag distances (location of these maxima on left and time evolution on right) in frontal impact configuration



**Figure 6-47: Maxima of intracerebral Von Mises stress calculated for the five head/airbag distances under (frontal impact configuration)**



**Figure 6-48: Elongation of the head-atlas capsular ligament for the five simulated frontal impact**

One of the limitations of this study is that no head injury criteria are available for the 6 year old child. Nevertheless for the adult and for the 3 year old child the Von Mises stress is well correlated to the diffuse axonal injury (Deck *et al.* 2008 and Roth *et al.* 2008). This is the reason why this parameter is analysed in this study.

In present parametric study it clearly appears that for a distance over 10 cm the injury parameter is divided by two. The Von Mises stress is estimated around 40 kPa for a distance under 8 cm. For a distance over 10 cm the Von Mises stress is computed approximately at 20 kPa. This is an important result even if the exact tolerance is not yet known.

Concerning the neck response for impact at distance under 12 cm the injury risk increase dramatically (Figure 6-48).

### Lateral airbag deployment

In this section, numerical result obtained in lateral impact configuration for five head/airbag distances 60 mm; 80 mm; 100 mm 120 mm and 135 mm are reported (Figure 6-49 - Figure 6-50).

Figure 6-51 represents the time evolution of the interaction between head and airbag obtained for the five distances. Maximum values of these forces reach 6 to 8kN for time duration of around 20 ms.

Figure 6-52 represents the maximum interaction forces calculated per head/airbag distance.

Figure 6-53 shows the intracerebral Von Mises stress computed (location and time evolution curves) for the five airbag distances in lateral impact configuration. Location of these maxima is similar in the five cases (and corresponds to the vertex area). On the right side of Figure 6-53 the mean value of Von Mises stress in 10 elements at these maxima location.

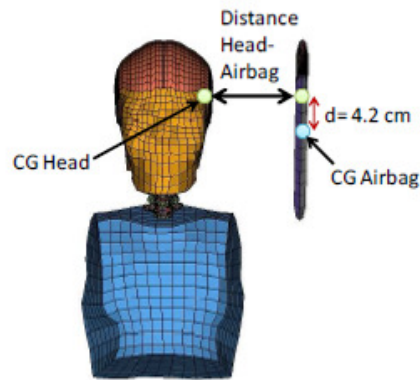


Figure 6-49: Child under airbag deployment in lateral configuration

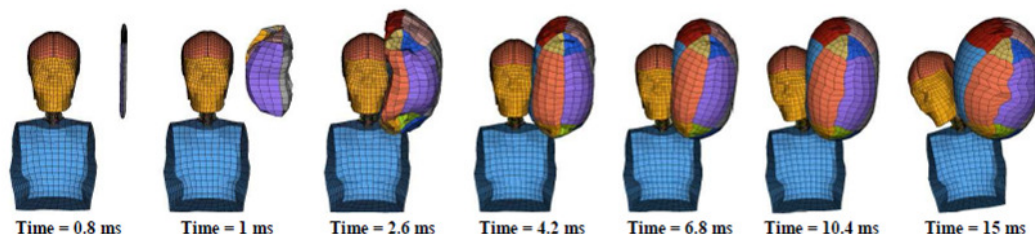


Figure 6-50: Overall kinematics of the head FEM under lateral airbag impact

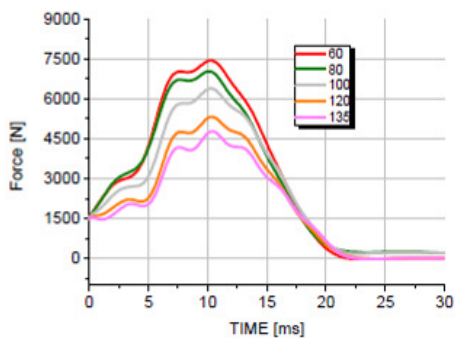


Figure 6-51: Interaction force calculated between the head and the airbag for each of the 5 distances (d=6 cm; d=8 cm; d=10 cm; d=12 cm; d=13.5 cm)

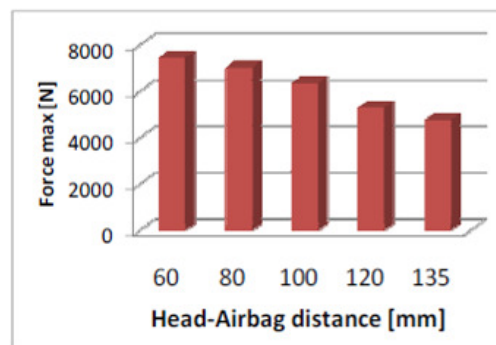


Figure 6-52: Maximal interaction force calculated for the 5 distances (d=6 cm; d=8 cm; d=10 cm; d=12 cm; d=13.5 cm)

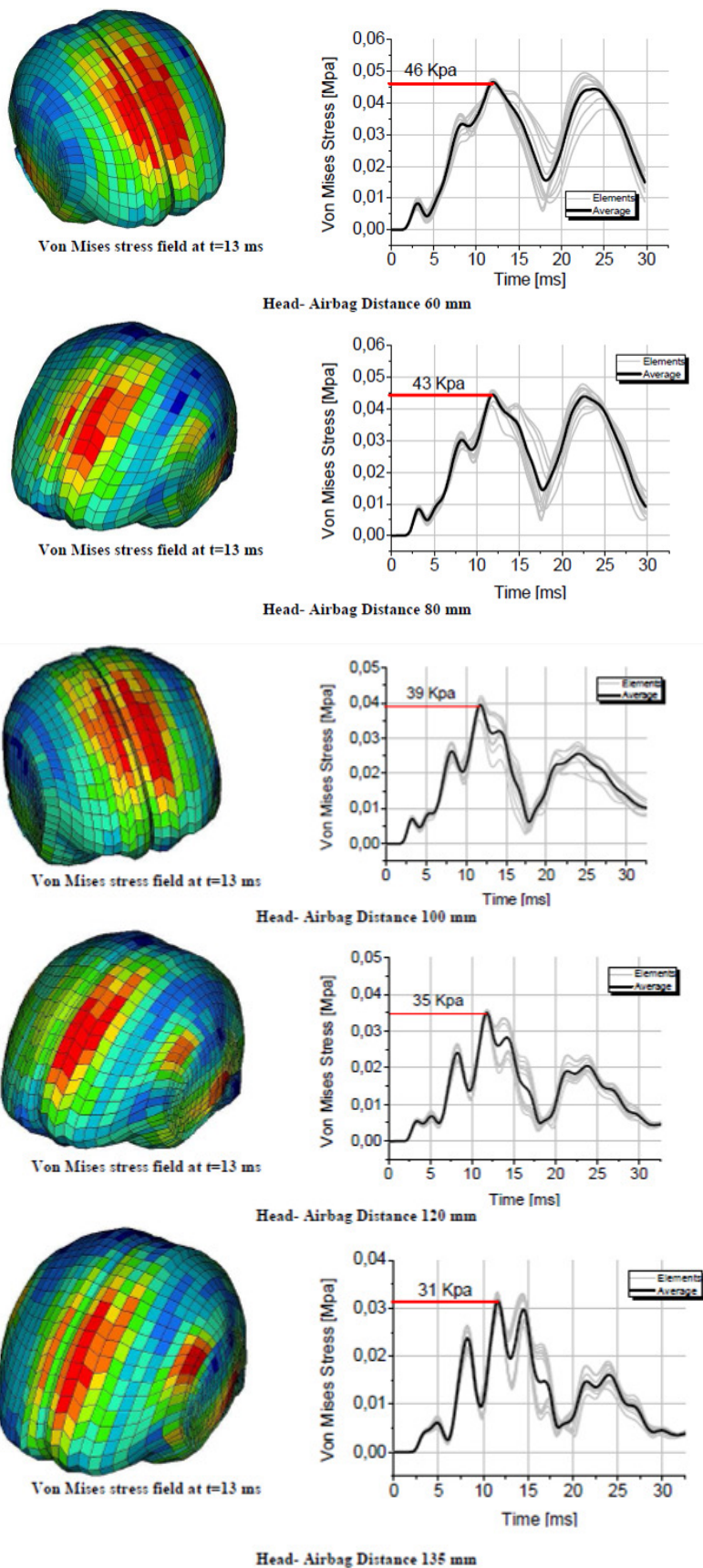


Figure 6-53: Illustration of the intracerebral Von Mises stress calculated for the five head airbag distances (location of these maxima on left and time evolution on right) in lateral impact configuration

Under lateral impact configuration it seems that there is a correlation between the head-airbag distance and the intracerebral Von Mises stress. The intracerebral Von Mises stress decrease linearly as a function of the distance. The Von Mises stress is estimated at around 40 kPa for a distance equal to 6 cm and at 12 cm around at 35 kPa.

For the head-atlas capsular ligament elongation the same conclusion can be underline. There is no threshold which can be defined in order to optimise the neck injury risk.

#### **6.3.4 Discussions**

After the development of a six-year-old child head–neck FE model and its use under airbag deployment, it is important to define the limitations of this study. A number of limitations exist at the biomechanical modelling level where clearly improvements are needed in the future, especially as far as neck injury criteria are concerned. The boundary conditions applied are not the same as in accident conditions as the simulations do not take into account the initial velocity of the whole body, the effect of the seatbelt and the initial position influence on the kinematics and the injury risk. The main originality of the proposed head–neck–thorax model is to consider a detailed geometry of the cervical spine and an FE head model with proposed tolerance limits for moderate neurological lesion. Therefore, it is a step towards numerical tools for the assessment of the child head and neck injury risk under airbag deployment.

#### **6.3.5 Conclusions**

In this study a coupling of the adult Head FEM and the adult neck FEM was perform. In order to obtain a Head-Neck FE Model of the six years old child, the geometry and the mechanical properties were adjusted with the scaling method available in the literature. The head-neck model was coupled to a simplified thorax and validated the head kinematics under frontal and lateral impact. Based on the NBDL test the accelerations and the head displacement were scale in accordance to the Irwin method's in order to provide the experimental validation data. Finally five distances were computed under frontal and lateral airbag impact in order to estimate the head and neck injury risk. For the frontal impact it clearly appears that over a distance of 10 cm the Von Mises stress is divide by two (41 kPa for a distance of 6 cm and 20 kPa for a distance of 12 cm). Based on the results obtained with the adult head the Von Mises stress is correlated to the diffuse axonal injury with a critical threshold at 20 kPa approximately. Coming to the neck injury it also appeared that the injury risk decrease significantly over a distance of 10 cm. Concerning the lateral airbag deployment, the Von Mises stress decrease linearly as a function of the distance or the impact force. It appeared that the Von Mises stress were however over 20 kPa for all distance, illustrating critical injury risk for all lateral impact. It can therefore be concluded that lateral airbag deployment is clearly more dangerous as frontal deployment as for head is concerned. Under lateral impact occipital-atlas capsular ligament are less stretched as under frontal impact. As injury mechanisms and injury criteria are not yet defined for these segments at this specific age, no definitive conclusion can be drawn at this level. Finally injury risk is higher for all the distances in lateral impact. This conclusion is in accordance to the medical knowledge; the head is more vulnerable in the temporal region.

#### **6.3.6 Acknowledgement**

The authors would like to thank the CASPER project (Grant agreement N°218564) for their support.

### 6.3.7 References

- Chazal, J., Tanguy, A., Bourges, M., Gaurel, G., Escande, G., Guillot, M. and Vanneuville, G. (1985) Biomechanical properties of spinal ligaments and a histological study of the supraspinal ligament in traction. *Journal of Biomechanics* (18)3: 167-176.
- Dauvilliers, F. (1994) Modélisation Tridimensionnelle et Dynamique du Rachis Cervical. PhD Thesis, ENSAM Paris.
- Deck C. and Willinger R.. (2008) Improved head injury criteria based on head FE model. *International Journal of Crashworthiness* 13 (6), 667-678. 6-12-2008. Oxon, UK, Taylor&Francis.
- De Jager, M., Sauren, A., Thunnissen, J. and Wismans, J. (1996) A Global and a Detailed Mathematical Model for Head-Neck Dynamics. Proc. 40th Stapp Car Crash Conference, pp. 269-281. Society of Automotive Engineers, Warrendale, PA. Paper 962430
- Ewing C., Thomas D., Beeler G., Patrick L. and Gillis D. (1969) Living human dynamic response to -Gx impact acceleration II - Accelerations measured on the head and neck. Proc.13th Stapp Car Crash Conference, pp. 400-415. Society of Automotive Engineers, Warrendale, PA. . Paper 690817
- Ewing, C., Thomas, D., Lustick, L., Muzzy, III W., Willems, G. and Majewski, P. (1977) Dynamic response of the human head and neck to +Gy impact acceleration. Proc. 21st Stapp Car Crash Conference, pp. 549-586. Society of Automotive Engineers, Warrendale, PA. Paper 770928.
- Kang H.S, Willinger R., Diaw B., Chinn B. (1998), Validation of a 3D anatomic human head model and replication of head impact in motorcycle accident by finite element modelling, Proc. Of the 41 st STAPP Car Crash Conf., pp 329-338.
- Khalil T.B., Hubbard R.P., Parametric study of head response by finite element modelling, *J. of Biomechanics*, (1977) Vol. 10, p119-132.
- Irwin, A. and Mertz, H. J. (1997) Biomechanical basis for the CRABI and hybrid III hild dummies, SAE paper 973317.
- Kleinberger, M. (1993) Application of finite element techniques to the study of cervical spine mechanics. Proc. 37th Stapp Car Crash Conference, pp. 261-272. Society of Automotive Engineers, Warrendale, PA. Paper 933131
- Kumaresan, S., Yoganandan, N., and Pintar, F. A., (2001). Pediatric neck injury scale factors and tolerance. *Biomedical Sciences Instrumentation* 37, 435-440
- Meyer F. Bourdet N., Deck C., Willinger R., Raul J.S. (2004) « Human neck finite element model development and validation against original experimental data » SAE paper :2004-22-0008 pp 177-206.
- Nahum, A.M., Smith, R., Ward, C.C., Intracranial pressure dynamics during head impact, Proceed. of the 21st Stapp Car Crash Conf., SAE Paper 770922 (1970)., pp. 339-366, 1977 Piekarski, Fracture of bone. *J. Appl. Phys.* 14, N°1, 215-223.
- Prasad, P., Kim, A. and Weerappuli, D.P.V. (1997) Biofidelity of Anthropomorphic Test

---

Devices for Rear Impact. Proc. 41st Stapp Car Crash Conference, pp. 387-415.  
Society of Automotive Engineers, Warrendale, PA. Paper 973342.

Reynolds, HM., Young, JW., Mc Conville, Jt., and Snyder, RG., (1976) Development and evaluation of masterbody forms for Three-Years old Child and Six Years old child Dummies. DOT HS-801 811, University of Michigan, Ann Arbor.

Troseille, X., Tarrière, C., Lavaste, F., Guillon, F., Domont, A., (1992) Development of a F.E.M. of the human head according to a specific test protocol, Proceed. of the 36th Stapp Car Crash Conf., pp. 235-253.

Weber, K. (2002). Pediatric biomechanics. Accidental injury: Biomechanics and prevention, A. Nahum and J. Melvin, eds., Springer-Verlag, New York, 523–549.

Willinger R., Taleb L., Pradoura P., (1995) Head biomechanics from the finite element model to the physical model. Proceed. Ircobi, pp 245-260, Brunnen.

Willinger R, Bourdet N., Fischer R., Legal F. (2005) Modal analysis of the human head neck in vivo as a criteria for crash test dummy evaluation . J. of Sound and Vib., vol 287 (3), 405-431

Yoganandan, N., Biomechanics of Skull Fracture, (1994) Proc. of Head Injury 94 Symposium, Washington DC.

Yoganandan, N. and Pintar, F. (2001) A. Single rear impact produces lower cervical spine soft tissue injuries. Proc. Ircobi conference pp. 201-211



## 7 Summary

The COVER project provided a framework for the exchange of information between the main EU FP7 projects on human injury biomechanics in road vehicle collisions, as well as aligning their dissemination strategies. This overview report is an example of the cooperation brought about by COVER in the area of child safety. It drew together the latest research and findings from two complimentary projects; CASPER and EPOCh, to provide a single source of information for researchers and stakeholders working in the field.

Directive 91/67/EEC (as amended by 2003/20/EC) made the use of a child restraint approved to UN Regulation 44 mandatory for children travelling in cars in the EU. The UN Regulation includes front and rear impact tests with the P-Series “family” of child dummies and specifies minimum standards of performance for child restraints in these tests. Whilst these measures have undoubtedly reduced the number of children killed or seriously injured in the EU, industry and regulators both agree that further improvements are both necessary and feasible to meet the demands of consumers. These improvements can be brought about by understanding the way children are injured in collisions and ensuring that test procedures and tools (such as dummies) are targeted at the key injury mechanisms and encourage improvements in restraint design.

Rates of child restraint use are relatively high across the EU, particularly in the original Member States due, in part to the legislation described above (as well as other initiatives). It is critical to maintain these high rates of child restraint use as new Member States join the EU, which have not traditionally operated or enforced such legislation. However, the research summarised in Chapter 2 also highlighted the importance of using a child restraint system correctly; around two-thirds of the child restraints observed in the field study were misused in some way, although significant regional differences in misuse rates were found between the three study locations (Berlin, Lyon and Naples). The effects of misuse are likely to vary according to the particular situation; nevertheless, sled tests undertaken within CASPER demonstrated that, overall, misuse tended to increase dummy head excursion and hence the risk of child head injury through head contact with the interior of the vehicle.

Children represent a relatively small proportion of the total number of people that are killed or seriously injured in road vehicle collisions each year. Nevertheless, the CASPER database (combined with CHILD cases) comprises 656 restrained children (with 416 in a child restraint system). Two hundred and three children received injuries at  $\text{MAIS} \geq 3$  (149 of these in a child restraint system). Whilst the database is not representative, it illustrates that children in child restraints are seriously injured in collisions and provides a valuable resource for researchers looking at the way children are injured in collisions. The analysis from CASPER presented in Section 3.1, highlighted that children that are seriously injured in front impact collisions tended to be involved in collisions that were more severe than the impact test in UN Regulation 44. For side impact, vehicle intrusion played an important role in the risk of injury for children seated on the struck side of the vehicle. A side impact test for child restraint systems is being introduced by a new UN Regulation on “Enhanced Child Restraint Systems” and it will be important, therefore, to ensure that the test is capable of encouraging child restraint designs that mitigate the risks associated with vehicle intrusion.

The EPOCh project studied injuries to older children in preparation for the development of the Q10 dummy. Section 3.2 presented the main body regions that are injured in older children and described the key injury mechanisms. The head was the most

frequently injured body region, in both front and side impact, through contact with the vehicle interior. The abdomen was noted as the next most significant body region to protect, highlighting the need for some means of detecting, and ideally measuring abdomen loading in the Q10 (as well as other dummies used for the assessment of non-integral child restraint systems).

Both CASPER and EPOCH contributed to the development of the Q-Series dummies and examples of their main research work were included in this overview report in Chapter 4. The Q-Series is expected to help bring about a step forward in the protection of children in cars and is specified in the new UN Regulation on “Enhanced Child Restraint Systems”. Section 4.1 presented an investigation of different solutions to improve the response of the dummy by removing the gap between the legs and pelvis (to prevent the belt from becoming trapped). The results of sled tests were promising, but the authors concluded that further work would be needed to develop a solution that is suitable for a regulation. Section 4.2 described the development and assessment of abdomen sensors for the Q-Series, undertaken within CASPER. The work verified the capacity of the sensors to detect abdomen loading, including first experiments with the sensors fitted in the Q10 dummy. Section 4.3 presented an evaluation of the biofidelity, sensitivity, repeatability and durability of the Q10 performed by the EPOCH project. The dummy performed according to its design specifications and within the expectations of the project.

With a new dummy, such as the Q-Series, it is essential to provide a means of interpreting the dummy measurements in terms of the risk of injury to children, as well as measurement thresholds that are suitable for use in test procedures. Chapter 5 described the latest work on the development of injury criteria and performance limits for the Q-Series. CASPER focussed on the existing Q-Series dummies and attempted to derive limits through accident reconstruction and scaling. This work was described in Section 5.1. There were sufficient data to derive a reliable injury risk curve for the head in front impact collisions, whilst some trends were discernible for the neck (also in front impact). However, neither chest acceleration, nor deflection, were capable of predicting injury. This was attributed to the interaction between the dummy and the diagonal part of the seat belt. A head injury risk curve was also derived for the head in side impact, but there were too few data for other body regions. The EPOCH project developed injury risk curves for the Q10 using scaling techniques and proposed regulatory performance limits. This was presented in Section 5.2. Limits were proposed for the head, neck and chest in the front impact conditions specified in UN Regulation 44. No work was undertaken on side impact.

Recognising the increasing role of numerical simulation in vehicle safety research (and the value of such techniques), the CASPER project sought to ensure that numerical tools were available to represent child dummies as well as real children. The principal work of CASPER in this field was presented in Chapter 6. Section 6.1 described the development of FE models of the Q-Series and the first experiences of their use. Sections 6.2 and 6.3 focussed on human body models of the head and neck complex. In Section 6.2, a FE model of a three-year-old child was used to derive new head injury criteria. The Von Mises stress in the brain was found to be a reasonable predictor of loss of consciousness whilst cranial strain energy predicted cranial fracture. Section 6.3 derived a FE model for a six-year-old child and used it to investigate the interaction between children and airbags.